CELL-BASED APPROACHES FOR MODULATING CARTILAGE AND BONE PHENOTYPE

EDITED BY: Roberto Narcisi and Elena Jones
PUBLISHED IN: Frontiers in Bioengineering and Biotechnology

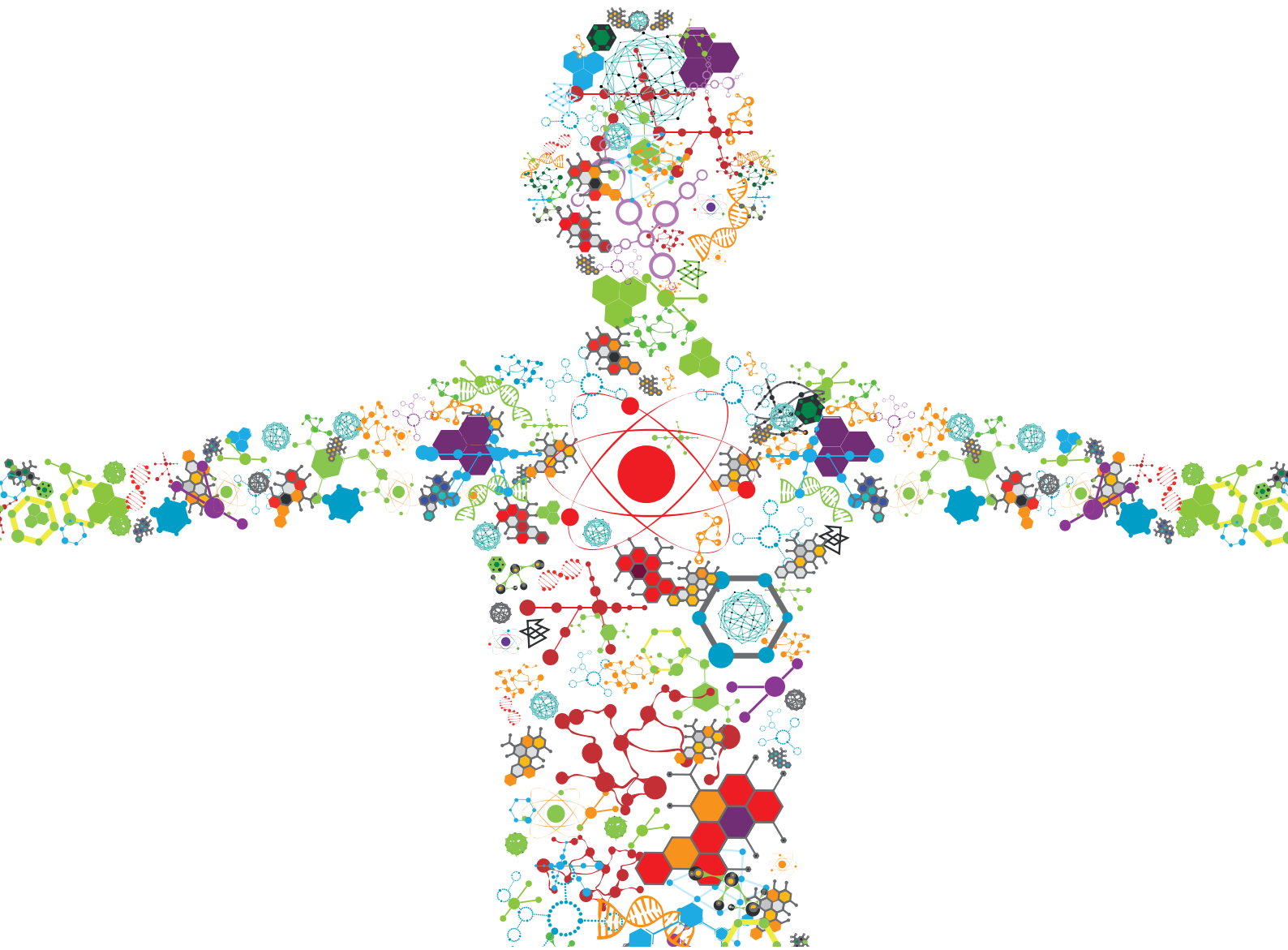

frontiers Research Topics

frontiers

ISSN 1664-8714
ISBN 978-2-88971-855-9
DOI 10.3389/978-2-88971-855-9

About Frontiers

Frontiers is more than just an open-access publisher of scholarly articles: it is a pioneering approach to the world of academia, radically improving the way scholarly research is managed. The grand vision of Frontiers is a world where all people have an equal opportunity to seek, share and generate knowledge. Frontiers provides immediate and permanent online open access to all its publications, but this alone is not enough to realize our grand goals.

Frontiers Journal Series

The Frontiers Journal Series is a multi-tier and interdisciplinary set of open-access, online journals, promising a paradigm shift from the current review, selection and dissemination processes in academic publishing. All Frontiers journals are driven by researchers for researchers; therefore, they constitute a service to the scholarly community. At the same time, the Frontiers Journal Series operates on a revolutionary invention, the tiered publishing system, initially addressing specific communities of scholars, and gradually climbing up to broader public understanding, thus serving the interests of the lay society, too.

Dedication to Quality

Each Frontiers article is a landmark of the highest quality, thanks to genuinely collaborative interactions between authors and review editors, who include some of the world's best academicians. Research must be certified by peers before entering a stream of knowledge that may eventually reach the public - and shape society; therefore, Frontiers only applies the most rigorous and unbiased reviews.
Frontiers revolutionizes research publishing by freely delivering the most outstanding research, evaluated with no bias from both the academic and social point of view. By applying the most advanced information technologies, Frontiers is catapulting scholarly publishing into a new generation.

What are Frontiers Research Topics?

Frontiers Research Topics are very popular trademarks of the Frontiers Journals Series: they are collections of at least ten articles, all centered on a particular subject. With their unique mix of varied contributions from Original Research to Review Articles, Frontiers Research Topics unify the most influential researchers, the latest key findings and historical advances in a hot research area! Find out more on how to host your own Frontiers Research Topic or contribute to one as an author by contacting the Frontiers Editorial Office: frontiersin.org/about/contact

CELL-BASED APPROACHES FOR MODULATING CARTILAGE AND BONE PHENOTYPE

Topic Editors:
Roberto Narcisi, Erasmus University Rotterdam, Netherlands
Elena Jones, University of Leeds, United Kingdom

Citation: Narcisi, R., Jones, E., eds. (2021). Cell-Based Approaches for Modulating Cartilage and Bone Phenotype. Lausanne: Frontiers Media SA.
doi: 10.3389/978-2-88971-855-9

Table of Contents

frontiers in Bioengineering and Biotechnology

EDITORIAL
published: 02 July 2021
doi: 10.3389/fbioe.2021.716323

Editorial: Cell-Based Approaches for Modulating Cartilage and Bone Phenotype

Roberto Narcisi[1]* *and Elena Jones*[2]

[1] Department of Orthopaedics and Sports Medicine, Erasmus MC, University Medical Center, Rotterdam, Netherlands,
[2] Leeds Institute of Rheumatic and Musculoskeletal Medicine, The University of Leeds, Leeds, United Kingdom

Keywords: cartilage, bone, mesenchymal stem cells, osteoarthritis, musculoskeletal disorders

Editorial on the Research Topic

Cell-Based Approaches for Modulating Cartilage and Bone Phenotype

With increasing aging populations, musculoskeletal tissue disorders including osteoarthritis (OA) and fracture non-unions have become a significant healthcare challenge. The discovery of multipotential mesenchymal stem/stromal cells (commonly termed MSCs) in virtually all musculoskeletal tissues (da Silva Meirelles et al., 2006), combined with significant advances in industrial-scale cell manufacture (Bellani et al., 2020), have made musculoskeletal tissue regeneration a realistic opportunity. And yet, the regulatory approvals and clinical uptake of new therapies progress at a frustratingly slow pace. Apart from commercial considerations, a slow uptake of these therapies may be due to our limited understanding of the effects of mechanical, cellular, inflammatory and metabolic environments on MSCs, both before and after implantation. The aim of this Research Topic was to bring together recent research on cell-based bone and cartilage regeneration focussing on extrinsic mechanisms controlling cell fate.

The Research Topic is framed by two comprehensive review articles, with Goodman and Lin centered on bone healing and Greif et al. on the infrapatellar fad pad (IFP) as a source of MSCs and therapeutic target for osteoarthritis, a joint pathology influencing all joint tissues and often characterized by inflammation. Common for both reviews and the Research Topic in general is the focus on MSC potency enhancement, be it in elderly individuals or patients with co-morbidities. Goodman and Lin emphasize *ex vivo* cell pre-conditioning, hypoxia, genetic manipulations, and the use of biomaterials as potent modulators of cell function. Gene activated matrices combine the latter two factors and enable MSC migration and differentiation to occur in a tissue-relevant, three-dimensional manner. Greif et al. emphasizes the cross-talk between MSCs and M1 (pro-inflammatory) or M2 (anti-inflammatory) macrophages as an important determinant of the cellular and molecular milieu at the site of regeneration.

Oxygen levels are a known parameter influencing cartilage homeostasis and chondrocyte phenotype. In their study, Dennis et al. found that human chondrocytes self-assembled into cartilage sheets and cultured under physiologic conditions, were able to deposit an higher amount of extracellular matrix components, such as glycosaminoglycans, and become stiffer compared to cartilage sheets cultured in atmospheric oxygen levels. Along this line, in their review Lin et al. highlighted the importance of lysyl oxidase enzymes in regulating hypoxia-inducible factors in chondrocytes which, in turn, are key regulators of cartilage homeostasis. Lysyl oxidase enzymes can mediate cartilage integrity by regulating the expression of extracellular matrix-degrading enzymes matrix metalloproteinases and collagen cross-links, and have been recently associated to aging-associated cartilage degeneration. For this reason they are becoming very interesting potential targets for cartilage pathologies. Other extracellular matrix components of cartilage are Aggrecan

OPEN ACCESS

Edited and reviewed by:
Andrea Banfi,
University of Basel, Switzerland

***Correspondence:**
Roberto Narcisi
r.narcisi@erasmusmc.nl

Specialty section:
This article was submitted to Preclinical Cell and Gene Therapy, a section of the journal Frontiers in Bioengineering and Biotechnology

Received: *28 May 2021*
Accepted: *10 June 2021*
Published: *02 July 2021*

Citation:
Narcisi R and Jones E (2021) Editorial: Cell-Based Approaches for Modulating Cartilage and Bone Phenotype. Front. Bioeng. Biotechnol. 9:716323. doi: 10.3389/fbioe.2021.716323

and COMP. In their research, Caron et al., investigated the possibility of culturing progenitor periosteal cells under the influence of these matrix components aiming to sustain the chondrogenic differentiation process of those cells, which is often hampered by unwanted hypertrophic differentiation. What they found is indeed that those extracellular cartilage components have a potential favorable influence for the *in vivo* generation of cartilage for regenerative medicine applications since hypertrophy was significantly reduced when Aggrecan and COMP were added to the cell culture.

Bone regeneration with non-autologous MSCs is explored in Longoni et al., which presents a comprehensive *in vivo* investigation of segmental bone repair in a rat model. Using collagen-embedded, chondrogenically pre-differentiated xenogenic or allogenic MSCs, the authors demonstrate that bone bridging (*via* endochondral ossification) is "proportional to the degree of host-donor relatedness," and that immune cell activation at both early and late stages of repair plays a major role in the healing outcome. These findings greatly improve our understanding of the immune cell mechanisms behind fracture non-union and fracture healing in general.

A controversial topic of platelet products (PPs), including platelet lysate (PL) for bone regeneration, is introduced in Goodman and Lin, where they call for a better standardization of PP/PL production and quality control. In this context, the study by Rikkers et al. presents an excellent example of good practice, where PL is thoroughly characterized for platelet purity as well as growth factor levels. The study describes the opposite effects of their PL formulation on chondrocyte expansion (enhancement) and re-differentiation (inhibition) thus emphasizing the complexity of chondrocyte responses to PL. Chondrogenesis enhancement for cartilage regeneration is also considered by Carroll et al., where the authors employ cell-seeded agarose hydrogels and a custom-designed oxygen sensor to compare the effects of different MSC sources (including IFP), cell density, and environmental oxygen tension on their chondrogenesis. The study opens up a possibility of sensor-monitored manufacturing of tissue engineered cartilage implants.

Sanjurjo-Rodriguez et al. compare MSCs derived from synovial fluid (SF) and subchondral bone (SB) of knee OA patients, and demonstrates a beneficial chondrogenesis-supporting gene expression in SF MSCs, particularly after joint distraction, a joint-preserving treatment for OA based on the correction of joint biomechanics. Together, the articles by Sanjurjo-Rodriguez et al. and Carroll et al. bring to the fore the effects of metabolic and biomechanical environments on MSC function.

Overall, in this Research Topic several important biological aspects regulating bone and cartilage phenotype at the cellular level have been discussed. Cell based-approaches for the treatment of musculoskeletal tissues are becoming more and more appealing for regenerative medicine and tissue engineering applications. A better understanding of the basic molecular processes governing cellular differentiation and commitment will allow us to explore new applications or further refine existing ones, in order to ameliorate the treatment of musculoskeletal disorders.

AUTHOR CONTRIBUTIONS

All authors listed have made a substantial, direct and intellectual contribution to the work, and approved it for publication.

ACKNOWLEDGMENTS

The Topic Editors would like to thank all the authors that contributed to the Research Topic.

REFERENCES

Bellani, C. F., Ajeian, J., Duffy, L., Miotto, M., Groenewegen, L., and Connon, C. J. (2020). Scale-up technologies for the manufacture of adherent cells. *Front. Nutr.* 7:575146. doi: 10.3389/fnut.2020.575146

da Silva Meirelles, L., Chagastelles, P. C., and Nardi, N. B. (2006). Mesenchymal stem cells reside in virtually all post-natal organs and tissues. *J. Cell Sci.* 119, 2204–2213. doi: 10.1242/jcs.02932

Conflict of Interest: The authors declare that the research was conducted in the absence of any commercial or financial relationships that could be construed as a potential conflict of interest.

frontiers in Bioengineering and Biotechnology

REVIEW
published: 30 April 2020
doi: 10.3389/fbioe.2020.00359

Molecular Insights Into Lysyl Oxidases in Cartilage Regeneration and Rejuvenation

Weiping Lin[1]†, Liangliang Xu[2†] and Gang Li[1,3]**

[1] Department of Orthopaedics and Traumatology, Stem Cells and Regenerative Medicine Laboratory, Li Ka Shing Institute of Health Sciences, The Chinese University of Hong Kong, Prince of Wales Hospital, Hong Kong, China, [2] The First Affiliated Hospital of Guangzhou University of Chinese Medicine, Lingnan Medical Research Center, Guangzhou University of Chinese Medicine, Guangzhou, China, [3] MOE Key Laboratory for Regenerative Medicine, School of Biomedical Sciences, The Chinese University of Hong Kong, Hong Kong, China

OPEN ACCESS

Edited by:
Roberto Narcisi,
Erasmus University Rotterdam, Netherlands

Reviewed by:
Guus van den Akker, Maastricht University, Netherlands
Ryan Michael Porter, University of Arkansas for Medical Sciences, United States

***Correspondence:**
Gang Li
gangli@cuhk.edu.hk
Weiping Lin
weipinglin@link.cuhk.edu.hk

† These authors have contributed equally to this work

Specialty section:
This article was submitted to Preclinical Cell and Gene Therapy, a section of the journal Frontiers in Bioengineering and Biotechnology

Received: 17 February 2020
Accepted: 31 March 2020
Published: 30 April 2020

Citation:
Lin W, Xu L and Li G (2020) Molecular Insights Into Lysyl Oxidases in Cartilage Regeneration and Rejuvenation. Front. Bioeng. Biotechnol. 8:359. doi: 10.3389/fbioe.2020.00359

Articular cartilage remains among the most difficult tissues to regenerate due to its poor self-repair capacity. The lysyl oxidase family (LOX; also termed as protein-lysine 6-oxidase), mainly consists of lysyl oxidase (LO) and lysyl oxidase-like 1-4 (LOXL1-LOXL4), has been traditionally defined as cuproenzymes that are essential for stabilization of extracellular matrix, particularly cross-linking of collagen and elastin. LOX is essential in the musculoskeletal system, particularly cartilage. LOXs-mediated collagen cross-links are essential for the functional integrity of articular cartilage. Appropriate modulation of the expression or activity of certain LOX members selectively may become potential promising strategy for cartilage repair. In the current review, we summarized the advances of LOX in cartilage homeostasis and functioning, as well as copper-mediated activation of LOX through hypoxia-responsive signaling axis during recent decades. Also, the molecular signaling network governing LOX expression has been summarized, indicating that appropriate modulation of hypoxia-responsive-signaling-directed LOX expression through manipulation of bioavailability of copper and oxygen is promising for further clinical implications of cartilage regeneration, which has emerged as a potential therapeutic approach for cartilage rejuvenation in tissue engineering and regenerative medicine. Therefore, targeted regulation of copper-mediated hypoxia-responsive signalling axis for selective modulation of LOX expression may become potential effective therapeutics for enhanced cartilage regeneration and rejuvenation in future clinical implications.

Keywords: lysyl oxidase, cartilage, hypoxia-inducible factor, copper, transcription activity, regeneration, rejuvenation

INTRODUCTION

The lysyl oxidase family (LOX; also termed as protein-lysine 6-oxidase) has been traditionally defined as cuproenzymes that are essential for stabilization of extracellular matrix (ECM), particularly cross-linking of collagen and elastin (Rucker et al., 1998; Kagan and Li, 2003). LOX mainly comprises of five members that were originally considered copper-dependent amine

oxidases, including lysyl oxidase and lysyl oxidase-like 1-4 (LOXL1-LOXL4), is a copper-containing amine oxidase belonging to a heterogeneous family of enzymes, which catalyzes oxidative deamination of the amino group in certain lysine and hydroxylysine residues of collagen molecules for stabilization of collagen fibrils (Kagan and Li, 2003). To date, LOX has been demonstrated to regulate a diverse range of cellular processes and biological functions (Smith-Mungo and Kagan, 1998), as well as certain pathogenesis of various diseases, particularly fibrotic diseases, ischemic cardiovascular diseases, and cancer progression, which is mainly mediated by ECM remodeling and elastogenesis (Schmelzer et al., 2019), epithelial-mesenchymal transition and intracellular signaling (Lopez et al., 2010; Busnadiego et al., 2013; Cox et al., 2013, 2015; Klingberg et al., 2013; Rimar et al., 2014; Schmelzer et al., 2019). The LOX has been demonstrated as crucial contributors for normal embryonic development of various tissue and organ systems, including cardiovascular (Martinez-Gonzalez et al., 2019), and respiratory systems (Maki et al., 2002; Maki, 2009; Maki et al., 2005), as well as essential for normal physiological and cellular properties, such as sprouting angiogenesis of endothelial cells (Lucero and Kagan, 2006; Bignon et al., 2011).

Cartilage is an avascular collagen-abundant tissue. Unlike bone, cartilage seems to lack efficient self-reparative/regenerative capacity, making arthritis common and costly, affecting the well-being and quality of life of millions of people worldwide (Huey et al., 2012; Mobasheri and Batt, 2016; Deng et al., 2019). Inflammatory arthritides, such as rheumatoid arthritis, and psoriatic arthritis, are among the most challenging auto-immune diseases and health problems worldwide (Mobasheri and Batt, 2016; Flores et al., 2019; Zhou B. et al., 2019). Of note, osteoarthritis (OA) is the most common form of arthritis, which is one of the most prevalent chronic immune diseases. OA is characterized by articular cartilage degeneration, subchondral bone remodeling, osteophyte formation and synovial changes (Yuan et al., 2014). OA is a multifactorial disease and various risk factors of OA have been reported, such as obesity (Aspden, 2011), body mass (Messier et al., 2005), and aging (Lotz and Loeser, 2012). Until now, the etiology and pathophysiology of OA have not been well documented. Various treatments, such as cellular therapies (Fu et al., 2014; Lee and Wang, 2017; Lin et al., 2017; Teo et al., 2019; Xu et al., 2019), administration of certain drugs or chemicals (Zhang et al., 2016, 2019; Yao et al., 2019), therapeutic surgeries (Chen Y. et al., 2015), and bio-fabrication approach (Tatman et al., 2015; Onofrillo et al., 2018; Lee et al., 2019), have been intensely studied and tested in various preclinical studies and clinical trials during recent decades (Lee and Wang, 2017; Zhang et al., 2019). However, several hurdles are required to be addressed for therapeutic optimization before clinical translation. And currently there are no effective clinical options treating OA (Mobasheri and Batt, 2016; Chen et al., 2018; Griffin and Scanzello, 2019).

Cross-linking is essential for the stabilization and mechanical support of collagen networks within native cartilage. Of note, the formation of lysine-derived, covalent pyridinoline (PYR) cross-links relies on the enzyme LOX, which is hypoxia-response element-directed upregulation during HIF1-transcriptional activation (van Vlimmeren et al., 2010; Gao et al., 2013). The activity of LOX is regulated by proteolytic cleavage of the LOX pro-peptides. Importantly, the activity of LOX is also mainly dependent on the presence of copper (Wang et al., 1996). The LOX family plays central roles in the musculoskeletal system, such as tendon (Danielsen, 1982; Robinson et al., 2005; Marturano et al., 2013), ligaments (Makris et al., 2014), and cartilage (Iftikhar et al., 2011; Makris et al., 2014).

Of note, copper, an important co-factor of various chaperones and enzymes, is vital for maintenance of integrity and homeostasis of cartilage tissues. However, until now, the underlying detailed mechanisms remain elusive. In the current review, we summarized the advances of LOXs family in cartilage homeostasis and regeneration, including embryogenesis, and potential involvement during pathophysiology of arthritis, as well as copper-mediated activation of LOXs and hypoxia-responsive signaling axis during recent decades, the main molecular modulation signaling network controlling LOXs expression, which is promising for potential clinical implications of cartilage regeneration in regenerative medicine and tissue engineering. Also, we propose potential links between the LOXs family and aging-related chronic inflammation and cartilage degeneration. Modulation of certain the LOXs family members may become a promising therapeutic approach for cartilage regeneration.

LYSYL OXIDASES IN CARTILAGE FUNCTIONING

Endochondral ossification is one of the two main forms of skeletal formation during embryogenesis. Mesenchymal chondroprogenitor cells differentiate into chondrocytes through cellular condensation processes, which are then surrounded by an abundant layer of extracellular matrix, including type II, IX, and XI collagens, which is the characteristics of cartilage (Mendler et al., 1989).

Generally, aging-induced cartilage degeneration in arthritis is becoming increasingly prevalent, which is accompanied with the changes in the components of ECM of cartilage (Loeser et al., 2016; Varela-Eirin et al., 2018). The expression of LO and LOXLs has been detected in chondrocytes near the joint cavity undergoing appositional growth, as well as in the epiphyseal plate of femur undergoing endochondral ossification. Strong expression of LO was observed in marrow cavity. And the localization of LOXL was mainly detected in chondrocytes of the reserve, proliferating cartilage, and hypertrophic zones, suggesting their vital functions during cartilage embryogenesis and potential roles for the normal function of adult cartilage (Hayashi et al., 2004; Thomassin et al., 2005). Further studies have indicated the expression of LO, LOXL2, and LOXL4 on chondrocytes of articular cartilage layers (Huang et al., 2010). Also, expression of LOXL2 has been detected in proliferating and hypertrophic chondrocytes of normal growth plate *in vivo* (Iftikhar et al., 2011). The general histologic structure of joint cartilage (mainly including growth plate and articular cartilage) has been presented in **Figure 1**.

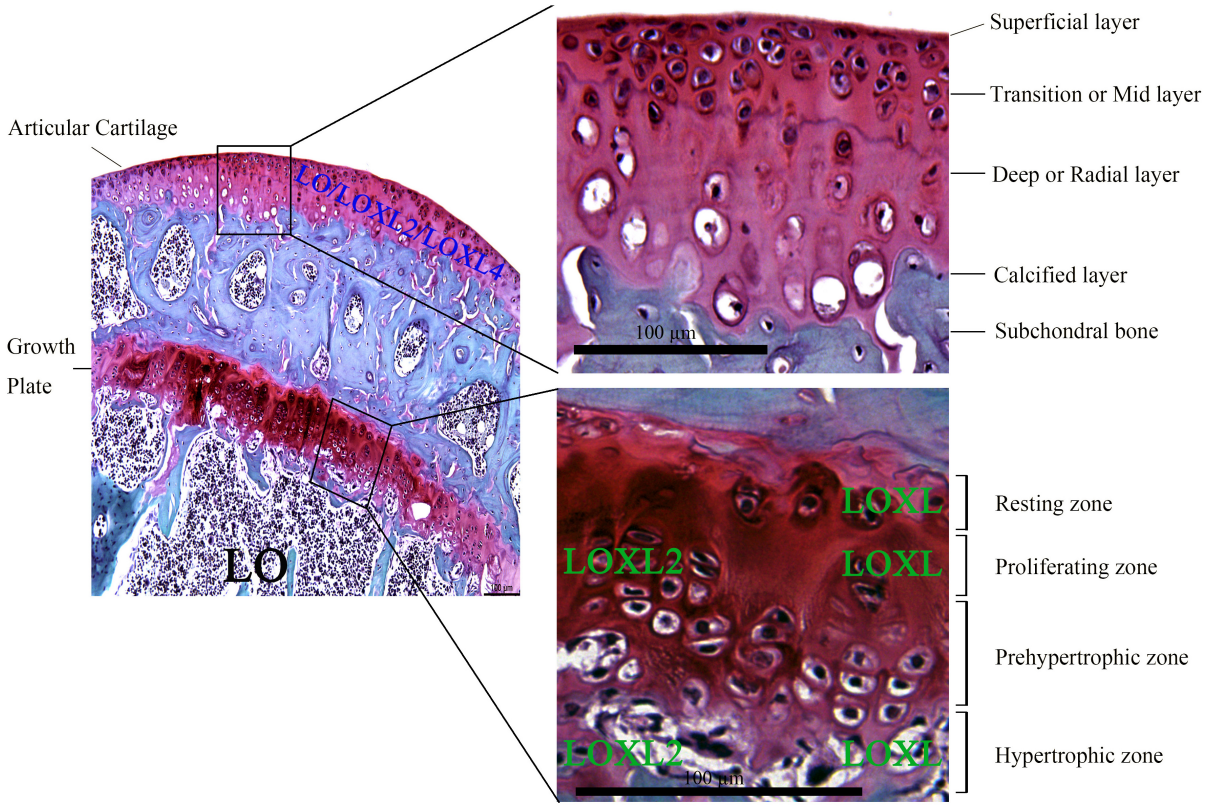

FIGURE 1 | Histology of growth plate and articular cartilage through Safranin O-Fast green staining of the proximal tibia from adult C57BL/6 mice. Mature articular cartilage is mainly comprised of four zones based on histologic features: superficial layer, transition or mid (middle) layer, deep or radial layer, and calcified layer that is lined by subchondral bone. Growth plate is mainly characterized by several morphologically distinct zones, including resting zone, proliferating zone, prehypertrophic zone, and hypertrophic zone. LO is mainly expressed in marrow cavity, while LOXL2 expression is mainly localized in proliferating and hypertrophic zones of growth plate. LOXL was mainly found on chondrocytes of resting, proliferating and hypertrophic zones of growth plate. The expression of LO, LOXL2, and LOXL4 was descended from superficial to deep layers of articular cartilage. Lysyl oxidase: LO; lysyl oxidase like-2: LOXL2; lysyl oxidase like-4: LOXL4; Lysyl oxidase-like enzymes: LOXL. Scale bar: 100 μm.

Notably, the activity of LOX is of pivotal importance for maintaining the tensile and elastic features of connective tissues in the musculoskeletal (Weiner and Traub, 1992; Herchenhan et al., 2015), cardiovascular and pulmonary systems (Ohmura et al., 2012; Nave et al., 2014). In cartilage, LOX is capable of modification of amino acids lysine and hydroxylysine into covalent PYR cross-linking (i.e., heterotypic collagen II/IX/XI) (Eyre et al., 2004), in particular the most abundant type of cross-links in native articular cartilage, which is tightly correlated with the tensile properties of native articular cartilage (Williamson et al., 2003; Eyre et al., 2008). Nevertheless, inactivation of LOXs induced by copper metabolic disorder or gene mutation would lead to dysfunction of connective tissues and collagen-containing organs (Kuivaniemi et al., 1982; Maki et al., 2002). To date, the discovery of crystal structures of copper-containing amine oxidase and lysyl oxidase-like 2 has been reported in the current literature (**Figure 2**) (Duff et al., 2003, 2004; Lunelli et al., 2005; Zhang X. et al., 2018).

To date, the LOX family has been reported essential for cartilage maturation, chondroprotection, and homeostasis maintenance of cartilage. LO and LOXL-3b have been demonstrated crucial for cartilage maturation during zebrafish development, respectively (Reynaud et al., 2008; van Boxtel et al., 2011). Further, studies have indicated the upregulation of LOXL2 in OA cartilage in response to injury, which may be considered as a naturally protective response that promotes anabolism while inhibiting specific catabolic response during OA pathophysiology (Alshenibr et al., 2017; Bais and Goldring, 2017). Likewise, a recent study further confirmed that systemic adenovirus-delivered LOXL2 expression or LOXL2 genetic overexpression both exhibited chondroprotective effects through inhibition of catabolic factors and IL-1β-induced NF-κB signaling in mice (Tashkandi et al., 2019). Also, Matrigel constructs of human chondrocytes from the knee joint and TMJ implanted in nude mice showed enhanced anabolic responses after LOXL2 transduction, including increased expression of sex determining region Y-box containing gene 9 (SOX9), aggrecan (ACAN), and COL2A1, whilst reduced the levels of extracellular matrix (ECM)-degrading enzymes matrix metalloproteinases and inhibited chondrocyte apoptosis (Alshenibr et al., 2017). Therefore, LOX-mediated collagen cross-links are essential for the functional integrity of articular

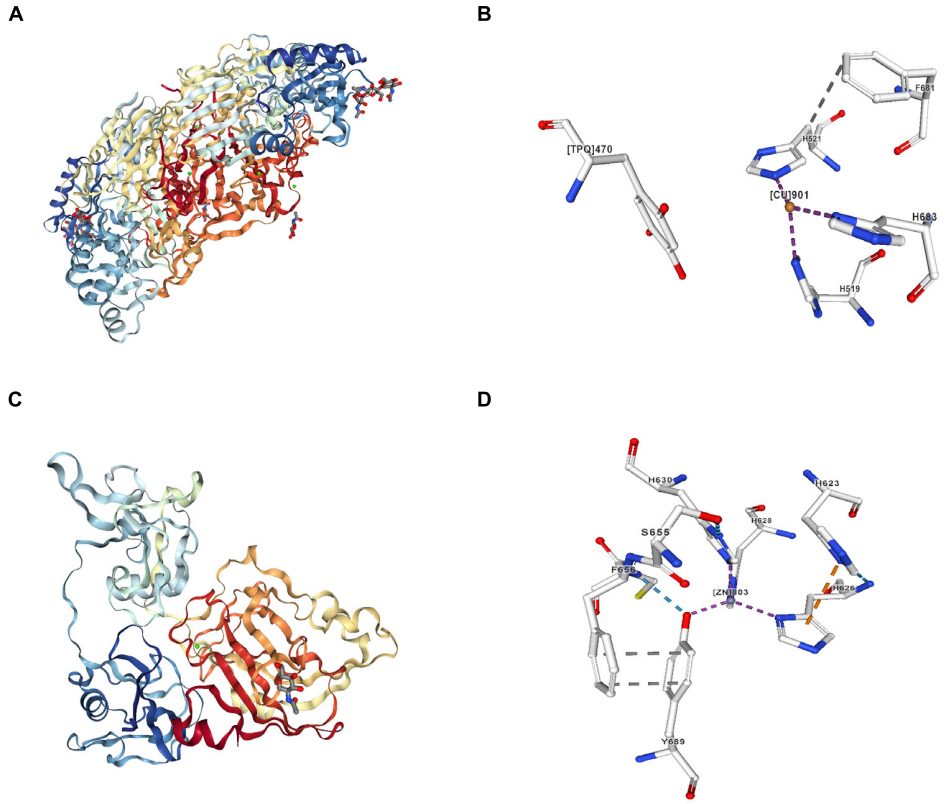

FIGURE 2 | Crystal structures and ligand interactions of copper-containing amine oxidase and human lysyl oxidase-like 2 (http://www.rcsb.org/). **(A)** Copper-containing amine oxidase extracted from bovine serum (BSAO) was crystallized and its three-dimensional structure at 2.37A resolution. The biological unit of BSAO is a homodimer, formed by two monomers related to each other by a non-crystallographic 2-fold axis. Each monomer is composed of three domains. **(B)** Ligand interaction of copper iron [(CU)901] in copper-containing amine oxidase extracted from BSAO. **(C)** Crystal structure of human lysyl oxidase-like 2 (hLOXL2) at 2.4-Å resolution. **(D)** Ligand interaction of zinc iron ([ZN]803:A) in hLOXL2. The copper-binding site of hLOXL2 is occupied by zinc, which blocks lysyl tyrosylquinone (LTQ) generation and the enzymatic activity of hLOXL2. The LTQ precursor residues in the structure are distanced by 16.6 Å, corroborating the notion that the present structure may represent a precursor state and that pronounced conformational rearrangements would be required for protein activation.

cartilage and cartilage homeostasis. Appropriate modulation of the expression or activity of certain LOXs family members selectively may become potential promising strategy for cartilage repair.

The components of extracellular matrix are vital for the maintenance of phenotype and function of chondrocytes (Shi et al., 2017; Li et al., 2018; Zhang et al., 2020). The expression of a novel LOX-related gene, named LOXC, has been detected in cartilage *in vivo*, which modulates the formation of collagenous extracellular matrix (Ito et al., 2001). A series of further studies have confirmed LOX as a key enzyme responsible for the formation of collagen cross-links. Furthermore, hypoxia-induced endogenous LOX expression has been applied in the repair of *de novo* multiple musculoskeletal tissues (i.e., cartilage, meniscus, tendons, and ligaments) as important regenerative strategies, which is mainly mediated through mechanisms of hypoxia-induced enhanced PYR crosslinking and increased tensile properties of collagen-rich tissues (Makris et al., 2014).

Simultaneously, studies have demonstrated that combined treatment of copper sulfate and hydroxylysine would additively or synergistically enhance collagen cross-linking in engineered articular cartilage, improving the tensile and biomechanical properties of the neocartilage (Makris et al., 2013). LOXL2 promotes chondrogenic differentiation through regulation of SOX9 and SNAIL (Iftikhar et al., 2011). Also, LOX activity has been reported vital for phenotypic modulation of chondrocytes (Farjanel et al., 2005). Therefore, modulation of endogenous LOX activity or expression selectively has been demonstrated effective for promotion of tensile properties and cross-linking of cartilage, as well as phenotypic control of chondrocytes, which appears as promising clinically applicable approaches of regenerative medicine and tissue engineering (Makris et al., 2014; Hadidi et al., 2017) (**Table 1**).

Regulation of Hypoxia-Inducible Factor-1 in Chondrogenesis and Cartilage Homeostasis

The physiological oxygen tension between 2%∼9% in healthy individuals, which is termed as 'physiologic normoxia' (Simon and Keith, 2008). Generally, hypoxia-inducible factor 1 (HIF-1) is expressed in a variety of organs and tissues in

TABLE 1 | Therapeutic approaches for enhanced cartilage regeneration through LOXs modulation.

Authors	Source/Species	Detailed Treatments	Experimental Model	Therapeutic Outcomes	Mechanisms
Makris et al., 2014	Calves	Continuous hypoxia conditioning or exogenous LOXL2 administration	Trochlea groove cartilage and knee meniscus explants	Enhanced neocartilage formation and functional properties	Increased collagen cross-linking
Tashkandi et al., 2019	Mice	Intra-articular injection with MIA (monosodium iodoacetate) or intraperitoneal injection of adenovirus vector (Adv)-RFP-LOXL2	MIA-induced OA in LOXL2-overexpressing transgenic mice or Cho/+ mice injected with Adv-RFP-LOXL2	Systemic LOXL2 adenovirus or LOXL2 genetic overexpression in mice protected against OA	Inhibition of IL-1β-induced phospho-NF-κB/p65 and MMP13 expression; upregulation of anabolic genes
Makris et al., 2013	Juvenile bovine knee joints	0.0016 mg/ml copper sulfate and 0.146% mg/ml hydroxylysine either or in combination	Chondrocytes-self-assembly-tissue culture constructs	Synergistic tensile properties in combination of copper sulfate and hydroxylysine-treated group	Enhanced PYR cross-links
Hadidi et al., 2017	Bovine hind limbs taken from skeletally immature calves	Exogenous LOXL2 administration along with copper and free hydroxylysine	Culture constructs: primary articular chondrocytes and meniscus cells seeded in non-adherent agarose wells	Enhanced tensile properties of and near-native tissue values in terms of glycosaminoglycan content in LOXL2-treated constructs	Increased collagen and PYR cross-links
Lin R. et al., 2019	New Zealand white rabbits	Copper-incorporated bioactive glass-ceramics (Cu-BGC)	Model of osteochondral defects with a diameter of 5 mm	Facilitated the regeneration of cartilage and osteochondral interface significantly by Cu-BGC treatment	Activation of HIF-1 signaling and inhibition of inflammatory response via inducing an anti-inflammatory M2 phenotype in macrophage
Alshenibr et al., 2017	Human	*In vivo* implantation of human articular and temporomandibular joints (TMJ) chondrocytes in nude mice; expression detection in human tissue sections	Human knee and hip joints and TMJ	Upregulated expression of LOXL2 in OA cartilage	A protective response that promotes anabolism while inhibition of specific catabolic responses (promoted specific chondrogenesis in implants lacked fibrosis and mineralization)
Iftikhar et al., 2011	Not available	Induction of chondrogenic differentiation	ATDC5 cell line	Expression of LOXL2 in ATDC5 chondrogenic cells and LOXL2 promoted ATDC5 chondrogenic differentiation	Through regulation of SOX9 and SNAIL

healthy mammalians under physiologic normoxic conditions, including brain, kidney, liver, heart, and cartilage (Stroka et al., 2001; Coimbra et al., 2004). Articular cartilage is residing in a hypoxic microenvironment of avascular hypoxic zone *in vivo* under normal physiological conditions, ranging from 7∼10% oxygen tensions in the superficial zone, and 1% oxygen in the deep zones (Ferrell and Najafipour, 1992). Hypoxia-inducible factor 1α (HIF-1α) have been demonstrated essential for cartilage maturation (Duval et al., 2009; Stegen et al., 2019). Also, local activation of HIF-1α is necessary for survival and homeostatic function of chondrocytes, as well as normal joint development (Aro et al., 2012; Long, 2019). Thus, hypoxia and HIF-1 have been exploited to modulate chondrocyte phenotype and represent an efficient approach to improve cell properties before implantation for cartilage repair.

Notably, HIF-1 is of pivotal significance for survival and growth arrest of chondrocytes during cartilage development, as well as cartilage homeostasis of osteoarthritic cartilage (Pfander et al., 2006; Gelse et al., 2008). HIF-1 is conducive to the maintenance of chondrogenic specific markers (SOX9, type II collagen, and aggrecan) and inhibition of cartilage hypertrophy (Duval et al., 2012). HIF-1 has been demonstrated as a positive regulator of SOX9 activity, which is required for chondrogenesis and synthesis of cartilage ECM (Robins et al., 2005; Zhang et al., 2011). Nevertheless, dysregulation of HIF-1α signaling axis would lead to skeletal dysplasia by interfering with cellular bioenergetics and biosynthesis

(Stegen et al., 2019). A recent study has indicated the increased expression of genes involved in matrix degradation, hypoxia-responsive, and inflammatory signaling in damaged cartilages comparing with healthy counterparts through whole genome microarray analysis, suggesting potential involvement of HIF-1α during the progression of OA pathophysiology (Yudoh et al., 2005; Aşık et al., 2019), which may be a natural protection response of the body since previous studies have demonstrated chondroprotection efficacy through activation of HIF-1 signaling axis (Gelse et al., 2008; Maes et al., 2012; Lin R. et al., 2019). Further comprehensive studies elucidating detailed roles of HIF-1α in certain stages of OA pathogenic progression, as well as detailed mechanisms on hypoxia-induced LOXs expression and activity, require further elucidation. Therefore, appropriate modulation of transcriptional activity of HIF-1α may become a potential feasible therapeutic approach for cartilage regeneration.

Chondroprotective Effects of Copper in Cartilage

Copper, an essential redox-active trace element, which is essential for most aerobic organisms (Tapiero et al., 2003; Solomon et al., 2014). Simultaneously, copper functions as a co-factor of various proteins and enzymes, including cytochrome C, superoxide dismutase, tyrosinase, ascorbate oxidase, lysyl oxidase, and amine oxidase, exhibiting diverse fundamental cellular functions in normal physiology, including energy generation, iron acquisition, oxygen transportation, cellular metabolism, peptide hormone maturation, blood clotting, neurotransmitter biosynthesis, and intracellular signal transduction (Huffman and O'Halloran, 2001; Hamza and Gitlin, 2002; Kim et al., 2008; Turski et al., 2012; Grubman and White, 2014; Wang et al., 2018; Miller et al., 2019). Generally, copper is able to exist in two oxidation states in the body of mammalians: Cu^{+} and Cu^{2+} (Lin and Kosman, 1990; Pushie et al., 2007; Solomon et al., 2014). The trafficking of copper into specific intracellular targets is delivered by metallochaperones (Hamza et al., 2001; Puig and Thiele, 2002; Chen G. F. et al., 2015). And there is no free copper in the cytoplasm under normal physiological conditions (Rae et al., 1999).

In general, moderate copper levels are essential for normal growth, development, health, such as the normal functioning of innate immune system (Djoko et al., 2015; Bost et al., 2016), and bone health (Eaton-Evans et al., 1996; Qu et al., 2018). Of note, copper is also vital for maintenance of integrity and homeostasis of cartilage tissues. Copper metabolic disorder correlates closely with ischemic cardiovascular diseases (Jiang et al., 2007; Kim et al., 2010), embryonic and neonatal abnormalities, and anemia (Cartwright and Wintrobe, 1964; Jensen et al., 2019), as well as the onset of osteoarthritis (Scudder et al., 1978; Yazar et al., 2005).

Supplementation of dietary copper has been reported to reduce the severity of osteochondrosis and other developmental cartilage lesions, which may result from enhanced collagen cross-linking and increased collagen II synthesis (Knight et al., 1990; Hurtig et al., 1993; Yuan et al., 2011). The chondroprotection efficacy of copper may be attributable to the anti-catabolic effects of Cu^{2+}, which abrogates the degradation of cartilage matrix proteoglycan via inhibition of nitric oxide release (Pasqualicchio et al., 1996). A recent study has reported that copper-incorporated bioactive glass-ceramics facilitated the regeneration of cartilage and osteochondral interface effectively, which was mediated in part through activated HIF-1 signaling and inhibited inflammatory response, representing a feasible approach for treating osteoarthritis associated with osteochondral defects (Lin R. et al., 2019). However, until now, the detailed mechanisms of interactions between copper and chondrocytes, as well as copper trafficking within chondrocytes remain elusive. To date, copper has been identified as a cofactor of several identified major cartilage formation-associated enzymes (Rucker et al., 1998; Heraud et al., 2002; Makris et al., 2013), however, cellular and molecular mechanisms underlying intracellular copper transportation in chondrocytes are not yet clearly understood. A cartilage matrix glycoprotein, a membrane-associated protein synthesized by chondrocytes, has been demonstrated to bind copper and exert some oxidase activity similar with ceruloplasmin, which may function as an important copper transporter in chondrocytes and a potential chondrogenic marker (Fife et al., 1986, 1993; Harris, 2000; Ranganathan et al., 2011; La Mendola et al., 2012; Ishihara et al., 2014; Linder, 2016; Magri et al., 2018). The proposed cellular model of copper intracellular transportation has been presented in **Figure 3** according to current literature (Okado-Matsumoto and Fridovich, 2001; Carr et al., 2005; Horng et al., 2005; Turski and Thiele, 2009; Ohrvik and Thiele, 2014; Urso and Maffia, 2015; Miller et al., 2019; Shi et al., 2019), illustrating the routes of copper trafficking and how it functions within chondrocytes and during ECM remodeling.

Further, emerging evidence has indicated that copper stabilizes the HIF-1α protein through inhibiting prolyl hydroxylases-mediated prolyl hydroxylation in an iron-independent manner, which is required for transcriptional activation of HIF-1 of a series of target genes (Martin et al., 2005; Feng et al., 2009; Himoto et al., 2016; Liu et al., 2018; Chen et al., 2020), suggesting that appropriate copper levels may be required for normal cartilage function through regulation of HIF-1α transcriptional activity. However, detailed mechanisms of transcriptional processes initiating specific target genes expression of HIF-1 require further elucidation. Therefore, copper may modulate cartilage homeostasis through regulation of activity of HIF-1 transcription and chondrogenic-associated proteins and markers, such as LOXL2, and SOX9 (Robins et al., 2005; Amarilio et al., 2007; Schietke et al., 2010), as well as VEGF, which is essential for chondrocyte survival (Cramer et al., 2004; Maes et al., 2004, 2012) (**Figure 4**). Also, further extensive studies on regulation of HIF-1 expression (such as heat shock protein 90, HSP90), and specific targeting of certain transcriptional activation of certain HIF-1 target genes (Minet et al., 1999; Isaacs et al., 2002; Katschinski et al., 2004), as well as regulation of systemic copper metabolism are promising

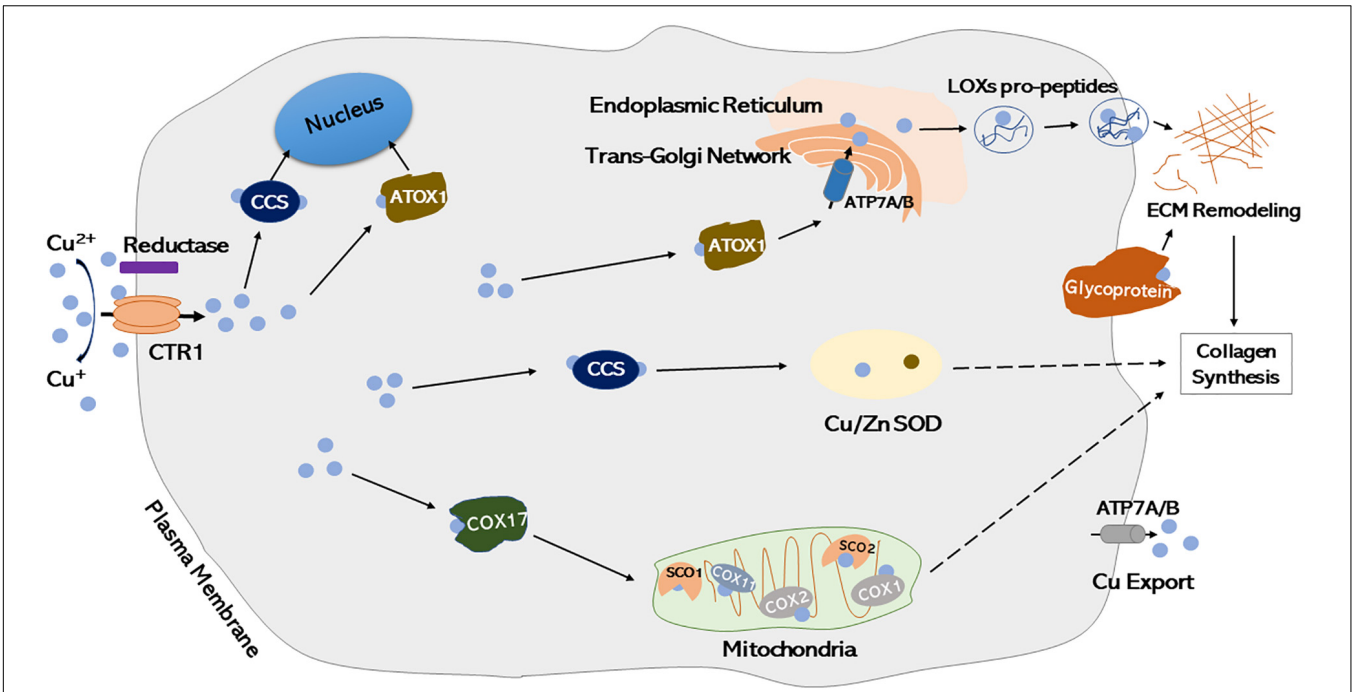

FIGURE 3 | Proposed cellular models of intracellular copper trafficking in chondrocytes. Cu^{2+} is transformed to Cu^{+} by a putative metalloreductase, which then enters the cell through plasma membrane importer CTR1. Once inside the cell, copper is handed off to copper chaperones. CCS incorporated copper into the cytosolic protein Cu/Zn-SOD. ATOX1 delivers copper into secretory compartments of Golgi and Endoplasmic Reticulum through ATP7A/B. Copper can be incorporated into copper-dependent proteins, such as LOXs pro-peptides (secreted forms of LOXs), which is involved in ECM remodeling. Once inside the intermembrane space of mitochondria, copper is handed off to COX17 and then passed onto either SCO1, which then transfers copper to COX2 subunit of cytochrome oxidase, or COX11, which transfers copper to COX1 subunit of cytochrome oxidase. Copper exporter ATP7A/B exports copper out of the cell by translocating to plasma membrane when intracellular copper concentrations are high. Glycoprotein interacts with copper and regulates ECM remodeling. Cu, Copper; Copper-transporter 1, CTR1 (a major copper importer); CCS, Copper chaperone for superoxide dismutase; Cu/Zn-SOD, copper/zinc-superoxide dismutase; ATOX1, a copper chaperone, also known as HAH1; LOXs, lysyl oxidases; COX, cytochrome oxidase; SCO, synthesis of cytochrome c oxidase; ATP, copper transporting P-type ATPases [systemic copper absorption (ATP7A) and copper excretion (ATP7B)]; ECM, extracellular matrix.

for potential therapeutic optimization (Isaacs et al., 2002; Kim et al., 2010).

Potential Links Between LOX and Aging-Associated Cartilage Degeneration

Aging, which is characterized by a chronic and low-grade inflammation, also termed as age-associated inflammation, which has been referred to as 'inflamm-aging' (Franceschi and Campisi, 2014; Huang et al., 2019; Josephson et al., 2019), is also a risk factor of osteoarthritis (Greene and Loeser, 2015). Inflammation is a normal process in healthy individuals. Acute inflammation initiates the regenerative response (Kyritsis et al., 2012). Whilst chronic inflammation is likely to cause various diseases (Akhurst et al., 2005; Liu et al., 2019). The signaling pathways that are implicated in chronic inflammation include NF-κB (Roman-Blas and Jimenez, 2008; Bamborough et al., 2010), signal transducer and activator of transcription (STAT) (He and Karin, 2011), mitogen-activated protein kinases (MAPKS) (Thalhamer et al., 2008). Interestingly, a recent study reported that LOXL3-mediated deacetylation/deacetylimination abolished the transcription activity of STAT3, thereby inhibiting differentiation of naïve $CD4^{+}$ T cells toward Th17/Treg cells (regulatory T cells) during inflammatory responses (Ma et al., 2017).

Aging-associated destruction of joints and cartilage degradation in osteoarthritis is correlated with changes in extracellular matrix of articular cartilage, such as cartilage ECM stiffness, and in the levels and solubility profiles of matrix crosslinks, especially pentosidine, as well as reduced thickness of cartilage, proteolysis, advanced glycation and calcification (Eyre et al., 1988; Pokharna et al., 1995; Lotz and Loeser, 2012). Notably, rejuvenation has emerged as a promising therapeutic regenerative approach for improvement or restoration of the self-repair capacity of injured or aging tissue and organ systems (Leung et al., 2006; Nelson et al., 2008; Luria and Chu, 2014; Sarkar et al., 2020), which has been proposed as a conversion into an embryonic-like state recapitulating many events during embryogenesis, including the reactivation of embryonic signature genes, and cytoskeletal/ECM components, and lineage specification (Vortkamp et al., 1998; Jankowski et al., 2009; Luo et al., 2009; Adam et al., 2015; Caldwell and Wang, 2015; Hu et al., 2017; Ransom et al., 2018; Feng et al., 2019; Lin W. et al., 2019; Miao et al., 2019). Consistently, the process of cartilage repair has been considered as recapitulation of various events during developmental morphogenesis. Chondrocytes in

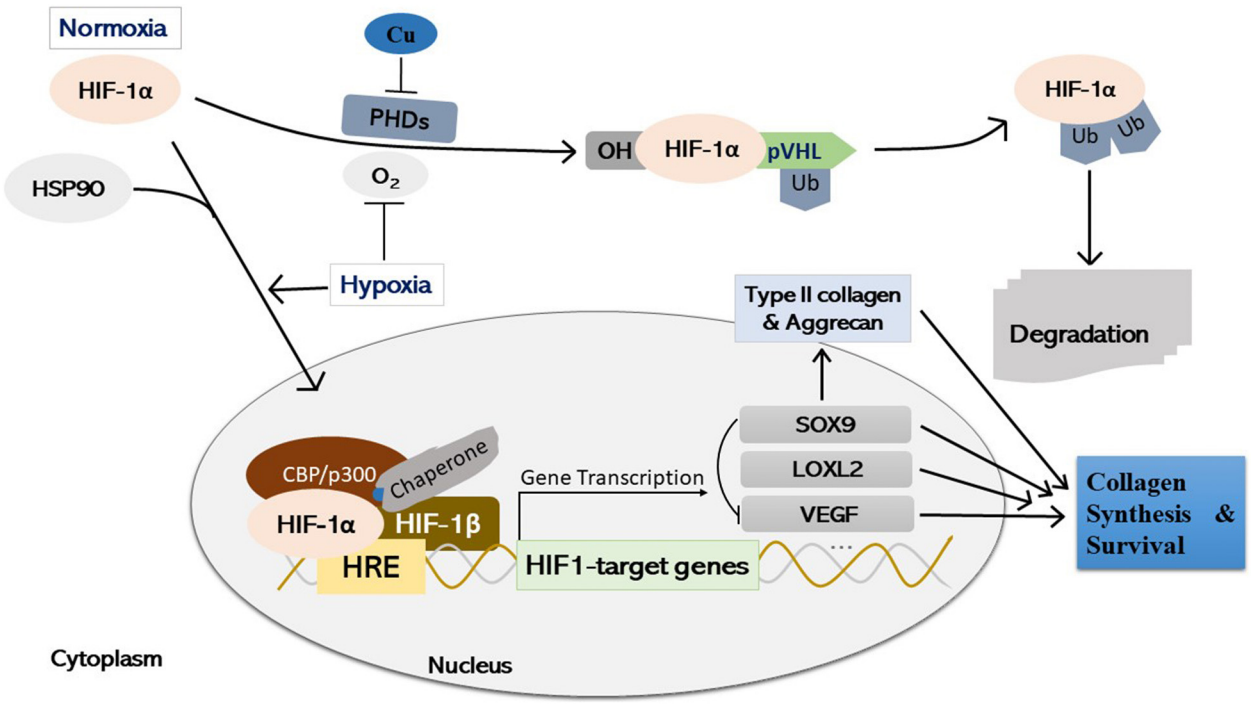

FIGURE 4 | Schematic illustration of copper-mediated hypoxia-response element (HRE)-directed transcriptional fine-tuning of cartilage homeostasis-associated genes in chondrocytes. Under normoxia, HIF-1α undergoes PHDs-mediated prolyl hydroxylation, and prolyl OH HIF-1α is ligated by pVHL, an E3 ubiquitin ligase, and degraded by the proteasome finally. Copper stabilizes HIF-1α protein by inhibiting PHDs activity in an iron-independent manner. Under hypoxia or through interaction with HSP90, HIF-1α stabilizes and accumulates in the cell nucleus, where it forms a dimer with the HIF-1β subunit and a putative unidentified copper-chaperone. The dimer then forms a transcriptional complex with coactivator CBP/p300 through binding with HRE, regulating the expression of various downstream target genes, such as LOXL2, SOX9, and VEGF. Simultaneously, SOX9 is a negative regulator of VEGF, whilst the expression of SOX9 target genes (i.e., Type II collagen, and Aggrecan) is initiated, which is essential for cartilage synthesis and survival during both embryonic joint development and cartilage homeostasis. HIF-1α, hypoxia-inducible factor-1α; PHDs, prolyl hydroxylases; OH: enzymatic hydroxylation; pVHL, von Hippel-Lindau tumor suppressor protein; HRE, hypoxia-response element; Ub, ubiquitinated; SOX9, SRY (sex determining region Y)-box 9; HSP90, heat shock protein 90; LOXL2, lysyl oxidase-like 2; VEGF, vascular endothelial growth factor; Cu, copper.

osteoarthritic articular cartilage usually undergoes a gradual dissolution of anisotropic organization along with re-expression of phenotypic biomarkers of immature cartilage, so tissue maturation is a potential approach for restoration of normal structure and function (Caterson et al., 1990; Khan et al., 2008; Hunziker, 2009; Jiang et al., 2015; Zhang et al., 2017).

Interestingly, copper is also involved in inflammatory responses, including both innate and adaptive immunity (Percival, 1998; Failla, 2003). Increasing evidence has indicated the potential link between copper metabolic disorder and aging-related diseases, such as aging-induced cartilage degradation and dysfunction (Yazar et al., 2005; Lotz and Loeser, 2012; Tao et al., 2019). And previous studies have demonstrated the vital roles of LOX in normal chondrocyte function (Sanada et al., 1978; Ahsan et al., 1999), which may be correlated with the pathogenesis of aging-associated osteoarthritis (Pokharna et al., 1995). Moreover, LOXL1 is expressed in major organs in late fetal and neonatal mice, but it generally diminishes in aging animals, which may be associated with aortic fragility resulting from abnormal remodeling of collagen and elastic fibers (Hayashi et al., 2004; Behmoaras et al., 2008). The decreased expression of LOXs may attribute to reduction of HIF-1 activity in aging organisms (Rivard et al., 2000; Ceradini et al., 2004). Meanwhile, LOXL2 has recently been demonstrated as a potential chondroprotective factor in aging related joint osteoarthritis, mainly through inducing anabolic gene expression and attenuating catabolic genes (Bais and Goldring, 2017; Tashkandi et al., 2019). Thus, restoration of collagen and elastic fiber synthesis in juvenile ECM components though regulation of signaling pathways governing LOX expression may become a promising therapeutic approach for amelioration of aging-associated cartilage degeneration and enhanced cartilage regeneration.

Meanwhile, changes in cell-ECM interactions are important features of aging phenomenon (Sun et al., 2011). During the progression of aging-associated degeneration diseases, altered cell fate of adult stem cells, or dysfunction of terminally differentiated mature cells occurs, which may result from the changed ECM niche modified with aging-related proteins and reduced expression of ECM-synthesis-associated proteins (Goupille et al., 1998; Chan et al., 2006; Sakai et al., 2012; Wang et al., 2015; Jeon et al., 2017; Zhang Y. et al., 2018; Patil et al., 2019), which may be correlated with the LOX family members. Therefore, reverting aging-associated genes in ECM may become an important strategy for joint rejuvenation (Chan et al., 2006;

Fuoco et al., 2014; Li et al., 2014; Sun et al., 2011; Wang et al., 2019; Zhou J. et al., 2019). Modulation of expression of LOXs family members through transcriptional regulation of HIF-1 may become promising therapeutic approaches for treating aging-induced cartilage degeneration as potential rejuvenating therapies.

CONCLUDING REMARKS

In summary, LOXs play pivotal roles in maintenance of cartilage function and chondrogenesis. Therapeutic modulation of LOX activity and expression selectively targeting copper-mediated hypoxia-responsive signaling pathways is promising for cartilage repair and OA attenuation. Meanwhile, further extensive basic and preclinical research is warranted for potential translational application of the LOX family in tissue-engineered neocartilage in tissue engineering and regenerative medicine in the future. Specific and moderate manipulation of activities of LOXs and transcriptional regulation of hypoxia-responsive transcription factors through copper bioavailability modulation or continuous hypoxia-conditioning may become effective interventions for enhanced cartilage regeneration, as well as promising rejuvenation therapeutics, which may exert further therapeutic implications in the upcoming clinical arena.

AUTHOR CONTRIBUTIONS

WL and LX made literature review and contributed equally. GL conceptualized the study and critically revised the manuscript. All authors read and approved the final manuscript.

FUNDING

This work was partially supported by grants from the National Natural Science Foundation of China (81772322), Hong Kong Government Research Grant Council, General Research Fund (14120118, 14160917, 9054014 N_CityU102/15, C7030-18G, and T13-402/17-N), Hong Kong Innovation Technology Commission Funds (PRP/050/19FX and ITS/448/18), and the Science and Technology Foundation of Guangdong Province (2017A050506046). This study also received support from the SMART program, Lui Che Woo Institute of Innovative Medicine, The Chinese University of Hong Kong.

REFERENCES

Adam, R. C., Yang, H., Rockowitz, S., Larsen, S. B., Nikolova, M., Oristian, D. S., et al. (2015). Pioneer factors govern super-enhancer dynamics in stem cell plasticity and lineage choice. *Nature* 521, 366–370. doi: 10.1038/nature14289

Ahsan, T., Lottman, L. M., Harwood, F., Amiel, D., and Sah, R. L. (1999). Integrative cartilage repair: inhibition by β-aminopropionitrile. *J. Orthop. Res.* 17, 850–857. doi: 10.1002/jor.1100170610

Akhurst, B., Matthews, V., Husk, K., Smyth, M. J., Abraham, L. J., and Yeoh, G. C. (2005). Differential lymphotoxin-β and interferon gamma signaling during mouse liver regeneration induced by chronic and acute injury. *Hepatology* 41, 327–335. doi: 10.1002/hep.20520

Alshenibr, W., Tashkandi, M. M., Alsaqer, S. F., Alkheriji, Y., Wise, A., Fulzele, S., et al. (2017). Anabolic role of lysyl oxidase like-2 in cartilage of knee and temporomandibular joints with osteoarthritis. *Arthritis Res. Ther.* 19:179. doi: 10.1186/s13075-017-1388-8

Amarilio, R., Viukov, S. V., Sharir, A., Eshkar-Oren, I., Johnson, R. S., and Zelzer, E. (2007). HIF1α regulation of *Sox9* is necessary to maintain differentiation of hypoxic prechondrogenic cells during early skeletogenesis. *Development* 134, 3917–3928. doi: 10.1242/dev.008441

Aro, E., Khatri, R., Gerard-O'Riley, R., Mangiavini, L., Myllyharju, J., and Schipani, E. (2012). Hypoxia-inducible factor-1 (HIF-1) but not HIF-2 is essential for hypoxic induction of collagen prolyl 4-hydroxylases in primary newborn mouse epiphyseal growth plate chondrocytes. *J. Biol. Chem.* 287, 37134–37144. doi: 10.1074/jbc.M112.352872

Aşık, M. D., Gürsoy, S., Akkaya, M., Kozacı, L. D., Doğan, M., and Bozkurt, M. (2019). Microarray analysis of cartilage: comparison between damaged and non-weight-bearing healthy cartilage. *Connect. Tissue Res.* doi: 10.1080/03008207.2019.1611797 [Epub ahead of print].

Aspden, R. M. (2011). Obesity punches above its weight in osteoarthritis. *Nat. Rev. Rheumatol.* 7, 65–68. doi: 10.1038/nrrheum.2010.123

Bais, M. V., and Goldring, M. B. (2017). LOXL2 as a protective in osteoarthritis cartilage. *Aging* 9, 2024–2025. doi: 10.18632/aging.101317

Bamborough, P., Morse, M. A., and Ray, K. P. (2010). Targeting IKKbeta for the treatment of rheumatoid arthritis. *Drug News Perspect.* 23, 483–490. doi: 10.1358/dnp.2010.23.8.1447844

Behmoaras, J., Slove, S., Seve, S., Vranckx, R., Sommer, P., and Jacob, M. P. (2008). Differential expression of lysyl oxidases LOXL1 and LOX during growth and aging suggests specific roles in elastin and collagen fiber remodeling in rat aorta. *Rejuvenation Res.* 11, 883–889. doi: 10.1089/rej.2008.0760

Bignon, M., Pichol-Thievend, C., Hardouin, J., Malbouyres, M., Brechot, N., Nasciutti, L., et al. (2011). Lysyl oxidase-like protein-2 regulates sprouting angiogenesis and type IV collagen assembly in the endothelial basement membrane. *Blood* 118, 3979–3989. doi: 10.1182/blood-2010-10-313296

Bost, M., Houdart, S., Oberli, M., Kalonji, E., Huneau, J. F., and Margaritis, I. (2016). Dietary copper and human health: current evidence and unresolved issues. *J. Trace Elem. Med. Biol.* 35, 107–115. doi: 10.1016/j.jtemb.2016.02.006

Busnadiego, O., Gonzalez-Santamaria, J., Lagares, D., Guinea-Viniegra, J., Pichol-Thievend, C., Muller, L., et al. (2013). LOXL4 is induced by transforming growth factor β1 through Smad and JunB/Fra2 and contributes to vascular matrix remodeling. *Mol. Cell. Biol.* 33, 2388–2401. doi: 10.1128/MCB.00036-13

Caldwell, K. L., and Wang, J. (2015). Cell-based articular cartilage repair: the link between development and regeneration. *Osteoarthritis Cartilage* 23, 351–362. doi: 10.1016/j.joca.2014.11.004

Carr, H. S., Maxfield, A. B., Horng, Y. C., and Winge, D. R. (2005). Functional analysis of the domains in Cox11. *J. Biol. Chem.* 280, 22664–22669. doi: 10.1074/jbc.M414077200

Cartwright, G. E., and Wintrobe, M. M. (1964). The question of copper deficiency in man. *Am. J. Clin. Nutr.* 15, 94–110. doi: 10.1093/ajcn/15.2.94

Caterson, B., Mahmoodian, F., Sorrell, J. M., Hardingham, T. E., Bayliss, M. T., Carney, S. L., et al. (1990). Modulation of native chondroitin sulphate structure in tissue development and in disease. *J. Cell Sci.* 97(Pt 3), 411–417.

Ceradini, D. J., Kulkarni, A. R., Callaghan, M. J., Tepper, O. M., Bastidas, N., Kleinman, M. E., et al. (2004). Progenitor cell trafficking is regulated by hypoxic gradients through HIF-1 induction of SDF-1. *Nat. Med.* 10, 858–864. doi: 10.1038/nm1075

Chan, D., Song, Y., Sham, P., and Cheung, K. M. (2006). Genetics of disc degeneration. *Eur. Spine J.* 15(Suppl. 3), S317–S325. doi: 10.1007/s00586-006-0171-3

Chen, G. F., Sudhahar, V., Youn, S. W., Das, A., Cho, J., Kamiya, T., et al. (2015). Copper transport protein antioxidant-1 promotes inflammatory neovascularization via chaperone and transcription factor function. *Sci. Rep.* 5:14780. doi: 10.1038/srep14780

Chen, X., Hu, J. G., Huang, Y. Z., Li, S., Li, S. F., Wang, M., et al. (2020). Copper promotes the migration of bone marrow mesenchymal stem cells via Rnd3-dependent cytoskeleton remodeling. *J. Cell. Physiol.* 235, 221–231. doi: 10.1002/jcp.28961

Chen, Y., Sun, Y., Pan, X., Ho, K., and Li, G. (2015). Joint distraction attenuates osteoarthritis by reducing secondary inflammation, cartilage degeneration and subchondral bone aberrant change. *Osteoarthritis Cartilage* 23, 1728–1735. doi: 10.1016/j.joca.2015.05.018

Chen, Y., Zhang, D., Ho, K. W., Lin, S., Suen, W. C., Zhang, H., et al. (2018). GPR120 is an important inflammatory regulator in the development of osteoarthritis. *Arthritis Res. Ther.* 20:163. doi: 10.1186/s13075-018-1660-6

Coimbra, I. B., Jimenez, S. A., Hawkins, D. F., Piera-Velazquez, S., and Stokes, D. G. (2004). Hypoxia inducible factor-1 α expression in human normal and osteoarthritic chondrocytes. *Osteoarthritis Cartilage* 12, 336–345. doi: 10.1016/j.joca.2003.12.005

Cox, T. R., Bird, D., Baker, A. M., Barker, H. E., Ho, M. W., Lang, G., et al. (2013). LOX-mediated collagen crosslinking is responsible for fibrosis-enhanced metastasis. *Cancer Res.* 73, 1721–1732. doi: 10.1158/0008-5472.CAN-12-2233

Cox, T. R., Rumney, R. M. H., Schoof, E. M., Perryman, L., Hoye, A. M., Agrawal, A., et al. (2015). The hypoxic cancer secretome induces pre-metastatic bone lesions through lysyl oxidase. *Nature* 522, 106–110. doi: 10.1038/nature14492

Cramer, T., Schipani, E., Johnson, R. S., Swoboda, B., and Pfander, D. (2004). Expression of VEGF isoforms by epiphyseal chondrocytes during low-oxygen tension is HIF-1 α dependent. *Osteoarthritis Cartilage* 12, 433–439. doi: 10.1016/j.joca.2004.02.003

Danielsen, C. C. (1982). Mechanical properties of reconstituted collagen fibrils. Influence of a glycosaminoglycan: dermatan sulfate. *Connect. Tissue Res.* 9, 219–225. doi: 10.3109/03008208209160265

Deng, Z., Gao, X., Sun, X., Amra, S., Lu, A., Cui, Y., et al. (2019). Characterization of articular cartilage homeostasis and the mechanism of superior cartilage regeneration of MRL/MpJ mice. *FASEB J.* 33, 8809–8821. doi: 10.1096/fj.201802132RR

Djoko, K. Y., Ong, C. L., Walker, M. J., and McEwan, A. G. (2015). The role of copper and zinc toxicity in innate immune defense against bacterial pathogens. *J. Biol. Chem.* 290, 18954–18961. doi: 10.1074/jbc.R115.647099

Duff, A. P., Cohen, A. E., Ellis, P. J., Kuchar, J. A., Langley, D. B., Shepard, E. M., et al. (2003). The crystal structure of *Pichia pastoris* lysyl oxidase. *Biochemistry* 42, 15148–15157. doi: 10.1021/bi035338v

Duff, A. P., Trambaiolo, D. M., Cohen, A. E., Ellis, P. J., Juda, G. A., Shepard, E. M., et al. (2004). Using xenon as a probe for dioxygen-binding sites in copper amine oxidases. *J. Mol. Biol.* 344, 599–607. doi: 10.1016/j.jmb.2004.09.075

Duval, E., Bauge, C., Andriamanalijaona, R., Benateau, H., Leclercq, S., Dutoit, S., et al. (2012). Molecular mechanism of hypoxia-induced chondrogenesis and its application in *in vivo* cartilage tissue engineering. *Biomaterials* 33, 6042–6051. doi: 10.1016/j.biomaterials.2012.04.061

Duval, E., Leclercq, S., Elissalde, J. M., Demoor, M., Galera, P., and Boumediene, K. (2009). Hypoxia-inducible factor 1α inhibits the fibroblast-like markers type I and type III collagen during hypoxia-induced chondrocyte redifferentiation: hypoxia not only induces type II collagen and aggrecan, but it also inhibits type I and type III collagen in the hypoxia-inducible factor 1α-dependent redifferentiation of chondrocytes. *Arthritis Rheum.* 60, 3038–3048. doi: 10.1002/art.24851

Eaton-Evans, J., Mcllrath, E., Jackson, W., McCartney, H., and Strain, J. J. (1996). Copper supplementation and the maintenance of bone mineral density in middle-aged women. *J. Trace Elem. Exp. Med.* 9, 87–94. doi: 10.1002/(sici)1520-670x(1996)9:3<87::aid-jtra1>3.0.co;2-e

Eyre, D. R., Dickson, I. R., and Van Ness, K. (1988). Collagen cross-linking in human bone and articular cartilage. Age-related changes in the content of mature hydroxypyridinium residues. *Biochem. J.* 252, 495–500. doi: 10.1042/bj2520495

Eyre, D. R., Pietka, T., Weis, M. A., and Wu, J. J. (2004). Covalent cross-linking of the NC1 domain of collagen type IX to collagen type II in cartilage. *J. Biol. Chem.* 279, 2568–2574. doi: 10.1074/jbc.M311653200

Eyre, D. R., Weis, M. A., and Wu, J. J. (2008). Advances in collagen cross-link analysis. *Methods* 45, 65–74. doi: 10.1016/j.ymeth.2008.01.002

Failla, M. L. (2003). Trace elements and host defense: recent advances and continuing challenges. *J. Nutr.* 133(5 Suppl. 1), 1443S–1447S. doi: 10.1093/jn/133.5.1443S

Farjanel, J., Seve, S., Borel, A., Sommer, P., and Hulmes, D. J. (2005). Inhibition of lysyl oxidase activity can delay phenotypic modulation of chondrocytes in two-dimensional culture. *Osteoarthritis Cartilage* 13, 120–128. doi: 10.1016/j.joca.2004.06.015

Feng, C., Chan, W. C. W., Lam, Y., Wang, X., Chen, P., Niu, B., et al. (2019). *Lgr5* and *Col22a1* mark progenitor cells in the lineage toward juvenile Articular chondrocytes. *Stem Cell Rep.* 13, 713–729. doi: 10.1016/j.stemcr.2019.08.006

Feng, W., Ye, F., Xue, W., Zhou, Z., and Kang, Y. J. (2009). Copper regulation of hypoxia-inducible factor-1 activity. *Mol. Pharmacol.* 75, 174–182. doi: 10.1124/mol.108.051516

Ferrell, W. R., and Najafipour, H. (1992). Changes in synovial PO2 and blood flow in the rabbit knee joint due to stimulation of the posterior articular nerve. *J. Physiol.* 449, 607–617. doi: 10.1113/jphysiol.1992.sp019104

Fife, R. S., Kluve-Beckerman, B., Houser, D. S., Proctor, C., Liepnieks, J., Masuda, I., et al. (1993). Evidence that a 550,000-dalton cartilage matrix glycoprotein is a chondrocyte membrane-associated protein closely related to ceruloplasmin. *J. Biol. Chem.* 268, 4407–4411.

Fife, R. S., Palmoski, M. J., and Brandt, K. D. (1986). Metabolism of a cartilage matrix glycoprotein in normal and osteoarthritic canine articular cartilage. *Arthritis Rheum.* 29, 1256–1262. doi: 10.1002/art.1780291011

Flores, R. R., Carbo, L., Kim, E., Van Meter, M., De Padilla, C. M. L., Zhao, J., et al. (2019). Adenoviral gene transfer of a single-chain IL-23 induces psoriatic arthritis-like symptoms in NOD mice. *FASEB J.* 33, 9505–9515. doi: 10.1096/fj.201900420R

Franceschi, C., and Campisi, J. (2014). Chronic inflammation (inflammaging) and its potential contribution to age-associated diseases. *J. Gerontol. A Biol. Sci. Med. Sci.* 69(Suppl. 1), S4–S9. doi: 10.1093/gerona/glu057

Fu, W. L., Zhou, C. Y., and Yu, J. K. (2014). A new source of mesenchymal stem cells for articular cartilage repair: MSCs derived from mobilized peripheral blood share similar biological characteristics in vitro and chondrogenesis in vivo as MSCs from bone marrow in a rabbit model. *Am. J. Sports Med.* 42, 592–601. doi: 10.1177/0363546513512778

Fuoco, C., Sangalli, E., Vono, R., Testa, S., Sacchetti, B., Latronico, M. V., et al. (2014). 3D hydrogel environment rejuvenates aged pericytes for skeletal muscle tissue engineering. *Front. Physiol.* 5:203. doi: 10.3389/fphys.2014.00203

Gao, S., Zhou, J., Zhao, Y., Toselli, P., and Li, W. (2013). Hypoxia-response element (HRE)-directed transcriptional regulation of the rat lysyl oxidase gene in response to cobalt and cadmium. *Toxicol. Sci.* 132, 379–389. doi: 10.1093/toxsci/kfs327

Gelse, K., Muhle, C., Knaup, K., Swoboda, B., Wiesener, M., Hennig, F., et al. (2008). Chondrogenic differentiation of growth factor-stimulated precursor cells in cartilage repair tissue is associated with increased HIF-1α activity. *Osteoarthritis Cartilage* 16, 1457–1465. doi: 10.1016/j.joca.2008.04.006

Goupille, P., Jayson, M. I., Valat, J. P., and Freemont, A. J. (1998). Matrix metalloproteinases: the clue to intervertebral disc degeneration? *Spine* 23, 1612–1626. doi: 10.1097/00007632-199807150-00021

Greene, M. A., and Loeser, R. F. (2015). Aging-related inflammation in osteoarthritis. *Osteoarthritis Cartilage* 23, 1966–1971. doi: 10.1016/j.joca.2015.01.008

Griffin, T. M., and Scanzello, C. R. (2019). Innate inflammation and synovial macrophages in osteoarthritis pathophysiology. *Clin. Exp. Rheumatol.* 37(Suppl. 120), 57–63.

Grubman, A., and White, A. R. (2014). Copper as a key regulator of cell signalling pathways. *Expert Rev. Mol. Med.* 16:e11. doi: 10.1017/erm.2014.11

Hadidi, P., Cissell, D. D., Hu, J. C., and Athanasiou, K. A. (2017). Temporal development of near-native functional properties and correlations with qMRI in self-assembling fibrocartilage treated with exogenous lysyl oxidase homolog 2. *Acta Biomater.* 64, 29–40. doi: 10.1016/j.actbio.2017.09.035

Hamza, I., Faisst, A., Prohaska, J., Chen, J., Gruss, P., and Gitlin, J. D. (2001). The metallochaperone Atox1 plays a critical role in perinatal copper homeostasis. *Proc. Natl. Acad. Sci. U.S.A.* 98, 6848–6852. doi: 10.1073/pnas.111058498

Hamza, I., and Gitlin, J. D. (2002). Copper chaperones for cytochrome *c* oxidase and human disease. *J. Bioenerg. Biomembr.* 34, 381–388. doi: 10.1023/a:1021254104012

Harris, E. D. (2000). Cellular copper transport and metabolism. *Annu. Rev. Nutr.* 20, 291–310. doi: 10.1146/annurev.nutr.20.1.291

Hayashi, K., Fong, K. S., Mercier, F., Boyd, C. D., Csiszar, K., and Hayashi, M. (2004). Comparative immunocytochemical localization of lysyl oxidase (LOX) and the lysyl oxidase-like (LOXL) proteins: changes in the expression of LOXL during development and growth of mouse tissues. *J. Mol. Histol.* 35, 845–855. doi: 10.1007/s10735-004-2340-1

He, G., and Karin, M. (2011). NF-κB and STAT3 - key players in liver inflammation and cancer. *Cell Res.* 21, 159–168. doi: 10.1038/cr.2010.183

Heraud, F., Savineau, C., and Harmand, M. F. (2002). Copper modulation of extracellular matrix synthesis by human articular chondrocytes. *Scand. J. Rheumatol.* 31, 279–284. doi: 10.1080/030097402760375179

Herchenhan, A., Uhlenbrock, F., Eliasson, P., Weis, M., Eyre, D., Kadler, K. E., et al. (2015). Lysyl oxidase activity is required for ordered collagen fibrillogenesis by tendon cells. *J. Biol. Chem.* 290, 16440–16450. doi: 10.1074/jbc.M115.641670

Himoto, T., Fujita, K., Nomura, T., Tani, J., Miyoshi, H., Morishita, A., et al. (2016). Roles of copper in hepatocarcinogenesis via the activation of hypoxia-inducible factor-1α. *Biol. Trace Elem. Res.* 174, 58–64. doi: 10.1007/s12011-016-0702-7

Horng, Y. C., Leary, S. C., Cobine, P. A., Young, F. B., George, G. N., Shoubridge, E. A., et al. (2005). Human Sco1 and Sco2 function as copper-binding proteins. *J. Biol. Chem.* 280, 34113–34122. doi: 10.1074/jbc.M506801200

Hu, D. P., Ferro, F., Yang, F., Taylor, A. J., Chang, W., Miclau, T., et al. (2017). Cartilage to bone transformation during fracture healing is coordinated by the invading vasculature and induction of the core pluripotency genes. *Development* 144, 221–234. doi: 10.1242/dev.130807

Huang, B., Wang, B., Yuk-Wai Lee, W., Pong, U. K., Leung, K. T., Li, X., et al. (2019). KDM3A and KDM4C regulate mesenchymal stromal cell senescence and bone aging via condensin-mediated heterochromatin reorganization. *iScience* 21, 375–390. doi: 10.1016/j.isci.2019.10.041

Huang, W., Sung, K. P., Xie, J., and Yang, J. J. (2010). Expression of lysyl oxidase family in different zones of articular cartilage. *Chin. J. Trauma* 26, 934–936.

Huey, D. J., Hu, J. C., and Athanasiou, K. A. (2012). Unlike bone, cartilage regeneration remains elusive. *Science* 338, 917–921. doi: 10.1126/science.1222454

Huffman, D. L., and O'Halloran, T. V. (2001). Function, structure, and mechanism of intracellular copper trafficking proteins. *Annu. Rev. Biochem.* 70, 677–701. doi: 10.1146/annurev.biochem.70.1.677

Hunziker, E. B. (2009). The elusive path to cartilage regeneration. *Adv. Mater.* 21, 3419–3424. doi: 10.1002/adma.200801957

Hurtig, M., Green, S. L., Dobson, H., Mikuni-Takagaki, Y., and Choi, J. J. E. V. J. (1993). Correlative study of defective cartilage and bone growth in foals fed a low-copper diet. *Equine Vet. J.* 25, 66–73. doi: 10.1111/j.2042-3306.1993.tb04857.x

Iftikhar, M., Hurtado, P., Bais, M. V., Wigner, N., Stephens, D. N., Gerstenfeld, L. C., et al. (2011). Lysyl oxidase-like-2 (LOXL2) is a major isoform in chondrocytes and is critically required for differentiation. *J. Biol. Chem.* 286, 909–918. doi: 10.1074/jbc.M110.155622

Isaacs, J. S., Jung, Y.-J., Mimnaugh, E. G., Martinez, A., Cuttitta, F., and Neckers, L. M. (2002). Hsp90 regulates a von Hippel Lindau-independent hypoxia-inducible factor-1α-degradative pathway. *J. Biol. Chem.* 277, 29936–29944. doi: 10.1074/jbc.m204733200

Ishihara, T., Kakiya, K., Takahashi, K., Miwa, H., Rokushima, M., Yoshinaga, T., et al. (2014). Discovery of novel differentiation markers in the early stage of chondrogenesis by glycoform-focused reverse proteomics and genomics. *Biochim. Biophys. Acta* 1840, 645–655. doi: 10.1016/j.bbagen.2013.10.027

Ito, H., Akiyama, H., Iguchi, H., Iyama, K., Miyamoto, M., Ohsawa, K., et al. (2001). Molecular cloning and biological activity of a novel lysyl oxidase-related gene expressed in cartilage. *J. Biol. Chem.* 276, 24023–24029. doi: 10.1074/jbc.M100861200

Jankowski, M. P., McIlwrath, S. L., Jing, X., Cornuet, P. K., Salerno, K. M., Koerber, H. R., et al. (2009). Sox11 transcription factor modulates peripheral nerve regeneration in adult mice. *Brain Res.* 1256, 43–54. doi: 10.1016/j.brainres.2008.12.032

Jensen, E. L., Gonzalez-Ibanez, A. M., Mendoza, P., Ruiz, L. M., Riedel, C. A., Simon, F., et al. (2019). Copper deficiency-induced anemia is caused by a mitochondrial metabolic reprograming in erythropoietic cells. *Metallomics* 11, 282–290. doi: 10.1039/c8mt00224j

Jeon, O. H., Kim, C., Laberge, R. M., Demaria, M., Rathod, S., Vasserot, A. P., et al. (2017). Local clearance of senescent cells attenuates the development of post-traumatic osteoarthritis and creates a pro-regenerative environment. *Nat. Med.* 23, 775–781. doi: 10.1038/nm.4324

Jiang, Y., Hu, C., Yu, S., Yan, J., Peng, H., Ouyang, H. W., et al. (2015). Cartilage stem/progenitor cells are activated in osteoarthritis via interleukin-1β/nerve growth factor signaling. *Arthritis Res. Ther.* 17:327. doi: 10.1186/s13075-015-0840-x

Jiang, Y., Reynolds, C., Xiao, C., Feng, W., Zhou, Z., Rodriguez, W., et al. (2007). Dietary copper supplementation reverses hypertrophic cardiomyopathy induced by chronic pressure overload in mice. *J. Exp. Med.* 204, 657–666. doi: 10.1084/jem.20061943

Josephson, A. M., Bradaschia-Correa, V., Lee, S., Leclerc, K., Patel, K. S., Muinos Lopez, E., et al. (2019). Age-related inflammation triggers skeletal stem/progenitor cell dysfunction. *Proc. Natl. Acad. Sci. U.S.A.* 116, 6995–7004. doi: 10.1073/pnas.1810692116

Kagan, H. M., and Li, W. (2003). Lysyl oxidase: properties, specificity, and biological roles inside and outside of the cell. *J. Cell. Biochem.* 88, 660–672. doi: 10.1002/jcb.10413

Katschinski, D., Le, L., Schindler, S., Thomas, T., Voss, A., Wenger, R. J. C. P., et al. (2004). Interaction of the PAS B domain with HSP90 accelerates hypoxia-inducible factor-1α stabilization. *Cell. Physiol. Biochem.* 14, 351–360. doi: 10.1159/000080345

Khan, I. M., Gilbert, S. J., Caterson, B., Sandell, L. J., and Archer, C. W. (2008). Oxidative stress induces expression of osteoarthritis markers procollagen IIA and 3B3(-) in adult bovine articular cartilage. *Osteoarthritis Cartilage* 16, 698–707. doi: 10.1016/j.joca.2007.10.004

Kim, B. E., Nevitt, T., and Thiele, D. J. (2008). Mechanisms for copper acquisition, distribution and regulation. *Nat. Chem. Biol.* 4, 176–185. doi: 10.1038/nchembio.72

Kim, B.-E., Turski, M. L., Nose, Y., Casad, M., Rockman, H. A., and Thiele, D. J. (2010). Cardiac copper deficiency activates a systemic signaling mechanism that communicates with the copper acquisition and storage organs. *Cell Metab.* 11, 353–363. doi: 10.1016/j.cmet.2010.04.003

Klingberg, F., Hinz, B., and White, E. S. (2013). The myofibroblast matrix: implications for tissue repair and fibrosis. *J. Pathol.* 229, 298–309. doi: 10.1002/path.4104

Knight, D. A., Weisbrode, S. E., Schmall, L. M., Reed, S. M., Gabel, A. A., Bramlage, L. R., et al. (1990). The effects of copper supplementation on the prevalence of cartilage lesions in foals. *Equine Vet. J.* 22, 426–432. doi: 10.1111/j.2042-3306.1990.tb04310.x

Kuivaniemi, H., Peltonen, L., Palotie, A., Kaitila, I., and Kivirikko, K. I. (1982). Abnormal copper metabolism and deficient lysyl oxidase activity in a heritable connective tissue disorder. *J. Clin. Invest.* 69, 730–733. doi: 10.1172/jci110503

Kyritsis, N., Kizil, C., Zocher, S., Kroehne, V., Kaslin, J., Freudenreich, D., et al. (2012). Acute inflammation initiates the regenerative response in the adult zebrafish brain. *Science* 338, 1353–1356. doi: 10.1126/science.1228773

La Mendola, D., Magri, A., Santoro, A. M., Nicoletti, V. G., and Rizzarelli, E. (2012). Copper(II) interaction with peptide fragments of histidine–proline-rich glycoprotein: speciation, stability and binding details. *J. Inorg. Biochem.* 111, 59–69. doi: 10.1016/j.jinorgbio.2012.02.027

Lee, C., O'Connell, C. D., Onofrillo, C., Choong, P. F. M., Di Bella, C., and Duchi, S. (2019). Concise review: human articular cartilage repair: sources and detection of cytotoxicity and genotoxicity in photo-crosslinkable hydrogel bioscaffolds. *Stem Cells Transl. Med.* 9, 302–315. doi: 10.1002/sctm.19-0192

Lee, W. Y., and Wang, B. (2017). Cartilage repair by mesenchymal stem cells: clinical trial update and perspectives. *J. Orthop. Translat.* 9, 76–88. doi: 10.1016/j.jot.2017.03.005

Leung, V. Y., Chan, D., and Cheung, K. M. (2006). Regeneration of intervertebral disc by mesenchymal stem cells: potentials, limitations, and future direction. *Eur. Spine J.* 15(Suppl. 3), S406–S413. doi: 10.1007/s00586-006-0183-z

Li, A., Wei, Y., Hung, C., and Vunjak-Novakovic, G. (2018). Chondrogenic properties of collagen type XI, a component of cartilage extracellular matrix. *Biomaterials* 173, 47–57. doi: 10.1016/j.biomaterials.2018.05.004

Li, J., Hansen, K. C., Zhang, Y., Dong, C., Dinu, C. Z., Dzieciatkowska, M., et al. (2014). Rejuvenation of chondrogenic potential in a young stem cell

microenvironment. *Biomaterials* 35, 642–653. doi: 10.1016/j.biomaterials.2013.09.099

Li, Y., Dai, G., Shi, L., Lin, Y., Chen, M., Li, G., et al. (2019). The potential roles of tendon stem/progenitor cells in tendon aging. *Curr. Stem Cell Res. Ther.* 14, 34–42. doi: 10.2174/1574888X13666181017112233

Lin, C. M., and Kosman, D. J. (1990). Copper uptake in wild type and copper metallothionein-deficient *Saccharomyces cerevisiae*, kinetics and mechanism. *J. Biol. Chem.* 265, 9194–9200.

Lin, R., Deng, C., Li, X., Liu, Y., Zhang, M., Qin, C., et al. (2019). Copper-incorporated bioactive glass-ceramics inducing anti-inflammatory phenotype and regeneration of cartilage/bone interface. *Theranostics* 9, 6300–6313. doi: 10.7150/thno.36120

Lin, S., Lee, W. Y. W., Xu, L., Wang, Y., Chen, Y., Ho, K. K. W., et al. (2017). Stepwise preconditioning enhances mesenchymal stem cell-based cartilage regeneration through epigenetic modification. *Osteoarthritis Cartilage* 25, 1541–1550. doi: 10.1016/j.joca.2017.05.008

Lin, W., Xu, L., Pan, Q., Lin, S., Feng, L., Wang, B., et al. (2019). Lgr5-overexpressing mesenchymal stem cells augment fracture healing through regulation of Wnt/ERK signaling pathways and mitochondrial dynamics. *FASEB J.* 33, 8565–8577. doi: 10.1096/fj.201900082RR

Linder, M. C. (2016). Ceruloplasmin and other copper binding components of blood plasma and their functions: an update. *Metallomics* 8, 887–905. doi: 10.1039/c6mt00103c

Liu, C. H., Abrams, N. D., Carrick, D. M., Chander, P., Dwyer, J., Hamlet, M. R. J., et al. (2019). Imaging inflammation and its resolution in health and disease: current status, clinical needs, challenges, and opportunities. *FASEB J.* 33, 13085–13097. doi: 10.1096/fj.201902024

Liu, X., Zhang, W., Wu, Z., Yang, Y., and Kang, Y. J. (2018). Copper levels affect targeting of hypoxia-inducible factor 1α to the promoters of hypoxia-regulated genes. *J. Biol. Chem.* 293, 14669–14677. doi: 10.1074/jbc.ra118.001764

Loeser, R. F., Collins, J. A., and Diekman, B. O. (2016). Ageing and the pathogenesis of osteoarthritis. *Nat. Rev. Rheumatol.* 12, 412–420. doi: 10.1038/nrrheum.2016.65

Long, F. (2019). Less is more: ditching mitochondria saves hypoxic cartilage. *Dev. Cell* 49, 656–658. doi: 10.1016/j.devcel.2019.05.030

Lopez, B., Gonzalez, A., Hermida, N., Valencia, F., de Teresa, E., and Diez, J. (2010). Role of lysyl oxidase in myocardial fibrosis: from basic science to clinical aspects. *Am. J. Physiol. Heart Circ. Physiol.* 299, H1–H9. doi: 10.1152/ajpheart.00335.2010

Lotz, M., and Loeser, R. F. (2012). Effects of aging on articular cartilage homeostasis. *Bone* 51, 241–248. doi: 10.1016/j.bone.2012.03.023

Lucero, H. A., and Kagan, H. M. (2006). Lysyl oxidase: an oxidative enzyme and effector of cell function. *Cell. Mol. Life Sci.* 63, 2304–2316. doi: 10.1007/s00018-006-6149-9

Lunelli, M., Di Paolo, M. L., Biadene, M., Calderone, V., Battistutta, R., Scarpa, M., et al. (2005). Crystal structure of amine oxidase from bovine serum. *J. Mol. Biol.* 346, 991–1004. doi: 10.1016/j.jmb.2004.12.038

Luo, J., Zhou, W., Zhou, X., Li, D., Weng, J., Yi, Z., et al. (2009). Regulation of bone formation and remodeling by G-protein-coupled receptor 48. *Development* 136, 2747–2756. doi: 10.1242/dev.033571

Luria, A., and Chu, C. R. (2014). Articular cartilage changes in maturing athletes: new targets for joint rejuvenation. *Sports Health* 6, 18–30. doi: 10.1177/1941738113514369

Ma, L., Huang, C., Wang, X. J., Xin, D. E., Wang, L. S., Zou, Q. C., et al. (2017). Lysyl oxidase 3 is a dual-specificity enzyme involved in STAT3 deacetylation and deacetylimination modulation. *Mol. Cell* 65, 296–309. doi: 10.1016/j.molcel.2016.12.002

Maes, C., Araldi, E., Haigh, K., Khatri, R., Van Looveren, R., Giaccia, A. J., et al. (2012). VEGF-independent cell-autonomous functions of HIF-1α regulating oxygen consumption in fetal cartilage are critical for chondrocyte survival. *J. Bone Miner. Res.* 27, 596–609. doi: 10.1002/jbmr.1487

Maes, C., Stockmans, I., Moermans, K., Van Looveren, R., Smets, N., Carmeliet, P., et al. (2004). Soluble VEGF isoforms are essential for establishing epiphyseal vascularization and regulating chondrocyte development and survival. *J. Clin. Invest.* 113, 188–199. doi: 10.1172/JCI19383

Magri, A., Grasso, G., Corti, F., Finetti, F., Greco, V., Santoro, A. M., et al. (2018). Peptides derived from the histidine-proline rich glycoprotein bind copper ions and exhibit anti-angiogenic properties. *Dalton Trans.* 47, 9492–9503. doi: 10.1039/c8dt01560k

Maki, J. M. (2009). Lysyl oxidases in mammalian development and certain pathological conditions. *Histol. Histopathol.* 24, 651–660. doi: 10.14670/HH-24.651

Maki, J. M., Rasanen, J., Tikkanen, H., Sormunen, R., Makikallio, K., Kivirikko, K. I., et al. (2002). Inactivation of the lysyl oxidase gene Lox leads to aortic aneurysms, cardiovascular dysfunction, and perinatal death in mice. *Circulation* 106, 2503–2509. doi: 10.1161/01.cir.0000038109.84500.1e

Maki, J. M., Sormunen, R., Lippo, S., Kaarteenaho-Wiik, R., Soininen, R., and Myllyharju, J. (2005). Lysyl oxidase is essential for normal development and function of the respiratory system and for the integrity of elastic and collagen fibers in various tissues. *Am. J. Pathol.* 167, 927–936. doi: 10.1016/S0002-9440(10)61183-2

Makris, E. A., MacBarb, R. F., Responte, D. J., Hu, J. C., and Athanasiou, K. A. (2013). A copper sulfate and hydroxylysine treatment regimen for enhancing collagen cross-linking and biomechanical properties in engineered neocartilage. *FASEB J.* 27, 2421–2430. doi: 10.1096/fj.12-224030

Makris, E. A., Responte, D. J., Paschos, N. K., Hu, J. C., and Athanasiou, K. A. (2014). Developing functional musculoskeletal tissues through hypoxia and lysyl oxidase-induced collagen cross-linking. *Proc. Natl. Acad. Sci. U.S.A.* 111, E4832–E4841. doi: 10.1073/pnas.1414271111

Martin, F., Linden, T., Katschinski, D. M., Oehme, F., Flamme, I., Mukhopadhyay, C. K., et al. (2005). Copper-dependent activation of hypoxia-inducible factor (HIF)-1: implications for ceruloplasmin regulation. *Blood* 105, 4613–4619. doi: 10.1182/blood-2004-10-3980

Martinez-Gonzalez, J., Varona, S., Canes, L., Galan, M., Briones, A. M., Cachofeiro, V., et al. (2019). Emerging roles of lysyl oxidases in the cardiovascular system: new concepts and therapeutic challenges. *Biomolecules* 9:610. doi: 10.3390/biom9100610

Marturano, J. E., Arena, J. D., Schiller, Z. A., Georgakoudi, I., and Kuo, C. K. (2013). Characterization of mechanical and biochemical properties of developing embryonic tendon. *Proc. Natl. Acad. Sci. U.S.A.* 110, 6370–6375. doi: 10.1073/pnas.1300135110

Mendler, M., Eich-Bender, S. G., Vaughan, L., Winterhalter, K. H., and Bruckner, P. (1989). Cartilage contains mixed fibrils of collagen types II, IX, and XI. *J. Cell Biol.* 108, 191–197. doi: 10.1083/jcb.108.1.191

Messier, S. P., Gutekunst, D. J., Davis, C., and DeVita, P. (2005). Weight loss reduces knee-joint loads in overweight and obese older adults with knee osteoarthritis. *Arthritis Rheum.* 52, 2026–2032. doi: 10.1002/art.21139

Miao, Q., Hill, M. C., Chen, F., Mo, Q., Ku, A. T., Ramos, C., et al. (2019). SOX11 and SOX4 drive the reactivation of an embryonic gene program during murine wound repair. *Nat. Commun.* 10:4042. doi: 10.1038/s41467-019-11880-9

Miller, K. A., Vicentini, F. A., Hirota, S. A., Sharkey, K. A., and Wieser, M. E. (2019). Antibiotic treatment affects the expression levels of copper transporters and the isotopic composition of copper in the colon of mice. *Proc. Natl. Acad. Sci. U.S.A.* 116, 5955–5960. doi: 10.1073/pnas.1814047116

Minet, E., Mottet, D., Michel, G., Roland, I., Raes, M., Remacle, J., et al. (1999). Hypoxia-induced activation of HIF-1: role of HIF-1α-Hsp90 interaction. *FEBS Lett.* 460, 251–256. doi: 10.1016/s0014-5793(99)01359-9

Mobasheri, A., and Batt, M. (2016). An update on the pathophysiology of osteoarthritis. *Ann. Phys. Rehabil. Med.* 59, 333–339. doi: 10.1016/j.rehab.2016.07.004

Nave, A. H., Mizikova, I., Niess, G., Steenbock, H., Reichenberger, F., Talavera, M. L., et al. (2014). Lysyl oxidases play a causal role in vascular remodeling in clinical and experimental pulmonary arterial hypertension. *Arterioscler. Thromb. Vasc. Biol.* 34, 1446–1458. doi: 10.1161/ATVBAHA.114.303534

Nelson, T. J., Behfar, A., and Terzic, A. (2008). Strategies for therapeutic repair: the "R(3)" regenerative medicine paradigm. *Clin. Transl. Sci.* 1, 168–171. doi: 10.1111/j.1752-8062.2008.00039.x

Ohmura, H., Yasukawa, H., Minami, T., Sugi, Y., Oba, T., Nagata, T., et al. (2012). Cardiomyocyte-specific transgenic expression of lysyl oxidase-like protein-1 induces cardiac hypertrophy in mice. *Hypertens. Res.* 35, 1063–1068. doi: 10.1038/hr.2012.92

Ohrvik, H., and Thiele, D. J. (2014). How copper traverses cellular membranes through the mammalian copper transporter 1, Ctr1. *Ann. N. Y. Acad. Sci.* 1314, 32–41. doi: 10.1111/nyas.12371

Okado-Matsumoto, A., and Fridovich, I. (2001). Subcellular distribution of superoxide dismutases (SOD) in rat liver: Cu, Zn-SOD in mitochondria. *J. Biol. Chem.* 276, 38388–38393. doi: 10.1074/jbc.M105395200

Onofrillo, C., Duchi, S., O'Connell, C. D., Blanchard, R., O'Connor, A. J., Scott, M., et al. (2018). Biofabrication of human articular cartilage: a path towards the development of a clinical treatment. *Biofabrication* 10:045006. doi: 10.1088/1758-5090/aad8d9

Pasqualicchio, M., Gasperini, R., Velo, G. P., and Davies, M. E. (1996). Effects of copper and zinc on proteoglycan metabolism in articular cartilage. *Mediators Inflamm.* 5, 95–99. doi: 10.1155/S0962935196000154

Patil, P., Dong, Q., Wang, D., Chang, J., Wiley, C., Demaria, M., et al. (2019). Systemic clearance of $p^{16^{INK4a}}$ -positive senescent cells mitigates age-associated intervertebral disc degeneration. *Aging Cell* 18:e12927. doi: 10.1111/acel.12927

Percival, S. S. (1998). Copper and immunity. *Am. J. Clin. Nutr.* 67(5 Suppl.), 1064S–1068S. doi: 10.1093/ajcn/67.5.1064S

Pfander, D., Swoboda, B., and Cramer, T. (2006). The role of HIF-1α in maintaining cartilage homeostasis and during the pathogenesis of osteoarthritis. *Arthritis Res. Ther.* 8:104. doi: 10.1186/ar1894

Pokharna, H. K., Monnier, V., Boja, B., and Moskowitz, R. W. (1995). Lysyl oxidase and Maillard reaction-mediated crosslinks in aging and osteoarthritic rabbit cartilage. *J. Orthop. Res.* 13, 13–21. doi: 10.1002/jor.1100130105

Puig, S., and Thiele, D. J. (2002). Molecular mechanisms of copper uptake and distribution. *Curr. Opin. Chem. Biol.* 6, 171–180. doi: 10.1016/s1367-5931(02)00298-3

Pushie, M. J., Ross, A. R., and Vogel, H. J. (2007). Mass spectrometric determination of the coordination geometry of potential copper(II) surrogates for the mammalian prion protein octarepeat region. *Anal. Chem.* 79, 5659–5667. doi: 10.1021/ac070312l

Qu, X., He, Z., Qiao, H., Zhai, Z., Mao, Z., Yu, Z., et al. (2018). Serum copper levels are associated with bone mineral density and total fracture. *J. Orthop. Translat.* 14, 34–44. doi: 10.1016/j.jot.2018.05.001

Rae, T. D., Schmidt, P. J., Pufahl, R. A., Culotta, V. C., and O'Halloran, T. V. (1999). Undetectable intracellular free copper: the requirement of a copper chaperone for superoxide dismutase. *Science* 284, 805–808. doi: 10.1126/science.284.5415.805

Ranganathan, P. N., Lu, Y., Jiang, L., Kim, C., and Collins, J. F. (2011). Serum ceruloplasmin protein expression and activity increases in iron-deficient rats and is further enhanced by higher dietary copper intake. *Blood* 118, 3146–3153. doi: 10.1182/blood-2011-05-352112

Ransom, R. C., Carter, A. C., Salhotra, A., Leavitt, T., Marecic, O., Murphy, M. P., et al. (2018). Mechanoresponsive stem cells acquire neural crest fate in jaw regeneration. *Nature* 563, 514–521. doi: 10.1038/s41586-018-0650-9

Reynaud, C., Baas, D., Gleyzal, C., Le Guellec, D., and Sommer, P. (2008). Morpholino knockdown of lysyl oxidase impairs zebrafish development, and reflects some aspects of copper metabolism disorders. *Matrix Biol.* 27, 547–560. doi: 10.1016/j.matbio.2008.03.002

Rimar, D., Rosner, I., Nov, Y., Slobodin, G., Rozenbaum, M., Halasz, K., et al. (2014). Brief report: lysyl oxidase is a potential biomarker of fibrosis in systemic sclerosis. *Arthritis Rheumatol.* 66, 726–730. doi: 10.1002/art.38277

Rivard, A., Berthou-Soulie, L., Principe, N., Kearney, M., Curry, C., Branellec, D., et al. (2000). Age-dependent defect in vascular endothelial growth factor expression is associated with reduced hypoxia-inducible factor 1 activity. *J. Biol. Chem.* 275, 29643–29647. doi: 10.1074/jbc.M001029200

Robins, J. C., Akeno, N., Mukherjee, A., Dalal, R. R., Aronow, B. J., Koopman, P., et al. (2005). Hypoxia induces chondrocyte-specific gene expression in mesenchymal cells in association with transcriptional activation of Sox9. *Bone* 37, 313–322. doi: 10.1016/j.bone.2005.04.040

Robinson, P. S., Huang, T. F., Kazam, E., Iozzo, R. V., Birk, D. E., and Soslowsky, L. J. (2005). Influence of decorin and biglycan on mechanical properties of multiple tendons in knockout mice. *J. Biomech. Eng.* 127, 181–185. doi: 10.1115/1.1835363

Roman-Blas, J. A., and Jimenez, S. A. (2008). Targeting NF-κB: a promising molecular therapy in inflammatory arthritis. *Int. Rev. Immunol.* 27, 351–374. doi: 10.1080/08830180802295740

Rucker, R. B., Kosonen, T., Clegg, M. S., Mitchell, A. E., Rucker, B. R., Uriu-Hare, J. Y., et al. (1998). Copper, lysyl oxidase, and extracellular matrix protein cross-linking. *Am. J. Clin. Nutr.* 67(5 Suppl.), 996S–1002S. doi: 10.1093/ajcn/67.5.996S

Sakai, D., Nakamura, Y., Nakai, T., Mishima, T., Kato, S., Grad, S., et al. (2012). Exhaustion of nucleus pulposus progenitor cells with ageing and degeneration of the intervertebral disc. *Nat. Commun.* 3:1264. doi: 10.1038/ncomms2226

Sanada, H., Shikata, J., Hamamoto, H., Ueba, Y., Yamamuro, T., and Takeda, T. (1978). Changes in collagen cross-linking and lysyl oxidase by estrogen. *Biochim. Biophys. Acta* 541, 408–413. doi: 10.1016/0304-4165(78)90199-x

Sarkar, T. J., Quarta, M., Mukherjee, S., Colville, A., Paine, P., Doan, L., et al. (2020). Transient non-integrative expression of nuclear reprogramming factors promotes multifaceted amelioration of aging in human cells. *Nat. Commun.* 11:1545. doi: 10.1038/s41467-020-15174-3

Schietke, R., Warnecke, C., Wacker, I., Schodel, J., Mole, D. R., Campean, V., et al. (2010). The lysyl oxidases LOX and LOXL2 are necessary and sufficient to repress E-cadherin in hypoxia: insights into cellular transformation processes mediated by HIF-1. *J. Biol. Chem.* 285, 6658–6669. doi: 10.1074/jbc.M109.042424

Schmelzer, C. E. H., Heinz, A., Troilo, H., Lockhart-Cairns, M. P., Jowitt, T. A., Marchand, M. F., et al. (2019). Lysyl oxidase-like 2 (LOXL2)-mediated cross-linking of tropoelastin. *FASEB J.* 33, 5468–5481. doi: 10.1096/fj.201801860RR

Scudder, P. R., Al-Timimi, D., McMurray, W., White, A. G., Zoob, B. C., and Dormandy, T. L. (1978). Serum copper and related variables in rheumatoid arthritis. *Ann. Rheum. Dis.* 37, 67–70. doi: 10.1136/ard.37.1.67

Shi, Q., Qian, Z., Liu, D., Sun, J., Xu, J., and Guo, X. (2017). Maintaining the phenotype stability of chondrocytes derived from MSCs by C-type natriuretic peptide. *Front. Physiol.* 8:143. doi: 10.3389/fphys.2017.00143

Shi, Y., Hu, X., Zhang, X., Cheng, J., Duan, X., Fu, X., et al. (2019). Superoxide dismutase 3 facilitates the chondrogenesis of bone marrow-derived mesenchymal stem cells. *Biochem. Biophys. Res. Commun.* 509, 983–987. doi: 10.1016/j.bbrc.2019.01.042

Simon, M. C., and Keith, B. (2008). The role of oxygen availability in embryonic development and stem cell function. *Nat. Rev. Mol. Cell Biol.* 9, 285–296. doi: 10.1038/nrm2354

Smith-Mungo, L. I., and Kagan, H. M. (1998). Lysyl oxidase: properties, regulation and multiple functions in biology. *Matrix Biol.* 16, 387–398. doi: 10.1016/s0945-053x(98)90012-9

Solomon, E. I., Heppner, D. E., Johnston, E. M., Ginsbach, J. W., Cirera, J., Qayyum, M., et al. (2014). Copper active sites in biology. *Chem. Rev.* 114, 3659–3853. doi: 10.1021/cr400327t

Stegen, S., Laperre, K., Eelen, G., Rinaldi, G., Fraisl, P., Torrekens, S., et al. (2019). HIF-1α metabolically controls collagen synthesis and modification in chondrocytes. *Nature* 565, 511–515. doi: 10.1038/s41586-019-0874-3

Stroka, D. M., Burkhardt, T., Desbaillets, I., Wenger, R. H., Neil, D. A., Bauer, C., et al. (2001). HIF-1 is expressed in normoxic tissue and displays an organ-specific regulation under systemic hypoxia. *FASEB J.* 15, 2445–2453. doi: 10.1096/fj.01-0125com

Sun, Y., Li, W., Lu, Z., Chen, R., Ling, J., Ran, Q., et al. (2011). Rescuing replication and osteogenesis of aged mesenchymal stem cells by exposure to a young extracellular matrix. *FASEB J.* 25, 1474–1485. doi: 10.1096/fj.10-161497

Tao, C., Wang, Y., Zhao, Y., Pan, J., Fan, Y., Liang, X., et al. (2019). Adipocyte-specific disruption of ATPase copper transporting α in mice accelerates lipoatrophy. *Diabetologia* 62, 2340–2353. doi: 10.1007/s00125-019-4966-2

Tapiero, H., Townsend, D. M., and Tew, K. D. (2003). Trace elements in human physiology and pathology. *Biomed. Pharmacother.* 57, 386–398. doi: 10.1016/s0753-3322(03)00012-x

Tashkandi, M., Ali, F., Alsaqer, S., Alhousami, T., Cano, A., Martin, A., et al. (2019). Lysyl oxidase-like 2 protects against progressive and aging related knee joint osteoarthritis in mice. *Int. J. Mol. Sci.* 20:4798. doi: 10.3390/ijms20194798

Tatman, P. D., Gerull, W., Sweeney-Easter, S., Davis, J. I., Gee, A. O., and Kim, D. H. (2015). Multiscale biofabrication of articular cartilage: bioinspired and biomimetic approaches. *Tissue Eng. Part B Rev.* 21, 543–559. doi: 10.1089/ten.TEB.2015.0142

Teo, A. Q. A., Wong, K. L., Shen, L., Lim, J. Y., Toh, W. S., Lee, E. H., et al. (2019). Equivalent 10-year outcomes after implantation of autologous bone marrow-derived mesenchymal stem cells versus autologous chondrocyte implantation for chondral defects of the knee. *Am. J. Sports Med.* 47, 2881–2887. doi: 10.1177/0363546519867933

Thalhamer, T., McGrath, M. A., and Harnett, M. M. (2008). MAPKs and their relevance to arthritis and inflammation. *Rheumatology* 47, 409–414. doi: 10.1093/rheumatology/kem297

Thomassin, L., Werneck, C. C., Broekelmann, T. J., Gleyzal, C., Hornstra, I. K., Mecham, R. P., et al. (2005). The Pro-regions of lysyl oxidase and lysyl oxidase-like 1 are required for deposition onto elastic fibers. *J. Biol. Chem.* 280, 42848–42855. doi: 10.1074/jbc.m506832200

Turski, M. L., Brady, D. C., Kim, H. J., Kim, B. E., Nose, Y., Counter, C. M., et al. (2012). A novel role for copper in Ras/mitogen-activated protein kinase signaling. *Mol. Cell. Biol.* 32, 1284–1295. doi: 10.1128/MCB.05722-11

Turski, M. L., and Thiele, D. J. (2009). New roles for copper metabolism in cell proliferation, signaling, and disease. *J. Biol. Chem.* 284, 717–721. doi: 10.1074/jbc.R800055200

Urso, E., and Maffia, M. (2015). Behind the link between copper and angiogenesis: established mechanisms and an overview on the role of vascular copper transport systems. *J. Vasc. Res.* 52, 172–196. doi: 10.1159/000438485

van Boxtel, A. L., Gansner, J. M., Hakvoort, H. W., Snell, H., Legler, J., and Gitlin, J. D. (2011). Lysyl oxidase-like 3b is critical for cartilage maturation during Zebrafish craniofacial development. *Matrix Biol.* 30, 178–187. doi: 10.1016/j.matbio.2010.12.002

van Vlimmeren, M. A., Driessen-Mol, A., van den Broek, M., Bouten, C. V., and Baaijens, F. P. (2010). Controlling matrix formation and cross-linking by hypoxia in cardiovascular tissue engineering. *J. Appl. Physiol.* 109, 1483–1491. doi: 10.1152/japplphysiol.00571.2010

Varela-Eirin, M., Loureiro, J., Fonseca, E., Corrochano, S., Caeiro, J. R., Collado, M., et al. (2018). Cartilage regeneration and ageing: Targeting cellular plasticity in osteoarthritis. *Ageing Res. Rev.* 42, 56–71. doi: 10.1016/j.arr.2017.12.006

Vortkamp, A., Pathi, S., Peretti, G. M., Caruso, E. M., Zaleske, D. J., and Tabin, C. J. (1998). Recapitulation of signals regulating embryonic bone formation during postnatal growth and in fracture repair. *Mech. Dev.* 71, 65–76. doi: 10.1016/s0925-4773(97)00203-7

Wang, A. M., Cao, P., Yee, A., Chan, D., and Wu, E. X. (2015). Detection of extracellular matrix degradation in intervertebral disc degeneration by diffusion magnetic resonance spectroscopy. *Magn. Reson. Med.* 73, 1703–1712. doi: 10.1002/mrm.25289

Wang, M. J., Chen, J., Chen, F., Liu, Q., Sun, Y., Yan, C., et al. (2019). Rejuvenating strategies of tissue-specific stem cells for healthy aging. *Aging Dis.* 10, 871–882. doi: 10.14336/AD.2018.1119

Wang, S. X., Mure, M., Medzihradszky, K. F., Burlingame, A. L., Brown, D. E., Dooley, D. M., et al. (1996). A crosslinked cofactor in lysyl oxidase: redox function for amino acid side chains. *Science* 273, 1078–1084. doi: 10.1126/science.273.5278.1078

Wang, T., Xiang, P., Ha, J. H., Wang, X., Doguer, C., Flores, S. R. L., et al. (2018). Copper supplementation reverses dietary iron overload-induced pathologies in mice. *J. Nutr. Biochem.* 59, 56–63. doi: 10.1016/j.jnutbio.2018.05.006

Weiner, S., and Traub, W. (1992). Bone structure: from angstroms to microns. *FASEB J.* 6, 879–885. doi: 10.1096/fasebj.6.3.1740237

Williamson, A. K., Chen, A. C., Masuda, K., Thonar, E. J., and Sah, R. L. (2003). Tensile mechanical properties of bovine articular cartilage: variations with growth and relationships to collagen network components. *J. Orthop. Res.* 21, 872–880. doi: 10.1016/S0736-0266(03)00030-5

Xu, L., Shunmei, E., Lin, S., Hou, Y., Lin, W., He, W., et al. (2019). Sox11-modified mesenchymal stem cells accelerate cartilage defect repair in SD rats. *Cell Tissue Res.* 376, 247–255. doi: 10.1007/s00441-018-02979-4

Yao, H., Xu, J. K., Zheng, N. Y., Wang, J. L., Mok, S. W., Lee, Y. W., et al. (2019). Intra-articular injection of magnesium chloride attenuates osteoarthritis progression in rats. *Osteoarthritis Cartilage* 27, 1811–1821. doi: 10.1016/j.joca.2019.08.007

Yazar, M., Sarban, S., Kocyigit, A., and Isikan, U. E. (2005). Synovial fluid and plasma selenium, copper, zinc, and iron concentrations in patients with rheumatoid arthritis and osteoarthritis. *Biol. Trace Elem. Res.* 106, 123–132. doi: 10.1385/bter:106:2:123

Yuan, X., Wang, J., Zhu, X., Zhang, Z., Ai, Y., Sun, G., et al. (2011). Effect of copper on levels of collagen and alkaline phosphatase activity from chondrocytes in newborn piglets *in vitro*. *Biol. Trace Elem. Res.* 144, 597–605. doi: 10.1007/s12011-011-9151-5

Yuan, X. L., Meng, H. Y., Wang, Y. C., Peng, J., Guo, Q. Y., Wang, A. Y., et al. (2014). Bone-cartilage interface crosstalk in osteoarthritis: potential pathways and future therapeutic strategies. *Osteoarthritis Cartilage* 22, 1077–1089. doi: 10.1016/j.joca.2014.05.023

Yudoh, K., Nakamura, H., Masuko-Hongo, K., Kato, T., and Nishioka, K. (2005). Catabolic stress induces expression of hypoxia-inducible factor (HIF)-1 α in articular chondrocytes: involvement of HIF-1 α in the pathogenesis of osteoarthritis. *Arthritis Res. Ther.* 7, R904–R914. doi: 10.1186/ar1765

Zhang, C., Yang, F., Cornelia, R., Tang, W., Swisher, S., and Kim, H. (2011). Hypoxia-inducible factor-1 is a positive regulator of Sox9 activity in femoral head osteonecrosis. *Bone* 48, 507–513. doi: 10.1016/j.bone.2010.10.006

Zhang, S., Hu, P., Liu, T., Li, Z., Huang, Y., Liao, J., et al. (2019). Kartogenin hydrolysis product 4-aminobiphenyl distributes to cartilage and mediates cartilage regeneration. *Theranostics* 9, 7108–7121. doi: 10.7150/thno.38182

Zhang, X., Cai, D., Zhou, F., Yu, J., Wu, X., Yu, D., et al. (2020). Targeting downstream subcellular YAP activity as a function of matrix stiffness with Verteporfin-encapsulated chitosan microsphere attenuates osteoarthritis. *Biomaterials* 232:119724. doi: 10.1016/j.biomaterials.2019.119724

Zhang, X., Wang, Q., Wu, J., Wang, J., Shi, Y., and Liu, M. (2018). Crystal structure of human lysyl oxidase-like 2 (hLOXL2) in a precursor state. *Proc. Natl. Acad. Sci. U.S.A.* 115, 3828–3833. doi: 10.1073/pnas.1720859115

Zhang, Y., Morgan, B. J., Smith, R., Fellows, C. R., Thornton, C., Snow, M., et al. (2017). Platelet-rich plasma induces post-natal maturation of immature articular cartilage and correlates with LOXL1 activation. *Sci. Rep.* 7:3699. doi: 10.1038/s41598-017-02297-9

Zhang, Y., Xiong, C., Kudelko, M., Li, Y., Wang, C., Wong, Y. L., et al. (2018). Early onset of disc degeneration in SM/J mice is associated with changes in ion transport systems and fibrotic events. *Matrix Biol.* 70, 123–139. doi: 10.1016/j.matbio.2018.03.024

Zhang, Z., Leong, D. J., Xu, L., He, Z., Wang, A., Navati, M., et al. (2016). Curcumin slows osteoarthritis progression and relieves osteoarthritis-associated pain symptoms in a post-traumatic osteoarthritis mouse model. *Arthritis Res. Ther.* 18:128. doi: 10.1186/s13075-016-1025-y

Zhou, B., Zhang, H., Su, X., Luo, Y., Li, X., Yu, C., et al. (2019). Therapeutic effects of a novel BAFF blocker on arthritis. *Signal Transduct. Target. Ther.* 4:19. doi: 10.1038/s41392-019-0051-z

Zhou, J., So, K. K., Li, Y., Li, Y., Yuan, J., Ding, Y., et al. (2019). Elevated H3K27ac in aged skeletal muscle leads to increase in extracellular matrix and fibrogenic conversion of muscle satellite cells. *Aging Cell* 18:e12996. doi: 10.1111/acel.12996

Conflict of Interest: The authors declare that the research was conducted in the absence of any commercial or financial relationships that could be construed as a potential conflict of interest.

frontiers in Bioengineering and Biotechnology

CORRECTION
published: 26 October 2020
doi: 10.3389/fbioe.2020.598323

Corrigendum: Molecular Insights Into Lysyl Oxidases in Cartilage Regeneration and Rejuvenation

Weiping Lin[1*†], *Liangliang Xu*[2†] *and Gang Li*[1,3*]

[1] Department of Orthopaedics and Traumatology, Stem Cells and Regenerative Medicine Laboratory, Li Ka Shing Institute of Health Sciences, The Chinese University of Hong Kong, Prince of Wales Hospital, Hong Kong, China, [2] The First Affiliated Hospital of Guangzhou University of Chinese Medicine, Lingnan Medical Research Center, Guangzhou University of Chinese Medicine, Guangzhou, China, [3] MOE Key Laboratory for Regenerative Medicine, School of Biomedical Sciences, The Chinese University of Hong Kong, Hong Kong, China

Keywords: lysyl oxidase, cartilage, hypoxia-inducible factor, copper, transcription activity, regeneration, rejuvenation

OPEN ACCESS

Approved by:
Frontiers Editorial Office, Frontiers Media SA, Switzerland

***Correspondence:**
Gang Li
gangli@cuhk.edu.hk
Weiping Lin
weipinglin@link.cuhk.edu.hk

†These authors have contributed equally to this work

Specialty section:
This article was submitted to Preclinical Cell and Gene Therapy, a section of the journal Frontiers in Bioengineering and Biotechnology

Received: *24 August 2020*
Accepted: *25 August 2020*
Published: *26 October 2020*

Citation:
Lin W, Xu L and Li G (2020) Corrigendum: Molecular Insights Into Lysyl Oxidases in Cartilage Regeneration and Rejuvenation. Front. Bioeng. Biotechnol. 8:598323. doi: 10.3389/fbioe.2020.598323

A Corrigendum on

Molecular Insights Into Lysyl Oxidases in Cartilage Regeneration and Rejuvenation
by Lin, W., Xu, L., and Li, G. (2020). Front. Bioeng. Biotechnol. 8:359. doi: 10.3389/fbioe.2020.00359

In the original article, there was a mistake in **Figure 4** as published. The corrected **Figure 4** and figure legend appear below.

The authors apologize for this error and state that they do not change the scientific conclusions of the article in any way. The original article has been updated.

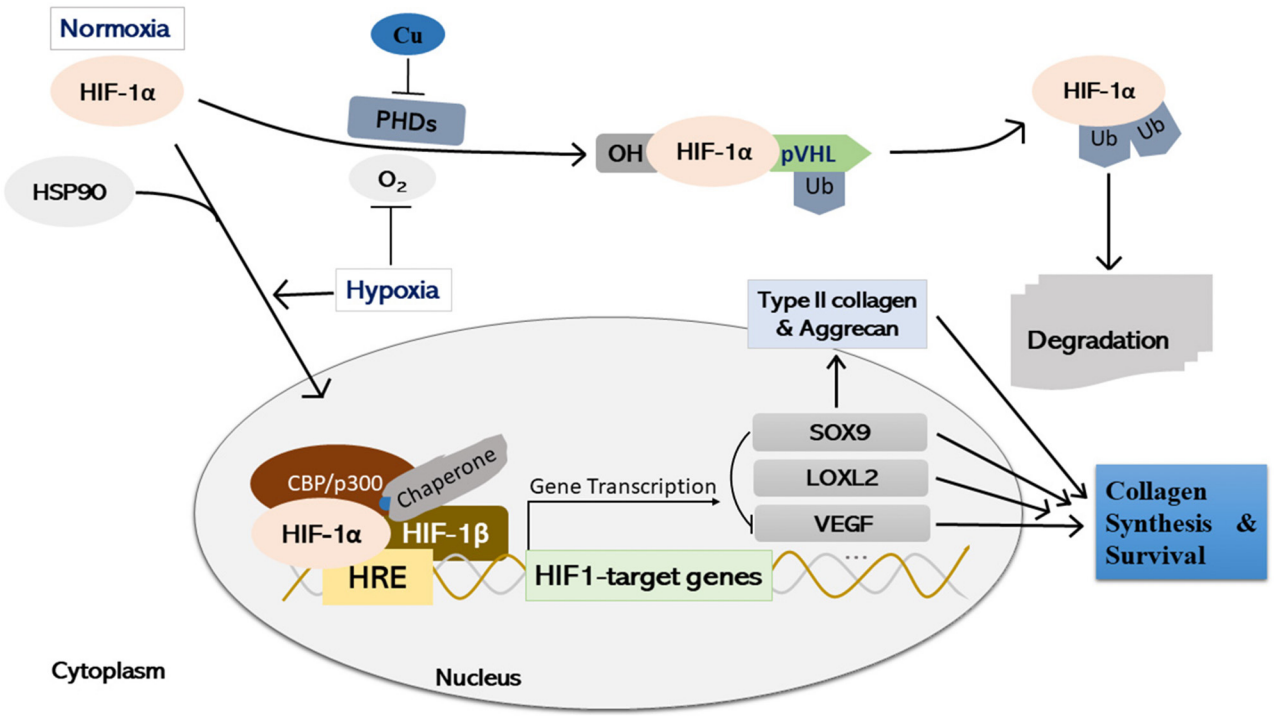

FIGURE 4 | Schematic illustration of copper-mediated hypoxia-response element (HRE)-directed transcriptional fine-tuning of cartilage homeostasis-associated genes in chondrocytes. Under normoxia, HIF-1α undergoes PHDs-mediated prolyl hydroxylation, and prolyl OH HIF-1α is ligated by pVHL, an E3 ubiquitin ligase, and degraded by the proteasome finally. Copper stabilizes HIF-1α protein by inhibiting PHDs activity in an iron-independent manner. Under hypoxia or through interaction with HSP90, HIF-1α stabilizes and accumulates in the cell nucleus, where it forms a dimer with the HIF-1β subunit and a putative unidentified copper-chaperone. The dimer then forms a transcriptional complex with coactivator CBP/p300 through binding with HRE, regulating the expression of various downstream target genes, such as LOXL2, SOX9, and VEGF. Simultaneously, SOX9 is a negative regulator of VEGF, whilst the expression of SOX9 target genes (i.e., Type II collagen, and Aggrecan) is initiated, which is essential for cartilage synthesis and survival during both embryonic joint development and cartilage homeostasis. HIF-1α, hypoxia-inducible factor-1α; PHDs, prolyl hydroxylases; OH: enzymatic hydroxylation; pVHL, von Hippel-Lindau tumor suppressor protein; HRE, hypoxia-response element; Ub, ubiquitinated; SOX9, SRY (sex determining region Y)-box 9; HSP90, heat shock protein 90; LOXL2, lysyl oxidase-like 2; VEGF, vascular endothelial growth factor; Cu, copper.

frontiers in Bioengineering and Biotechnology

REVIEW
published: 24 June 2020
doi: 10.3389/fbioe.2020.00641

Modifying MSC Phenotype to Facilitate Bone Healing: Biological Approaches

Stuart B. Goodman[1,2*] *and Tzuhua Lin*[3†]

[1] *Department of Orthopaedic Surgery, Stanford University School of Medicine, Redwood City, CA, United States,* [2] *Department of Bioengineering, Stanford University, Stanford, CA, United States,* [3] *Orthopaedic Research Laboratories, Stanford University, Stanford, CA, United States*

OPEN ACCESS

Edited by:
Roberto Narcisi, Erasmus University Rotterdam, Netherlands

Reviewed by:
Elena Jones, University of Leeds, United Kingdom
Bram van der Eerden, Erasmus University Rotterdam, Netherlands

****Correspondence:***
Stuart B. Goodman
goodbone@stanford.edu

†Present address:
Tzuhua Lin, Calico Life Sciences LLC, South San Francisco, CA, United States

Specialty section:
This article was submitted to Preclinical Cell and Gene Therapy, a section of the journal Frontiers in Bioengineering and Biotechnology

Received: *15 April 2020*
Accepted: *26 May 2020*
Published: *24 June 2020*

Citation:
Goodman SB and Lin T (2020) Modifying MSC Phenotype to Facilitate Bone Healing: Biological Approaches. Front. Bioeng. Biotechnol. 8:641. doi: 10.3389/fbioe.2020.00641

Healing of fractures and bone defects normally follows an orderly series of events including formation of a hematoma and an initial stage of inflammation, development of soft callus, formation of hard callus, and finally the stage of bone remodeling. In cases of severe musculoskeletal injury due to trauma, infection, irradiation and other adverse stimuli, deficient healing may lead to delayed or non-union; this results in a residual bone defect with instability, pain and loss of function. Modern methods of mechanical stabilization and autologous bone grafting are often successful in achieving fracture union and healing of bone defects; however, in some cases, this treatment is unsuccessful because of inadequate biological factors. Specifically, the systemic and local microenvironment may not be conducive to bone healing because of a loss of the progenitor cell population for bone and vascular lineage cells. Autologous bone grafting can provide the necessary scaffold, progenitor and differentiated lineage cells, and biological cues for bone reconstruction, however, autologous bone graft may be limited in quantity or quality. These unfavorable circumstances are magnified in systemic conditions with chronic inflammation, including obesity, diabetes, chronic renal disease, aging and others. Recently, strategies have been devised to both mitigate the necessity for, and complications from, open procedures for harvesting of autologous bone by using minimally invasive aspiration techniques and concentration of iliac crest bone cells, followed by local injection into the defect site. More elaborate strategies (not yet approved by the U.S. Food and Drug Administration-FDA) include isolation and expansion of subpopulations of the harvested cells, preconditioning of these cells or inserting specific genes to modulate or facilitate bone healing. We review the literature pertinent to the subject of modifying autologous harvested cells including MSCs to facilitate bone healing. Although many of these techniques and technologies are still in the preclinical stage and not yet approved for use in humans by the FDA, novel approaches to accelerate bone healing by modifying cells has great potential to mitigate the physical, economic and social burden of non-healing fractures and bone defects.

Keywords: mesenchymal stem cell, mesenchymal stromal cell, inflammation, preconditioning, hypoxia, genetic manipulation

INTRODUCTION

Complex fractures and bone defects due to musculoskeletal trauma, infection, irradiation, tumor excision, periprosthetic osteolysis, and other etiologies do not always heal without intervention. In the USA alone, non-union constitutes ∼1.9 to 10% of fractures and number ∼100,000 cases per year (Thomas and Kehoe, 2020). Systemic factors that depress bone healing include specific medical conditions (e.g., chronic renal disease, diabetes, obesity, anemia, and others), older age, hormonal deficiency (e.g., hypothyroidism), poor nutrition, excessive alcohol use, smoking, and medications that interfere with bone formation or remodeling such as certain cancer chemotherapeutic agents and biologics for treating rheumatoid arthritis, non-steroidal anti-inflammatory drugs (NSAIDs), corticosteroids, some anti-coagulants, and others (Giannoudis et al., 2007; Santolini et al., 2015; Zura et al., 2016; Thomas and Kehoe, 2020). Autologous bone graft (ABG) is the gold standard to obtain healing of bone defects and fracture non-union (Sen and Miclau, 2007). ABG contains all elements for bone regeneration including a calcified collagen-based scaffold, viable differentiated, and progenitor cells of the mesenchymal and vascular lineages, and the appropriate proteins and other factors that function as biological cues for cell-guided matrix deposition. Non-union in the elderly patient is particularly challenging, and will only increase due to the aging of our general population; in the USA, individuals over 65 years of age are estimated to double in about 30 years, from 48 million in 2015 to 88 million by 2050 (Wan et al., 2016). The elderly comprises about 13% of the population in the USA, however admissions to hospitals by the elderly, mostly for fracture care, constitute 50% of all cases (Wagner et al., 2019). Elderly patients present a unique problem, because the bone graft harvested from the iliac crest and other accessible areas is often deficient in the quality and quantity of bone (Hobby and Lee, 2013). Furthermore, mesenchymal stem cells (MSCs) from elderly patients demonstrate reduced proliferative capacity, chemotactic ability, and the potential for differentiation (Wagner et al., 2019). Similarly, endothelial progenitor cells also show decreased proliferation, migration and function.

Given the above challenges to obtain bone union in patient populations with different demographics and co-morbidities, novel strategies must be devised to augment or replace autologous bone. Potential approaches include the use of improved scaffolds and addition of exogenous growth factors; however, the most difficult aspect of this equation is to renew or revitalize the host cells locally or provide additional cells of the MSC-osteoblast cell lineage, the endothelial cell lineage, and other cells that could engraft or provide critical signaling mechanisms to enhance bone healing (Prockop, 2009). Although there has been extensive literature on the use of bone substitutes, novel scaffolds and growth factors, studies focused on providing or augmenting the deficient cellular components that are needed for bone healing have received less attention (Bravo et al., 2013; Park et al., 2018; Marongiu et al., 2020; Pereira et al., 2020).

The current review summarizes the latest *in vitro* and *in vivo* research on the manipulation of the cellular elements, focusing on MSCs, to be grafted directly into an area of bone deficiency or fracture non-union to enhance bone formation and in some instances, decrease bone degradation. Although the majority of these technologies are in the preclinical stage, the opportunities are far-reaching. To become a mainstay in the clinician's armamentarium in the future, these tools need to be thoroughly validated, and shown to be safe, efficacious and cost-effective (Gomez-Barrena et al., 2015).

One issue immediately comes to the forefront: should the medical practitioner replenish the deficient bone tissue using autologous or allogeneic cell grafting? As a general rule in any medical or surgical procedure, if there are cells or tissues available of sufficient number and quality in the host that are potentially usable with known and limited morbidity, this is normally the first option chosen. Autologous grafts are derived from the patient's own tissues; thus, these cells are non-immunogenic and will not transmit potential diseases that may be harbored by the donor (Dimitriou et al., 2011a; Egol et al., 2015; Nauth et al., 2015). However, harvesting of cells or tissues from the host takes time and therefore has an associated cost and potential morbidity (Dimitriou et al., 2011b; Hernigou P. et al., 2014; Egol et al., 2015). Furthermore, especially for larger bone defects, there may be autologous tissues or cells of insufficient quality or quantity for healing. Allogeneic tissues or in the present discussion, cells are harvested from another individual and processed under strict sterile and regulatory conditions. These cells may potentially transmit diseases, known or unknown to the host; the desired cell population(s) are usually selected and expanded, and packaged by the manufacturer prior to delivery. In addition to the potential transmission of disease and cost, when discussing MSCs, there are recent reports challenging their previously touted immune-privileged nature (Griffin et al., 2010, 2013; Ankrum et al., 2014; Berglund et al., 2017; Almeida-Porada et al., 2020). Autologous concentrated marrow cell aspirates or techniques such as the use of the reamer-aspirator also contain many different and important cell lineages and populations, as well as other factors that may enhance bone healing to a greater degree than a graft

Abbreviations: AAV, adeno-associated virus; ABG, autologous bone graft; ALK, alkaline phosphatase; ASC, Adipose-derived stem cell; bFGF, basic fibroblast growth factor; BM-MSC, bone marrow derived MSC; BMP, bone morphogenetic protein; CCL2, C-C motif ligand 2; CD, cluster differentiation; CFU-F, colony forming unit-fibroblast; COX, cyclo-oxygenase; CXCR, C-X-C motif receptor; DNA, deoxyribonucleic acid; dsDNA, double stranded DNA; EP, prostaglandin E receptor; EPC, endothelial progenitor cells; ECFC, endothelial colony-forming unit; GAMs, gene activated matrices; GMP, Good Manufacturing Practices; hASC, human adipose stem cells; HGF, hepatocyte growth factor; HIP, hypoxia-inducible factor; hSSC, human skeletal stem cell; IDO, indoleamine 2,3-dioxygenase; IL, interleukin; iNOS, inducible nitric oxide synthase; ISCT, International Society for Cell and Gene Therapy; IFNγ, interferon gamma; LIMP-1, lysosomal integral membrane protein-1; LMP-1, latent membrane protein 1; MCP-1, macrophage chemotactic protein 1; MSC, mesenchymal stromal cell. In some of the text, specific quoted authors have referred to MSC as mesenchymal stem cell. Please refer to this usage in the text below; NF-κB, nuclear factor-κB; NK cells, natural killer cells; pDNA, plasmid DNA; PDGF, platelet-derived growth factor; PG, prostaglandin; PRP, platelet rich plasma; PTH, parathyroid hormone; RANKL, receptor activator of nuclear factor-κB ligand; RBC, red blood cell; RNA, ribonucleic acid; Runx2, runt-related transcription factor 2; SDF, stroma cell-derived factor; STAT3, Signal Transducer and Activator of Transcription 3; SVF, stromal vascular fraction; TET, tetracycline; TGFβ, transforming growth factor beta; TNFα, tumor necrosis factor alpha; Tregs, T regulatory cells; VEGF, vascular endothelial growth factor.

composed of a single cell lineage (Henrich et al., 2010; Sagi et al., 2012; Seebach et al., 2015). This topic of discussion has yet to be resolved.

Although this review will focus on MSCS, all tissues require a robust vascular supply to maintain sufficient amounts of oxygen and nutrients, and rid the tissues of toxic waste. These concepts are also relevant to fracture healing and bone regeneration (Lee et al., 2008; Giles et al., 2017; Bahney et al., 2019). Endothelial progenitor cells are found in aspirates of the iliac crest, and in other sources commonly harvested for bone graft, however the numbers of endothelial colony-forming units (ECFCs) from these sources is very low (Pittenger et al., 1999). ECFCs, also called late outgrowth progenitor cells (late EPCs) come from progenitor cells in the peripheral or umbilical cord blood, and are phenotypic and functional precursors for cells of the endothelial lineage (Tasev et al., 2016). Early outgrowth progenitor cells (early EPCs) originate from the myeloid-monocytic lineage, are $CD14^+$ and $CD45^+$ and function mainly in a paracrine manner. ECFCs provide cells that incorporate into the endothelial lining of newly formed blood vessels. Combinations of ECFCs and MSCs or Adipose-derived stem cells (ASCs) are even more potent in neovascularization than ECFCs alone (Lin et al., 2012). Although ECFCs have been used extensively in scenarios of compromised vascularity and ischemia, there are also opportunities to use these cells in conjunction with MSCs for fracture healing and the regeneration of bone (Liu et al., 2012, 2013; Zigdon-Giladi et al., 2015; Sun et al., 2016; Tasev et al., 2016; Giles et al., 2017; Grosso et al., 2017).

METHODS OF CELL HARVESTING

General Comments Concerning Cell Sources

Traditionally, bone graft for the purposes of obtaining union of fractures or healing of bone defects was harvested from the anterior or posterior iliac crest, because this area contained an abundance of all of the elements for osteogenesis. Other areas for obtaining bone graft are sometimes used, especially when working in local areas, such as the spine during decompression and fusion, greater trochanter, proximal or distal tibia, humerus etc. As an alternative, the reamer aspirator device can be used to harvest the contents of the medullary canal of long bones. The resultant aspirate has excellent regenerative capacity for bone healing, equivalent or in some studies superior to that of iliac crest graft (Henrich et al., 2010; Sagi et al., 2012; Seebach et al., 2015). Furthermore, aspirate from the reamer device can be used for grafting of large critical sized defects (Egol et al., 2015).

An alternative source of cells for bone healing is fat, which is usually abundant and can be accessed via liposuction. Fat is composed of ∼90% mature fat cells and ∼10% of a stromal vascular fraction (SVF). The SVF is composed of a heterogeneous population of cells including fibroblasts, vascular smooth muscle cells and pericytes, endothelial cells, monocyte/macrophages, lymphocytes, ASCs, and other precursor cells. It has been reported that up to 1 X 10^7 ASCs can be isolated from ∼300 cc of fat aspirate (Romagnoli and Brandi, 2014). ASCs have been reported to have very similar properties to bone marrow derived MSCs, although there are differences in some of the cell surface markers such as adhesion molecules (De Ugarte et al., 2003). ASCs are capable of differentiation into mesenchymal-based cells such as adipocytes, osteoblasts, chondrocytes, myocytes, and other cells (Tajima et al., 2018). The fat-derived cell population can be used either as a point-of care product or processed further to isolate, expand and concentrate the desired cell population (Romagnoli and Brandi, 2014; Grayson et al., 2015; Alt et al., 2020). Studies have shown that differentiated ASC-derived osteoblast lineage cells are effective in forming bone and healing bone defects (Parrilla et al., 2011; Mizuno et al., 2012; Tajima et al., 2018). Several recent reviews have summarized the preclinical and clinical data relevant to the use of ASCs for bone healing (Romagnoli and Brandi, 2014; Grayson et al., 2015; Tajima et al., 2018). Despite the known efficacy of ASCs for healing of bone, the use of this source is uncommon in orthopaedic surgery and is more common in the plastic surgery, perhaps because of the concurrent liposuction procedure.

Harvesting From the Iliac Crest

Autologous bone graft harvested from the iliac crest is the gold standard by which other sources and techniques are measured. The technique of cell harvesting for the purposes of grafting of bone defects, non-union, osteonecrosis and other bone deficiencies has been well-described (Hernigou et al., 2005, 2015; Piuzzi et al., 2018). The technique should be mastered with a clear understanding of how to accomplish the technique safely, according to considerations of pelvic anatomy (Hernigou J. et al., 2014). Although some will report that red blood cells (RBCs) constitute the majority of cells in the marrow, by definition, RBCs are not cells because they do not possess a nucleus. The same objection could be made for platelets. It should be recognized that the majority of "true" cells in the iliac crest are not progenitor cells for osteoblasts or endothelial cells. The pelvic marrow is mostly composed of myelopoietic white blood cells (about 50%), erythropoietic cells (25%) and lymphocytic lineage cells, in a stroma containing fibroblasts, adipocytes, osteoblasts, osteoclasts, and endothelial cells. With aging, the normally "red" marrow becomes "yellow," due to a predominance of adipocytes. Colony forming unit-fibroblast (CFU-F) cells that are precursors of the mesenchymal stem cell lineage are rare, and constitute approximately one out of every 30,000+ nucleated cells harvested from the anterior iliac crest, or ∼600–1,200 progenitor cells per milliliter (cc) of aspirated unconcentrated bone marrow (Muschler et al., 1997; Hernigou et al., 2005, 2015). Repeated aspiration from the same location further dilutes the number of nucleated cells harvested, because the void quickly fills with red blood cells and plasma, that are less dense compared to the more densely packed cellular elements (Batinic et al., 1990; Muschler et al., 1997). It is therefore recommended that only 2 milliliters (ml) of marrow be aspirated in any one location, prior to repositioning the needle to another location. This can be done through the same insertion point or using another point of entry

into the bone. Additionally, there are age-related and gender-related differences in the number of nucleated cells harvested. Muschler et al. noted that the number of nucleated cells in aspirates from elderly individuals (age 70 or older) are 50% (or substantially) less than those from teenagers (Muschler et al., 2001). Furthermore, the number of CFU-F cells derived from these nucleated cells was proportionally the same for aged men but was significantly less for elderly woman. The autologous iliac crest cell aspirates are gathered into heparinized syringes to avoid clotting.

Because of the paucity of cells, especially progenitor cells, in the aspirates, a method of concentration of the nucleated cells is normally used prior to local injection. Several studies have demonstrated that the desired outcome, namely fracture union or bone healing, is directly proportional to the number and concentration of progenitor cells that are injected locally (Hernigou and Beaujean, 2002; Hernigou et al., 2005, 2009). Concentration of the aspirated marrow also decreases the eventual volume that is injected locally, usually into a very confined space.

One classification system for describing different methods of cell separation and isolation of MSCs is as follows: (a) cell adherence to plastic surfaces; (b) gradient centrifugation methods; (c) membrane filtration methods; (d) Fluorescently labeled antibodies that bind to surface or intracellular molecules; and e. magnetically labeled antibodies that bind to surface molecules (Nicodemou and Danisovic, 2017). These methods all have their strengths and limitations. To maximize efficiency and minimize cost, the delivery of autologous byproducts, whether cells or biologics or both, would be optimized if these substances were delivered at the point-of-care, i.e., when the fracture, non-union or bone defect was undergoing additional invasive procedures such as surgical stabilization. Thus, centrifugation is the method that is most commonly used to concentrate the nucleated cell portion of bone aspirates for management of bone defects. Centrifugation separates different fluidic composites based on their differential densities. Centrifugation may be combined with the use of Ficoll, Ficoll-Paque, or other density gradient media or devices for cell separation. The above methods disperse and isolate the components of the marrow aspirate into various layers based on their density; the layer containing the mononuclear cells is called the buffy coat. The buffy coat contains a higher percentage of osteoprogenitor cells than in the harvested uncentrifuged marrow. Although the exact degree of concentration is controversial, most systems state that the level of concentration is ∼2X-7X (Hegde et al., 2014; Dragoo and Guzman, 2020). There is also some controversy as to which commercial aspiration and concentration system is the optimal one for clinical use. The results of these systems are generally very similar (Hegde et al., 2014; Dragoo and Guzman, 2020). However, it must be emphasized that the manufacturers' instructions should be followed carefully to optimize cell retrieval. There are other techniques, often more expensive and/or limited in availability, to concentrate the buffy coat or subsets thereof, including fluorescence-activated cell sorting (FACS), selective retention that uses a special device incorporating a semipermeable membrane for cell selection based on their surface markers, magnetic separation using hyaluronan surface markers, the use of active and passive microfluidic devices, buoyancy activated cell sorting and others (Muschler et al., 2005; Caralla et al., 2012, 2013; Joshi et al., 2015).

METHODS OF CELL EXPANSION AND SELECTION

One issue that needs to be addressed initially pertains to the cell type(s) that the clinician would want to select for injection/grafting into a defect to enhance bone healing. Osteoblasts are differentiated cells that do not divide. Thus, a more logical option for regeneration of bone is to revert to an earlier stage in the lineage, such as the pre-osteoblast or the MSC. In preclinical studies, and in limited clinical trials (Gomez-Barrena et al., 2015, 2020; Lee et al., 2019; Hutchings et al., 2020), MSCs have been the target cell for isolation. As outlined above, MSCs are rare in the bone marrow; the approach most commonly used is expansion *in vitro*, and then injection or open grafting in a suitable carrier. This technique for bone regeneration is being performed outside of the USA, because it constitutes more than "minimal manipulation" of cells (U. S. Food and Drug Administration, 2017).

The definition of an MSC is controversial (Caplan, 2017a,b). Indeed, the International Society for Cell and Gene Therapy (ISCT) has distinguished the two terms mesenchymal stem cell and mesenchymal stromal cell (Viswanathan et al., 2019). In a position statement on nomenclature published in 2005 and updated in 2019, the ISCT states (*author: bracketed references omitted*): "The former (author: i.e., *mesenchymal stem cell*) refers to a stem cell population with demonstrable progenitor cell functionality of self-renewal and differentiation, whereas the latter (*author:* i.e., *mesenchymal stromal cell*) refers to a bulk population with notable secretory, immunomodulatory and homing properties." (Horwitz et al., 2005; Viswanathan et al., 2019). Furthermore, they stated: "a minimal criteria to define multipotent MSCs as being plastic adherent, expressing CD73, CD90, and CD105, lacking the expression of hematopoietic and endothelial markers CD11b, CD14, CD19, CD34, CD45, CD79a, and HLA-DR and capable of *in vitro* differentiation into adipocyte, chondrocyte and osteoblast lineages" (Dominici et al., 2006). In the latest definition, the ISCT has endorsed continued use of the term MSC (Mesenchymal Stromal Cell) but recommends that (1) the tissue source or origin of the cells be clearly specified, (2) functional definitions must clarify whether one is referring to mesenchymal stromal cells or mesenchymal stem cells, (3) the term mesenchymal stromal cell be used to describe bulk unfractionated cell populations to recognize the fact that this may include other cell types, but not hematopoietic or endothelial cells (Viswanathan et al., 2019). This discussion is even more complex, due to the recent description of the Mouse Skeletal Stem Cell and the Human Skeletal Stem Cell (hSSC) (Chan et al., 2018; Gulati et al., 2018). The hSSC is defined as a self-renewing multipotent skeletal stem cell that is $PDPN^{+}CD146^{-}CD73^{+}CD164^{+}$, and

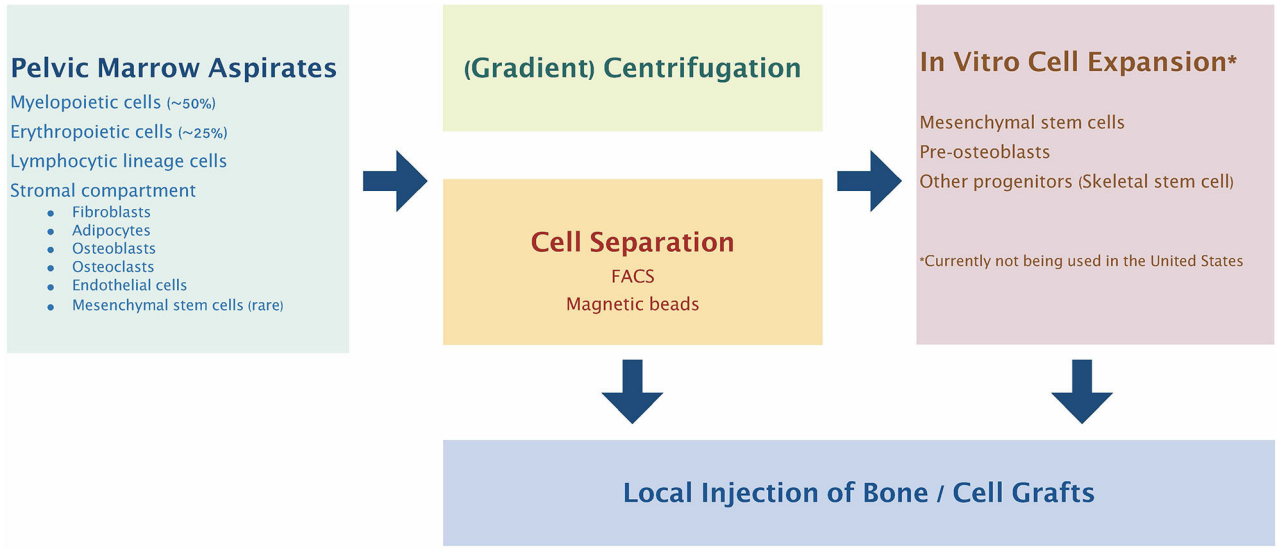

FIGURE 1 | Bone marrow cell harvesting, selection, and expansion process most commonly used clinically. Pelvic marrow aspirates are concentrated by centrifugation and/or selection of specific cell populations before injection into the bone defect site. Alternatively, the selected progenitor cells can be expanded and manipulated *in vitro* to further enhance their therapeutic potential.

generates progenitors of bone, cartilage, and stroma, but not fat.

Given the above controversy, there have been many different methods for isolation of what the authors describe as mesenchymal stem cells (Kanczler et al., 2019) (**Figure 1**). One such methodology for GMP compliant generation of bone marrow derived MSCs and expansion on a large scale for a multicenter study of fracture healing in Europe has been described in detail (Fekete et al., 2012; Rojewski et al., 2013; Gomez-Barrena et al., 2020). This and other studies using MSCs are ongoing. However, it must be emphasized that such studies must be interpreted in light of the particular cell source, isolation and identification protocols, methods and details of cell delivery, the particular application for which these cells are given, and the methods of assessment of outcomes.

One further point needs emphasis. It is clear that MSCs interact with many other cells in the hematopoietic and mesenchymal lineages. In fact, there is substantial evidence that interactions with macrophages, T cells and other cells in the hematopoietic lineage are critical to the preconditioning and activation of MSCs and provide important cues and guides for their immunomodulatory function (see below). Thus, it might be prudent to consider not just the delivery of MSCs alone, but combinations of different cell lineages for optimal healing of bone defects (Konnecke et al., 2014; Croes et al., 2015, 2016; Kovach et al., 2015; Bastian et al., 2016; Loi et al., 2016b; El Khassawna et al., 2017; Pajarinen et al., 2019).

Given the fact that the first step in bone formation is inflammation, it is logical to concentrate on the cell lineages that have been shown to be most impactful to inflammation in the context of bone healing (Marsell and Einhorn, 2011). As outlined below, pro-inflammatory mediators from cells of the innate immune system including macrophages, mast cells, polymorphonuclear leukocytes and others are critical initially to preconditioning, priming and activating MSCs into an immunomodulatory and pro-reconstructive phenotype (Kouroupis et al., 2019). Furthermore, MSCs possess Toll-like receptors which are important to the specific pro- or anti-inflammatory phenotype of MSCs (Delarosa et al., 2012; Najar et al., 2017; Kouroupis et al., 2019). In this respect, interactions between macrophages and MSCs are the prototype for studying innate immune system-MSC communication. These interactions are highly contextual; although the innate system presents a preprogrammed sequence of events when subjected to an adverse stimulus, the specific interactions occur in the setting of the local physical, chemical and biologic microenvironment characteristic of a specific organ system (Kouroupis et al., 2019). Thus, different cell lineages provide distinctive signals to MSCs, and alter their function according to local cues. For example, within the hematopoietic cell niche, T cell subpopulations interact with MSCs to determine the balance between myeloid differentiation and adipogenesis (Najar et al., 2018). With respect to bone, T regulatory cells (Tregs) have been noted to play a significant role in regulating MSC differentiation and osteoclast function (Li et al., 2018). Other interactions between T and B cell subsets and MSCs modulate the proliferation and differentiation of MSCs, affecting bone formation and remodeling (Konnecke et al., 2014; Ono et al., 2016). These complex interactions have fostered the field of osteoimmunology in which innate and adaptive immune cells interact with cells of the MSC-osteoblast-osteocyte lineage to regulate bone healing and remodeling (Kovach et al., 2015; Ono and Takayanagi, 2017).

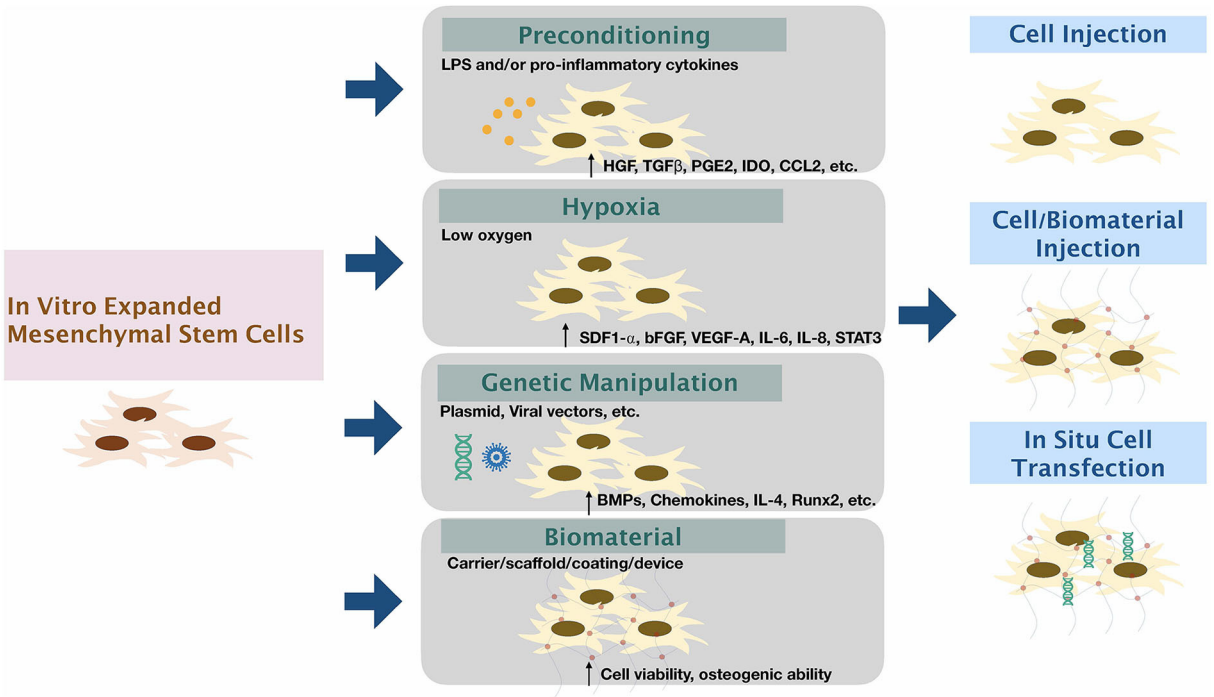

FIGURE 2 | Modifying mesenchymal stem cells to enhance therapeutic functions. The expanded mesenchymal stem cells can be modified via (1) Preconditioning by stimulation by inflammatory factors/substances; (2) Exposure of cells to low oxygen tension; (3) Genetic manipulation using viral or non-viral vectors; and (4) using biomaterial carriers/scaffolds/coatings/devices along or in combination with other methods to enhance the function of MSCs.

METHODS TO ENHANCE THE FUNCTION OF HARVESTED CELLS (FIGURE 2)

Preconditioning of MSCs With Biologics

MSCs engage in crosstalk with other cells of different lineages, and in this way, are exposed to biological cues from the local microenvironment and other regional tissues. This intercellular crosstalk is accomplished directly or indirectly through processes that introduce MSCs to signals and byproducts from neighboring cells. This may occur directly via cell-to-cell contact, or indirectly by exposure to secreted cytokines, chemokines, exosomes, or other substances that interact with receptors or through other signaling mechanisms (e.g., by phagocytosis) by MSCs (Zhang et al., 2019).

Macrophages are much more than phagocytic cells within the innate immune system. Indeed, macrophages are versatile cells with numerous functions and capabilities with respect to immunomodulation and tissue regeneration; this is due to the macrophage's phenotypic plasticity that is responsive to local biological and mechanical signals and cues (Mantovani et al., 2013). MSCs and macrophages have a particularly intricate bidirectional system of interaction. The activation or priming of MSCs by macrophages is one such example. Pro-inflammatory substances such as Tumor Necrosis Factor alpha (TNFα), Interferon gamma (IFNγ), Interleukin-1 (IL-1) and other substances prime MSCs into a state facilitating the resolution of inflammation, vasculogenesis, and tissue healing/reconstruction (Kim and Hematti, 2009; Glass et al., 2011; Carvalho et al., 2013; Croes et al., 2015; Karnes et al., 2015). One paradigm emanates from the concept of polarization of MSCs into MSC1 and MSC2 phenotypes (Waterman et al., 2010). MSC1 cells release primarily pro-inflammatory mediators whereas MSC2 cells are primarily immunosuppressive/pro-reconstructive. Thus, exposure of "uncommitted" MSCs in the stroma to inflammatory mediators (cytokines, chemokines etc.) from macrophages, polymorphonuclear leukocytes (PMNs) and other cells polarizes the MSC into an immunomodulating, tissue regenerative phenotype. Teleologically, this system of checks and balances would tend to preserve the integrity of the local tissues when faced with potentially lethal stimuli, which if persistent, would overwhelm the organism.

Preconditioning of MSCs with IFNγ upregulates many growth factors [such as hepatocyte growth factor (HGF), Transforming Growth Factor beta (TGFβ), and others], Prostaglandin E2 (PGE2), Indoleamine 2,3-dioxygenase (IDO)- an immune checkpoint molecule, the chemokine CCL2 (also known as Macrophage Chemotactic Protein 1 or MCP-1), suppresses $CD4^+$ and CD 8^+ T cell and NK cell proliferation, and polarizes macrophages from a pro-inflammatory M1 to an anti-inflammatory M2 phenotype (de Witte et al., 2015; Lin et al., 2017a; Philipp et al., 2018; Noronha Nc et al., 2019). Preconditioning of MSCs with TNFα leads to similar though less pronounced results compared to IFNγ (de Witte et al., 2015; Noronha Nc et al., 2019). Some of the reported studies

have used adipose-derived MSCs (ASCs) whereas others have used bone marrow derived MSCs (BM-MSCs). Results of preconditioning with TNFα on bone regeneration have varied for different cell sources. However, the majority of studies suggests that preconditioning with low dose TNFα enhances immunomodulation and osteogenesis (Lu Z. et al., 2013; Croes et al., 2015; Bastidas-Coral et al., 2016; Lu et al., 2017). However, Lin et al. found that neither IFNγ nor TNFα preconditioning, alone or in combination, promoted osteogenesis using murine primary MSCs. In contrast, TNFα in combination with lipopolysaccharide promoted alkaline phosphatase activity and new bone formation *in vitro* (Lin et al., 2017a).

Bastidas-Coral and colleagues explored how exposure to the cytokines TNF-α, IL-6, IL-8, IL-17F, and IL-4 affected the proliferation and osteogenic differentiation of human adipose stem cells (hASCs) *in vitro* for 72 h (Bastidas-Coral et al., 2016). The different cytokines had variable effects on different markers of bone formation including alkaline phosphatase expression and bone nodule formation. Interestingly, addition of IL-6 increased both of the above markers in dramatic fashion and was thought to be a candidate for future studies on bone repair.

It is clear that preconditioning of MSCs with pro-inflammatory factors from macrophages and other cells alters MSC phenotype, and generally supports bone formation. The reverse is true as well: byproducts from MSCs affect macrophage phenotype, generally providing a faciliatory stimulus for bone formation (Prockop et al., 2010; Pajarinen et al., 2019). In fact, MSCs were found to provide an important immunomodulatory function on inflammatory processes via iNOS and a COX2 dependent pathway to enhance PGE2 production (Nemeth et al., 2009; Maggini et al., 2010). These events increase IL-10 secretion by macrophages through binding with Prostaglandin E receptors (EP)2 and EP4. The effects of MSCs on macrophages and other cells is of immense importance; further details can be found in other publications (Kim and Hematti, 2009; Cho et al., 2014; Pajarinen et al., 2019).

Platelet Rich Plasma (PRP) is a derivative of blood, and consists of plasma, plasma proteins, and in addition, the contents of the alpha granules of activated platelets which contain growth factors, cytokines, chemokines and other substances. *In vitro* studies have shown that PRP increases the proliferation and differentiation of MSCs and ASCs, important cells for the formation of bone (Kasten et al., 2006; Vogel et al., 2006; McLaughlin et al., 2016). A recent systematic review on the subject, which summarized the preclinical and clinical data on the subject concluded that the utility of PRP for bone healing is still controversial. Although *in vitro* studies are suggestive of potential utility of PRP in facilitating bone healing, the many different methods and techniques of preparation and use of PRP, including numerous animal models and methods of evaluation have yielded research literature of low quality (Roffi et al., 2017). Clinical studies in humans on the use of PRP for the treatment of acute fractures, delayed unions and non-unions were also guarded (Roffi et al., 2017). The majority of the studies that the authors reviewed led them to the finding that key aspects that could potentially affect the final outcome including platelet concentrations, leukocyte components, activation modality and others were either inconsistent or not stipulated in the publication (Roffi et al., 2017). The authors' final conclusion was the following: "Overall, the available literature presents major limitations in terms of low quality and extreme heterogeneity, which hamper the possibility to optimize PRP treatment and translate positive preclinical findings on its biological potential to favor bone healing into a real clinical benefit." (Roffi et al., 2017). A recent study examining the effect of PRP on a healing osteotomy for anterior cruciate deficiency in dogs found no significant effect of PRP on healing of the osteotomy as assessed using radiographs, ultrasound, or MRI (Franklin et al., 2017). This skepticism is echoed in other reviews of the use of PRP in fractures and non-unions in humans (Nauth et al., 2015; Marongiu et al., 2020). A systematic review and meta-analysis of the use of PRP in oral surgery concluded that the studies were of low quality; in periodontal defects the addition of PRP may have a slight benefit (Franchini et al., 2019). It is clear that further well-designed prospective studies with appropriate controls need to be performed prior to widespread use of PRP as an adjunct for bone healing.

Numerous cytokines, growth factors, pharmacological agents and chemicals have been shown to activate or prime MSCs for various applications in different organ systems (Noronha Nc et al., 2019). Some of these methods and applications are relevant to bone. The reader is referred to these publications for further information.

Exposure of Cells to Low Oxygen Environments

Though ambient conditions (i.e., room air) contain ∼21% oxygen (O_2) and *in vitro* cell culture O_2 tension is about 18%, the physiological O_2 tension in bone marrow and in the peripheral tissues *in vivo* is only 1–7% (Mohyeldin et al., 2010; Wagegg et al., 2012). This low oxygen tension is also seen locally after musculoskeletal trauma and fracture, and in other instances of inflammation. Hypoxic conditions locally are important determinants of the subsequent function of osteogenic and vasculogenic progenitor cells (Volkmer et al., 2010; Garcia-Sanchez et al., 2019). The cellular response to hypoxia is generally controlled by the transcription factor hypoxia-inducible factor (HIF)-1. HIF-1 is activated under hypoxic conditions and controls numerous cellular processes including the method of cellular metabolism (favoring anaerobic glycolysis over aerobic oxidative metabolism), angiogenesis, and erythropoiesis. There has been some controversy concerning the effects of hypoxia on MSCs and their downstream lineage cells. Currently, with reference to human cells, hypoxia has been shown to stabilize the immunophenotype of MSCs and shifts their differentiation from the adipogenic to the osteogenic lineage in a HIF dependent manner (Wagegg et al., 2012). Furthermore, hypoxia induces the secretion of stroma cell-derived factor 1 alpha (SDF1-α or CXCL12), a potent chemotactic factor for MSCs and other cells; SDF1-α functions together with the chemokine receptor CXCR4 (Park et al., 2017). Numerous other anti-inflammatory and pro-reconstructive cytokines and chemokines are also upregulated by hypoxia (Gabrielyan et al., 2017; Quade et al., 2020). In mice, both

MSCs and the media from bone marrow-derived MSCs cultured under hypoxic conditions demonstrated increased amounts of basic fibroblast growth factor (bFGF), vascular endothelial growth factor A (VEGF-A), interleukin 6 (IL-6), and interleukin 8 (IL-8), and enhanced the proliferation and migration of endothelial cells and other cells including macrophages (Chen et al., 2014). Osteogenesis and angiogenesis are also controlled by the transcription factor Signal Transducer and Activator of Transcription 3 (STAT3), an important regulator of bone homeostasis (Yu et al., 2019). Using murine MSCs *in vitro* and a femoral defect model, hypoxia was shown to upregulate the phosphorylation of STAT and was important to the healing of a bone defect. Interestingly, the duration of hypoxia was critical to osteogenesis and angiogenesis, with 3 days of exposure being optimal (Yu et al., 2019). Other studies in animals have confirmed hypoxic preconditioning as a method to enhance osteogenesis, angiogenesis and bone healing, even in aged animals (Fan et al., 2015; Zhang et al., 2018). Hypoxic preconditioning of MSCs has also been suggested as a treatment for osteonecrosis of the femoral head, where local hypoxic conditions are present (Ciapetti et al., 2016).

Genetic Manipulation of Cells

Gene therapy was originally conceived as a treatment for specific intractable genetically-based diseases in which the gene to be transferred was either missing or significantly altered, resulting in a phenotype that was deficient in a clinically significant manner. This classic approach to gene therapy might be applied to Mendelian based diseases such as hemophilia, sickle cell disease, Gaucher's disease, osteogenesis imperfecta, and others. Current definitions of gene therapy have changed due to recent technical advances in genetic engineering of cells. Presently, potential treatments include vector-delivered gene therapy, gene-modified cell therapy and gene editing (Salzman et al., 2018). Salzman et al. summarized the clinical aim of these treatment concepts succinctly: "Rather than treating disease symptoms, gene therapy can address the root causes of genetic diseases by modifying expression of a patient's genes or by repairing or replacing abnormal genes." (Salzman et al., 2018).

Although non-union of fractures and deficient healing of bone defects are usually not life-threatening, these conditions often cause significant pain and functional impairment. In this regard, methods to expedite the healing of bone defects and fractures has merit. Thus, the concept of gene therapy has entered the realm of bone tissue engineering and repair (Evans, 2010; Lu C. H. et al., 2013; Balmayor and van Griensven, 2015; Evans and Huard, 2015; Atasoy-Zeybek and Kose, 2018; Ball et al., 2018; Betz et al., 2018; Bougioukli et al., 2018; Shapiro et al., 2018; Freitas et al., 2019). The advantages of gene delivery include the persistent release of a growth factor(s) or other substance(s) over a period of weeks to months, which is generally longer than with local protein delivery devices. Some of the disadvantages of gene delivery include less control over the timing and dose of delivery of a biological agent, safety concerns such as the potential for unintended adverse effects, including carcinogenicity on non-target cells and limitations regarding irreversibility of treatment.

On a practical level, gene therapy has been accomplished using different methods including: non-viral chemical and physical methods to deliver DNA or microparticles into cells, gene activated matrices (GAMs) or scaffolds that enable the slow release of genetic material to the surrounding cells, the use of viral vectors to transfer genes into cells *in vivo*, and genetically engineered autologous or allogeneic cells *ex vivo* with subsequent delivery of these cells *in vivo* (Atasoy-Zeybek and Kose, 2018; Shapiro et al., 2018). All of these methods have been used in preclinical studies to facilitate bone formation, and some are in early clinical trials (see summaries in references D'Mello et al., 2017; Atasoy-Zeybek and Kose, 2018; Betz et al., 2018; Freitas et al., 2019). A variety of genes that have been delivered in various ways including BMP-2, BMP-4, BMP-7, HIF-1, lysosomal integral membrane protein-1 (LIMP-1), PTH 1-34, PDGF-B, VEGF, caALK2 (a BMP receptor), Runx2, RANKL, and combinations thereof (D'Mello et al., 2017; Atasoy-Zeybek and Kose, 2018).

Non-viral based vector therapy is usually accomplished using circular plasmid dsDNA. This method is generally inexpensive, relatively fast, and is accomplished in one step via direct injection, with less concern regarding multistep contamination seen with *ex vivo* methods (Atasoy-Zeybek and Kose, 2018). However, there are concerns regarding the generally low levels of transfection of the specific target cells, unintended transfection of other cells, the short duration of gene expression *in vivo* and therefore the low levels of protein expression. Techniques that have been employed include electroporation, sonoporation, microinjection and other mechanical and biological methods.

Gene activated matrices (GAMs) use a three-dimensional scaffold which is porous and usually biodegradable to transfer plasmid DNA (pDNA) to the local environment (D'Mello et al., 2017; Atasoy-Zeybek and Kose, 2018). The pDNA is transfected into neighboring cells that infiltrate the GAM; these cells subsequently produce the desired protein. The method is relatively inexpensive and easy to produce even on a large scale, is locally effective in producing the desired biological factors, and generally demonstrates low toxicity, pathogenicity, mutagenicity, carcinogenicity and immunogenicity. Commonly used scaffolds include collagen, gelatin, alginate, chitosan, and silk. More mechanically stable structures, such as allograft bone, calcium-based ceramics, and combinations of polymers with/without calcium-based compounds have been used. The physical and chemical properties of the scaffold are key to cellular infiltration and attachment, as well as gene delivery. The GAM technique has been successfully used in pre-clinical studies to release various growth factors (such as VEGF, BMPs, and others) in a balanced manner to optimize the desired effects and limit toxicity. Recently, the use of RNA-based scaffolds for delivery of mRNA, miRNA, and siRNA has been described (Leng et al., 2020). This novel technology can deliver one or more RNA factors simultaneously to the tissues locally. However, the exact cells that are transfected cannot be precisely controlled.

Viral vectors are employed to aid in the transmission of DNA into the host cell (Evans and Huard, 2015; Ball et al., 2018). The virus is altered to make it less virulent and pathogenic, and the genetic sequence of the intended biological factor to be delivered is added to the viral DNA to form a recombinant structure. This

recombinant viral vector can be used as a stand-alone circular plasmid (episome) for short term effects or can be integrated into the DNA of the host cell for longer term expression (Balmayor and van Griensven, 2015; Atasoy-Zeybek and Kose, 2018; Ball et al., 2018; Betz et al., 2018). Some of the considerations for viral-associated gene therapy include the capacity of the virus for packaging DNA, the efficiency of transduction and gene expression, the desired timing and duration of gene activity, the target cell for potential gene incorporation, the complexity and cost of the construction, the regulation and monitoring of gene and protein expression, whether the virus affects dividing and non-dividing cells alike, and how toxic/mutagenic/immunogenic will the construct be for the host. The most commonly used viral vectors include adenovirus, adeno-associated virus (AAV), lentivirus, and retrovirus. Each of these has different characteristics, risks and benefits (Evans and Huard, 2015; Atasoy-Zeybek and Kose, 2018). Of these, adenovirus has been the most commonly used for bone healing, although they are highly immunogenic and evoke a host response that often limits protein expression (Evans, 2010; Evans and Huard, 2015; Atasoy-Zeybek and Kose, 2018; Bougioukli et al., 2018).

Ex vivo genetically engineered autologous or allogeneic cells for *in vivo* cell delivery have been used for several decades in preclinical studies (Balmayor and van Griensven, 2015; Ball et al., 2018; Betz et al., 2018). Autologous cells are harvested from bone marrow or other sources (e.g., ADSCs, muscle cells etc.), selected out (if desired), expanded and then genetically manipulated with insertion of genes using viral or non-viral methods. Allogeneic cells, though less commonly used, are generally MSCs because of their relatively immune-privileged status to the host (although this is controversial) (Berglund et al., 2017; Kiernan et al., 2018). All of the considerations outlined above concerning viral non-cellular infection are relevant to viral cellular infection as well. The cells are transduced *ex vivo* and then implanted into the bone defect or fracture gap in orthopaedic applications. Adenoviral based constructs are the most commonly used viral agents, but other vectors have their proponents (Balmayor and van Griensven, 2015; Ball et al., 2018; Betz et al., 2018). Growth factors relevant to osteogenesis including BMP-2, BMP-4, BMP-7, Epstein-Barr virus latent membrane protein 1 (LMP-1) and others have been inserted into healing defects with some success. Concerns regarding safety and efficacy, as outlined above for viral vectors are applicable. Furthermore, *ex vivo* transfection is rather complex, laborious, time-consuming and expensive. To control the delivery spatially and temporally, novel concepts have been introduced including aptamers which are oligonucleotide or peptide molecules that bind to specific molecules on targeted cells, on-off switches that modulate gene expression (e.g., TET-on/TET-off systems with control by the administration of doxycycline), sensing receptors linked with effector molecules that control subsequent gene expression in a negative feedback loop and the use of tissue specific promoters (Balmayor and van Griensven, 2015).

Can the process of *ex vivo* viral gene infection be linked to *in vivo* cell administration in a more expeditious manner? Lieberman's group has performed extensive studies in rodents with human cells to examine the over-expression of BMP-2 using ASCs and BM-MSCs to enhance bone healing. Recently, they showed that lentiviral transduction of the BMP-2 gene into human mononuclear bone marrow cells using a "next day" or overnight protocol was less effective than the standard "two-step" tissue expansion approach in healing of a rat critical sized femoral defect (Bougioukli et al., 2019). However, both approaches showed improved new bone formation compared to the controls using plain radiographs, microCT imaging, and histomorphological analysis.

Acute inflammation is the first stage of fracture healing (Gerstenfeld et al., 2003; Loi et al., 2016a). Healing of fractures and bone defects cannot proceed through the typical course of biological events if acute inflammation persists beyond several days to a week. Chronic inflammation and fibrosis are associated with non-union of fractures and decreased healing of bone defects. These facts suggest opportunities for genetic manipulation of the microenvironment of the fracture gap and chronic bone defect. One strategy is to encourage migration of cells into the hematoma, non-union or defect site via the local delivery of genetically altered cells that overexpress key chemokines for MSCs and vascular progenitor cells (Herrmann et al., 2015). Some of the chemokines which have been used for this and related purpose (such as osteoporosis) include Stromal Cell-derived Factor 1 (SDF-1), CCL7 (Monocyte Chemotactic Protein 3 or MCP-3), and others (Lien et al., 2009; Herrmann et al., 2015). Growth factors such as BMP-2 and PDGF and others have chemotactic properties in addition to their direct osteogenic and vasculogenic effects (Lu C. H. et al., 2013; Chen et al., 2015; Bougioukli et al., 2019).

Our laboratory's approach to regulate the healing of bone defects is centered on the modulation of the inflammatory response. Interleukin-4 is an anti-inflammatory cytokine that facilitates the resolution of inflammation and promotes tissue regeneration (Loi et al., 2016a,b). We have generated several genetically engineered constructs that over-express IL-4 to facilitate the healing of chronic bone defects. These include transduced murine bone marrow-derived mesenchymal stromal cells (MSCs) that are NF-κB responsive and IL-4 over-expressing, or contain constitutively active IL-4 expression lentiviral vectors (Lin et al., 2017b, 2018a,b). These constructs have been shown to produce clinically significant amounts of IL-4 either continuously, or only when NF-κB is upregulated in a negative-feedback loop. These constructs change M1 pro-inflammatory macrophages into an M2 anti-inflammatory pro-reconstructive phenotype and have been shown to reverse the suppression of bone formation by an adverse stimulus: contaminated polyethylene particles. The genetically modified cells showed *in vivo* survival similar to the vector only controls, and a significant biological effect (increased bone mineral density) for at least 4 weeks when implanted into the bone marrow cavity. NFκB sensing IL-4 secreting MSCs appear to function as an "on demand" drug delivery system to modulate chronic inflammation. Current efforts are focused on constructs to modulate acute inflammation and cellular chemotaxis.

As outlined above, there appears to be numerous potential opportunities for the use of gene therapies to facilitate bone healing and mitigate chronic inflammation; however, these

therapies are not yet FDA approved, and must first demonstrate obligatory safety and efficacy profiles and show cost effectiveness, in order to be used in clinical practice.

Other Techniques to Enhance the Function of MSCs

Bone healing is dependent on both biological and mechanical cues and the local environment to which it is subjected. When composite grafting techniques are used i.e., a material together with MSCs or cell aspirate, the physical, chemical and material properties of the carrier/scaffold/coating/device used will determine, in part, the phenotype of the cells (Nava et al., 2012; Luangphakdy et al., 2013; Hanson et al., 2014; Chen et al., 2019). Although a detailed discussion of the physical, chemical and material determinants affecting MSC phenotype is beyond the scope of this review, some general points can be made.

In tissue engineering applications for the healing of bone defects, various biomaterials are often used in conjunction with MSCs. These materials are composed of different hydrogels and polymers, mineralized proteins, ceramics, porous metals etc. In clinical scenarios relevant to healing of bone defects, cell fate is determined in part by numerous properties of the materials used including the composition, morphology, viscosity, stiffness, porosity, topography, surface wettability, surface energy, surface charge, molecular attachments, protein absorption and numerous other factors (Wilson et al., 2005; Luangphakdy et al., 2013; Hanson et al., 2014; Bilem et al., 2016; Chen et al., 2019). For example, in *in vitro* studies, the topographical differences between 2D and 3D culture conditions have been shown to alter the crosstalk between MSCs and macrophages, and their immune profile (Valles et al., 2015). In studies of healing of critical sized bone defects in canines, cancellous allograft bone proved to be the optimal scaffold, compared to numerous other polymers (Luangphakdy et al., 2013). This seems intuitive, given the material architectural and biomechanical similarities of allograft cancellous bone to host bone. For the facilitation of bone healing for critical size defects with insufficient autologous bone, the optimal biomaterial template might be decellularized functionalized cancellous allograft bone, in which the surface is coated with molecules to increase cell attachment preferentially for the MSC-osteoblast and the vascular cell lineages. The processing of this bone could be optimized to ensure that it was of sufficient mechanical strength for the indication proposed. Further basic research in this area would provide exciting opportunities for novel preclinical studies and subsequent translation to the clinic.

DISCUSSION

Although the majority of fractures heal uneventfully, up to 10% result in delayed or non-union (Thomas and Kehoe, 2020). Moreover, bone defects due to traumatic and non-traumatic etiologies will not heal if the defect is large, and the biological and mechanical environments are unfavorable (Giannoudis et al., 2007). Autologous bone graft is the gold standard for treatment of non-unions, bone defects and other causes of localized deficiencies in bone stock. In fact, autologous bone graft is the second most frequent tissue that is transplanted worldwide, second only to blood transfusion (Campana et al., 2014). However, autologous bone graft may be insufficient in quantity and/or quality to fulfill the requirements for bone union or healing of a large bone defect. Bone graft substitutes with osteoconductive and even osteoinductive capabilities are generally insufficient to heal critical size long bone defects, in part because they do not provide viable cells for osteogenesis and paracrine signaling, and do not simulate the bone microenvironment sufficiently (Fillingham and Jacobs, 2016; Lee et al., 2019).

In an effort to decrease the potential morbidity of open harvesting of autologous bone graft, less invasive procedures have been introduced (Dimitriou et al., 2011b). In a systematic review by Dimitriou et al. 19.37% of patients who underwent bone graft harvesting from the iliac crest had a complication, whereas only 6% of patients who underwent harvesting using the long bone intramedullary reamer-irrigator-aspirator (RIA) device sustained an adverse event. A recent study has shown an even lower complication rate using the reamer-aspirator; the complication rate of 1.76% was accompanied by a prolonged post-operative pain rate of 6.45% (Haubruck et al., 2018). In a prospective randomized comparative study (Level 1), the reamer-aspirator was found to have the same union rate and less donor-site pain compared with iliac crest autograft for long bone non-unions (Dawson et al., 2014). The use of harvested autologous iliac crest cells (rather than bulk pieces of bone graft) for enhancement of bone healing has been known for over 3 decades. Connolly et al. did not concentrate the mononuclear cell component after bone marrow harvest at first, but later realized the benefits of centrifugation in providing a more compact osteogenic pellet (Connolly et al., 1989, 1991; Connolly, 1995).

Concentrated bone marrow aspirate has been used for the treatment of delayed and non-union of fractures, defects due to chronic inflammation, infection, tumor and other bone deficiencies, osteonecrosis and in other applications for healing of bone (Hernigou et al., 2005, 2009). Despite these successes, there remains significant opportunities for enrichment of the concentrated bone marrow aspirate, and in particular, the isolation and augmentation of osteoprogenitor cells and vascular progenitor cells. The purpose of this review is to summarize the current literature regarding biological treatments of MSCs for augmentation of bone healing. It is recognized that other methods, including mechanical, chemical, pharmacological etc., are also putative solutions to this problem; however, restriction to biological treatments alone reveals a substantial amount of literature for focused review and commentary. Three main treatments of MSCs are highlighted: preconditioning also known as priming or activation of MSCs by biological factors, exposure of MSCs to a hypoxic environment, and genetic manipulation of cells.

Preconditioning of MSCs by cytokines, chemokines, and other substances is "natural," in the sense that this process currently is the paradigm by which the innate immune system and MSC lineage cells interact to resolve the inflammatory response and reconstruct host tissue. Indeed, these events are

common to all organ systems, in which continuous cellular crosstalk among inflammatory cells, MSCs and numerous other cell types is the norm. Without this intercellular "on-line" signaling, adverse stimuli would potentially destroy critical tissues, thereby jeopardizing the long-term viability of the organism.

Biologic preconditioning of cells *ex vivo* is evidence based; however, even though the cells may be autologous, the processes involved in preconditioning are more than "minimal manipulation" (U. S. Food and Drug Administration, 2017). This is especially true if the cells are selected and expanded in culture, such as with MSCs. Ongoing *in vitro*, *in vivo* and restricted clinical trials will hopefully see this technique translate to the clinic. The first step might be isolation and concentration of harvested autogenous iliac crest cells, which are then exposed to a "benign" treatment, perhaps one (or two) pro-inflammatory cytokine(s), prior to washing and local implantation. This would potentially activate both the progenitor cells and innate immune cells alike, the combination of which is more effective than progenitor cells alone (Kovach et al., 2015; Loi et al., 2016b). This first stage preconditioning concept using autologous concentrated but non-expanded cells might also be extended to the use of low oxygen environments, another effective stimulus.

Genetic manipulation of cells and tissues *ex vivo* and *in vivo* has already been instituted clinically on a limited basis, for severe incurable illnesses in which genetically-based diseases are associated with a devastating phenotype. Once the principles of gene therapy are better understood, and the questions related to safety and efficacy are answered more clearly, other less serious but debilitating conditions might be considered. It is in this realm that accelerated bone healing using genetic manipulation of the cells may find a suitable application. Many questions still need to be answered regarding the optimal platform, appropriate dosing and timing, potential immunogenicity, mutagenicity, carcinogenicity, unintended adverse effects on neighboring cells, as well as cost effectiveness of treatment.

FUTURE DIRECTIONS

There are major efficacy and regulatory concerns as well as issues related to cost that need to be addressed prior to the widespread introduction and use of new technologies to improve bone healing using modified MSCs and their byproducts. Indeed, some of the issues relevant to even the use of *unmodified* MSCs and their byproducts alone have only recently been posed and reviewed (Diederichs et al., 2013; Marolt Presen et al., 2019; Robb et al., 2019). Exhaustive *in vitro* and *in vivo* preclinical studies in small and large animals must be performed, as what may work in the culture plate and small animals may be quite different from what works in larger animals and humans. There are major issues related to which cell types or lineages are most appropriate for selection, the methods by which these cells will be confirmed, harvested, isolated, expanded, and their purity, potency, stability, and sterility assured. Storage mechanisms for easy access to the end-user and user-friendly delivery mechanisms and technologies must be invented. Importantly, the cells must be shown to be efficacious and safe and cost effective. This should be accomplished by well-designed prospective, randomized studies, with meticulous documentation and oversight, for clear indications in specific populations. Databases for long-term follow-up of biological therapies should be established. Performing novel cutting edge therapies with substantial potential risk for serious life threating diseases such as cancer and end-stage heart disease is one end of the spectrum. Non-union of fractures and bone defects are not life threatening, although their impact on quality of life is often substantial. Nonetheless, eventually graduated clinical trials must be performed according to the principles outlined by groups such as with the IDEAL recommendations and others (McCulloch et al., 2009; Ergina et al., 2013). All of these concerns must be addressed in a very complex regulatory environment, which in the USA has rather strict regulations concerning the modification of cells, which can only be "minimally manipulated" (U. S. Food and Drug Administration, 2017). Finally, cost-effective analyses and value-based health care decision making will be important determinants as to whether these new technologies translate to the clinic, or remain only a subject of scientific inquiry (Burnham et al., 2017).

CONCLUSION

Complete healing of fractures and bone defects in specific patient populations and difficult clinical scenarios is still an unmet medical need. Novel approaches and techniques are challenging the belief that autologous bone graft procedures are always the best surgical solutions for obtaining bone union. The harvesting, concentration, and possible manipulation of the phenotype of osteoprogenitor and vascular progenitor cells using preconditioning protocols, exposure to low oxygen environments and genetic manipulation may provide new opportunities for obtaining healing of bone, while minimizing the morbidity associated with open bone grafting. However, these new technologies have substantial scientific, regulatory, and financial hurdles that must be overcome prior to widespread use.

AUTHOR CONTRIBUTIONS

All authors listed have made a substantial, direct and intellectual contribution to the work, and approved it for publication.

ACKNOWLEDGMENTS

The authors acknowledge the generous support of the National Institute of Arthritis and Musculoskeletal and Skin Diseases of the National Institute of Health, grant numbers R01AR063717, R01AR073145, R01AR072613, and the Ellenburg Chair in Surgery, and the Stanford University Medical Scholars Research Grant.

REFERENCES

Almeida-Porada, G., Atala, A. J., and Porada, C. D. (2020). Therapeutic mesenchymal stromal cells for immunotherapy and for gene and drug delivery. *Mol. Ther. Methods Clin. Dev.* 16, 204–224. doi: 10.1016/j.omtm.2020.01.005

Alt, E. U., Winnier, G., Haenel, A., Rothoerl, R., Solakoglu, O., Alt, C., et al. (2020). Towards a comprehensive understanding of UA-ADRCs (uncultured, autologous, fresh, unmodified, adipose derived regenerative cells, isolated at point of care) in regenerative medicine. *Cells* 9:e1097. doi: 10.3390/cells9051097

Ankrum, J. A., Ong, J. F., and Karp, J. M. (2014). Mesenchymal stem cells: immune evasive, not immune privileged. *Nat. Biotechnol.* 32, 252–260. doi: 10.1038/nbt.2816

Atasoy-Zeybek, A., and Kose, G. T. (2018). Gene therapy strategies in bone tissue engineering and current clinical applications. *Adv. Exp. Med. Biol.* 1119, 85–101. doi: 10.1007/5584_2018_253

Bahney, C. S., Zondervan, R. L., Allison, P., Theologis, A., Ashley, J. W., Ahn, J., et al. (2019). Cellular biology of fracture healing. *J. Orthop. Res.* 37, 35–50. doi: 10.1002/jor.24170

Ball, A. N., Donahue, S. W., Wojda, S. J., McIlwraith, C. W., Kawcak, C. E., Ehrhart, N., et al. (2018). The challenges of promoting osteogenesis in segmental bone defects and osteoporosis. *J. Orthop. Res.* 36, 1559–1572. doi: 10.1002/jor.23845

Balmayor, E. R., and van Griensven, M. (2015). Gene therapy for bone engineering. *Front. Bioeng. Biotechnol.* 3:9. doi: 10.3389/fbioe.2015.00009

Bastian, O. W., Koenderman, L., Alblas, J., Leenen, L. P., and Blokhuis, T. J. (2016). Neutrophils contribute to fracture healing by synthesizing fibronectin+ extracellular matrix rapidly after injury. *Clin. Immunol.* 164, 78–84. doi: 10.1016/j.clim.2016.02.001

Bastidas-Coral, A. P., Bakker, A. D., Zandieh-Doulabi, B., Kleverlaan, C. J., Bravenboer, N., Forouzanfar, T., et al. (2016). Cytokines TNF-alpha, IL-6, IL-17F, and IL-4 differentially affect osteogenic differentiation of human adipose stem cells. *Stem Cells Int.* 2016:1318256. doi: 10.1155/2016/1318256

Batinic, D., Marusic, M., Pavletic, Z., Bogdanic, V., Uzarevic, B., Nemet, D., et al. (1990). Relationship between differing volumes of bone marrow aspirates and their cellular composition. *Bone Marrow Transplant.* 6, 103–107.

Berglund, A. K., Fortier, L. A., Antczak, D. F., and Schnabel, L. V. (2017). Immunoprivileged no more: measuring the immunogenicity of allogeneic adult mesenchymal stem cells. *Stem Cell Res. Ther.* 8:288. doi: 10.1186/s13287-017-0742-8

Betz, V. M., Kochanek, S., Rammelt, S., Muller, P. E., Betz, O. B., and Messmer, C. (2018). Recent advances in gene-enhanced bone tissue engineering. *J. Gene Med.* 20:e3018. doi: 10.1002/jgm.3018

Bilem, I., Chevallier, P., Plawinski, L., Sone, E. D., Durrieu, M. C., and Laroche, G. (2016). RGD and BMP-2 mimetic peptide crosstalk enhances osteogenic commitment of human bone marrow stem cells. *Acta Biomater.* 36, 132–142. doi: 10.1016/j.actbio.2016.03.032

Bougioukli, S., Alluri, R., Pannell, W., Sugiyama, O., Vega, A., Tang, A., et al. (2019). *Ex vivo* gene therapy using human bone marrow cells overexpressing BMP-2: "Next-day" gene therapy versus standard "two-step" approach. *Bone* 128:115032. doi: 10.1016/j.bone.2019.08.005

Bougioukli, S., Evans, C. H., Alluri, R. K., Ghivizzani, S. C., and Lieberman, J. R. (2018). Gene therapy to enhance bone and cartilage repair in orthopaedic surgery. *Curr. Gene Ther.* 18, 154–170. doi: 10.2174/1566523218666180410152842

Bravo, D., Jazrawi, L., Cardone, D. A., Virk, M., Passias, P. G., Einhorn, T. A., et al. (2013). Orthobiologics a comprehensive review of the current evidence and use in orthopedic subspecialties. *Bull. Hosp. Jt. Dis.* 76, 223–231.

Burnham, J. M., Meta, F., Lizzio, V., Makhni, E. C., and Bozic, K. J. (2017). Technology assessment and cost-effectiveness in orthopedics: how to measure outcomes and deliver value in a constantly changing healthcare environment. *Curr. Rev. Musculoskelet. Med.* 10, 233–239. doi: 10.1007/s12178-017-9407-6

Campana, V., Milano, G., Pagano, E., Barba, M., Cicione, C., Salonna, G., et al. (2014). Bone substitutes in orthopaedic surgery: from basic science to clinical practice. *J. Mater. Sci. Mater. Med.* 25, 2445–2461. doi: 10.1007/s10856-014-5240-2

Caplan, A. I. (2017a). Mesenchymal stem cells: time to change the name! *Stem Cells Transl. Med.* 6, 1445–1451. doi: 10.1002/sctm.17-0051

Caplan, A. I. (2017b). New MSC: MSCs as pericytes are Sentinels and gatekeepers. *J. Orthop. Res.* 35, 1151–1159. doi: 10.1002/jor.23560

Caralla, T., Boehm, C., Hascall, V., and Muschler, G. (2012). Hyaluronan as a novel marker for rapid selection of connective tissue progenitors. *Ann. Biomed. Eng.* 40, 2559–2567. doi: 10.1007/s10439-012-0608-2

Caralla, T., Joshi, P., Fleury, S., Luangphakdy, V., Shinohara, K., Pan, H., et al. (2013). *in vivo* transplantation of autogenous marrow-derived cells following rapid intraoperative magnetic separation based on hyaluronan to augment bone regeneration. *Tissue Eng. Pt. A.* 19, 125–134. doi: 10.1089/ten.tea.2011.0622

Carvalho, J. L., Braga, V. B., Melo, M. B., Campos, A. C., Oliveira, M. S., Gomes, D. A., et al. (2013). Priming mesenchymal stem cells boosts stem cell therapy to treat myocardial infarction. *J. Cell. Mol. Med.* 17, 617–625. doi: 10.1111/jcmm.12036

Chan, C. K. F., Gulati, G. S., Sinha, R., Tompkins, J. V., Lopez, M., Carter, A. C., et al. (2018). Identification of the human skeletal stem cell. *Cell* 175, 43–56 e21. doi: 10.1016/j.cell.2018.07.029

Chen, L., Xu, Y., Zhao, J., Zhang, Z., Yang, R., Xie, J., et al. (2014). Conditioned medium from hypoxic bone marrow-derived mesenchymal stem cells enhances wound healing in mice. *PLoS ONE* 9:e96161. doi: 10.1371/journal.pone.0096161

Chen, W., Baylink, D. J., Brier-Jones, J., Neises, A., Kiroyan, J. B., Rundle, C. H., et al. (2015). PDGFB-based stem cell gene therapy increases bone strength in the mouse. *Proc. Natl. Acad. Sci. U.S.A.* 112, E3893–E3900. doi: 10.1073/pnas.1501759112

Chen, Y., Shu, Z., Qian, K., Wang, J., and Zhu, H. (2019). Harnessing the properties of biomaterial to enhance the immunomodulation of mesenchymal stem cells. *Tissue Eng. Pt. B. Rev.* 25, 492–499. doi: 10.1089/ten.teb.2019.0131

Cho, D. I., Kim, M. R., Jeong, H. Y., Jeong, H. C., Jeong, M. H., Yoon, S. H., et al. (2014). Mesenchymal stem cells reciprocally regulate the M1/M2 balance in mouse bone marrow-derived macrophages. *Exp. Mol. Med.* 46:e70. doi: 10.1038/emm.2013.135

Ciapetti, G., Granchi, D., Fotia, C., Savarino, L., Dallari, D., Del Piccolo, N., et al. (2016). Effects of hypoxia on osteogenic differentiation of mesenchymal stromal cells used as a cell therapy for avascular necrosis of the femoral head. *Cytotherapy* 18, 1087–1099. doi: 10.1016/j.jcyt.2016.06.005

Connolly, J. F. (1995). Injectable bone marrow preparations to stimulate osteogenic repair. *Clin. Orthop. Relat. Res.* 1995, 8–18.

Connolly, J. F., Guse, R., Tiedeman, J., and Dehne, R. (1989). Autologous marrow injection for delayed unions of the tibia: a preliminary report. *J. Orthop. Trauma* 3, 276–282. doi: 10.1097/00005131-198912000-00002

Connolly, J. F., Guse, R., Tiedeman, J., and Dehne, R. (1991). Autologous marrow injection as a substitute for operative grafting of tibial nonunions. *Clin. Orthop. Relat. Res.* 1991, 259–270.

Croes, M., Oner, F. C., Kruyt, M. C., Blokhuis, T. J., Bastian, O., Dhert, W. J., et al. (2015). Proinflammatory mediators enhance the osteogenesis of human mesenchymal stem cells after lineage commitment. *PLoS ONE* 10:e0132781. doi: 10.1371/journal.pone.0132781

Croes, M., Oner, F. C., van Neerven, D., Sabir, E., Kruyt, M. C., Blokhuis, T. J., et al. (2016). Proinflammatory T cells and IL-17 stimulate osteoblast differentiation. *Bone* 84, 262–270. doi: 10.1016/j.bone.2016.01.010

Dawson, J., Kiner, D., Gardner, W. II., Swafford, R., and Nowotarski, P. J. (2014). The reamer-irrigator-aspirator as a device for harvesting bone graft compared with iliac crest bone graft: union rates and complications. *J. Orthop. Trauma* 28, 584–590. doi: 10.1097/BOT.0000000000000086

De Ugarte, D. A., Alfonso, Z., Zuk, P. A., Elbarbary, A., Zhu, M., Ashjian, P., et al. (2003). Differential expression of stem cell mobilization-associated molecules on multi-lineage cells from adipose tissue and bone marrow. *Immunol. Lett.* 89, 267–270. doi: 10.1016/S0165-2478(03)00108-1

de Witte, S. F., Franquesa, M., Baan, C. C., and Hoogduijn, M. J. (2015). Toward development of imesenchymal stem cells for immunomodulatory therapy. *Front. Immunol.* 6:648. doi: 10.3389/fimmu.2015.00648

Delarosa, O., Dalemans, W., and Lombardo, E. (2012). Toll-like receptors as modulators of mesenchymal stem cells. *Front. Immunol.* 3:182. doi: 10.3389/fimmu.2012.00182

Diederichs, S., Shine, K. M., and Tuan, R. S. (2013). The promise and challenges of stem cell-based therapies for skeletal diseases: stem cell applications in skeletal medicine: potential, cell sources and characteristics, and challenges of clinical translation. *Bioessays* 35, 220–230. doi: 10.1002/bies.201200068

Dimitriou, R., Jones, E., McGonagle, D., and Giannoudis, P. V. (2011a). Bone regeneration: current concepts and future directions. *BMC Med.* 9:66. doi: 10.1186/1741-7015-9-66

Dimitriou, R., Mataliotakis, G. I., Angoules, A. G., Kanakaris, N. K., and Giannoudis, P. V. (2011b). Complications following autologous bone graft harvesting from the iliac crest and using the RIA: a systematic review. *Injury* 42(Suppl. 2), S3–S15. doi: 10.1016/j.injury.2011.06.015

D'Mello, S., Atluri, K., Geary, S. M., Hong, L., Elangovan, S., and Salem, A. K. (2017). Bone regeneration using gene-activated matrices. *AAPS J.* 19, 43–53. doi: 10.1208/s12248-016-9982-2

Dominici, M., Le Blanc, K., Mueller, I., Slaper-Cortenbach, I., Marini, F., Krause, D., et al. (2006). Minimal criteria for defining multipotent mesenchymal stromal cells. *Int. Soc. Cell. Ther. Posit. Statement Cytother.* 8, 315–317. doi: 10.1080/14653240600855905

Dragoo, J. L., and Guzman, R. A. (2020). Evaluation of the consistency and composition of commercially available bone marrow aspirate concentrate systems. *Orthop. J. Sports Med.* 8:2325967119893634. doi: 10.1177/2325967119893634

Egol, K. A., Nauth, A., Lee, M., Pape, H. C., Watson, J. T., and Borrelli, J Jr. (2015). Bone grafting: sourcing, timing, strategies, and alternatives. *J Orthop Trauma* 29(Suppl. 12), S10–S14. doi: 10.1097/BOT.0000000000000460

El Khassawna, T., Serra, A., Bucher, C. H., Petersen, A., Schlundt, C., Konnecke, I., et al. (2017). T lymphocytes influence the mineralization process of bone. *Front. Immunol.* 8:562. doi: 10.3389/fimmu.2017.00562

Ergina, P. L., Barkun, J. S., McCulloch, P., Cook, J. A., Altman, D. G., and Group, I. (2013). IDEAL framework for surgical innovation 2: observational studies in the exploration and assessment stages. *BMJ* 346:f3011. doi: 10.1136/bmj.f3011

Evans, C. H. (2010). Gene therapy for bone healing. *Expert Rev. Mol. Med.* 12:e18. doi: 10.1017/S1462399410001493

Evans, C. H., and Huard, J. (2015). Gene therapy approaches to regenerating the musculoskeletal system. *Nat. Rev. Rheumatol.* 11, 234–242. doi: 10.1038/nrrheum.2015.28

Fan, L., Zhang, C., Yu, Z., Shi, Z., Dang, X., and Wang, K. (2015). Transplantation of hypoxia preconditioned bone marrow mesenchymal stem cells enhances angiogenesis and osteogenesis in rabbit femoral head osteonecrosis. *Bone* 81, 544–553. doi: 10.1016/j.bone.2015.09.005

Fekete, N., Rojewski, M. T., Furst, D., Kreja, L., Ignatius, A., Dausend, J., et al. (2012). GMP-compliant isolation and large-scale expansion of bone marrow-derived MSC. *PLoS ONE* 7:e43255. doi: 10.1371/journal.pone.0043255

Fillingham, Y., and Jacobs, J. (2016). Bone grafts and their substitutes. *Bone Joint J.* 98 (Suppl. A), 6–9. doi: 10.1302/0301-620X.98B.36350

Franchini, M., Cruciani, M., Mengoli, C., Masiello, F., Marano, G., D'Aloja, E., et al. (2019). The use of platelet-rich plasma in oral surgery: a systematic review and meta-analysis. *Blood Transfus.* 17, 357–367. doi: 10.2450/2019.0177-19

Franklin, S. P., Burke, E. E., and Holmes, S. P. (2017). The effect of platelet-rich plasma on osseous healing in dogs undergoing high tibial osteotomy. *PLoS ONE* 12:e0177597. doi: 10.1371/journal.pone.0177597

Freitas, J., Santos, S. G., Goncalves, R. M., Teixeira, J. H., Barbosa, M. A., and Almeida, M. I. (2019). Genetically engineered-MSC therapies for non-unions, delayed unions and critical-size bone defects. *Int. J. Mol. Sci.* 20:3430. doi: 10.3390/ijms20143430

Gabrielyan, A., Neumann, E., Gelinsky, M., and Rosen-Wolff, A. (2017). Metabolically conditioned media derived from bone marrow stromal cells or human skin fibroblasts act as effective chemoattractants for mesenchymal stem cells. *Stem Cell Res. Ther.* 8:212. doi: 10.1186/s13287-017-0664-5

Garcia-Sanchez, D., Fernandez, D., Rodriguez-Rey, J. C., and Perez-Campo, F. M. (2019). Enhancing survival, engraftment, and osteogenic potential of mesenchymal stem cells. *World J. Stem Cells* 11, 748–763. doi: 10.4252/wjsc.v11.i10.748

Gerstenfeld, L. C., Cullinane, D. M., Barnes, G. L., Graves, D. T., and Einhorn, T. A. (2003). Fracture healing as a post-natal developmental process: molecular, spatial, and temporal aspects of its regulation. *J. Cell. Biochem.* 88, 873–884. doi: 10.1002/jcb.10435

Giannoudis, P. V., Einhorn, T. A., and Marsh, D. (2007). Fracture healing: the diamond concept. *Injury* 38(Suppl. 4), S3–S6. doi: 10.1016/S0020-1383(08)70003-2

Giles, E. M., Godbout, C., Chi, W., Glick, M. A., Lin, T., Li, R., et al. (2017). Subtypes of endothelial progenitor cells affect healing of segmental bone defects differently. *Int. Orthop.* 41, 2337–2343. doi: 10.1007/s00264-017-3613-0

Glass, G. E., Chan, J. K., Freidin, A., Feldmann, M., Horwood, N. J., and Nanchahal, J. (2011). TNF-alpha promotes fracture repair by augmenting the recruitment and differentiation of muscle-derived stromal cells. *Proc. Natl. Acad. Sci. U.S.A.* 108, 1585–1590. doi: 10.1073/pnas.1018501108

Gomez-Barrena, E., Padilla-Eguiluz, N., Rosset, P., Gebhard, F., Hernigou, P., Baldini, N., et al. (2020). Early efficacy evaluation of mesenchymal stromal cells (MSC) combined to biomaterials to treat long bone non-unions. *Injury* 51, S63–S73. doi: 10.1016/j.injury.2020.02.070

Gomez-Barrena, E., Rosset, P., Lozano, D., Stanovici, J., Ermthaller, C., and Gerbhard, F. (2015). Bone fracture healing: cell therapy in delayed unions and nonunions. *Bone* 70, 93–101. doi: 10.1016/j.bone.2014.07.033

Grayson, W. L., Bunnell, B. A., Martin, E., Frazier, T., Hung, B. P., and Gimble, J. M. (2015). Stromal cells and stem cells in clinical bone regeneration. *Nat. Rev. Endocrinol.* 11, 140–150. doi: 10.1038/nrendo.2014.234

Griffin, M. D., Ritter, T., and Mahon, B. P. (2010). Immunological aspects of allogeneic mesenchymal stem cell therapies. *Hum. Gene Ther.* 21, 1641–1655. doi: 10.1089/hum.2010.156

Griffin, M. D., Ryan, A. E., Alagesan, S., Lohan, P., Treacy, O., and Ritter, T. (2013). Anti-donor immune responses elicited by allogeneic mesenchymal stem cells: what have we learned so far? *Immunol. Cell Biol.* 91, 40–51. doi: 10.1038/icb.2012.67

Grosso, A., Burger, M. G., Lunger, A., Schaefer, D. J., Banfi, A., and Di Maggio, N. (2017). It takes two to tango: coupling of angiogenesis and osteogenesis for bone regeneration. *Front. Bioeng. Biotechnol.* 5:68. doi: 10.3389/fbioe.2017.00068

Gulati, G. S., Murphy, M. P., Marecic, O., Lopez, M., Brewer, R. E., Koepke, L. S., et al. (2018). Isolation and functional assessment of mouse skeletal stem cell lineage. *Nat. Protoc.* 13, 1294–1309. doi: 10.1038/nprot.2018.041

Hanson, S., D'Souza, R. N., and Hematti, P. (2014). Biomaterial-mesenchymal stem cell constructs for immunomodulation in composite tissue engineering. *Tissue Eng. Pt. A.* 20, 2162–2168. doi: 10.1089/ten.tea.2013.0359

Haubruck, P., Ober, J., Heller, R., Miska, M., Schmidmaier, G., and Tanner, M. C. (2018). Complications and risk management in the use of the reaming-irrigator-aspirator (RIA) system: RIA is a safe and reliable method in harvesting autologous bone graft. *PLoS ONE* 13:e0196051. doi: 10.1371/journal.pone.0196051

Hegde, V., Shonuga, O., Ellis, S., Fragomen, A., Kennedy, J., Kudryashov, V., et al. (2014). A prospective comparison of 3 approved systems for autologous bone marrow concentration demonstrated nonequivalency in progenitor cell number and concentration. *J. Orthop. Trauma* 28, 591–598. doi: 10.1097/BOT.0000000000000113

Henrich, D., Seebach, C., Sterlepper, E., Tauchmann, C., Marzi, I., and Frank, J. (2010). RIA reamings and hip aspirate: a comparative evaluation of osteoprogenitor and endothelial progenitor cells. *Injury* 41(Suppl. 2), S62–S68. doi: 10.1016/S0020-1383(10)70012-7

Hernigou, J., Picard, L., Alves, A., Silvera, J., Homma, Y., and Hernigou, P. (2014). Understanding bone safety zones during bone marrow aspiration from the iliac crest: the sector rule. *Int. Orthop.* 38, 2377–2384. doi: 10.1007/s00264-014-2343-9

Hernigou, P., and Beaujean, F. (2002). Treatment of osteonecrosis with autologous bone marrow grafting. *Clin Orthop Relat Res.* 405, 14–23. doi: 10.1097/00003086-200212000-00003

Hernigou, P., Desroches, A., Queinnec, S., Flouzat Lachaniette, C. H., Poignard, A., Allain, J., et al. (2014). Morbidity of graft harvesting versus bone marrow aspiration in cell regenerative therapy. *Int. Orthop.* 38, 1855–1860. doi: 10.1007/s00264-014-2318-x

Hernigou, P., Flouzat-Lachaniette, C. H., Delambre, J., Poignard, A., Allain, J., Chevallier, N., et al. (2015). Osteonecrosis repair with bone marrow cell therapies: state of the clinical art. *Bone* 70, 102–109. doi: 10.1016/j.bone.2014.04.034

Hernigou, P., Poignard, A., Beaujean, F., and Rouard, H. (2005). Percutaneous autologous bone-marrow grafting for nonunions. Influence of the number and concentration of progenitor cells. *J. Bone Jt. Surg. Am. Vol.* 87, 1430–1437. doi: 10.2106/00004623-200507000-00003

Hernigou, P., Poignard, A., Zilber, S., and Rouard, H. (2009). Cell therapy of hip osteonecrosis with autologous bone marrow grafting. *Indian J. Orthop.* 43, 40–45. doi: 10.4103/0019-5413.45322

Herrmann, M., Verrier, S., and Alini, M. (2015). Strategies to stimulate mobilization and homing of endogenous stem and progenitor cells for bone tissue repair. *Front. Bioeng. Biotechnol.* 3:79. doi: 10.3389/fbioe.2015.00079

Hobby, B., and Lee, M. A. (2013). Managing atrophic nonunion in the geriatric population: incidence, distribution, and causes. *Orthop. Clin. North Am.* 44, 251–256. doi: 10.1016/j.ocl.2013.01.011

Horwitz, E. M., Le Blanc, K., Dominici, M., Mueller, I., Slaper-Cortenbach, I., Marini, F. C., et al. (2005). Clarification of the nomenclature for MSC: the International Society for Cellular Therapy position statement. *Cytotherapy* 7, 393–395. doi: 10.1080/14653240500319234

Hutchings, G., Moncrieff, L., Dompe, C., Janowicz, K., Sibiak, R., Bryja, A., et al. (2020). Bone regeneration, reconstruction and use of osteogenic cells; from basic knowledge, animal models to clinical trials. *J. Clin. Med.* 9:139. doi: 10.3390/jcm9010139

Joshi, P., Williams, P. S., Moore, L. R., Caralla, T., Boehm, C., Muschler, G., et al. (2015). Circular Halbach array for fast magnetic separation of hyaluronan-expressing tissue progenitors. *Anal. Chem.* 87, 9908–9915. doi: 10.1021/acs.analchem.5b02431

Kanczler, J., Tare, R. S., Stumpf, P., Noble, T. J., Black, C., and Oreffo, R. O. C. (2019). Isolation, differentiation, and characterization of human bone marrow stem cells *in vitro* and *in vivo*. *Methods Mol. Biol.* 1914, 53–70. doi: 10.1007/978-1-4939-8997-3_4

Karnes, J. M., Daffner, S. D., and Watkins, C. M. (2015). Multiple roles of tumor necrosis factor-alpha in fracture healing. *Bone* 78, 87–93. doi: 10.1016/j.bone.2015.05.001

Kasten, P., Vogel, J., Luginbuhl, R., Niemeyer, P., Weiss, S., Schneider, S., et al. (2006). Influence of platelet-rich plasma on osteogenic differentiation of mesenchymal stem cells and ectopic bone formation in calcium phosphate ceramics. *Cells Tissues Organs.* 183, 68–79. doi: 10.1159/000095511

Kiernan, C. H., Wolvius, E. B., Brama, P. A. J., and Farrell, E. (2018). The immune response to allogeneic differentiated mesenchymal stem cells in the context of bone tissue engineering. *Tissue Eng. Pt. B. Rev.* 24, 75–83. doi: 10.1089/ten.teb.2017.0175

Kim, J., and Hematti, P. (2009). Mesenchymal stem cell-educated macrophages: a novel type of alternatively activated macrophages. *Exp. Hematol.* 37, 1445–1453. doi: 10.1016/j.exphem.2009.09.004

Konnecke, I., Serra, A., El Khassawna, T., Schlundt, C., Schell, H., Hauser, A., et al. (2014). T and B cells participate in bone repair by infiltrating the fracture callus in a two-wave fashion. *Bone* 64, 155–165. doi: 10.1016/j.bone.2014.03.052

Kouroupis, D., Sanjurjo-Rodriguez, C., Jones, E., and Correa, D. (2019). Mesenchymal stem cell functionalization for enhanced therapeutic applications. *Tissue Eng. Pt. B. Rev.* 25, 55–77. doi: 10.1089/ten.teb.2018.0118

Kovach, T. K., Dighe, A. S., Lobo, P. I., and Cui, Q. (2015). Interactions between MSCs and immune cells: implications for bone healing. *J. Immunol. Res.* 2015:752510. doi: 10.1155/2015/752510

Lee, C. C., Hirasawa, N., Garcia, K. G., Ramanathan, D., and Kim, K. D. (2019). Stem and progenitor cell microenvironment for bone regeneration and repair. *Regen. Med.* 14, 693–702. doi: 10.2217/rme-2018-0044

Lee, D. Y., Cho, T. J., Kim, J. A., Lee, H. R., Yoo, W. J., Chung, C. Y., et al. (2008). Mobilization of endothelial progenitor cells in fracture healing and distraction osteogenesis. *Bone* 42, 932–941. doi: 10.1016/j.bone.2008.01.007

Leng, Q., Chen, L., and Lv, Y. (2020). RNA-based scaffolds for bone regeneration: application and mechanisms of mRNA, miRNA and siRNA. *Theranostics* 10, 3190–3205. doi: 10.7150/thno.42640

Li, J., Tan, J., Martino, M. M., and Lui, K. O. (2018). Regulatory T-cells: potential regulator of tissue repair and regeneration. *Front. Immunol.* 9:585. doi: 10.3389/fimmu.2018.00585

Lien, C. Y., Chih-Yuan Ho, K., Lee, O. K., Blunn, G. W., and Su, Y. (2009). Restoration of bone mass and strength in glucocorticoid-treated mice by systemic transplantation of CXCR4 and cbfa-1 co-expressing mesenchymal stem cells. *J. Bone Miner. Res.* 24, 837–848. doi: 10.1359/jbmr.081257

Lin, R. Z., Moreno-Luna, R., Zhou, B., Pu, W. T., and Melero-Martin, J. M. (2012). Equal modulation of endothelial cell function by four distinct tissue-specific mesenchymal stem cells. *Angiogenesis* 15, 443–455. doi: 10.1007/s10456-012-9272-2

Lin, T., Kohno, Y., Huang, J. F., Romero-Lopez, M., Pajarinen, J., Maruyama, M., et al. (2018a). NFkappaB sensing IL-4 secreting mesenchymal stem cells mitigate the proinflammatory response of macrophages exposed to polyethylene wear particles. *J. Biomed. Mater. Res. A* 106, 2744–2752. doi: 10.1002/jbm.a.36504

Lin, T., Pajarinen, J., Kohno, Y., Maruyama, M., Romero-Lopez, M., Huang, J. F., et al. (2018b). Transplanted interleukin-4–secreting mesenchymal stromal cells show extended survival and increased bone mineral density in the murine femur. *Cytotherapy* 20, 1028–1036. doi: 10.1016/j.jcyt.2018.06.009

Lin, T., Pajarinen, J., Nabeshima, A., Lu, L., Nathan, K., Jamsen, E., et al. (2017a). Preconditioning of murine mesenchymal stem cells synergistically enhanced immunomodulation and osteogenesis. *Stem Cell Res. Ther.* 8:277. doi: 10.1186/s13287-017-0730-z

Lin, T., Pajarinen, J., Nabeshima, A., Lu, L., Nathan, K., Yao, Z., et al. (2017b). Establishment of NF-kappaB sensing and interleukin-4 secreting mesenchymal stromal cells as an "on-demand" drug delivery system to modulate inflammation. *Cytotherapy* 19, 1025–1034. doi: 10.1016/j.jcyt.2017.06.008

Liu, Y., Teoh, S. H., Chong, M. S., Lee, E. S., Mattar, C. N., Randhawa, N. K., et al. (2012). Vasculogenic and osteogenesis-enhancing potential of human umbilical cord blood endothelial colony-forming cells. *Stem Cells* 30, 1911–1924. doi: 10.1002/stem.1164

Liu, Y., Teoh, S. H., Chong, M. S., Yeow, C. H., Kamm, R. D., Choolani, M., et al. (2013). Contrasting effects of vasculogenic induction upon biaxial bioreactor stimulation of mesenchymal stem cells and endothelial progenitor cells cocultures in three-dimensional scaffolds under *in vitro* and *in vivo* paradigms for vascularized bone tissue engineering. *Tissue Eng. Pt. A.* 19, 893–904. doi: 10.1089/ten.tea.2012.0187

Loi, F., Cordova, L. A., Pajarinen, J., Lin, T. H., Yao, Z., and Goodman, S. B. (2016a). Inflammation, fracture and bone repair. *Bone* 86, 119–130. doi: 10.1016/j.bone.2016.02.020

Loi, F., Cordova, L. A., Zhang, R., Pajarinen, J., Lin, T. H., Goodman, S. B., et al. (2016b). The effects of immunomodulation by macrophage subsets on osteogenesis *in vitro*. *Stem Cell Res. Ther.* 7:15. doi: 10.1186/s13287-016-0276-5

Lu, C. H., Chang, Y. H., Lin, S. Y., Li, K. C., and Hu, Y. C. (2013). Recent progresses in gene delivery-based bone tissue engineering. *Biotechnol. Adv.* 31, 1695–1706. doi: 10.1016/j.biotechadv.2013.08.015

Lu, Z., Chen, Y., Dunstan, C., Roohani-Esfahani, S., and Zreiqat, H. (2017). Priming adipose stem cells with tumor necrosis factor-alpha preconditioning potentiates their exosome efficacy for bone regeneration. *Tissue Eng. Part A.* 23, 1212–1220. doi: 10.1089/ten.tea.2016.0548

Lu, Z., Wang, G., Dunstan, C. R., Chen, Y., Lu, W. Y., Davies, B., et al. (2013). Activation and promotion of adipose stem cells by tumour necrosis factor-alpha preconditioning for bone regeneration. *J. Cell. Physiol.* 228, 1737–1744. doi: 10.1002/jcp.24330

Luangphakdy, V., Walker, E., Shinohara, K., Pan, H., Hefferan, T., Bauer, T. W., et al. (2013). Evaluation of osteoconductive scaffolds in the canine femoral multi-defect model. *Tissue Eng. Pt. A.* 19, 634–648. doi: 10.1089/ten.tea.2012.0289

Maggini, J., Mirkin, G., Bognanni, I., Holmberg, J., Piazzon, I. M., Nepomnaschy, I., et al. (2010). Mouse bone marrow-derived mesenchymal stromal cells turn activated macrophages into a regulatory-like profile. *PLoS ONE* 5:e9252. doi: 10.1371/journal.pone.0009252

Mantovani, A., Biswas, S. K., Galdiero, M. R., Sica, A., and Locati, M. (2013). Macrophage plasticity and polarization in tissue repair and remodelling. *J. Pathol.* 229, 176–185. doi: 10.1002/path.4133

Marolt Presen, D., Traweger, A., Gimona, M., and Redl, H. (2019). Mesenchymal stromal cell-based bone regeneration therapies: from cell transplantation and tissue engineering to therapeutic secretomes and extracellular vesicles. *Front. Bioeng. Biotechnol.* 7:352. doi: 10.3389/fbioe.2019.00352

Marongiu, G., Dolci, A., Verona, M., and Capone, A. (2020). The biology and treatment of acute long-bones diaphyseal fractures: overview of the current options for bone healing enhancement. *Bone Rep.* 12:100249. doi: 10.1016/j.bonr.2020.100249

Marsell, R., and Einhorn, T. A. (2011). The biology of fracture healing. *Injury* 42, 551–555. doi: 10.1016/j.injury.2011.03.031

McCulloch, P., Altman, D. G., Campbell, W. B., Flum, D. R., Glasziou, P., Marshall, J. C., et al. (2009). No surgical innovation without

evaluation: the IDEAL recommendations. *Lancet* 374, 1105–1112. doi: 10.1016/S0140-6736(09)61116-8

McLaughlin, M., Gagnet, P., Cunningham, E., Yeager, R., D'Amico, M., Guski, K., et al. (2016). Allogeneic platelet releasate preparations derived via a novel rapid thrombin activation process promote rapid growth and increased BMP-2 and BMP-4 expression in human adipose-derived stem cells. *Stem Cells Int.* 2016:7183734. doi: 10.1155/2016/7183734

Mizuno, H., Tobita, M., and Uysal, A. C. (2012). Concise review: adipose-derived stem cells as a novel tool for future regenerative medicine. *Stem Cells* 30, 804–810. doi: 10.1002/stem.1076

Mohyeldin, A., Garzon-Muvdi, T., and Quinones-Hinojosa, A. (2010). Oxygen in stem cell biology: a critical component of the stem cell niche. *Cell Stem Cell* 7, 150–161. doi: 10.1016/j.stem.2010.07.007

Muschler, G. F., Boehm, C., and Easley, K. (1997). Aspiration to obtain osteoblast progenitor cells from human bone marrow: the influence of aspiration volume. *J. Bone Jt. Surg. Am. Vol.* 79, 1699–1709. doi: 10.2106/00004623-199711000-00012

Muschler, G. F., Matsukura, Y., Nitto, H., Boehm, C. A., Valdevit, A. D., Kambic, H. E., et al. (2005). Selective retention of bone marrow-derived cells to enhance spinal fusion. *Clin. Orthop. Relat. Res.* 2005, 242–251. doi: 10.1097/01.blo.0000149812.32857.8b

Muschler, G. F., Nitto, H., Boehm, C. A., and Easley, K. A. (2001). Age- and gender-related changes in the cellularity of human bone marrow and the prevalence of osteoblastic progenitors. *J. Orthop. Res.* 19, 117–125. doi: 10.1016/S0736-0266(00)00010-3

Najar, M., Krayem, M., Merimi, M., Burny, A., Meuleman, N., Bron, D., et al. (2018). Insights into inflammatory priming of mesenchymal stromal cells: functional biological impacts. *Inflamm. Res.* 67, 467–477. doi: 10.1007/s00011-018-1131-1

Najar, M., Krayem, M., Meuleman, N., Bron, D., and Lagneaux, L. (2017). Mesenchymal stromal cells and toll-like receptor priming: a critical review. *Immune Netw.* 17, 89–102. doi: 10.4110/in.2017.17.2.89

Nauth, A., Lane, J., Watson, J. T., and Giannoudis, P. (2015). Bone graft substitution and augmentation. *J. Orthop. Trauma* 29(Suppl. 12), S34–S38. doi: 10.1097/BOT.0000000000000464

Nava, M. M., Raimondi, M. T., and Pietrabissa, R. (2012). Controlling self-renewal and differentiation of stem cells via mechanical cues. *J. Biomed. Biotechnol.* 2012:797410. doi: 10.1155/2012/797410

Nemeth, K., Leelahavanichkul, A., Yuen, P. S., Mayer, B., Parmelee, A., Doi, K., et al. (2009). Bone marrow stromal cells attenuate sepsis via prostaglandin E(2)-dependent reprogramming of host macrophages to increase their interleukin-10 production. *Nat. Med.* 15, 42–49. doi: 10.1038/nm.1905

Nicodemou, A., and Danisovic, L. (2017). Mesenchymal stromal/stem cell separation methods: concise review. *Cell Tissue Bank.* 18, 443–460. doi: 10.1007/s10561-017-9658-x

Noronha Nc, N. C., Mizukami, A., Caliari-Oliveira, C., Cominal, J. G., Rocha, J. L. M., Covas, D. T., et al. (2019). Priming approaches to improve the efficacy of mesenchymal stromal cell-based therapies. *Stem Cell Res. Ther.* 10:131. doi: 10.1186/s13287-019-1224-y

Ono, T., Okamoto, K., Nakashima, T., Nitta, T., Hori, S., Iwakura, Y., et al. (2016). IL-17-producing gammadelta T cells enhance bone regeneration. *Nat. Commun.* 7:10928. doi: 10.1038/ncomms10928

Ono, T., and Takayanagi, H. (2017). Osteoimmunology in Bone Fracture Healing. *Curr. Osteoporos. Rep.* 15, 367–375. doi: 10.1007/s11914-017-0381-0

Pajarinen, J., Lin, T., Gibon, E., Kohno, Y., Maruyama, M., Nathan, K., et al. (2019). Mesenchymal stem cell-macrophage crosstalk and bone healing. *Biomaterials* 196, 80–89. doi: 10.1016/j.biomaterials.2017.12.025

Park, J. Y., Park, S. H., Kim, M. G., Park, S. H., Yoo, T. H., and Kim, M. S. (2018). Biomimetic scaffolds for bone tissue engineering. *Adv. Exp. Med. Biol.* 1064, 109–121. doi: 10.1007/978-981-13-0445-3_7

Park, S., Jang, H., Kim, B. S., Hwang, C., Jeong, G. S., and Park, Y. (2017). Directional migration of mesenchymal stem cells under an SDF-1alpha gradient on a microfluidic device. *PLoS ONE* 12:e0184595. doi: 10.1371/journal.pone.0184595

Parrilla, C., Saulnier, N., Bernardini, C., Patti, R., Tartaglione, T., Fetoni, A. R., et al. (2011). Undifferentiated human adipose tissue-derived stromal cells induce mandibular bone healing in rats. *Arch. Otolaryngol. Head Neck Surg.* 137, 463–470. doi: 10.1001/archoto.2011.61

Pereira, H. F., Cengiz, I. B., Silva, F. S., Reis, R. L., and Oliveira, J. M. (2020). Scaffolds and coatings for bone regeneration. *J. Mater. Sci. Mater. Med.* 31:27. doi: 10.1007/s10856-020-06364-y

Philipp, D., Suhr, L., Wahlers, T., Choi, Y. H., and Paunel-Gorgulu, A. (2018). Preconditioning of bone marrow-derived mesenchymal stem cells highly strengthens their potential to promote IL-6-dependent M2b polarization. *Stem Cell Res. Ther.* 9:286. doi: 10.1186/s13287-018-1039-2

Pittenger, M. F., Mackay, A. M., Beck, S. C., Jaiswal, R. K., Douglas, R., Mosca, J. D., et al. (1999). Multilineage potential of adult human mesenchymal stem cells. *Science* 284, 143–147. doi: 10.1126/science.284.5411.143

Piuzzi, N. S., Mantripragada, V. P., Sumski, A., Selvam, S., Boehm, C., and Muschler, G. F. (2018). Bone marrow-derived cellular therapies in orthopaedics: part i: recommendations for bone marrow aspiration technique and safety. *JBJS Rev.* 6:e4. doi: 10.2106/JBJS.RVW.18.00007

Prockop, D. J. (2009). Repair of tissues by adult stem/progenitor cells (MSCs): controversies, myths, and changing paradigms. *Mol. Ther.* 17, 939–946. doi: 10.1038/mt.2009.62

Prockop, D. J., Kota, D. J., Bazhanov, N., and Reger, R. L. (2010). Evolving paradigms for repair of tissues by adult stem/progenitor cells (MSCs). *J. Cell. Mol. Med.* 14, 2190–2199. doi: 10.1111/j.1582-4934.2010.01151.x

Quade, M., Munch, P., Lode, A., Duin, S., Vater, C., Gabrielyan, A., et al. (2020). The secretome of hypoxia conditioned hMSC loaded in a central depot induces chemotaxis and angiogenesis in a biomimetic mineralized collagen bone replacement material. *Adv. Healthc. Mater.* 9:e1901426. doi: 10.1002/adhm.201901426

Robb, K. P., Fitzgerald, J. C., Barry, F., and Viswanathan, S. (2019). Mesenchymal stromal cell therapy: progress in manufacturing and assessments of potency. *Cytotherapy* 21, 289–306. doi: 10.1016/j.jcyt.2018.10.014

Roffi, A., Di Matteo, B., Krishnakumar, G. S., Kon, E., and Filardo, G. (2017). Platelet-rich plasma for the treatment of bone defects: from pre-clinical rational to evidence in the clinical practice. A systematic review. *Int. Orthop.* 41, 221–237. doi: 10.1007/s00264-016-3342-9

Rojewski, M. T., Fekete, N., Baila, S., Nguyen, K., Furst, D., Antwiler, D., et al. (2013). GMP-compliant isolation and expansion of bone marrow-derived MSCs in the closed, automated device quantum cell expansion system. *Cell Transplant.* 22, 1981–2000. doi: 10.3727/096368912X657990

Romagnoli, C., and Brandi, M. L. (2014). Adipose mesenchymal stem cells in the field of bone tissue engineering. *World J. Stem Cells* 6, 144–152. doi: 10.4252/wjsc.v6.i2.144

Sagi, H. C., Young, M. L., Gerstenfeld, L., Einhorn, T. A., and Tornetta, P. (2012). Qualitative and quantitative differences between bone graft obtained from the medullary canal (with a Reamer/Irrigator/Aspirator) and the iliac crest of the same patient. *J. Bone Jt. Surg. Am. Vol.* 94, 2128–2135. doi: 10.2106/JBJS.L.00159

Salzman, R., Cook, F., Hunt, T., Malech, H. L., Reilly, P., Foss-Campbell, B., et al. (2018). Addressing the value of gene therapy and enhancing patient access to transformative treatments. *Mol. Ther.* 26, 2717–2726. doi: 10.1016/j.ymthe.2018.10.017

Santolini, E., West, R., and Giannoudis, P. V. (2015). Risk factors for long bone fracture non-union: a stratification approach based on the level of the existing scientific evidence. *Injury* 46(Suppl. 8), S8–S19. doi: 10.1016/S0020-1383(15)30049-8

Seebach, C., Henrich, D., Schaible, A., Relja, B., Jugold, M., Bonig, H., et al. (2015). Cell-based therapy by implanted human bone marrow-derived mononuclear cells improved bone healing of large bone defects in rats. *Tissue Eng. Pt. A.* 21, 1565–1578. doi: 10.1089/ten.tea.2014.0410

Sen, M. K., and Miclau, T. (2007). Autologous iliac crest bone graft: should it still be the gold standard for treating nonunions? *Injury* 38(Suppl. 1), S75–S80. doi: 10.1016/j.injury.2007.02.012

Shapiro, G., Lieber, R., Gazit, D., and Pelled, G. (2018). Recent advances and future of gene therapy for bone regeneration. *Curr. Osteoporos. Rep.* 16, 504–511. doi: 10.1007/s11914-018-0459-3

Sun, K., Zhou, Z., Ju, X., Zhou, Y., Lan, J., Chen, D., et al. (2016). Combined transplantation of mesenchymal stem cells and endothelial progenitor cells for

tissue engineering: a systematic review and meta-analysis. *Stem Cell Res. Ther.* 7:151. doi: 10.1186/s13287-016-0390-4

Tajima, S., Tobita, M., and Mizuno, H. (2018). Current status of bone regeneration using adipose-derived stem cells. *Histol. Histopathol.* 33, 619–627. doi: 10.14670/HH-11-942

Tasev, D., Koolwijk, P., and van Hinsbergh, V. W. (2016). Therapeutic potential of human-derived endothelial colony-forming cells in animal models. *Tissue Eng. Pt. B. Rev.* 22, 371–382. doi: 10.1089/ten.teb.2016.0050

Thomas, J. D., and Kehoe, J. L. (2020). *Bone Nonunion.* Treasure Island, FL: StatPearls Publishing.

U. S. Food and Drug Administration (2017). *Regulatory Considerations for Human Cells, Tissues, and Cellular and Tissue- Based Products: Minimal Manipulation and Homologous Use*. FDA. Available online at: https://www.fda.gov/BiologicsBloodVaccines/GuidanceComplianceRegulatoryInformation/Guidances/default.htm (accessed April 5, 2020).

Valles, G., Bensiamar, F., Crespo, L., Arruebo, M., Vilaboa, N., and Saldana, L. (2015). Topographical cues regulate the crosstalk between MSCs and macrophages. *Biomaterials* 37, 124–133. doi: 10.1016/j.biomaterials.2014.10.028

Viswanathan, S., Shi, Y., Galipeau, J., Krampera, M., Leblanc, K., Martin, I., et al. (2019). Mesenchymal stem versus stromal cells: International Society for Cell and Gene Therapy (ISCT(R)) Mesenchymal Stromal Cell committee position statement on nomenclature. *Cytotherapy* 21, 1019–1024. doi: 10.1016/j.jcyt.2019.08.002

Vogel, J. P., Szalay, K., Geiger, F., Kramer, M., Richter, W., and Kasten, P. (2006). Platelet-rich plasma improves expansion of human mesenchymal stem cells and retains differentiation capacity and *in vivo* bone formation in calcium phosphate ceramics. *Platelets* 17, 462–469. doi: 10.1080/09537100600758867

Volkmer, E., Kallukalam, B. C., Maertz, J., Otto, S., Drosse, I., Polzer, H., et al. (2010). Hypoxic preconditioning of human mesenchymal stem cells overcomes hypoxia-induced inhibition of osteogenic differentiation. *Tissue Eng. Pt. A.* 16, 153–164. doi: 10.1089/ten.tea.2009.0021

Wagegg, M., Gaber, T., Lohanatha, F. L., Hahne, M., Strehl, C., Fangradt, M., et al. (2012). Hypoxia promotes osteogenesis but suppresses adipogenesis of human mesenchymal stromal cells in a hypoxia-inducible factor-1 dependent manner. *PLoS ONE* 7:e46483. doi: 10.1371/journal.pone.0046483

Wagner, D. R., Karnik, S., Gunderson, Z. J., Nielsen, J. J., Fennimore, A., Promer, H. J., et al. (2019). Dysfunctional stem and progenitor cells impair fracture healing with age. *World J. Stem Cells* 11, 281–296. doi: 10.4252/wjsc.v11.i6.281

Wan, H. E., Goodkind, D., and Kowal, P. (2016). *U.S. Census Bureau, International Population Reports*. Washington, DC: U.S. Government Publishing Office. Available online at: http://www.census.gov/newsroom/press-releases/2016/cb16-54.html

Waterman, R. S., Tomchuck, S. L., Henkle, S. L., and Betancourt, A. M. (2010). A new mesenchymal stem cell (MSC) paradigm: polarization into a pro-inflammatory MSC1 or an immunosuppressive MSC2 phenotype. *PLoS ONE* 5:e10088. doi: 10.1371/journal.pone.0010088

Wilson, C. J., Clegg, R. E., Leavesley, D. I., and Pearcy, M. J. (2005). Mediation of biomaterial-cell interactions by adsorbed proteins: a review. *Tissue Eng.* 11, 1–18. doi: 10.1089/ten.2005.11.1

Yu, X., Wan, Q., Ye, X., Cheng, Y., Pathak, J. L., and Li, Z. (2019). Cellular hypoxia promotes osteogenic differentiation of mesenchymal stem cells and bone defect healing via STAT3 signaling. *Cell. Mol. Biol. Lett.* 24:64. doi: 10.1186/s11658-019-0191-8

Zhang, J., Feng, Z., Wei, J., Yu, Y., Luo, J., Zhou, J., et al. (2018). Repair of critical-sized mandible defects in aged rat using hypoxia preconditioned BMSCs with up-regulation of Hif-1alpha. *Int. J. Biol. Sci.* 14, 449–460. doi: 10.7150/ijbs.24158

Zhang, Z., Huang, S., Wu, S., Qi, J., Li, W., Liu, S., et al. (2019). Clearance of apoptotic cells by mesenchymal stem cells contributes to immunosuppression via PGE2. *EBioMedicine* 45, 341–350. doi: 10.1016/j.ebiom.2019.06.016

Zigdon-Giladi, H., Michaeli-Geller, G., Bick, T., Lewinson, D., and Machtei, E. E. (2015). Human blood-derived endothelial progenitor cells augment vasculogenesis and osteogenesis. *J. Clin. Periodontol.* 42, 89–95. doi: 10.1111/jcpe.12325

Zura, R., Mehta, S., Della Rocca, G. J., and Steen, R. G. (2016). Biological risk factors for nonunion of bone fracture. *JBJS Rev.* 4:01874474-201601000-00005. doi: 10.2106/JBJS.RVW.O.00008

Conflict of Interest: The authors declare that the research was conducted in the absence of any commercial or financial relationships that could be construed as a potential conflict of interest.

frontiers in Bioengineering and Biotechnology

ORIGINAL RESEARCH
published: 08 July 2020
doi: 10.3389/fbioe.2020.00804

Importance of Timing of Platelet Lysate-Supplementation in Expanding or Redifferentiating Human Chondrocytes for Chondrogenesis

Margot Rikkers[1], Riccardo Levato[1,2], Jos Malda[1,2] and Luciënne A. Vonk[1†]*

[1] Department of Orthopaedics, University Medical Center Utrecht, Utrecht University, Utrecht, Netherlands, [2] Department of Equine Sciences, Faculty of Veterinary Medicine, Utrecht University, Utrecht, Netherlands

OPEN ACCESS

Edited by:
Roberto Narcisi,
Erasmus University Rotterdam,
Netherlands

Reviewed by:
Andrea Lolli,
Erasmus Medical Center, Netherlands
Chiara Gentili,
University of Genoa, Italy

***Correspondence:**
Luciënne A. Vonk
l.a.vonk-3@umcutrecht.nl

†Present address:
Luciënne A. Vonk,
CO.DON AG, Teltow, Germany

Specialty section:
This article was submitted to Preclinical Cell and Gene Therapy, a section of the journal Frontiers in Bioengineering and Biotechnology

Received: 13 March 2020
Accepted: 22 June 2020
Published: 08 July 2020

Citation:
Rikkers M, Levato R, Malda J and Vonk LA (2020) Importance of Timing of Platelet Lysate-Supplementation in Expanding or Redifferentiating Human Chondrocytes for Chondrogenesis. Front. Bioeng. Biotechnol. 8:804. doi: 10.3389/fbioe.2020.00804

Osteoarthritis (OA) in articular joints is a prevalent disease. With increasing life expectancy, the need for therapies other than knee replacement arises. The intrinsic repair capacity of cartilage is limited, therefore alternative strategies for cartilage regeneration are being explored. The purpose of this study is first to investigate the potential of platelet lysate (PL) as a xeno-free alternative in expansion of human OA chondrocytes for cell therapy, and second to assess the effects of PL on redifferentiation of expanded chondrocytes in 3D pellet cultures. Chondrocytes were isolated from human OA cartilage and subjected to PL in monolayer culture. Cell proliferation, morphology, and expression of chondrogenic genes were assessed. Next, PL-expanded chondrocytes were cultured in 3D cell pellets and cartilage matrix production was assessed after 28 days. In addition, the supplementation of PL to redifferentiation medium for the culture of expanded chondrocytes in 3D pellets was evaluated. Glycosaminoglycan (GAG) and collagen production were evaluated by quantitative biochemical analyses, as well as by (immuno)histochemistry. A dose-dependent effect of PL on chondrocyte proliferation was found, but expression of chondrogenic markers was decreased when compared to FBS-expanded cells. After 28 days of subsequent 3D pellet culture, GAG production was significantly higher in pellets consisting of chondrocytes expanded with PL compared to controls. However, when used to supplement redifferentiation medium for chondrocyte pellets, PL significantly decreased the production of GAGs and collagen. In conclusion, chondrocyte proliferation is stimulated by PL and cartilage production in subsequent 3D culture is maintained. Furthermore, the presences of PL during redifferentiation of 3D chondrocyte strongly inhibits GAG and collagen content. The data presented in the current study indicate that while the use of PL for expansion in cartilage cell therapies is possibly beneficial, intra-articular injection of the product in the treatment of OA might be questioned.

Keywords: platelet lysate, chondrocyte, cartilage regeneration, ACI, xeno-free

INTRODUCTION

Focal cartilage defects occur frequently in young and active patients and cause serious limitations on both joint function and the patient's mobility and quality of life (Heir et al., 2010). As cartilage is an avascular tissue, spontaneous healing of the tissue is limited. In addition, with increasing life expectancy, the patient population with osteoarthritis (OA) is growing continuously (Cross et al., 2014).

A well-established surgical procedure to treat cartilage defects is autologous chondrocyte implantation (ACI). Long-term follow-up studies have demonstrated hyaline-like cartilage formation and satisfactory clinical outcome up to 20 years post-surgery (Brittberg, 2008; Peterson et al., 2010). Nevertheless, a major part of treated patients shows signs of fibrocartilage formation in the regenerated area (McCarthy et al., 2018). As fibrocartilage is mechanically inferior to hyaline cartilage, it is unfit to fulfill the natural functions of hyaline cartilage and therefore more prone to degradation (Messner and Maletius, 1996; Knutsen et al., 2004). One of the causes of the fibrocartilage formation is dedifferentiation of chondrocytes during the *in vitro* expansion phase (Schnabel et al., 2002), which is a requirement to obtain a sufficient amount of cells for autologous cell transplantation. Maintaining chondrogenic redifferentiation capacity of chondrocytes during expansion is essential for improving the quality of the regenerated cartilage and thus potentially improves clinical outcome.

Platelet-rich plasma (PRP) is a blood product containing high growth factor levels that has been used for various applications over the past decades (Sánchez et al., 2007; Mei-Dan et al., 2012; Smith, 2015; Zhang et al., 2018). While variations in content and production methods exist, PRP consistently contains a high concentration of blood platelets. In orthopedics, PRP and PRP-derivates like platelet lysate (PL) can be used for applications such as intra-articular injection for the treatment of knee osteoarthritis (Filardo et al., 2015b). Moreover, as it is a rich source of growth factors, human PL also shows potential to be used in cell culture as a xeno-free alternative to bovine serum, possibly as a pooled off-the-shelf media supplement. In clinical cell therapy, PL is already used for the expansion of cells (de Windt et al., 2016).

The effect of *in vitro* expansion in the presence of PL on the chondrogenic potential of chondrocytes remains unclear. While most studies agree that PRP and PL have a stimulatory effect on chondrocyte proliferation (Drengk et al., 2008; Pereira et al., 2013), contradictory results have been reported on anabolic effects of PRP-derivates on cartilage matrix formation by chondrocytes (Drengk et al., 2008; Pereira et al., 2013; Xie et al., 2014).

Therefore, the current study aims to investigate the effect of PL on the chondrogenic potential of chondrocytes. More specifically, this study looked into the effect of PL on chondrocytes during expansion and subsequent 3D culture, as well as effects on matrix production in 3D cultures while being exposed to PL.

MATERIALS AND METHODS

Experimental Design and Study Outline

To test the hypothesis whether PL will maintain chondrogenic capacity of culture expanded chondrocytes, chondrocyte monolayers were subjected to various concentrations of PL and compared to culture in fetal bovine serum (FBS). To subsequently assess cartilage-like matrix formation, chondrocytes were harvested and cultured in 3D cell pellets. The production of sulfated GAGs and collagens was measured biochemically, as well as histologically and by gene expression to compare between groups. In addition, the hypothesis that PL will improve redifferentiation of chondrocytes was tested using a similar 3D cell pellet culture system where PL was added fresh into the redifferentiation medium each medium change. Production of GAGs and collagens was assessed similarly as above.

Platelet Lysate Preparation and Growth Factor Quantification

Platelet lysate was prepared from human blood collected in 3.2% sodium citrate-containing tubes. Blood was obtained through the Mini Donor Service, a blood donation facility for research purposes approved by the medical ethics committee of the University Medical Center Utrecht, Netherlands. All donors have provided written informed consent, in accordance with the declaration of Helsinki. All donors were reported being healthy and free from antiplatelet drugs or non-steroid anti-inflammatory drugs. Platelet-rich plasma was prepared by centrifugation of whole blood at 130 *g* for 15 min, upon which pelleted erythrocytes were discarded and the plasma layer was concentrated by a second centrifugation cycle at 250 *g* for 15 min. Platelet count was measured using a CELL-42 DYN Emerald Hematology Analyzer (Abbott, United States). Platelets were activated to release their growth factors by three freeze-thaw cycles, after which samples were centrifuged at 8,000 *g* for 10 min and supernatant PL was stored at −20°C until use. Pooled PL from at least three donors was used in each experiment. The concentrations of human growth factors PDGF-AB, TGF-β1, VEGF, and FGF-2 were quantitatively determined using enzyme-linked immunosorbent assays (ELISA) according to the manufacturer's instructions (DuoSet ELISA kits, R&D Systems, Minneapolis, MN, United States).

Donors and Cell Isolation

Osteoarthritic cartilage was obtained from redundant material from patients who had undergone total knee arthroplasty. The material is collected anonymously according to the Medical Ethics regulations of the University Medical Center Utrecht and approved by the local medical ethics committee (University Medical Center Utrecht). Cartilage was dissected from the underlying bone, rinsed in phosphate-buffered saline (PBS) and cut into 2 mm pieces. The pieces were digested in 0.2% (w/v) pronase (Sigma-Aldrich) in Dulbecco's modified Eagle's medium (DMEM, 31966; Gibco, Netherlands) with 1% penicillin/streptomycin (100 U/mL, 100 mg/mL; Gibco)

at 37°C for 2 h, followed by overnight digestion in 0.075% (w/v) collagenase type II (CLS-2, Worthington, Lakewood, NJ, United States) in DMEM supplemented with 10% (v/v) heat-inactivated FBS (Biowest) and 1% penicillin/streptomycin under agitation. The cells were then filtered through a 70-μm cell strainer (Greiner Bio-One), washed, and counted. Chondrocytes were expanded using Expansion medium (DMEM supplemented with 1% penicillin/streptomycin and 10% FBS). Cells were cryopreserved in liquid nitrogen until use.

Cell Culture

Passage 1 chondrocytes (n = 6 donors, age 61–75, average 69 years) were seeded in 24-well plates at 1,500 cells/cm^2 and cultured for 7 days in Expansion medium, where FBS was replaced with 0.01, 0.1, 1, 2, or 5% PL (all v/v). All media containing PL were supplemented with 3.3 U/mL heparin (Sigma-Aldrich) to prevent coagulation. Control conditions were cultured in Expansion medium with 10% FBS, with and without heparin. As a negative control, chondrocytes were expanded with serum-free medium (DMEM supplemented with 2% human serum albumin (HSA; Sanquin Blood Supply Foundation), 2% insulin-transferrin-selenium-ethanolamine (ITS-X; Gibco), 0.2 mM L-ascorbic acid 2-phosphate (ASAP; Sigma-Aldrich), and 1% penicillin/streptomycin). This did not lead to a sufficient number of chondrocytes to be used for further pellet culture and therefore this condition was not included in the following experiments. Photomicrographs can be found in **Supplementary Figure S1**.

For the 3D pellet culture, chondrocytes (n = 5 donors, age 55–75, average 65 years) were expanded in monolayers in Expansion medium with either 10% FBS, 1, or 5% PL and heparin up to passage 2. Following expansion, pellets containing 2.5 × 10^5 cells were formed in ultra-low attachment 96-well round-bottom plate wells (Corning) by centrifugation at 300 g for 5 min. Pellets were cultured for 28 days in Redifferentiation medium (DMEM supplemented with 2% HSA, 2% ITS-X, 0.2 ASAP, and 1% penicillin/streptomycin).

For evaluating the effects of PL on chondrogenic redifferentiation, chondrocytes (n = 6 donors, age 54–84, average 65 years) were first expanded in Expansion medium with 10% FBS. Pellets were then cultured for 28 days in Redifferentiation medium either or not supplemented with 1 or 5% PL and heparin.

Immunofluorescent Staining

Expanded monolayers were fixed after 7 days with 10% buffered formalin. Fixed monolayers were permeabilized using 0.2% Triton X-100 (Sigma-Aldrich) in PBS for 20 min, followed by incubation with phalloidin (TRITC-conjugated; 1/200 dilution in PBS; Sigma-Aldrich) for 1 h. Nuclei were stained with 100 ng/mL 4',6-diamidino-2-phenylindole (DAPI; Sigma-Aldrich) in PBS for 5 min. Monolayers were imaged using an upright fluorescent microscope (BX51; Olympus).

Biochemical Analysis of Pellets

Pellets were harvested after 28 days to measure glycosaminoglycan (GAG), collagen, and DNA content. Samples were digested overnight in a papain digestion buffer (250 μg/mL papain; Sigma-Aldrich, 0.2 M NaH_2PO_4, 0.1M EDTA, 0.01M cysteine, pH 6) at 60°C.

Sulfated GAG content was quantified using a dimethylmethylene blue (DMMB; pH 3) assay. The 525/595 nm absorbance ratio was measured using chondroitin-6-sulfate (Sigma-Aldrich) as a standard.

Total collagen content was calculated from the hydroxyproline content (Neuman and Logan, 1950). Papain digests were lyophilized and hydrolyzed in 4 M NaOH (Sigma-Aldrich) in Milli-Q water overnight at 108°C, after which samples were neutralized with 1.4 M citric acid (Sigma-Aldrich) in Milli-Q water. 50 mM freshly prepared Chloramin-T (Merck) in oxidation buffer was added and incubated for 20 min under agitation. Subsequently, 1.1 M freshly prepared dimethylaminobenzoaldehyde (Merck) in 25% (v/v) perchloric acid (Merck) in 2-propanol (Sigma-Aldrich) was added and incubated for 20 min at 60°C. Samples were cooled and absorbance read at 570 nm using hydroxyproline (Merck) as a standard.

Total DNA content was quantified using a Quant-iT PicoGreen dsDNA assay (Invitrogen) according to the manufacturer's instructions. Fluorescence was measured at 485 nm excitation and 535 nm emission by a microplate fluorometer (Fluoroskan Ascent).

Histology

Pellets were processed for histology by fixation in 10% buffered formalin, dehydration through graded ethanol steps, clearing in xylene, and subsequent embedding in paraffin. 5 μm sections were cut and deparaffinised before staining. Sections were stained for GAGs with 0.125% safranin-O (Merck) counterstained with 0.4% fast green (Sigma-Aldrich) and Weigert's hematoxylin (Clin-Tech). Collagen deposition was evaluated by immunohistochemistry, with appropriate primary antibodies for type II collagen (II-II6B3; DHSB; 1:100 in PBS/BSA 5%) and type I collagen (EPR7785, BioConnect; 1:400 in PBS/BSA 5%). Samples were blocked using 0.3% H_2O_2, followed by antigen retrieval with pronase (1 mg/mL; Sigma-Aldrich) for 30 min at 37°C and hyaluronidase (10 mg/mL; Sigma-Aldrich) for 30 min at 37°C. Next, sections were blocked using bovine serum albumin (BSA; 5% (w/v) in PBS) for 30 min, followed by overnight incubation with the primary antibody at 4°C. After washing, type II collagen sections were incubated with a goat-anti-mouse IgG HRP-conjugated (DAKO, P0447; 1:100 in PBS/BSA 5%) and type I collagen sections with Envision + System-HRP anti-rabbit (DAKO, K4003), both for 1 h at room temperature. Next, both stainings were developed using 3,3'-diaminobenzidine (DAB, Sigma-Aldrich). Sections were counterstained with Mayer's hematoxylin (Klinipath) and mounted in DPX mounting medium (Merck).

Real-Time PCR

Total RNA was isolated from monolayers and pellets using TRIzol (Invitrogen) according to the manufacturer's instructions. Total RNA (200–500 ng) was reverse transcribed using the High-Capacity cDNA Reverse Transcription Kit (Applied

Biosystems). Real-time polymerase chain reactions (PCRs) were performed using iTaq Universal SYBR Green Supermix (Bio-Rad) in a LightCycler 96 (Roche Diagnostics) according to the manufacturer's instructions. The amplified PCR fragments extended over at least one exon border (except for 18S). Relative gene expression was calculated using 18S as a housekeeping gene. Primers (Invitrogen) used for real-time PCR are listed in **Table 1**.

Statistical Analysis

Each experiment was performed with cells from six donors. For the monolayer expansion, three wells were used for each condition. For pellet cultures, three pellets were used for biochemical analyses, three for gene expression analysis, and two for histology. Data are expressed as mean ± standard deviation (SD). Data were statistically analyzed using the GraphPad Prism 7.0 software package (GraphPad Software, United States). Normal distribution of the data was checked with a Shapiro-Wilk test ($p > 0.05$) and homogeneity with a Levene's test. When the data was normally distributed and samples were homogeneous, a one-way analysis of variance (ANOVA) was performed with Dunnett's *post hoc* test. When the data was non-normally distributed, a Kruskal-Wallis test was performed with Dunn's *post hoc*. A value of $p < 0.05$ was considered statistically significant.

RESULTS

Platelet Lysate Characterization

To characterize the PL product, cell and platelet concentrations were counted and growth factor concentrations were determined in six batches of PL by ELISA (**Table 2**). Manually prepared PL was deprived from erythrocytes ($19 \pm 4 \times 10^9$/L) and leukocytes ($0.3 \pm 0.1 \times 10^9$/L), while platelet concentrations were maintained ($458 \pm 87 \times 10^9$/L). Furthermore, we found high concentrations of PDGF-AB (36142 ± 2518 pg/mL) and TGF-β1 (65379 ± 3889 pg/mL), while concentrations of FGF-2 (49 ± 10 pg/mL) and VEGF (150 ± 53 pg/mL) were less.

TABLE 1 | Primer sequences used for real-time PCR.

Target gene	Oligonucleotide sequence (5' to 3')	Annealing temperature (°C)	Product size (bp)
18S	Fw: GTAACCCGTTGAACCCCATT Rv: CCATCCAATCGGTAGTAGCG	57	151
COL2A1	Fw: AGGGCCAGGATGTCCGGCA Rv: GGGTCCCAGGTTCTCCATCT	57	195
ACAN	Fw: CAACTACCCGGCCATCC Rv: GATGGCTCTGTAATGGAACAC	56	160
COL1A1	Fw: TCCAACGAGATCGAGATCC Rv: AAGCCGAATTCCTGGTCT	57	191
SOX9	Fw: CCCAACGCCATCTTCAAGG Rv: CTGCTCAGCTCGCCGATGT	60	242
ACTA2	Fw: ATGCCATCATGCGTCTGGAT Rv: ACGCTCAGCAGTAGTAACGA	60	101
NOTCH1	Fw: AAGCTGCATCCAGAGGCAAAC Rv: TGGCATACACACTCCGAGAACAC	60	172
CDH2	Fw: GCGTCTGTAGAGGCTTCTGG Rv: GCCACTTGCCACTTTTCCTG	60	293

Forward (Fw) and reverse (Rev) primers. COL2A1, collagen type II alpha 1 chain; ACAN, aggrecan; COL1A1, collagen type I alpha 1 chain; SOX9, SRY-box transcription factor 9; ACTA2, actin alpha 2, smooth muscle; NOTCH1, notch receptor 1; CDH2, cadherin 2.

TABLE 2 | Cell and growth factor concentrations in platelet lysate.

	Content (mean ± SEM)
Erythrocytes (10^9/L)	19 ± 4
Leukocytes (10^9/L)	0.3 ± 0.1
Platelets (10^9/L)	458 ± 87
PDGF-AB (pg/mL)	36, 142 ± 2, 518
TGF-β1 (pg/mL)	65, 379 ± 3, 889
FGF-2 (pg/mL)	49 ± 10
VEGF (pg/mL)	150 ± 53

Cell concentrations in PL were determined using a CELL-42 DYN Emerald Hematology Analyzer. Growth factor concentrations in PL were quantified by enzyme-linked immunosorbent assays (ELISA). All values are expressed as mean ± SEM (n = 6).

Chondrocyte Proliferation Is Stimulated in the Presence of Platelet Lysate During Expansion

Supplementation of Expansion medium with PL enhanced chondrocyte proliferation in a dose-dependent manner. Immunocytochemical staining of monolayers with phalloidin suggested an increase in cell amount after 7 days of exposure to PL (**Figure 1A**). These findings were confirmed by quantification of DNA content (**Figure 1C**). Furthermore, changes in cellular morphology were observed. Chondrocytes cultured in the presence of PL exhibited an elongated shape opposed to a more spindle-like shape for cells in control expansion cultures (**Figure 1B**).

In contrast to the dose-dependent increase in DNA content, expression of chondrogenic genes coding for type II collagen (COL2A1), aggrecan (ACAN), and SRY-box transcription factor 9 (SOX9) decreased in a dose-dependent manner compared to the control group (**Figures 2A–D**). Expression of dedifferentiation marker type I collagen (COL1A1) was increased with increasing PL concentrations, while fibroblast marker actin alpha 2, smooth muscle (ACTA2) did not show significant changes (**Figures 2E,F**). Notch receptor 1 (NOTCH1) and cadherin 2 (CDH2), genes associated with stemness, were significantly increased when chondrocytes were exposed to culture medium containing 5% PL (**Figures 2G,H**).

Chondrocytes Expanded in the Presence of Platelet Lysate Maintain Their Redifferentiation Potential

To compare chondrogenic potential of PL-expanded chondrocytes and chondrocytes expanded in the presence of FBS, 3D pellet cultures were performed to allow for neo-cartilage extracellular matrix (ECM) formation. Pellets

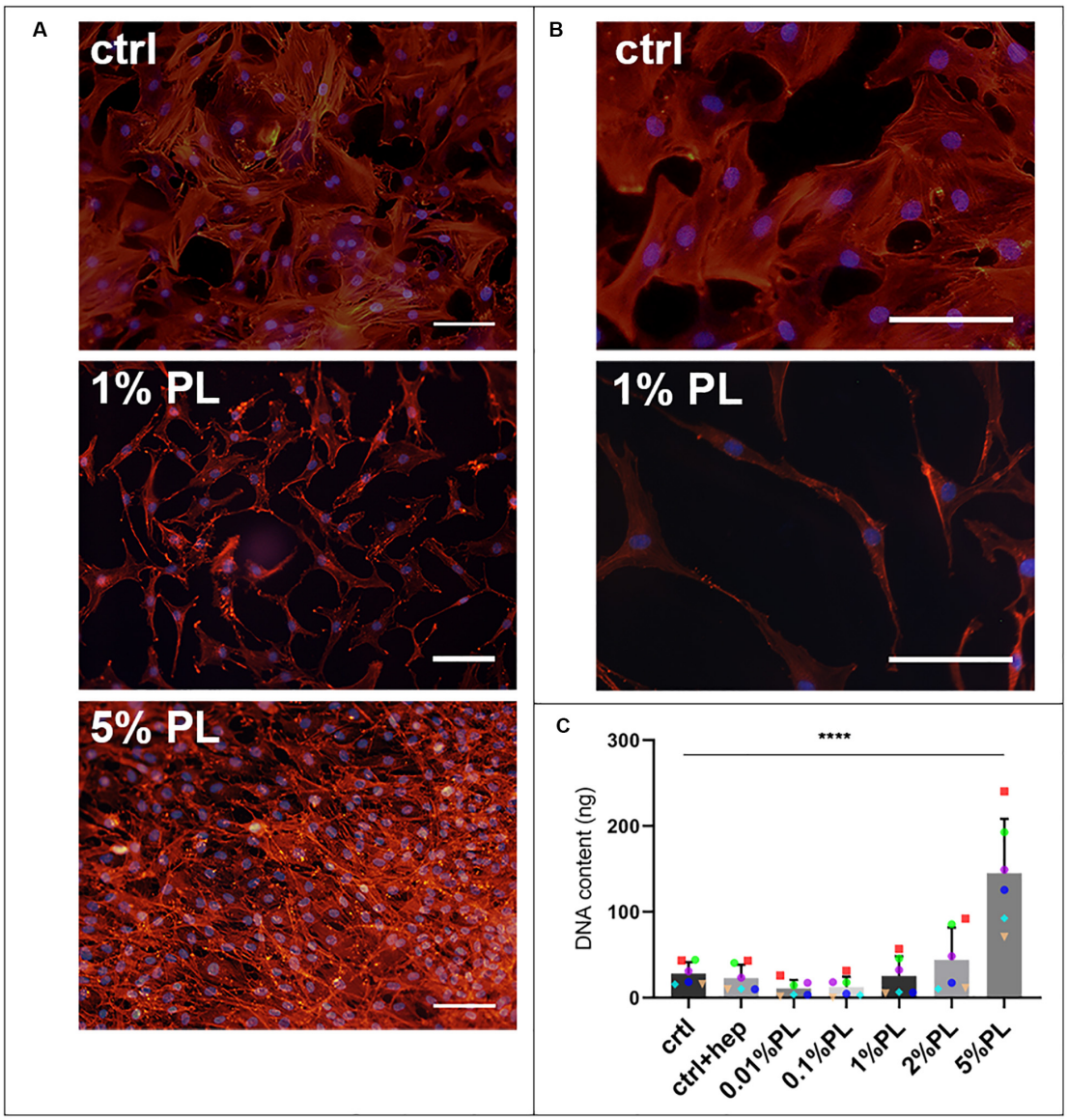

FIGURE 1 | Effect of platelet lysate on chondrocyte proliferation. Phalloidin/DAPI staining of passage 1 chondrocytes after 7 days in monolayer culture in expansion medium supplemented with 10% FBS, 1, and 5% PL **(A)**. Higher magnification of the photomicrographs showing the morphology of chondrocytes expanded with 10% FBS and 1% PL **(B)**. DNA content of the monolayer conditions **(C)**. All scale bars = 100 μm. Data are presented as mean ± SD. ****$p < 0.0001$.

consisting of PL-expanded chondrocytes were found to produce significantly more GAGs after 28 days when compared to the control conditions (**Figure 3A**). A slight qualitative increase in GAG production was seen across all chondrocyte donors used in this experiment (**Figure 3B** and **Supplementary Figure S2**). However, pellets consisting of 5% PL-expanded chondrocytes did not evidently show an improvement in GAG production on histology when compared to 1% PL-expanded chondrocyte pellets. Additionally, PL-expanded chondrocyte pellets did not present an increase in ACAN gene expression (**Figure 3A**).

To further investigate the chondrogenic potential of PL-expanded chondrocytes, production of collagen was determined. Quantitative biochemical analysis of total collagen content revealed an increase in 1% PL-expanded chondrocyte pellets compared to the control conditions. However, no differences were found on gene expression level of COL2A1 and COL1A1 (**Figure 4A**). Immunohistochemical staining revealed a slight increase in type II collagen production in two out of five donors. Overall, no evident increase of type II collagen was seen in experimental groups, in line with the mRNA data (**Figure 4B** and **Supplementary Figure S2**). Furthermore, staining for type I collagen was absent in all conditions (**Figure 4B**).

Taken together, these data suggest that the chondrogenic differentiation capacity is preserved in osteoarthritic chondrocytes upon expansion with PL.

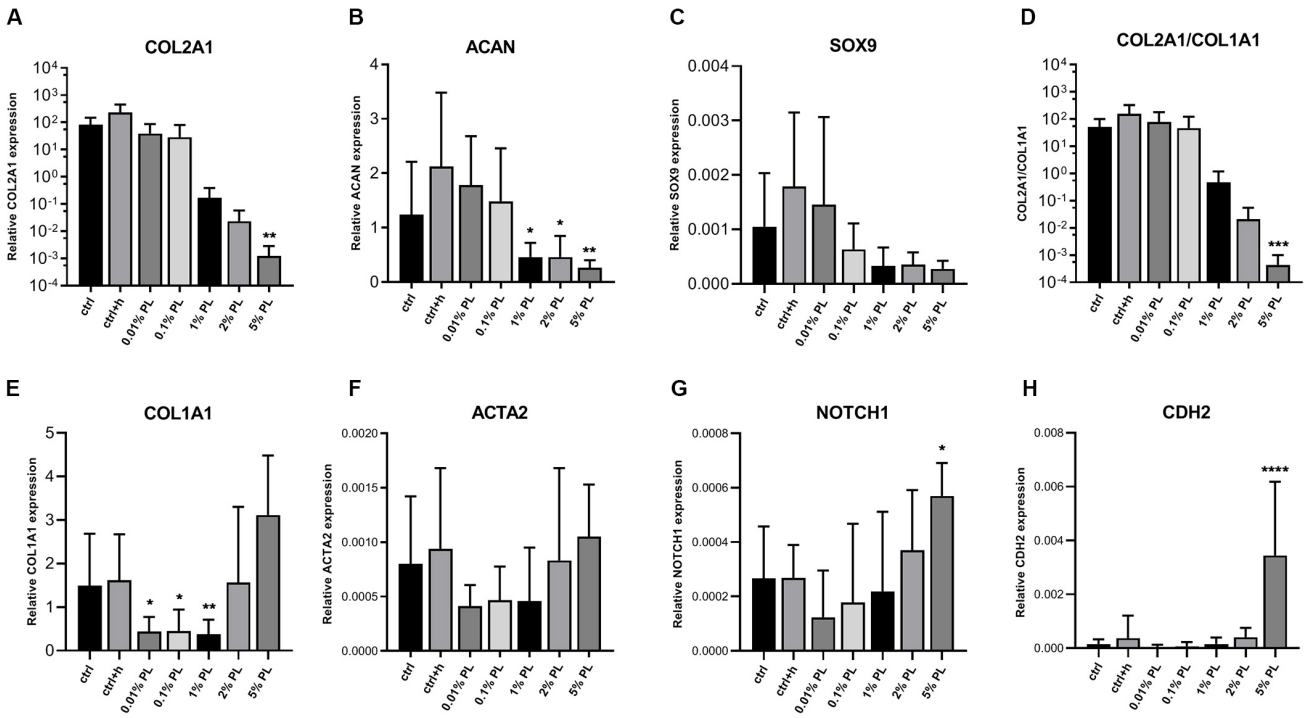

FIGURE 2 | Gene expression of platelet lysate-expanded chondrocytes in monolayers. Gene expression type II collagen (COL2A1, **A**), aggrecan (ACAN, **B**), SRY-box transcription factor 9 (SOX9, **C**), ratio of type II/type I collagen (COL2A1/COL1A1, **D**), type I collagen (COL1A1, **E**), actin alpha 2, smooth muscle (ACTA2, **F**), notch receptor 1 (NOTCH1, **G**) and cadherin 2 (CDH2, **H**) by chondrocytes in monolayer culture in expansion medium supplemented with 10% FBS (ctrl), 10% FBS and 3.3 U/mL heparin (ctrl + h), 0.01% platelet lysate (PL), 0.1, 1, 2, and 5% PL (all PL conditions contain heparin), normalized for the housekeeping gene 18S. Data are shown as mean ± SD. $^{*}p < 0.05$; $^{**}p < 0.005$; $^{***}p < 0.0005$; $^{****}p < 0.0001$.

Platelet Lysate Strongly Inhibits Matrix Production During Redifferentiation of Chondrocytes

To test whether PL has a chondrogenic effect on osteoarthritic chondrocytes *in vitro*, chondrocytes were cultured in 3D pellets, after which PL was added to the Redifferentiation medium. For these experiments, all cells were expanded using conventional Expansion medium containing 10% FBS, instead of PL.

Biochemical analyses revealed a significant decrease in GAG production in pellets differentiated in the presence of 1 or 5% PL. Further, cell numbers also decreased as confirmed by DNA quantification analysis. Quantitative analysis for total collagen did not reveal any difference between experimental and control conditions (**Figure 5A**). For donors with high chondrogenic capacity (**Figure 5B**, Donor 1) as well as donors having low chondrogenic capacity (**Figure 5B**, Donor 2), addition of PL during redifferentiation strongly inhibited GAG, type II and type I collagen formation. Histological stainings for GAGs and type II collagen of all donors used in this experiment are displayed in **Supplementary Figure S3**, confirming the uniform effect of PL on inhibition of cartilage matrix formation. Expression of chondrogenic marker COL2A1 significantly decreased in pellets cultured in the presence of 1 and 5% PL, while no difference was found in the expression of ACAN and COL1A1 (**Figure 5C**).

These data reveal a considerable inhibition of cartilage matrix production by PL in chondrocyte pellets, independent of chondrogenic capacity of the donor.

DISCUSSION

The dedifferentiation of chondrocytes during expansion is a major challenge in the successful application of ACI as this causes the formation of fibrocartilage. PRP and PL provide a rich source of growth factors, which can provide an autologous supplement for *in vitro* cell culture. While some studies report on the stimulation of chondrocyte proliferation, chondrogenesis, and diminishing catabolic effects in the treatment of OA, consensus on this topic does not exist. Moreover, very limited work has been done on the capacity of PL to rescue cartilage matrix production in cultured OA chondrocytes.

The aim of this study was to elucidate the effects of PL on OA chondrocytes *in vitro*. We confirmed that PL exerts a stimulatory effect on the proliferation of chondrocytes. A dose-dependent effect on chondrocyte proliferation by PL was found, as determined by the quantification of DNA in the monolayer samples. This result is in line with previous studies where PL was compared to FBS-containing expansion medium (Choi et al., 1980; Gaissmaier et al., 2005; Pereira et al., 2013; Hildner et al., 2015). In addition to the

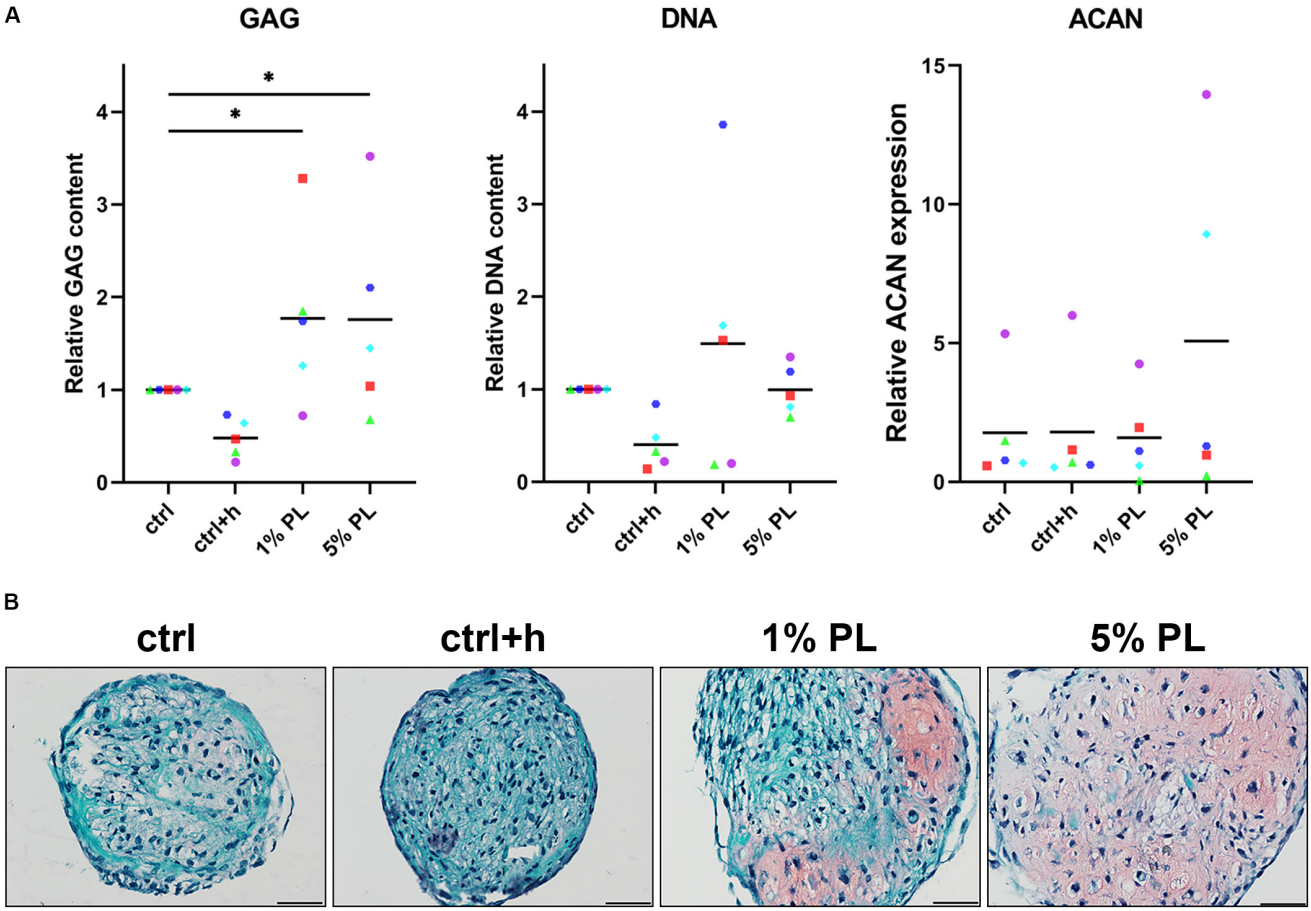

FIGURE 3 | Glycosaminoglycan production of chondrocytes in 3D pellet cultures. Glycosaminoglycan (GAG) deposition and aggrecan (ACAN) gene expression in pellet cultures of passage 2 chondrocytes expanded in medium supplemented with 10% FBS (ctrl) with and without heparin (+h), 1- and 5% human platelet lysate (PL) cultured for 28 days in redifferentiation medium. **(A)** Biochemical analysis of GAGs and DNA content and relative expression of ACAN (normalized against the housekeeping gene 18S). Data are presented per donor and overall mean. *$p < 0.05$. **(B)** Histological assessment by safranin-O. Scale bar = 100 μm.

stimulation of proliferation, we found a decreased expression of chondrogenic marker genes COL2A1 and ACAN, and an increase of the dedifferentiation marker COL1A1 compared to FBS-expanded chondrocytes. Taken together, this suggests an increased dedifferentiation of chondrocytes during expansion in PL-supplemented medium. Interestingly, a recent study reports on increased expression of chondrogenic markers and decreased expression of dedifferentiation markers in MSCs and cartilage progenitor cells expanded using different concentrations of PL and the same effect was to a lesser extent visible in chondrocytes (Wang et al., 2019). Additionally, we found that chondrocytes expanded with the highest concentration of PL exhibited an increased expression of CDH2 and NOTCH1. CDH2 has been described to be involved in embryonic limb chondrogenesis and is associated with (cartilage) stemness (Oberlender and Tuan, 1994). Specific expression of NOTCH1 has been described at the developing cartilage surface of mouse knee joints (Hayes et al., 2003) and in cells with enhanced clonality at the articular surface of bovine cartilage (Dowthwaite et al., 2004). Therefore, we suggest that the specific combination and concentration of growth factors in PL as used in the current study drives chondrocytes into a dedifferentiated state with increased chondroprogenitor-like potential.

Next, our data demonstrated that chondrocytes that were expanded with PL maintain their chondrogenic differentiation capacities when subsequently cultured in a 3D environment. The deposition of GAGs was slightly increased in PL-expanded chondrocyte pellets, while type II collagen deposition was unaltered. Moreover, type I collagen production was absent in both FBS-expanded chondrocyte pellets as well as in PL-expanded chondrocyte pellets. This supports our suggestion that chondrocytes expanded in PL do dedifferentiate but maintain progenitor-like chondrogenic potential. Several previous studies also reported on an increase (Choi et al., 1980; Hildner et al., 2015) or maintenance (Pereira et al., 2013) of chondrogenic potential of chondrocytes after expansion in PL, while another study observed opposite outcomes (Sykes et al., 2018). This makes it hard to draw a conclusive statement on the effects of PL on chondrogenic capacities of chondrocytes is still lacking.

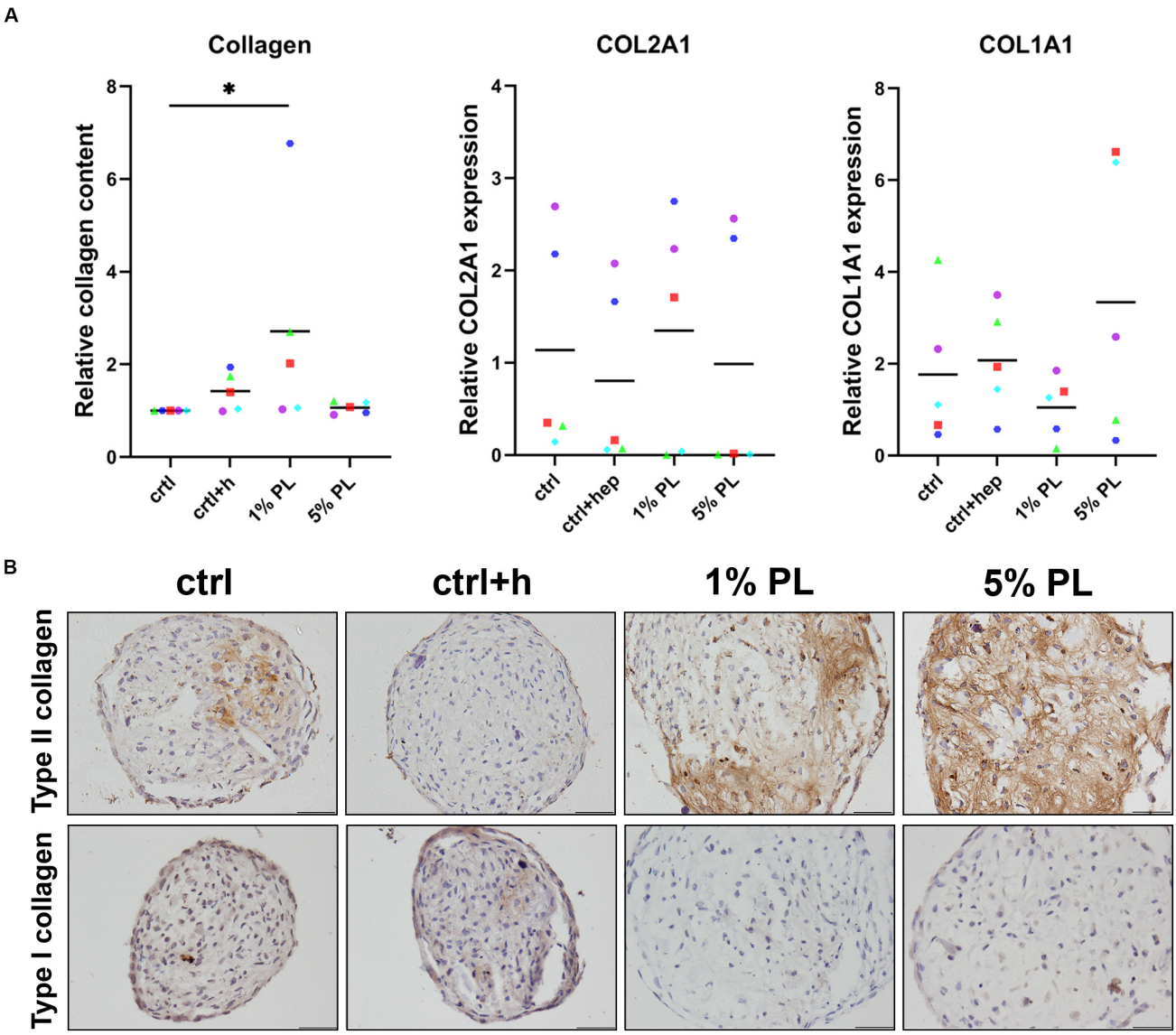

FIGURE 4 | Collagen production of chondrocytes in 3D pellet cultures. Collagen deposition and type II (COL2A1) and I collagen (COL1A1) gene expression in pellet cultures of passage 2 chondrocytes expanded in medium supplemented with 10% FBS (ctrl) with and without heparin (+h), 1- and 5% human platelet lysate (PL) cultured for 28 days in redifferentiation medium. **(A)** Biochemical analysis of total collagen content and relative expression of COL2A1 and COL1A1 (normalized against the housekeeping gene 18S). Data are presented per donor and overall mean. *$p < 0.05$. **(B)** Histological assessment by type II and I collagen immunohistochemistry. Scale bar = 100 μm.

The effect of intra-articular PRP injections in the treatment of OA has been evaluated in various randomized controlled trials (Kon et al., 2011; Cerza et al., 2012; Patel et al., 2013; Filardo et al., 2015a; Smith, 2015; Cole et al., 2017; Jubert et al., 2017). Since some of these studies found a positive effect on pain and function (Kon et al., 2011; Cerza et al., 2012; Cole et al., 2017), we hypothesized that PL would have a stimulatory effect on chondrogenesis in pellets consisting of OA chondrocytes that are expanded in FBS-supplemented expansion medium. Interestingly, our results showed that culture in the presence of PL remarkably inhibited GAG deposition in the pellets when compared to control conditions and complete absence of type II collagen production was observed. Furthermore, real-time PCR data revealed a strong decrease in COL2A1 expression, indicating a dedifferentiation of the chondrocyte phenotype in presence of PL, even in 3D. To the best of our knowledge, no other studies have been performed in which the direct effect of PL on OA chondrocytes in 3D pellet culture is assessed. One paper reported on the effect of PL supplementation to the differentiation medium during only the first 3 days of chondrocyte pellet culture. However, these chondrocytes were also expanded using PL. These pellets performed significantly worse in cartilage matrix production when compared to pellets cultured in regular differentiation medium (Hildner et al., 2015).

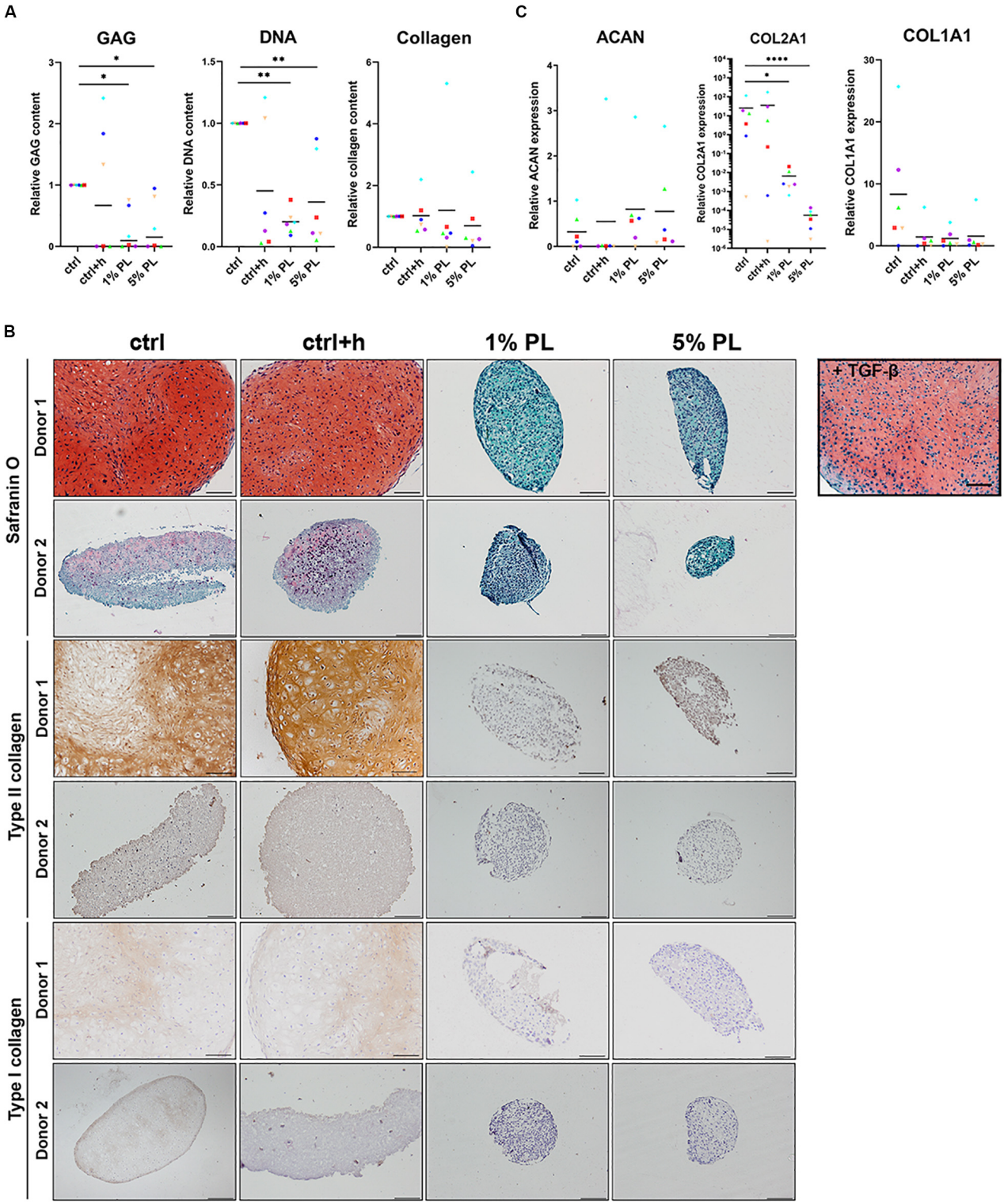

FIGURE 5 | Matrix production and gene expression of chondrocytes in 3D pellet cultures supplemented with platelet lysate. **(A)** Glycosaminoglycan (GAG), collagen, and DNA content after 28 days of culture in redifferentiation medium (ctrl) with and without heparin (+h) and in the presence of 1- and 5% human platelet lysate (PL). **(B)** Cartilage production for one donor with high chondrogenic potential (Donor 1) and one donor with low chondrogenic potential (Donor 2) as determined by histological staining of GAGs by safranin-O, and immunohistochemical staining for type II and I collagen. Scale bar = 100 μm. **(C)** Relative gene expression of type II collagen (COL2A1), aggrecan (ACAN), and type I collagen (COL1A1), normalized for the housekeeping gene 18S. Data are presented per donor and overall mean. $^{*}p < 0.05$; $^{**}p < 0.005$; $^{****}p < 0.0001$.

Outcomes of studies focusing on other 3D culture models are inconsistent. When chondrocytes were cultured in alginate beads and subjected to platelet supernatant, a product similar to PL, a distinct decrease in chondrogenic genes was measured when compared to control conditions lacking platelet supernatant (Gaissmaier et al., 2005). Others reported on induction of chondrogenesis when adding PRP or PL to a 3D culture system. When PL was incorporated in a dextran-containing hydrogel, it was able to enhance proliferation, and simultaneously, induce chondrogenesis, both for MSCs and for cocultures of MSCs and chondrocytes (Moreira Teixeira et al., 2012). The different findings might be explained by differences in the growth factor concentrations and ratios between the various growth factors.

The concentrated growth factors present in PL stimulate chondrocytes to proliferate. It is known that FGF and PDGF stimulate proliferation (Green et al., 2015; Zhao et al., 2016), while TGF-β inhibits proliferation and mediates initiation of differentiation in chondrocytes (Green et al., 2015). Furthermore, the cocktail of growth factors in the current study seems to maintain the cells in a progenitor-like state during expansion, demonstrated by enhanced expression of NOTCH1 and CDH2. These markers are involved in pathways that have been described to be of importance in chondrocyte proliferation during development. Proliferation and regeneration of chondrocytes *in vitro* are two distinct processes that do not go hand in hand. Upon expansion, chondrocytes present a dedifferentiated phenotype, with increased type I collagen gene expression (Darling and Athanasiou, 2005). However, the cells can recover their phenotype and redifferentiate when brought back into 3D culture (Marijnissen et al., 2000). Further in-depth characterization of PL-treated chondrocytes will be necessary to elucidate their phenotypical change in relation to chondroprogenitor cells and MSCs.

The same cocktail of growth factors seems to be ineffective in stimulating chondrocytes to produce cartilage matrix in a 3D pellet environment. Possibly the high concentrations of FGF in PRP may interfere with the redifferentiation process by suppressing cellular senescence and inhibition of the TGF-β pathway (Ito et al., 2007). Human platelets are a rich source of TGF-β and PRP can contain up to 100-fold increased concentrations of TGF-β (Eppley et al., 2004; Sundman et al., 2011). Accordingly, this study also found high concentrations of TGF-β in the used PL. It is known that overstimulation by TGF-β inhibits FGF- and Wnt-mediated proliferation of chondrocytes (Cleary et al., 2015). Besides that, it is likely that high concentrations of TGF-β play a role in *in vitro* fibrocartilage formation by chondrocytes (Narcisi et al., 2012). Future studies looking into molecular mechanisms causing chondrocytes to dedifferentiate upon PL-exposure can shed more light on the observations in the study presented here.

The variations in outcomes between this study and previous research can partly be explained by the numerous methods available to prepare PRP. Firstly, there is a great variation in platelet and growth factor concentration that is used in PRP, caused by both donor variability, as well as by the variety of preparation methods (Sundman et al., 2011; Mazzocca et al., 2012; Dhurat and Sukesh, 2014). Secondly, it remains unclear whether the concentration of growth factors in PRP is related to the concentration of platelets (Eppley et al., 2004; Sundman et al., 2011). Thirdly, there is a difference between leukocyte-rich (LR-) and leukocyte-poor (LP-)PRP. It is generally assumed that leukocytes and immune modulating cytokines present in PRP contribute to a pro-inflammatory environment and is undesirable in the treatment of OA (Anitua et al., 2015; Riboh et al., 2016; Simental-Mendía et al., 2018). Nonetheless, direct comparison in a clinical study between LP- and LR-PRP injections has not given conclusive outcomes which type of PRP is most effective in the treatment of OA (Filardo et al., 2012). However, an *ex vivo* study examining the effects of different PRP preparations on cartilage and meniscal explants suggested a pro-inflammatory effect of LR-PRP preparations (Kisiday et al., 2012). Clinical studies mainly use LP-PRP for injection, containing either similar numbers of leukocytes compared to whole blood (Kon et al., 2011; Filardo et al., 2015a), reduced amounts (Cerza et al., 2012; Cole et al., 2017; Jubert et al., 2017), or are deprived of leukocytes (Patel et al., 2013). There is a need for additional clinical studies to make clear which type of PRP is effective in the treatment of OA, and for PRP and PL preparation methods to be aligned between different laboratories, clinics, and hospitals (Fice et al., 2019). Objective measurements of cartilage quality after PRP treatment are not available to date. Comprehensive studies including objective analysis of cartilage quality after PRP injection are needed in addition to current analysis using mainly patient questionnaire outcomes. Furthermore, there are some limitations to *in vitro* models to consider. Laboratory models are usually limited to a single tissue or cell type, whereas PRP *in vivo* affects the whole joint environment (Filardo et al., 2015b). Moreover, positive clinical outcomes may be explained by mechanisms other than a direct effect of PL on the cells in the cartilage. It has been previously shown that PRP can act anti-inflammatory both *in vitro* as well as *in vivo* (Liu et al., 2014; Moussa et al., 2017). The inflammatory mediators in PRP and PL might create an improvement in the intra-articular environment, upon which cartilage matrix production by the resident chondrocytes is stimulated. An *in vitro* model as presented in the current study is unable to take these additional factors into account. More extensive studies using multiple cell types or tissues, or animal models are necessary to answer this question. Finally, *in vitro* culture does not mimic growth factor clearance, unless a bioreactor system is used. These factors should be taken into account when comparing *in vitro* results to clinical outcomes.

CONCLUSION

The current study provides insights into the effects of PL on chondrogenic differentiation of human chondrocytes and its potential to be used for two different clinical applications. We propose that platelet lysate has potential to be used in the expansion of chondrocytes for application in cartilage defects. Nonetheless, PL exerts a strong inhibitory effect on chondrogenesis *in vitro*, suggesting caution for its utilization in intra-articular injections.

DATA AVAILABILITY STATEMENT

All datasets generated for this study are included in the article/**Supplementary Material**.

AUTHOR CONTRIBUTIONS

MR and LV: conception and design. MR: collection and assembly of data. MR, RL, and LV: analysis and interpretation of the data. MR, RL, JM, and LV: drafting of the article and reviewing, final approval of the article. All authors contributed to the article and approved the submitted version.

FUNDING

This work was supported by the partners of Regenerative Medicine Crossing Borders (RegMed XB), a public-private partnership that uses regenerative medicine strategies to cure common chronic diseases. This collaboration project was financed by the Dutch Ministry of Economic Affairs by means of the PPP Allowance made available by the Top Sector Life Sciences & Health to stimulate public-private partnerships. The research was also supported by the Dutch Arthritis Foundation (LLP-12 and LLP-22) and the European Research Council under grant agreement no. 647426 (3D-JOINT).

ACKNOWLEDGMENTS

The antibody against collagen type II, developed by T. F. Linsenmayer, was obtained from the Developmental Studies Hybridoma Bank, created by the NICHD and maintained at The University of Iowa, Department of Biology, Iowa City, IA, United States.

SUPPLEMENTARY MATERIAL

The Supplementary Material for this article can be found online at: https://www.frontiersin.org/articles/10.3389/fbioe.2020.00804/full#supplementary-material

FIGURE S1 | Photomicrographs of control conditions of chondrocyte expansion. Chondrocytes expanded for 7 days with serum-free medium (negative control), medium containing 10% FBS (positive control), and experimental medium containing 5% platelet lysate (platelet lysate). Scale bars are 200 μm.

FIGURE S2 | Histological evaluation of pellets consisting of platelet lysate-expanded chondrocytes. Safranin O staining **(top panel)** visualizing glycosaminoglycans (GAG) and type II collagen deposition visualized by immunohistochemistry **(bottom panel)** of all donors used in the experiment. Scale bars in the top panel are 100 μm. Scale bars in the bottom panel are 400 μm.

FIGURE S3 | Histological evaluation of platelet lysate-treated pellets. Safranin O staining **(top panel)** visualizing glycosaminoglycans (GAG) and type II collagen deposition visualized by immunohistochemistry **(bottom panel)** of all donors used in the experiment. All scale bars are 100 μm.

REFERENCES

Anitua, E., Zalduendo, M., Troya, M., Padilla, S., and Orive, G. (2015). Leukocyte inclusion within a platelet rich plasma-derived fibrin scaffold stimulates a more pro-inflammatory environment and alters fibrin properties. *PLoS One* 10:121713. doi: 10.1371/journal.pone.0121713

Brittberg, M. (2008). Autologous chondrocyte implantation-technique and long-term follow-up. *Injury* 39, S40–S49. doi: 10.1016/j.injury.2008.01.040

Cerza, F., Carnì, S., Carcangiu, A., Di Vavo, I., Schiavilla, V., Pecora, A., et al. (2012). Comparison between hyaluronic acid and platelet-rich plasma, intra-articular infiltration in the treatment of gonarthrosis. *Am. J. Sports Med.* 40, 2822–2827. doi: 10.1177/0363546512461902

Choi, Y. C., Morris, G. M., and Sokoloff, L. (1980). Effect of platelet lysate on growth and sulfated glycosaminoglycan synthesis in articular chondrocyte cultures. *Arthrit. Rheum.* 23, 220–224. doi: 10.1002/art.1780230213

Cleary, M., van Osch, G., Brama, P., Hellingman, C., and Narcisi, R. (2015). FGF, TGFβ and Wnt crosstalk: embryonic to in vitro cartilage development frommesenchymal stem cells. *J. Tissue Eng. Regen. Med.* 9, 332–342. doi: 10.1002/term.1744

Cole, B. J., Karas, V., Hussey, K., Pilz, K., and Fortier, L. A. (2017). Hyaluronic acid versus platelet-rich plasma. *Am. J. Sports Med.* 45, 339–346. doi: 10.1177/0363546516665809

Cross, M., Smith, E., Hoy, D., Nolte, S., Ackerman, I., Fransen, M., et al. (2014). The global burden of hip and knee osteoarthritis: estimates from the global burden of disease 2010 study. *Ann. Rheum. Dis.* 73, 1323–1330. doi: 10.1136/annrheumdis-2013-204763

Darling, E. M., and Athanasiou, K. A. (2005). Rapid phenotypic changes in passaged articular chondrocyte subpopulations. *J. Orthop. Res.* 23, 425–432. doi: 10.1016/j.orthres.2004.08.008

de Windt, T. S., Vonk, L. A., Slaper-Cortenbach, I. C. M., van den Broek, M. P. H., Nizak, R., van Rijen, M. H. P., et al. (2016). Allogeneic mesenchymal stem cells stimulate cartilage regeneration and are safe for single-stage cartilage repair in humans upon mixture with recycled autologous chondrons. *Stem Cells* 10, 256–264. doi: 10.1002/stem.2475

Dhurat, R., and Sukesh, M. (2014). Principles and methods of preparation of platelet-rich plasma: a review and author's perspective. *J. Cutan. Aesthet. Surg.* 7, 189–197. doi: 10.4103/0974-2077.150734

Dowthwaite, G. P., Bishop, J., Redman, S., Khan, I., Rooney, P., Evans, D., et al. (2004). The surface of articular cartilage contains a progenitor cell population. *J. Cell Sci.* 117, 889–897. doi: 10.1242/jcs.00912

Drengk, A., Zapf, A., Stürmer, E. K., Stürmer, K. M., and Frosch, K.-H. (2008). Influence of platelet-rich plasma on chondrogenic differentiation and proliferation of chondrocytes and mesenchymal stem cells. *Cells Tissues Organ.* 189, 317–326. doi: 10.1159/000151290

Eppley, B. L., Woodell, J. E., and Higgins, J. (2004). Platelet quantification and growth factor analysis from platelet-rich plasma: implications for wound healing. *Plast. Reconstr. Surg.* 114, 1502–1508. doi: 10.1097/01.PRS.0000138251.07040.51

Fice, M. P., Miller, J. C., Christian, R., Hannon, C. P., Smyth, N., Murawski, C. D., et al. (2019). The role of platelet-rich plasma in cartilage pathology: an updated systematic review of the basic science evidence. *Arthrosc. J. Arthrosc. Relat. Surg.* 35, 961–976. doi: 10.1016/j.arthro.2018.10.125

Filardo, G., Di Matteo, B., Di Martino, A., Merli, M., Cenacchi, A., Fornasari, P., et al. (2015a). Platelet-rich plasma intra-articular knee injections show no superiority versus viscosupplementation: a randomized controlled trial. *Am. J. Sports Med.* 43, 1575–1582. doi: 10.1177/0363546515582027

Filardo, G., Kon, E., Roffi, A., Di Matteo, B., Merli, M., and Marcacci, M. (2015b). Platelet-rich plasma: why intra-articular? A systematic review of preclinical studies and clinical evidence on PRP for joint degeneration. *Knee Surg. Sport. Traumatol. Arthrosc.* 23, 2459–2474. doi: 10.1007/s00167-013-2743-2741

Filardo, G., Kon, E., Pereira Ruiz, M. T., Vaccaro, F., Guitaldi, R., Di Martino, A., et al. (2012). Platelet-rich plasma intra-articular injections for cartilage degeneration and osteoarthritis: single- versus double-spinning approach. *Knee Surgery Sport Traumatol. Arthrosc.* 20, 2082–2091. doi: 10.1007/s00167-011-1837-x

Gaissmaier, C., Fritz, J., Krackhardt, T., Flesch, I., Aicher, W. K., and Ashammakhi, N. (2005). Effect of human platelet supernatant on proliferation and matrix synthesis of human articular chondrocytes in monolayer and three-dimensional alginate cultures. *Biomaterials* 26, 1953–1960. doi: 10.1016/j.biomaterials.2004.06.031

Green, J. D., Tollemar, V., Dougherty, M., Yan, Z., Yin, L., Ye, J., et al. (2015). Multifaceted signaling regulators of chondrogenesis: implications in cartilage regeneration and tissue engineering. *Genes Dis.* 2, 307–327. doi: 10.1016/j.gendis.2015.09.003

Hayes, A. J., Dowthwaite, G. P., Webster, S., and Archer, C. W. (2003). The distribution of Notch receptors and their ligands during articular cartilage development. *J. Anat.* 202, 495–502. doi: 10.1046/j.1469-7580.2003.00185.x

Heir, S., Nerhus, T. K., Røtterud, J. H., Løken, S., Ekeland, A., Engebretsen, L., et al. (2010). Focal cartilage defects in the knee impair quality of life as much as severe osteoarthritis: a comparison of knee injury and osteoarthritis outcome score in 4 patient categories scheduled for knee surgery. *Am. J. Sports Med.* 38, 231–237. doi: 10.1177/0363546509352157

Hildner, F., Eder, M., Hofer, K., Aberl, J., van Griensven, M., Gabriel, C., et al. (2015). Human platelet lysate successfully promotes proliferation and subsequent chondrogenic differentiation of adipose-derived stem cells: a comparison with articular chondrocytes. *J. Tissue Eng. Regen. Med.* 9, 808–818. doi: 10.1002/term.1649

Ito, T., Sawada, R., Fujiwara, Y., Seyama, Y., and Tsuchiya, T. (2007). FGF-2 suppresses cellular senescence of human mesenchymal stem cells by down-regulation of TGF-β2. *Biochem. Biophys. Res. Commun.* 359, 108–114. doi: 10.1016/j.bbrc.2007.05.067

Jubert, N. J., Rodríguez, L., Reverté-Vinaixa, M. M., and Navarro, A. (2017). Platelet-rich plasma injections for advanced knee osteoarthritis: a prospective, randomized, double-blinded clinical trial. *Orthop. J. Sport Med.* 5, 1–11. doi: 10.1177/2325967116689386

Kisiday, J. D., McIlwraith, C. W., Rodkey, W. G., Frisbie, D. D., and Steadman, J. R. (2012). Effects of platelet-rich plasma composition on anabolic and catabolic activities in equine cartilage and meniscal explants. *Cartilage* 3, 245–254. doi: 10.1177/1947603511433181

Knutsen, G., Isaksen, V., Johansen, O., Engebretsen, L., Ludvigsen, T. C., Drogset, J. O., et al. (2004). *Autologous chondrocyte* implantation compared with microfracture in the knee: a randomized trial. *J. Bone Jt. Surg. Ser. A* 86, 455–464. doi: 10.2106/00004623-200403000-00403001

Kon, E., Mandelbaum, B., Buda, R., Filardo, G., Delcogliano, M., Timoncini, A., et al. (2011). Platelet-rich plasma intra-articular injection versus hyaluronic acid viscosupplementation as treatments for cartilage pathology: from early degeneration to osteoarthritis. *Arthrosc. J. Arthrosc. Relat. Surg.* 27, 1490–1501. doi: 10.1016/j.arthro.2011.05.011

Liu, J., Song, W., Yuan, T., Xu, Z., Jia, W., and Zhang, C. (2014). A comparison between platelet-rich plasma (PRP) and hyaluronate acid on the healing of cartilage defects. *PLoS One* 9:e097293. doi: 10.1371/journal.pone.0097293

Marijnissen, W. J. C. M., van Osch, G. J. V. M., Aigner, J., Verwoerd-Verhoef, H. L., and Verhaar, J. A. N. (2000). Tissue-engineered cartilage using serially passaged articular chondrocytes. *Chondrocytes in alginate*, combined in vivo with a synthetic (E210) or biologic biodegradable carrier (DBM). *Biomaterials* 21, 571–580. doi: 10.1016/S0142-9612(99)00218-215

Mazzocca, A. D., McCarthy, M. B. R., Chowaniec, D. M., Cote, M. P., Romeo, A. A., Bradley, J. P., et al. (2012). Platelet-rich plasma differs according to preparation method and human variability. *J. Bone Jt. Surg.* 94, 308–316. doi: 10.2106/JBJS.K.00430

McCarthy, H. S., Mccall, I. W., Williams, J. M., Mennan, C., Dugard, M. N., Richardson, J. B., et al. (2018). Magnetic resonance imaging parameters at 1 year correlate with clinical outcomes up to 17 years after autologous chondrocyte implantation. *Orthop. J. Sport Med.* 6, 1–10. doi: 10.1177/2325967118788280

Mei-Dan, O., Carmont, M. R., Laver, L., Mann, G., Maffulli, N., and Nyska, M. (2012). Platelet-rich plasma or hyaluronate in the management of osteochondral lesions of the talus. *Am. J. Sports Med.* 40, 534–541. doi: 10.1177/0363546511431238

Messner, K., and Maletius, W. (1996). The long-term prognosis for severe damage to weight-bearing cartilage in the knee: a 14-year clinical and radiographic follow-up in 28 young athletes. *Acta Orthop. Scand.* 67, 165–168. doi: 10.3109/17453679608994664

Moreira Teixeira, L. S., Leijten, J. C. H., Wennink, J. W. H., Chatterjea, A. G., Feijen, J., van Blitterswijk, C. A., et al. (2012). The effect of platelet lysate supplementation of a dextran-based hydrogel on cartilage formation. *Biomaterials* 33, 3651–3661. doi: 10.1016/j.biomaterials.2012.01.051

Moussa, M., Lajeunesse, D., Hilal, G., El Atat, O., Haykal, G., Serhal, R., et al. (2017). Platelet rich plasma (PRP) induces chondroprotection via increasing autophagy, anti-inflammatory markers, and decreasing apoptosis in human osteoarthritic cartilage. *Exp. Cell Res.* 352, 146–156. doi: 10.1016/j.yexcr.2017.02.012

Narcisi, R., Signorile, L., Verhaar, J., Giannoni, P., and van Osch, G. (2012). TGFβ inhibition during expansion phase increases the chondrogenic re-differentiation capacity of human articular chondrocytes. *Osteoarthr. Cartil.* 20, 1152–1160. doi: 10.1016/j.joca.2012.06.010

Neuman, R., and Logan, M. (1950). The determination of hydroxyproline. *J. Biol. Chem.* 184, 299–306.

Oberlender, S. A., and Tuan, R. S. (1994). Expression and functional involvement of N-cadherin in embryonic limb chondrogenesis. *Development* 120, 177–187.

Patel, S., Dhillon, M. S., Aggarwal, S., Marwaha, N., and Jain, A. (2013). Treatment with platelet-rich plasma is more effective than placebo for knee osteoarthritis: a prospective, double-blind, randomized trial. *Am. J. Sports Med.* 41, 356–364. doi: 10.1177/0363546512471299

Pereira, C., Scaranari, M., Benelli, R., Strada, P., Reis, R. L., Cancedda, R., et al. (2013). Dual effect of platelet lysate on human articular cartilage: a maintenance of chondrogenic potential and a transient pro-inflammatory activity followed by an inflammation resolution. *Tissue Eng. Part A* 19, 1476–1488. doi: 10.1089/ten.TEA.2012.0225

Peterson, L., Vasiliadis, H. S., Brittberg, M., and Lindahl, A. (2010). Autologous chondrocyte implantation: a long term follow-up. *Am. J. Sports Med.* 38, 1117–1124. doi: 10.1177/0363546509357915

Riboh, J. C., Saltzman, B. M., Yanke, A. B., Fortier, L., and Cole, B. J. (2016). Effect of leukocyte concentration on the efficacy of platelet-rich plasma in the treatment of knee osteoarthritis. *Am. J. Sports Med.* 44, 792–800. doi: 10.1177/0363546515580787

Sánchez, M., Anitua, E., Azofra, J., Andía, I., Padilla, S., and Mujika, I. (2007). Comparison of surgically repaired achilles tendon tears using platelet-rich fibrin matrices. *Am. J. Sports Med.* 35, 245–251. doi: 10.1177/0363546506294078

Schnabel, M., Marlovits, S., Eckhoff, G., Fichtel, I., Gotzen, L., Vécsei, V., et al. (2002). Dedifferentiation-associated changes in morphology and gene expression in primary human articular chondrocytes in cell culture. *Osteoarthr. Cartil.* 10, 62–70. doi: 10.1053/joca.2001.0482

Simental-Mendía, M., Vilchez-Cavazos, F., García-Garza, R., Lara-Arias, J., Montes-De-Oca-Luna, R., Said-Fernández, S., et al. (2018). The matrix synthesis and anti-inflammatory effect of autologous leukocyte-poor platelet rich plasma in human cartilage explants. *Histol. Histopathol.* 33, 609–618. doi: 10.14670/HH-11-961

Smith, P. A. (2015). Intra-articular autologous conditioned plasma injections provide safe and efficacious treatment for knee osteoarthritis. *Am. J. Sports Med.* 44, 884–891. doi: 10.1177/0363546515624678

Sundman, E. A., Cole, B. J., and Fortier, L. A. (2011). Growth factor and catabolic cytokine concentrations are influenced by the cellular composition of platelet-rich plasma. *Am. J. Sports Med.* 39, 2135–2140. doi: 10.1177/0363546511417792

Sykes, J. G., Kuiper, J. H., Richardson, J. B., Roberts, S., Wright, K. T., and Kuiper, N. J. (2018). Impact of human platelet lysate on the expansion and chondrogenic capacity of cultured human chondrocytes for cartilage cell therapy. *Eur. Cells Mater.* 35, 255–267. doi: 10.22203/eCM.v035a18

Wang, K., Li, J., Li, Z., Wang, B., Qin, Y., Zhang, N., et al. (2019). Chondrogenic progenitor cells exhibit superiority over mesenchymal stem cells and chondrocytes in platelet-rich plasma scaffold-based cartilage regeneration. *Am. J. Sports Med.* 47, 2200–2215. doi: 10.1177/0363546519854219

Xie, X., Zhang, C., and Tuan, R. S. (2014). Biology of platelet-rich plasma and its clinical application in cartilage repair. *Arthrit. Res. Ther.* 16:204. doi: 10.1186/ar4493

Zhang, H., Chen, S., Qiu, M., Zhou, A., Yan, W., and Zhang, J. (2018). Lateral meniscus allograft transplantation with platelet-rich plasma injections: a minimum two-year follow-up study. *Knee* 25, 568–576. doi: 10.1016/j.knee.2018.03.005

Zhao, G. Z., Zhang, L. Q., Liu, Y., Fang, J., Li, H. Z., Gao, K. H., et al. (2016). Effects of platelet-derived growth factor on chondrocyte proliferation, migration and apoptosis via regulation of GIT1 expression. *Mol. Med. Rep.* 14, 897–903. doi: 10.3892/mmr.2016.5291

Conflict of Interest: The authors declare that the research was conducted in the absence of any commercial or financial relationships that could be construed as a potential conflict of interest.

frontiers in Bioengineering and Biotechnology

ORIGINAL RESEARCH
published: 09 July 2020
doi: 10.3389/fbioe.2020.00651

Endochondral Bone Regeneration by Non-autologous Mesenchymal Stem Cells

Alessia Longoni[1,2], *I. Pennings*[1,2], *Marta Cuenca Lopera*[3], *M. H. P. van Rijen*[1,2,4], *Victor Peperzak*[3], *A. J. W. P. Rosenberg*[1], *Riccardo Levato*[2,4,5] *and Debby Gawlitta*[1,2*]

[1] *Department of Oral and Maxillofacial Surgery & Special Dental Care, University Medical Center Utrecht, Utrecht University, Utrecht, Netherlands,* [2] *Regenerative Medicine Center Utrecht, Utrecht, Netherlands,* [3] *Laboratory for Translational Immunology, University Medical Center Utrecht, Utrecht, Netherlands,* [4] *Department of Orthopaedics, University Medical Center Utrecht, Utrecht University, Utrecht, Netherlands,* [5] *Department of Clinical Sciences, Faculty of Veterinary Medicine, Utrecht University, Utrecht, Netherlands*

OPEN ACCESS

Edited by:
Roberto Narcisi, Erasmus University Rotterdam, Netherlands

Reviewed by:
Solvig Diederichs, Heidelberg University Hospital, Germany
Melanie Haffner-Luntzer, University of Ulm, Germany

***Correspondence:**
Debby Gawlitta
d.gawlitta@umcutrecht.nl

Specialty section:
This article was submitted to Preclinical Cell and Gene Therapy, a section of the journal Frontiers in Bioengineering and Biotechnology

Received: *12 March 2020*
Accepted: *27 May 2020*
Published: *09 July 2020*

Citation:
Longoni A, Pennings I, Cuenca Lopera M, van Rijen MHP, Peperzak V, Rosenberg AJWP, Levato R and Gawlitta D (2020) Endochondral Bone Regeneration by Non-autologous Mesenchymal Stem Cells. Front. Bioeng. Biotechnol. 8:651. doi: 10.3389/fbioe.2020.00651

Mimicking endochondral bone formation is a promising strategy for bone regeneration. To become a successful therapy, the cell source is a crucial translational aspect. Typically, autologous cells are used. The use of non-autologous mesenchymal stromal cells (MSCs) represents an interesting alternative. Nevertheless, non-autologous, differentiated MSCs may trigger an undesired immune response, hampering bone regeneration. The aim of this study was to unravel the influence of the immune response on endochondral bone regeneration, when using xenogeneic (human) or allogeneic (Dark Agouti) MSCs. To this end, chondrogenically differentiated MSCs embedded in a collagen carrier were implanted in critical size femoral defects of immunocompetent Brown Norway rats. Control groups were included with syngeneic/autologous (Brown Norway) MSCs or a cell-free carrier. The amount of neo-bone formation was proportional to the degree of host-donor relatedness, as no full bridging of the defect was observed in the xenogeneic group whereas 2/8 and 7/7 bridges occurred in the allogeneic and the syngeneic group, respectively. One week post-implantation, the xenogeneic grafts were invaded by pro-inflammatory macrophages, T lymphocytes, which persisted after 12 weeks, and anti-human antibodies were developed. The immune response toward the allogeneic graft was comparable to the one evoked by the syngeneic implants, aside from an increased production of alloantibodies, which might be responsible for the more heterogeneous bone formation. Our results demonstrate for the first time the feasibility of using non-autologous MSC-derived chondrocytes to elicit endochondral bone regeneration *in vivo*. Nevertheless, the pronounced immune response and the limited bone formation observed in the xenogeneic group undermine the clinical relevance of this group. On the contrary, although further research on how to achieve robust bone formation with allogeneic cells is needed, they may represent an alternative to autologous transplantation.

Keywords: allograft, xenograft, graft rejection, adaptive and innate immune response, bone regeneration, chondrogenic differentiation, endochondral bone formation, MSCs

INTRODUCTION

Endochondral bone formation represents a key process in bone development and fracture healing (Gerstenfeld et al., 2003; Shapiro, 2008). In particular, the growth plate and the fracture callus are characterized by a highly organized cartilaginous structure where chondrocytes progressively acquire a hypertrophic phenotype (Gerstenfeld et al., 2003). Once hypertrophic, chondrocytes switch their expression profile, upregulate genes involved in osteogenesis and start secreting proangiogenic factors and metalloproteinases (Gawlitta et al., 2010). This promotes blood vessel invasion, the infiltration of osteoprogenitor cells and osteoclasts, and the final remodeling of the cartilaginous template into new bone (Gawlitta et al., 2010).

Over the last decade, tissue engineering has successfully mimicked this process to regenerate bone defects *in vivo* (Thompson et al., 2015). Various types of cells, including multipotent mesenchymal stromal cells (MSCs) (Scotti et al., 2013; Harada et al., 2014; van der Stok et al., 2014; Matsiko et al., 2018; McDermott et al., 2019), embryonic stem cells (Jukes et al., 2008) and adipose-derived stem cells (Osinga et al., 2016) were used alone or in combination with biomaterials to develop a cartilaginous template that, upon implantation, would trigger new bone formation. Despite these promising results, the clinical translation of endochondral bone regeneration (EBR) is in an early stage for several reasons. One of the major challenges is represented by the variability of chondrogenic potential between MSC donors (Gawlitta et al., 2012; van der Stok et al., 2014) and its unpredictability (Sivasubramaniyan et al., 2018). In other words, the successful treatment of all patients with autologous MSCs is not feasible, as the differentiation potential of the isolated MSCs would vary from highly potent to completely incapable, in a patient-dependent manner. Furthermore, the personalized use of cells is associated with high costs when performed under Good Manufacturing Practice (GMP) (Evans et al., 2007; Evans, 2013). Here, we propose the use of non-autologous MSCs (*i.e.*, allogeneic or xenogeneic) as a potential strategy to increase the clinical translatability of EBR, ideally in a single-step surgical procedure. Non-autologous cells could be screened and pre-selected for their high chondrogenic potential in advance, circumventing the issue of the donor-to-donor variability, and leading to an off-the-shelf product. In addition, if MSCs with high chondrogenic potential could be pooled and used to treat multiple patients, the high costs associated with isolating and differentiating these cells under GMP restrictions would decrease. Finally, the use of non-autologous MSCs will eliminate any discomfort for the patients related to taking a bone marrow biopsy.

It is evident that the use of allogeneic or xenogeneic cells represents a clinically and economically attractive option. However, the immunogenicity of non-autologous grafts poses a potential obstacle to the clinical implementation, as it could affect the integration and functionality of the grafted tissues (Longoni et al., 2018). Nevertheless, differently from other types of transplantation (e.g., heart, lungs, or liver), in which the grafted organ represents the final functional tissue; in EBR, the cartilage template produced *in vitro* solely serves as a transient substrate that is remodeled into new, mostly recipient-derived bone tissue (Farrell et al., 2011; Scotti et al., 2013). As a result, the host is only gradually and temporarily exposed to the non-autologous MSC-derived chondrocytes and matrix during the remodeling process. Thus, it can be hypothesized that, if the initial remodeling steps would not be hampered by the immune reaction to the engineered non-autologous cartilage, the graft could be replaced by new, partially autologous (Farrell et al., 2011; Scotti et al., 2013) bone tissue. Only a limited number of *in vitro* studies have provided clues about the retention of the MSC immunomodulatory and immunoevasive properties after differentiation. It was shown that allogeneic MSC-derived chondrocytes retain their capability to actively suppress allogeneic T lymphocyte proliferation (Le Blanc et al., 2003; Zheng et al., 2008), decrease the secretion of pro-inflammatory cytokines such as interferon gamma and tumor necrosis factor alpha (Zheng et al., 2008) and inhibit the natural killer cell-mediated cytotoxicity (Du et al., 2016). Additionally, chondrogenically differentiated MSCs do not induce dendritic cell (DC) maturation nor increase in their antigen uptake or migration (Kiernan et al., 2018). On the contrary, it has been reported that xenogeneic, MSC-derived chondrocytes trigger T lymphocyte proliferation, cytotoxicity, and DC maturation, increasing antigen presentation and further activation of the adaptive immune response (Chen et al., 2007). All together, these *in vitro* findings hint that the intensity of the host immune response to the non-autologous implants is different, depending on whether they are allogeneic or xenogeneic. Nevertheless, no study has explored how potential changes in immunological response could affect EBR *in vivo*. As a consequence, based on the available information, it is not possible to predict if in any of these two cases, the host immune response will prevent new bone formation *in vivo*. Therefore, the aim of this study was to evaluate the impact of the immune response evoked by non-autologous MSC-derived chondrocytes on the conversion from cartilage to bone during EBR. To do so, cartilaginous constructs derived from full major histocompatibility complex class I and II (in rats RT1 class I and II) mismatched (Dark Agouti rat) or xenogeneic (human) MSCs were implanted in a critical size femur defect of an immunocompetent rat (Brown Norway) to closely monitor both the elicited immune response and the new bone formation.

MATERIALS AND METHODS

Study Design and Overview

Four experimental groups were included in this study: two different types of a non-autologous cell source, namely allogeneic (Dark Agouti rat, full RT1 mismatch) and xenogeneic (human). These were pre-selected based on their high and similar chondrogenic potential and compared to the syngeneic group (Brown Norway, autologous transplantation). Additionally, a control group consisting of the collagen carrier only was included. A critical size femoral defect introduced in Brown Norway immunocompetent rats was used as a model to observe the immune reaction and EBR induced by the different groups. Two end-points were analyzed, at one ($n = 5$ per group)

and 12 weeks ($n = 8$ per group for the syngeneic, allogeneic, and xenogeneic and $n = 5$ for the collagen control group) post-implantation. Mineralization over time was monitored by micro-CT at 0, 4, 8, and 12 weeks after surgery. Systemic immune response was monitored by checking the blood for the presence of an inflammation marker (α-1-acid glycoprotein) and antibody production (IgG and IgM) at 0, 1, 2, 4, 8, and 12 weeks. After euthanasia at 1 or 12 weeks post-implantation, the local immune response was analyzed via immunohistological stainings. Markers belonging to the innate (macrophages: CD68, CD163, iNOS, and CD206) and adaptive (T lymphocytes: CD3) immune response were investigated. Finally, bone formation and remodeling were investigated via histological analysis and histomorphometry (H&E, Safranin-O/Fast Green, and TRAP staining) after 12 weeks.

Isolation and Expansion of Bone Marrow-Derived MSCs

Human MSCs were isolated from the bone marrow aspirate of a 20-year old female patient. The aspirate was obtained after informed consent, according to a protocol approved by the local Medical Ethics Committee (University Medical Center Utrecht). The mononuclear fraction was separated using Ficoll-paque (Sigma-Aldrich, Zwijndrecht, the Netherlands) and seeded on plastic to select for adherence, as previously described (Gawlitta et al., 2012). The adherent cells were cultured at 37°C under humidified conditions and 5% carbon dioxide (CO_2) in MSC expansion medium consisting of α-MEM (22561, Invitrogen), supplemented with 10% heat-inactivated fetal bovine serum (S14068S1810, Biowest), 0.2 mM L-ascorbic acid 2-phosphate (A8960, Sigma), 100 U/mL penicillin with 100 mg/mL streptomycin (15140, Invitrogen) and 1 ng/ml basic fibroblast growth factor (233-FB; R&D Systems).

Rat MSCs were isolated from 4 weeks old female Dark Agouti and Brown Norway rats. Briefly, rats were euthanized through CO_2 asphyxiation and femur and tibia were collected. After removing the epiphysis, bone-marrow was obtained by flushing through the diaphysis with MSC expansion medium supplemented with 0.025% EDTA and cells were plated in a Petri dish. After 24 h, the medium was switched to StemXVivo (CCM004, R&D Systems) and refreshed three times per week. MSCs were passaged at subconfluency until passage 4. MSC multilineage potential (**Supplementary Figure 1**) was confirmed as reported previously (Gawlitta et al., 2012).

Chondrogenic Differentiation of MSC Spheroids

At passage 4, human and rat MSCs were harvested for chondrogenic differentiation. Collagen spheroids were created by encapsulating MSCs ($20*10^6$/ml) into 50 µl collagen type I gel (4 mg/ml) (CB354249, Corning) according to the manufacturer's instruction. Gelation was allowed for 45 min at 37°C. The spheroids were cultured in chondrogenic differentiation medium consisting of high glucose DMEM (31966, Invitrogen) with 1% ITS + premix (354352; BD Biosciences), 10^{-7} M dexamethasone (D8893; Sigma), 0.2 mM L-ascorbic acid 2-phosphate (A8960, Sigma), 100 U/mL penicillin with 100 mg/mL streptomycin (15140, Invitrogen). Chondrogenic differentiation medium for human MSCs was supplemented with 10 ng/ml TGFβ1 (100-21, PeproTech), whereas for rat MSCs, also 100 ng/ml BMP-2 was added. Medium was refreshed every day for the first 4 days and thereafter three times per week. Chondrogenic differentiation was confirmed via histological analysis.

Construct Preparation

Comparable spheroid sizes were obtained among the different groups after 28 days of differentiation. For each construct, eight chondrogenic spheroids were placed in a square cuboid custom-made mold (3.5 mm × 3.5 mm × 6 mm). Collagen (CB354249, Corning) gels (4 mg/ml) were casted into the mold around the eight spheroids and gelation was allowed for 45 min according to manufacturer's instruction. The constructs were prepared the day before implantation and incubated overnight in chondrogenic differentiation medium without TGFβ1 and BMP-2.

Animal Experiment and Surgical Procedure

The research protocol and procedures were approved by the animal ethical committee of the University Medical Center Utrecht (2465-2-01) and was in accordance with the national law on animal experiments. Forty-nine male Brown Norway rats (Envigo, the Netherlands) were housed in pairs in the animal facility of the University Medical Center Utrecht. Animals received standard food pellets and water *ad libitum*, under climate-controlled conditions (21°C; 12 h light/12 h darkness). At the age of 12 weeks, after at least 7 days of acclimatization, a 6 mm critical-size segmental bone defect was created under general anesthesia (1–3.5% isoflurane in oxygen, AST Farma, Oudewater, the Netherlands) as previously described (van der Stok et al., 2014). Briefly, the right hind leg was shaved and disinfected. The right femur was exposed through a lateral skin incision and dissection of soft tissue. Three proximal and three distal screws were used to stabilize a 23 × 3 × 2 mm polyether ether ketone (PEEK) plate to the femur in the anterolateral plane. After the bone's fixation to the PEEK plate, a 6 mm bone segment was removed using a saw guide and a wire saw (RISystem, Davos, Switzerland). The collagen constructs were press-fit in the defects and a single dose of antibiotic (Duplocillin LA, 22.000 IE/kg) was injected intramuscularly. Finally, the fascia and skin were sutured in layers using Vicryl Rapide 4-0 (VR 2297, Ethicon). Subcutaneous injection of pain medication (buprenorphine, 0.05 mg/kg bodyweight, AST Farma, Oudewater, the Netherlands) was given pre-operatively and twice a day for the following 3 days. Rats were euthanized after either 1 or 12 weeks with an overdose of barbiturates (phenobarbital; 200 mg/kg body weight, TEVA Pharma, Haarlem, the Netherlands). The femora were analyzed by histology and micro-computed tomography (microCT) scanning.

MicroCT Scanning

To evaluate tissue mineralization at 0, 4, 8, and 12 weeks after surgery, the hind leg of the rat was fixed in a custom-made support under anesthesia (1–3.5% isoflurane in oxygen) and scanned with a microCT imaging system (Quantum FX;

PerkinElmer, Waltham, MA, USA). Three minutes of scanning time was required per leg at an isotropic voxel size of 42 μm resolution (voltage 90 kV, current 180 mA, field of view = 21 mm). All scans were oriented in the same fashion using the ImageJ plugin Reorient3 TP and the same volume of interest (VOI: $6.3 \times 5 \times 5$ mm^3) was selected for all samples. VOIs were segmented with a global threshold and mineralized volumes were measured in mm^3 using the image processing software plugin BoneJ (Doube et al., 2010) (Image-J 2.0.0; Java, Redwood Shores, CA, USA). 3D reconstructions of the femur defect were based on the microCT data and created using ParaView (ParaView, Kitware Inc., USA).

Blood Sampling and Systemic Immune Response

Blood was sampled at 0, 1, 2, 4, 8, and 12 weeks from the tail vein using a catheter (BD angiocath, Becton Dickinson, Vianen, the Netherlands). Serum and plasma were collected in non-coated or EDTA coated MiniCollect tubes (450534 and 450532 Greiner Bio-one), respectively. Sample types were centrifuged for 15 min at 1,500 g and the supernatant was stored at −80°C.

In the serum, the acute-phase protein α-1-acid glycoprotein (AGP), indicative for inflammation, was quantified using an ELISA kit (AGP-2, Life Diagnostic, West Chester, USA), according to the manufacturer's instructions. Total IgG content in the plasma was quantified using the IgG Rat Uncoated ELISA kit (88-50490-86, Invitrogen), according to the manufacturer's instructions.

Detection of Anti-donor Immunoglobulin in Serum

To assess the production of alloreactive and xenoreactive IgM and IgG by the host, donor MSCs (either syngeneic, allogeneic, or xenogeneic) were expanded until 80% of confluency and chondrogenically differentiated for 10 days (Le Blanc et al., 2003; Chen et al., 2007) in a 96 wells plate. The monolayers were fixed in 10% buffered formalin solution for 30 min and incubated in 5% BSA-PBS for 30 min at room temperature. Rat sera were heat-inactivated for 30 min at 56°C, diluted 1:100 in 5% BSA-PBS and incubated with the donor MSC monolayer correspondent to the type of graft they received *in vivo* for 1 h at room temperature (adapted from Mathieux et al., 2014). After extensive washing with PBS, monolayers were incubated with a TRITC-conjugated antibody [8 μg/ml, goat-anti-rat IgM and IgG (H&L), 3010-03, SouthernBiotech] for 1 h at room temperature. Finally, samples were washed and counterstained with DAPI for 10 min. Representative pictures of the anti-donor immunoglobulin produced 0, 2, and 4 weeks post-implantation were taken for displaying purposes using a confocal microscope (Leica SP8X confocal). At 4 weeks, six pictures per sample (Olympus IX53) taken at random locations were used for the quantification. TRITC pixel quantification and nuclei count were performed using image-J after applying a global threshold. Data are presented as TRITC-positive pixels normalized to the number of nuclei per field of view. Controls for sample cross-reactivity are included in **Supplementary Figure 2**.

T Cell Proliferation Assay

To evaluate if the donor cells specifically triggered a T lymphocyte response, at 12 weeks the inguinal and popliteal lymph node were retrieved, crushed, and T cells were stained with CellTrace Violet (C34571, Thermo Fisher) for 20 min at 37°C, according to the manufacturer's instruction. After washing, 2^*10^5 stained T cells were resuspended in RPMI (11875093, Invitrogen) supplemented with 10% FBS 100 U/mL penicillin with 100 mg/mL streptomycin and added to the respective donor MSCs, which were beforehand expanded until 80% of confluency and chondrogenically differentiated for 10 days in a 96 wells plate. T cell-donor:MSC co-cultures were incubated for 4 days at 37°C under humidified conditions and 5% CO_2 (protocol adapted from Ryan et al., 2014). Afterward, cells were detached with trypsin and resuspended in FACS buffer consisting of PBS supplemented with 2% FBS. T cells were stained with CD3-PE conjugated antibody (0.4 μg/ml, 201411, BioLegend, San Diego, USA) for 30 min at 4°C and analyzed on an LSR-Fortessa flow cytometer (BD Bioscience, California, USA). Proliferation peaks were analyzed performing a deconvolution analysis with FlowJo and compared to lymphocytes that were not exposed to any other cell types (Nil) and T lymphocytes co-cultured with a third-party Sprague Dawley MSCs (Aspecific).

Histology and Immunohistochemistry

At week 1 and 12, the right femora were retrieved for histological processing. All specimens were fixed in a 10% neutral buffered formalin solution for 1 week. After fixation, they were decalcified in a 10% EDTA-phosphate buffered saline solution (pH 7.4), dehydrated in graded ethanol solutions (70–100%) and cleared in xylene. The samples were subsequently embedded in paraffin and sliced into 5 μm thick sections (Microm HM340E). *In vitro* samples were fixed, dehydrated and sliced following a similar procedure. Before staining, samples were deparaffinized with xylene and gradually rehydrated through decreasing ethanol solutions (100–70%).

Overall appearance of sections and new bone formation was evaluated using H&E staining (Sigma). A triple staining of Weigert's hematoxylin (640490; Klinipath BV), fast green (FN1066522; Merck), and Safranin O (FN1164048213; Merck) was applied to identify cell nuclei, collagenous fibers and GAGs. For the TRAP staining, hydrated sections were incubated for 20 min in 0.2 M acetate buffer at room temperature. To identify the osteoclasts, sections were incubated in 0.2 M acetate buffer supplemented with 0.5 mg/ml naphthol AS-MX phosphate (855, Sigma) and 1.1 mg/ml fast red TR salt (F8764, Sigma) for 4 h at 37°C. Mayer's hematoxylin was used for nuclear counterstaining. Histomorphometric analysis was performed on samples stained with H&E. Briefly, an overview of the whole sample was made by merging images (1.25x/0.04 FN26.5 objective) into a panoramic image in Adobe Photoshop C6. For each image, a region of interest (ROI) of 5×2.5 mm^2 was selected in the center of the defect. The titanium screw holes present on each side of the defect were used as reference point in order to ensure an equivalent positioning of ROI in all samples. Three different areas were manually selected for each ROI: bone, hypertrophic cartilage and bone marrow. The amount of pixel for each area was quantified

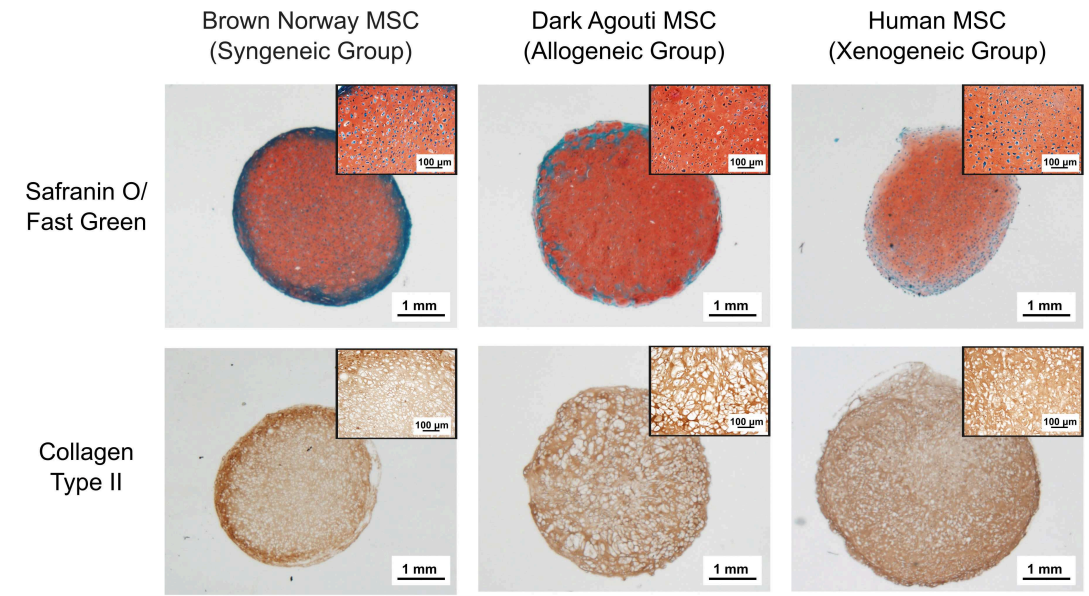

FIGURE 1 | Chondrogenic differentiation of the different MSCs donors. Chondrogenic differentiation is confirmed by the presence of GAGs (red) and Collagen Type II (brown). Inserts contain higher magnification pictures of the collagen spheroids.

via the function "recording measurement" and normalized for the ROI area. Osteoclasts in the ROI were counted using the cell counter plugin from Image-J.

For collagen type II (II-II6B3), CD68 (ab31630, Abcam), CD206 (AF2535, R&D Systems), CD163 (ab182422, Abcam), CD3 (ab16669, Abcam), and iNOS (ab15323, Abcam) staining, endogenous peroxidase activity was blocked by incubating samples for 15 min with 0.5% H_2O_2, followed by aspecific protein blocking with 5% BSA-PBS for 45 min at room temperature. Details about the antigen retrieval, primary and secondary antibody used can be found in **Supplementary Table 1**. The labels were visualized by DAB oxidation. Sections were then counterstained with hematoxylin, washed, dehydrated and mounted in depex. Rabbit and mouse isotypes (X0903 and X0931, Dako) were used as negative controls at concentrations matched with those of the primary antibodies. All sections were visualized using an Olympus BX51 microscope (Olympus DP73 camera, Olympus). Immune cells were quantified in three different areas of the defect site: the collagen carrier, the infiltrating tissue and the spheroids (**Supplementary Figure 3**). Three images per sample per area were taken and positive cells were counted using the cell counter plug-in from Image-J. The operator was blinded during the staining, acquisition and counting phases.

Statistics

The data are presented as means with standard deviations. For the analysis of the microCT results, AGP and IgG levels, a mixed linear model was used. The tests were adjusted for multiple comparisons by a Bonferroni's *post-hoc* comparison test (IBM SPSS 22.0, New York, USA). For the analysis of the immune cells infiltrating the defects (IHC slides) after 1 week and the histomorphometric measures, a Kruskal-Wallis test was performed, followed by a Dunn's *post-hoc* test (GraphPad Prism 6, San Diego, CA, USA). For the analysis of the T cell proliferation a one-way ANOVA was performed, followed by a Dunnet's *post-hoc* test (GraphPad Prism 6). A $p < 0.05$ was considered statistically significant.

RESULTS

Macroscopic Observations

At the time of surgery, the mean bodyweight of the rats was 258 ± 27 g and increased to 344 ± 28 g after 12 weeks. In total, three animals (1 xenogeneic, 1 syngeneic, and 1 collagen group) were euthanized before the experimental endpoint was reached due to failure of the PEEK plate and were therefore not included in the analyses. No external signs of adverse reactions (i.e., swelling or redness) to the implants were observed for any of the rats during the course of the experiment.

In vitro Chondrogenic Differentiation

After 4 weeks, the collagen spheroids derived from human, Dark Agouti or Brown Norway MSCs displayed abundant glycosaminoglycan (GAG) and collagen type II deposition (**Figure 1**). Cells displayed the typical chondrocyte morphology, with a rounded shape and were embedded in lacunae.

New Bone Formation

After 12 weeks, new bone formation was observed close to the extremities of the osteotomy gap in all samples. 7/7 defects of the syngeneic control group and 2/8 of the allogeneic group were fully bridged whereas no full bridges were observed in the xenogeneic or the collagen groups (**Figures 2A,B**). Furthermore, bone regeneration in the center of the defect was

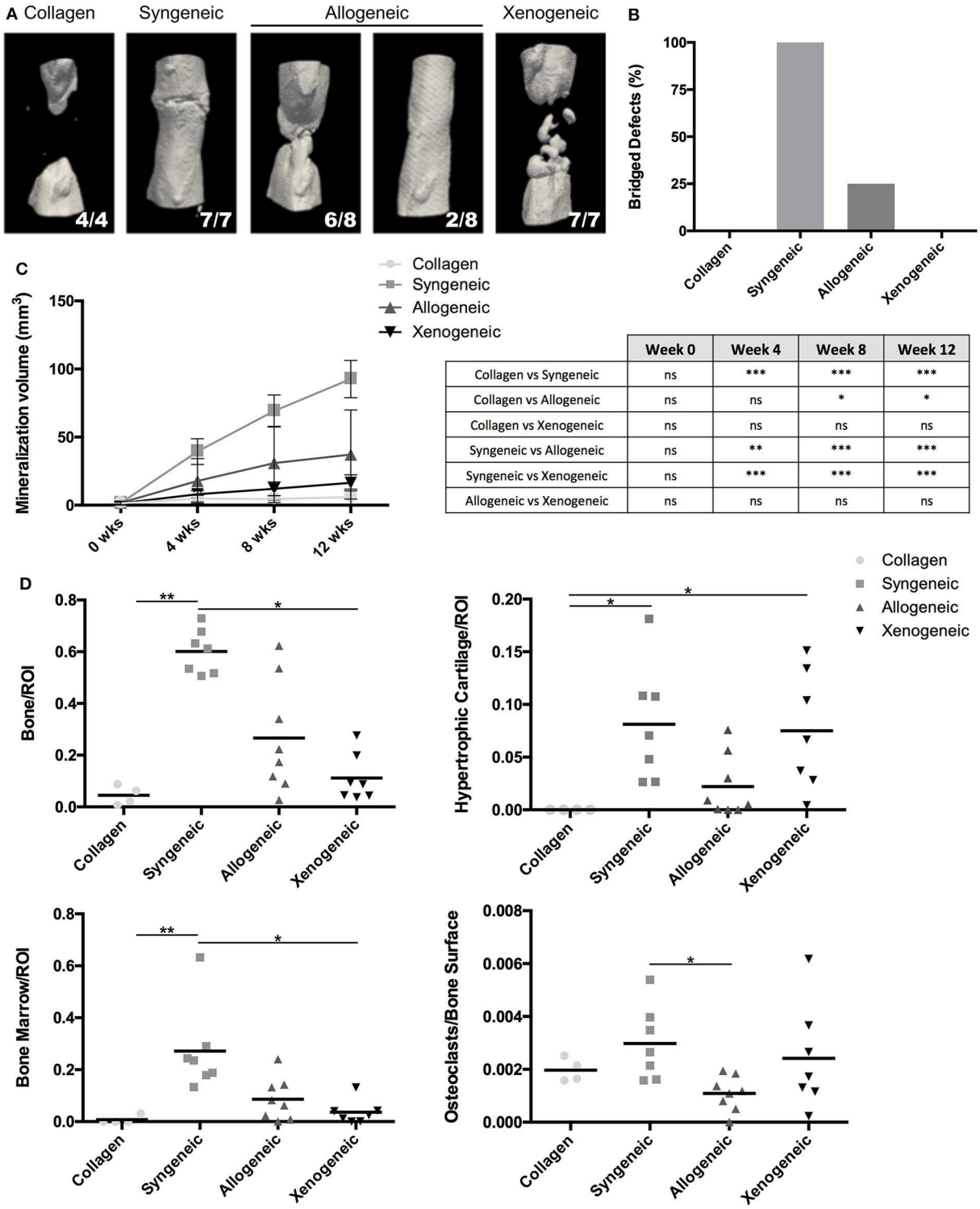

	Week 0	Week 4	Week 8	Week 12
Collagen vs Syngeneic	ns	***	***	***
Collagen vs Allogeneic	ns	ns	*	*
Collagen vs Xenogeneic	ns	ns	ns	ns
Syngeneic vs Allogeneic	ns	**	***	***
Syngeneic vs Xenogeneic	ns	***	***	***
Allogeneic vs Xenogeneic	ns	ns	ns	ns

FIGURE 2 | Evaluation of bone formation in the defect area. **(A)** The 3D microCT reconstructions of the defect areas after 12 weeks highlight the presence of mineralized areas with the shape of the implanted cartilaginous spheroids in the allogeneic and xenogeneic groups. **(B)** Heterogeneous results were observed in the allogeneic group, with 2/8 full bridging of the defect (25%) whereas 7/7 defects were bridged in the syngeneic group (100%). **(C)** Quantification of the mineralization over time confirmed that new bone formation was enhanced in the syngeneic group. **(D)** Results of the histomorphometric analysis performed 12 weeks post-implantation presented a similar trend. $^{*}p < 0.05$; $^{**}p < 0.01$; and $^{***}p < 0.001$. ns: not significant.

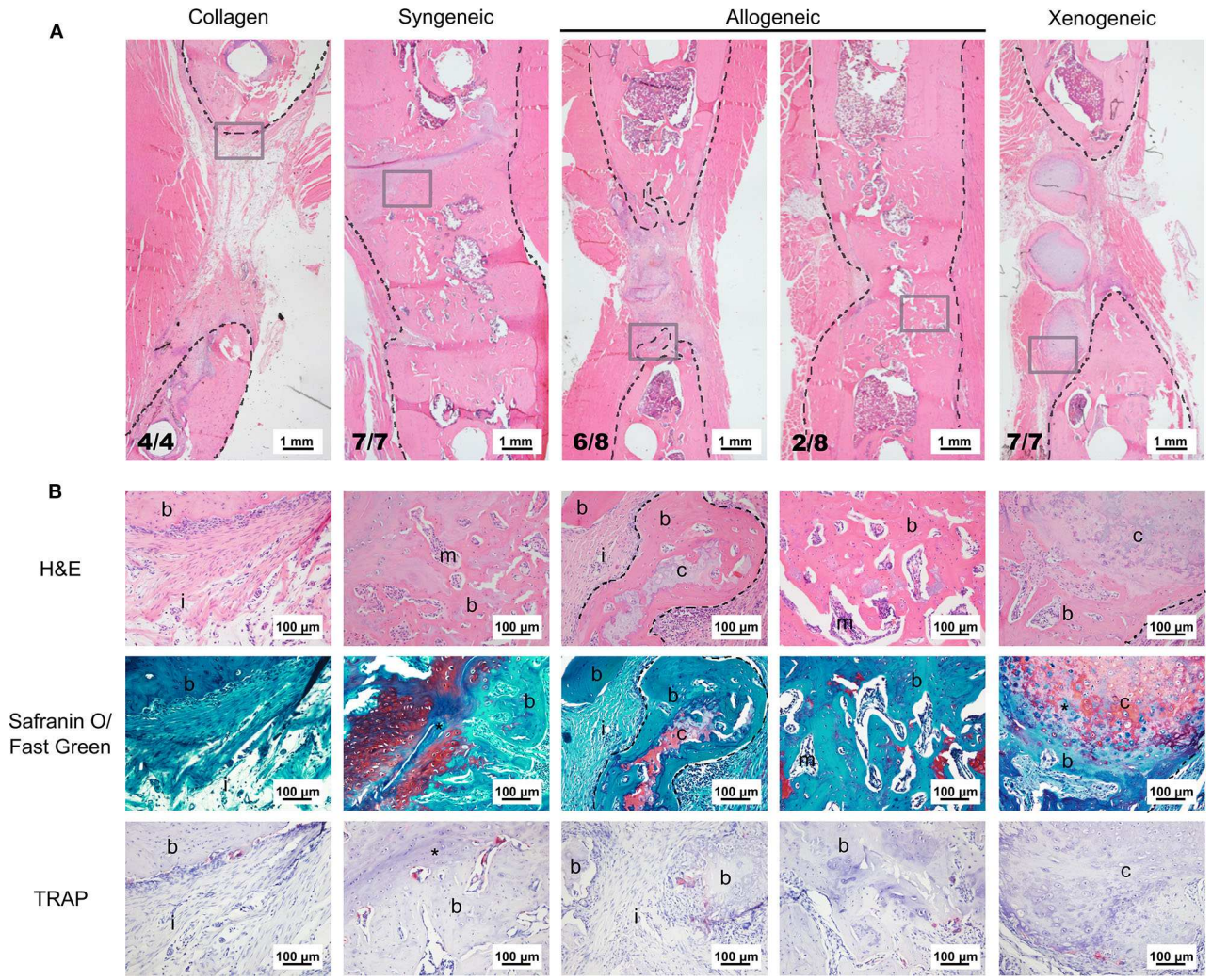

FIGURE 3 | Representative images of the bone defect repair after 12 weeks. **(A)** Overview of the defect area stained with H&E. The black dotted lines indicate the bone edges whereas the gray boxes highlight the area depicted in the higher magnification in **(B)**. **(B)** H&E staining shows that the edges of the cartilaginous spheroids (limited by the dotted line) were converted into bone. Safranin O/fast green staining highlights active EBR in the syngeneic group and the presence of some non-remodeled cartilage (red) in the core of the spheroids of the allogeneic and xenogeneic groups. TRAP staining (bright pink) indicates the presence of active osteoclasts in all groups. i, tissue infiltration; b, bone; m, bone marrow; c, cartilaginous spheroids; *EBR.

observed in all the samples in which MSCs were implanted, but not in the collagen control (**Figure 2A**). In particular, mineralized volumes resembling the shape and size of the implanted spheroid structures were still evident, especially in the xenogeneic group (**Figure 2A**). In these areas, human cells were found in the newly formed bone, suggesting the direct involvement of the cartilaginous templates in the regenerative process (**Supplementary Figure 4**).

Based on microCT data, mineralization was highest in the syngeneic group (92.6 ± 13.7 mm^3), followed by 37.2 ± 32.6 mm^3 for allogeneic, 16.4 ± 5.9 mm^3 for xenogeneic, and 5.96 ± 5.9 mm^3 for the collagen control (**Figure 2C**). A similar trend was observed after histomorphometric analysis (**Figure 2D**). Interestingly, hypertrophic cartilage was present also in the syngeneic group, indicating that remodeling is still ongoing at the proximal edge of the defect. On the contrary, in the allogeneic and xenogeneic group the hypertrophic cartilage was predominantly found in the non-remodeled parts of the spheroids. Consistent with the 3D reconstructions, the H&E staining highlighted the presence of bone islands at the edges of the spheroidal structures (**Figure 3**). Finally, in areas of active EBR, it was possible to discern osteoclasts, confirming that remodeling was ongoing after 12 weeks (**Figures 2D**, **3B**).

Implant-Induced Early Macrophage Polarization and T-Cell Infiltration

One week after implantation, macrophages positive for CD68 were most abundant in the xenogeneic group, especially when considering the tissue infiltration in the implanted spheroids

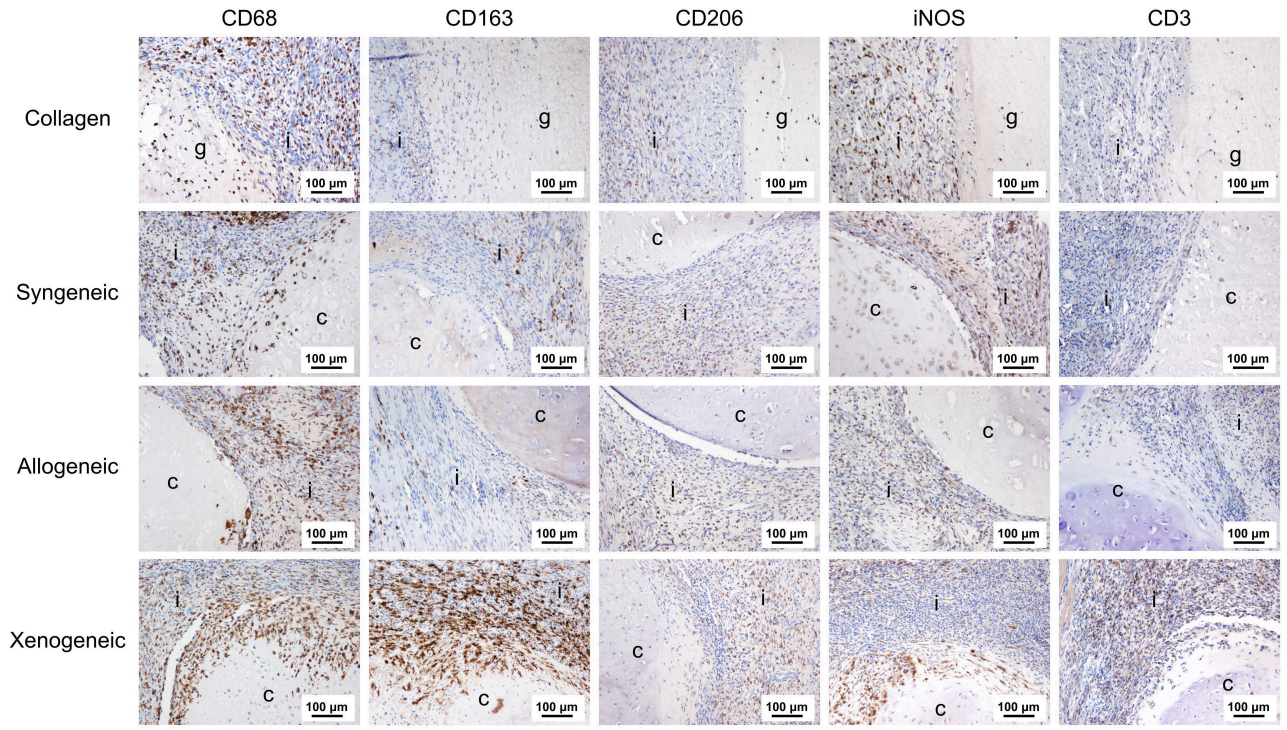

FIGURE 4 | Local adaptive and innate immune response after 1 week from the implantation. CD68+ and CD163+ macrophages were particularly abundant in the xenogeneic group, especially in the spheroids infiltration. No differences were evident in CD206+ macrophages distribution whereas more iNOS + cells were infiltrating the cartilaginous spheroids. CD3+ lymphocytes were predominant in the osteotomy gap of the xenogeneic samples compared to the other groups. Brown color indicates the positive staining. i, tissue infiltration; c, cartilaginous spheroids; g, collagen gel.

(**Figures 4**, **5**). Similarly, CD163+ macrophages were most abundant in the xenogeneic group in all the three analyzed areas (**Figures 4**, **5**). When analyzing the polarization of the macrophages, a significantly higher (p-value 0.01) amount of pro-inflammatory iNOS+ cells was detected in the spheroids of the xenogeneic group whereas no differences in anti-inflammatory CD206+ macrophages were observed (**Figure 5**). Finally, CD3+ lymphocytes were higher for the xenogeneic group in all three analyzed areas; the collagen carrier, the infiltrating tissue and the spheroids (**Figures 4**, **5**). On the contrary, no differences in T-cell infiltration or macrophage polarization were observed between the collagen, syngeneic and allogeneic groups.

Late T Cell Response

Only the chondrogenically differentiated donor MSCs form the xenogeneic group stimulated the proliferation of T-cells isolated from the draining lymph nodes adjacent to the implant during the *in vitro* co-culturing with donor cells (**Figure 6A**). Accordingly, the xenogeneic group presented the highest level of T-lymphocyte infiltration *in vivo*, after 12 weeks from implantation (**Figure 6B**). No T-cell proliferation was observed in the co-culture model for the allogeneic and the syngeneic group. Consistently, a limited amount of CD3+ lymphocytes was present in the defect after 12 weeks.

Systemic Immune Response and Antibody Production

An increase in serum concentration of AGP, an acute phase protein produced by the liver, was observed for all groups 1 week after the surgery (**Supplementary Figure 5**) as a consequence of the tissue injury during surgery. However, the AGP level had returned to baseline values in all animals after 2 weeks. On the contrary, the total IgG concentration in the plasma continued to increase over the 12 weeks, without any statistically significant differences between groups at any of the analyzed time-points (**Figure 7A**). However, when analyzing the binding of IgM and IgG to the implanted MSCs by immunocytochemistry, differences were observed (**Figures 7B,C**). In particular, lower levels of specific anti-donor immunoglobulins were detected in the syngeneic group (mean of 213 ± 74 positive pixels/nuclei) compared to both, the xenogeneic (mean of 14,382 ± 2,259 positive pixels/nuclei) and the allogeneic groups (mean of 1,032 ± 1,276 positive pixels/nuclei).

DISCUSSION

The use of non-autologous MSCs with high chondrogenic differentiation capability has the potential to open up new avenues for the clinical translation of cell-based methods for EBR. For such a therapy to be viable, it is crucial to unravel

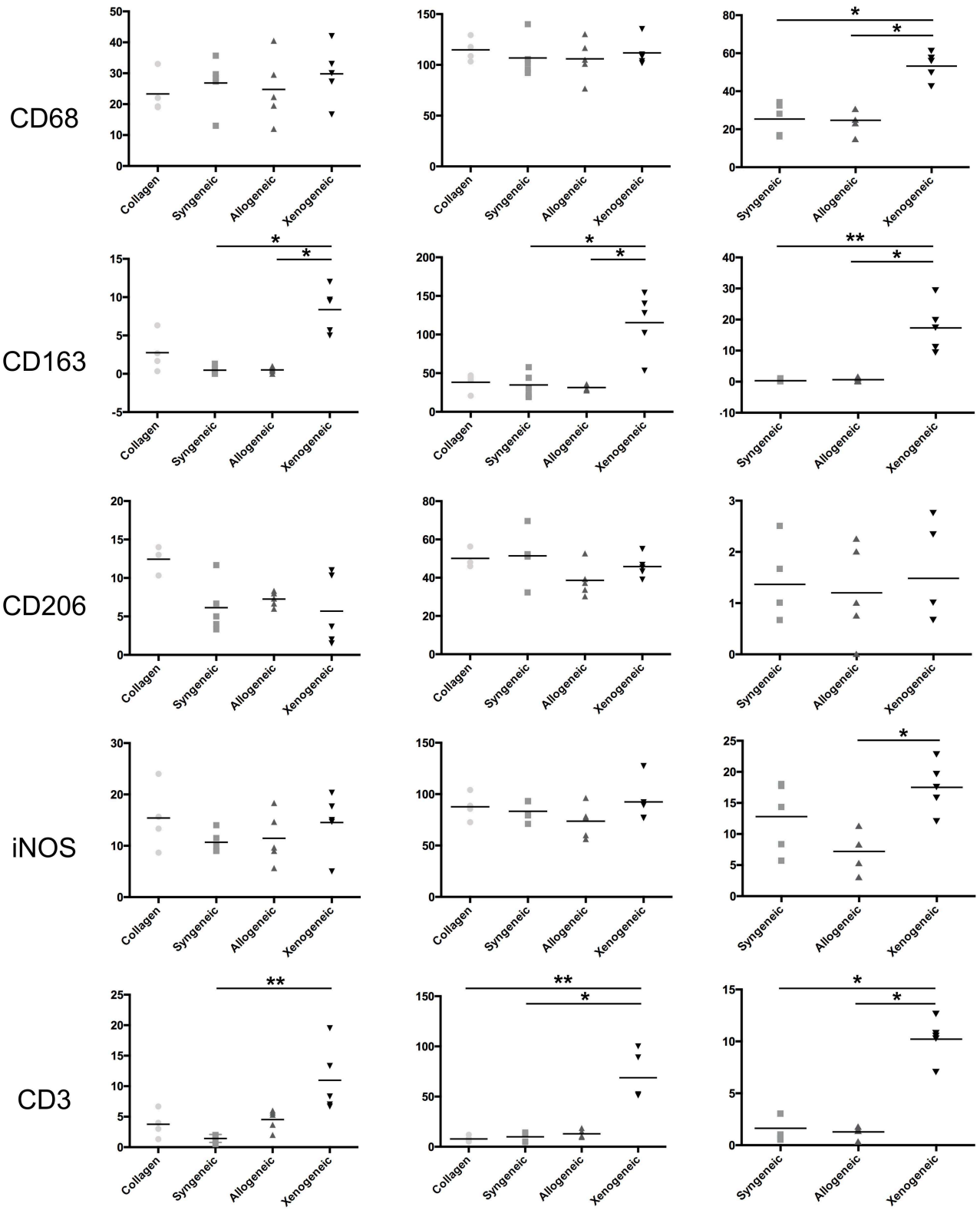

FIGURE 5 | Quantification of the immune cell infiltration in the different defect areas (collagen remnant, infiltration, and spheroids) after 1 week. The major differences were observed in the spheroids, where significantly more CD68+ and CD163+ macrophages, iNOS+ cells and CD3+ lymphocytes were found in the xenogeneic group. *$p < 0.05$; **$p < 0.01$.

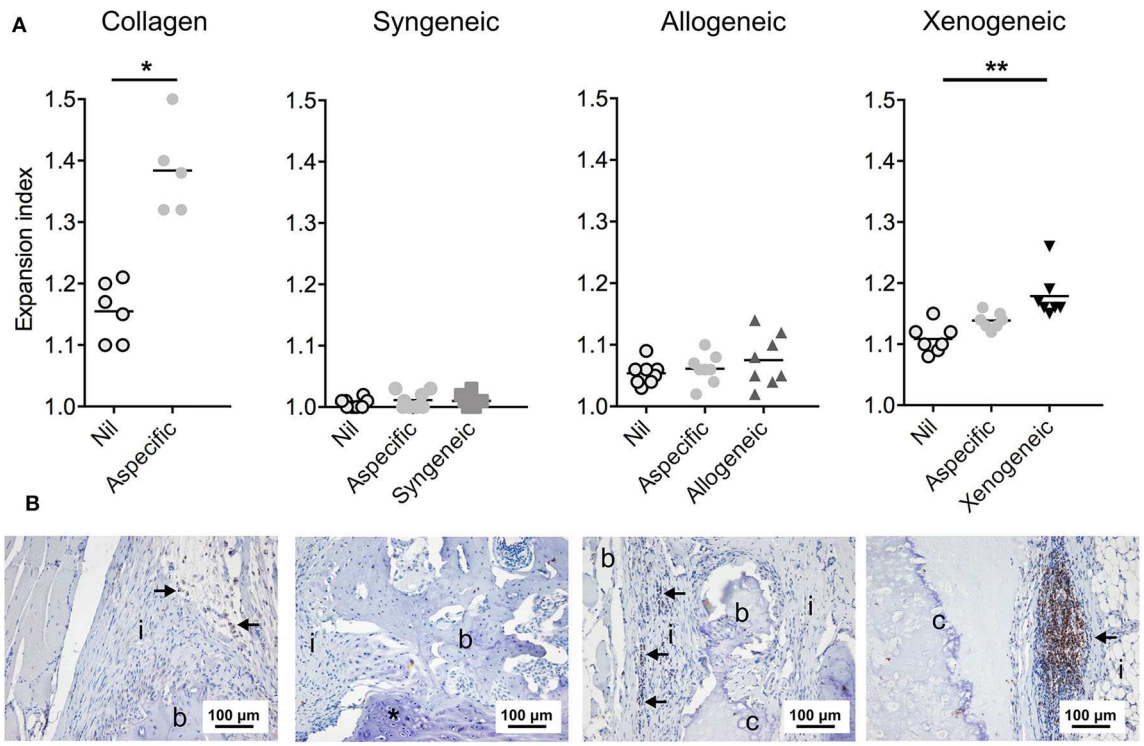

FIGURE 6 | T lymphocyte reaction to the non-autologous implants after 12 weeks. **(A)** Proliferation of the T cells isolated from the draining lymph nodes was assessed in a co-culture model with the donor cells. Specific proliferation induced by the donor cells was observed only in the xenogeneic group. Nil: lymphocytes that were not exposed to any other cell type; Aspecific: lymphocytes co-cultured with third-party Sprague Dawley MSCs; $^{*}p < 0.05$; $^{**}p < 0.01$. **(B)** CD3+ T lymphocytes (indicated by the arrows) were still prominent in the local immune response against the xenogeneic implants. Fewer CD3+ cells were spotted in the collagen and allogeneic samples. Brown color indicates the positive staining; i, tissue infiltration; b, bone; c, cartilaginous construct; *EBR.

if, and to which extent, the host immune reaction against the foreign implants prevents new bone formation. Here, using immunocompetent animals as a model, we proved that the conversion of the xenogeneic or allogeneic cartilaginous substrates into new bone is feasible even in the presence of a functional immune system. However, the extent of tissue mineralization was found to increase as a function of how close the donor cells are related to the recipient. This suggests that the activation of the immune system played a role in hampering EBR.

Xenogeneic cartilaginous spheroids suffered from an immune rejection, which impaired bone healing. Interestingly, despite this rejection, bone formation was not entirely inhibited in this group. The strong immune response was mediated by multiple immune cell types, belonging to both the innate and adaptive branch of the immune system. In particular, CD68+ and CD163+ macrophages were significantly more present within and in the proximity of the xenogeneic spheroids. This is in line with previous observations, where macrophages were found to be one of the driving forces responsible for the rejection of xenogeneic primary chondrocytes in an orthotopic minipig model (Niemietz et al., 2014). The direct involvement of macrophages in xenotransplantation rejection is probably due to their intrinsic capability of identifying non-self-cells, through the recognition of species-specific surface antigens such as CD47 (Ide et al., 2007; Navarro-Alvarez and Yang, 2014). The expression of iNOS in the majority of the cells that infiltrated the xenogeneic spheroids further supports their involvement in the cartilaginous spheroid rejection, as iNOS is a marker that usually indicates macrophage polarization toward a pro-inflammatory phenotype. Furthermore, the presence of iNOS positive macrophages usually correlates with poor regenerative outcomes (Brown et al., 2009). B and T lymphocytes were also involved in the rejection of the xenogeneic implants. In particular, CD3+ T lymphocytes infiltrated both the implanted construct and the surrounding tissue already within 1 week, and their presence persisted until the explantation at 12 weeks. This could have negatively affected the remodeling of the cartilaginous constructs, as T lymphocytes can promote the lysis of the grafted cells and stimulate the activation of other immune cells, including macrophages and B lymphocytes (Moreau et al., 2013). In addition, a correlation between the prolonged presence of effector T cells and delayed fracture repair was previously established (Reinke et al., 2013; Kovach et al., 2015; Schlundt et al., 2019). We further confirmed that the xenogeneic antigens specifically activated host lymphocytes, as in the co-culture model chondrogenically differentiated human MSCs induced the proliferation of T cells isolated from the draining lymph node. Similarly, by exposing the rat serum to human MSC-derived

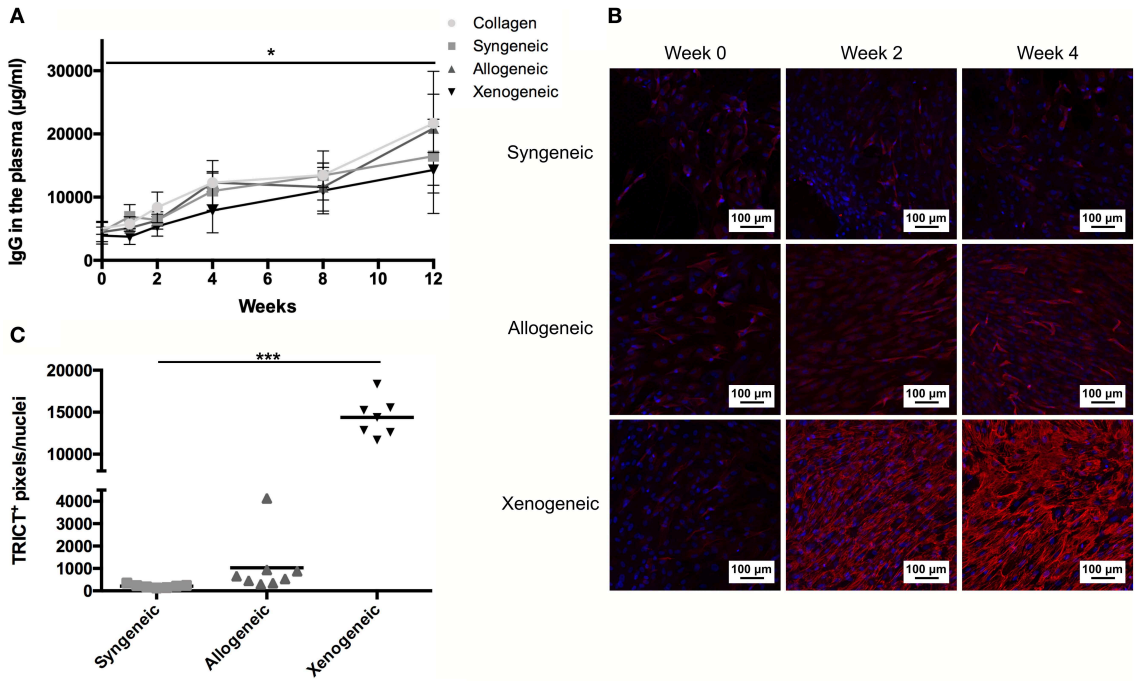

FIGURE 7 | Humoral response to the non-autologous implants. **(A)** Systemic IgG quantification shows a significant increase over time for all samples, but no differences between groups at any time-points. **(B)** Specific anti-donor IgG and IgM (red staining) were observed in all groups, but in particular in the xenogeneic group. **(C)** Quantification of the fluorescent staining confirmed that significantly more antibodies are produced against the xenogeneic implant. Although not statistically significant, more antibodies are produced on average against the allogeneic implants compared to the syngeneic ones. $^{*}p < 0.05$ and $^{***}p < 0.001$.

chondrocytes, the presence of antibodies against the xenogeneic antigens was observed. These findings are in line with the activation pattern of the adaptive branch of the immune system during both acute and chronic transplant rejection (Grinnemo et al., 2004; Mathieux et al., 2014; Vadori and Cozzi, 2015).

In contrast to the xenogeneic group, only a limited immune response was observed in the allogeneic group. More specifically, 1 week post-implantation no differences between the syngeneic and the allogeneic group were found in terms of CD68+ and CD163+ macrophage infiltration and M1 (iNOS)/M2 (CD206) polarization in the defect area and in the cartilaginous spheroids. Similarly, when comparing CD3+ T cell infiltration within the engineered constructs and in the surrounding tissues *in vivo*, no differences between the allogeneic and the syngeneic groups were observed at both 1 and 12 weeks post-implantation. Furthermore, no T cell proliferation was induced *in vitro* after co-culture with allogeneic MSCs. This outcome reinforces previous *in vitro* findings that suggest retention of immunoevasive or immunomodulatory properties in allogeneic chondrogenically differentiated MSCs (Le Blanc et al., 2003; Kiernan et al., 2016, 2017). To the best of our knowledge, only two other studies analyzed the immune response elicited by allogeneic MSCs-derived chondrocytes *in vivo* albeit for cartilage TE applications (Butnariu-Ephrat et al., 1996; Ryan et al., 2014). Here, chondrogenically differentiated MSCs were encapsulated in an alginate (Ryan et al., 2014) or hyaluronic acid carrier (Butnariu-Ephrat et al., 1996) and implanted subcutaneously (Ryan et al., 2014) or in an articular cartilage defect (Butnariu-Ephrat et al., 1996). CD68+ macrophage and CD3+ lymphocyte infiltration (Ryan et al., 2014) and fibrosis (Butnariu-Ephrat et al., 1996) were reported after 6 (Ryan et al., 2014) and 12 (Butnariu-Ephrat et al., 1996) weeks, respectively. Based on our findings, such an exacerbated immune response was not stimulated upon implantation in a segmental bone defect. Furthermore, differently from these studies, which aimed at obtaining stable cartilage, the unique goal of our study was to exploit the allogeneic spheroids only as a temporary substrate to trigger EBR. Thus, at the 12 weeks mark, the allogeneic graft was partially or entirely remodeled into new, partially autologous bone tissue. As a consequence, it is possible that this gradual remodeling over time and the cartilage conversion to non-immunogenic host neo-tissue did not trigger any additional immune cell activation and migration. Nevertheless, in spite of an immune reaction comparable to the syngeneic control in terms of early inflammation, macrophage and T lymphocyte infiltration and activation, the extent of bone formation showed more variability across the animals within the allogeneic group. In particular, 2/8 animals displayed full regeneration, comparable to the one induced by the syngeneic constructs whereas in 6/8 rats only partial regeneration was observed. While the origin of this difference could be multifaceted, one important contribution could be the production of IgM and IgG by the B lymphocytes. A trend toward increased IgM and IgG production against the

allogeneic implant was observed after 4 weeks. Production of alloreactive antibodies against different antigens, including the major histocompatibility complex (MHC) class I and class II molecules, the ABO blood-group antigens and other minor alloantigens, has been reported in several preclinical models (Colvin and Smith, 2005; Ryan et al., 2014; Lohan et al., 2017), marking the pivotal role of B cells in allorejection. In our study, the presence of immunoglobulin might have induced the activation of the complement system (Colvin and Smith, 2005; Su et al., 2019), interfering with the total remodeling of the construct in a host-dependent fashion. In particular, it is known that receptors for the complement anaphylatoxins (e.g., C5aR and C3aR) are expressed not only by immune cells, but also by cells involved in the fracture repair like osteoblasts, hypertrophic chondroblasts and osteoclasts (Huber-Lang et al., 2013; Mödinger et al., 2018). In addition, altering their expression pattern was shown to alter of the inflammatory phase of fracture healing and ultimately impaired bone repair (Bergdolt et al., 2017; Mödinger et al., 2018). Thus, future studies in the field could unravel if transient suppression of the B cell response would allow a more homogeneous and predictable extent of bone formation from allogeneic engineered cartilage grafts. Furthermore, investigating the role played by other immune cells, including polymorphonuclear cells, natural killer cells and the complement system could shed the light on additional reasons behind the heterogeneous outcome observed in the allogeneic group.

Importantly, in our study we explored the feasibility of EBR in the context of a full RT1 class I and II allogeneic mismatch (Gill et al., 1987). Nevertheless, even in such a challenging immune mismatch, successful bone regeneration comparable to the one induced by the syngeneic grafts was observed in 25% of the cases. These results present first hints toward a potential clinical translation, provided that a more homogeneous and predictable outcome could be achieved. An interesting option that could be explored is a partial donor-recipient MHC match. A partial RT 1 match might decrease the alloantibody production and promote a more reliable regenerative outcome, opening the way to a fully reproducible protocol for optimizing allogeneic EBR-based strategies.

On a final note, controversial evidence exists in literature regarding the direct contribution of MSCs to tissue regeneration. In particular, MSC secretome also exhibits regenerative capacity, as it promotes immune modulation, cell survival and reduces tissue fibrosis (Spees et al., 2016). Nevertheless, it has been established in several studies that in EBR, the implanted cells directly contribute to new bone formation, as part of the non-autologous chondrocytes transdifferentiate toward osteoblasts or osteocytes, and persist in the implanted matrix (Farrell et al., 2011; Scotti et al., 2013; Bahney et al., 2014; Yang et al., 2014). Thus, it must be considered that the newly formed tissue could contain donor cells and this might still affect bone homeostasis at a later stage, as an immune system reactivation could damage the newly formed bone. Although further analyses are required to exclude this possibility, our results suggest that the rejection of the newly deposited tissue is not a likely event. Our histological analyses do not show any sign of degradation of the newly formed bone after 12 weeks, underlining the safety and feasibility of using allogeneic cell sources for EBR.

CONCLUSION

The use of non-autologous MSCs for EBR offers great benefits from a translational clinical perspective, such as enabling a pre-selection of MSCs with high chondrogenic differentiation potential to guarantee a beneficial therapeutic outcome. Our results represent the first proof-of-concept of the feasibility of using non-autologous, chondrogenically differentiated MSCs to trigger EBR. A severe immune response did result in a low level of bone formation in the xenogeneic group, rendering it unsuitable for clinical translation applications. On the contrary, a milder immune response, mainly characterized by the production of specific anti-donor IgM and IgG was observed in the allogeneic group. While this might have affected the variability in terms of percentage of defect bridging between the different experimental animals, the successful bone formation observed in the allogeneic group provides encouraging evidence of its potential as an alternative to autologous transplantation. Overall, these findings provide fundamental information for the design and translation of the next generation of EBR-based strategies.

DATA AVAILABILITY STATEMENT

All datasets generated for this study are included in the article/**Supplementary Material**.

ETHICS STATEMENT

This animal study was reviewed and approved by Animal Welfare Body Utrecht (approved work Protocol No. 2465-2-01).

AUTHOR CONTRIBUTIONS

AL: conception and design, collection and assembly of the data, data analysis and interpretation, manuscript writing, and final approval of the manuscript. IP: collection and assembly of the data, data analysis and interpretation, and final approval of the manuscript. MC: conception and design, collection and assembly of the data, data analysis and interpretation, and final approval of the manuscript. MR, VP, and RL: data analysis and interpretation and final approval of the manuscript. AR: financial support, data analysis and interpretation, and final approval of the manuscript. DG: conception and design, data analysis and interpretation, financial and administrative support, and final approval of the manuscript. All authors contributed to the article and approved the submitted version.

FUNDING

This work was supported by the AO Foundation (Project No. S-16-130G).

ACKNOWLEDGMENTS

The antibody against collagen type II (II-II6B3), developed by T. F. Linsenmayer, was obtained from the DSHB developed under the auspices of the NICHD and maintained by the University of Iowa, Department of Biology, Iowa City, IA52242. Furthermore, the help of Imke Jansen, Irina Mancini, and Lizette Utomo was highly appreciated. Finally, the authors would like to thank Anja van der Sar and Nicky van Kronenburg for all the support during the animal experiment.

SUPPLEMENTARY MATERIAL

The Supplementary Material for this article can be found online at: https://www.frontiersin.org/articles/10.3389/fbioe.2020.00651/full#supplementary-material

REFERENCES

Bahney, C. S., Hu, D. P., Taylor, A. J., Ferro, F., Britz, H. M., Hallgrimsson, B., et al. (2014). Stem cell-derived endochondral cartilage stimulates bone healing by tissue transformation. *J. Bone Miner Res.* 29, 1269–1282. doi: 10.1002/jbmr.2148

Bergdolt, S., Kovtun, A., Hägele, Y., Liedert, A., Schinke, T., Amling, M., et al. (2017). Osteoblast-specific overexpression of complement receptor C5aR1 impairs fracture healing. *PLoS ONE* 12:e0179512. doi: 10.1371/journal.pone.0179512

Brown, B. N., Valentin, J. E., Stewart-Akers, A. M., McCabe, G. P., and Badylak, S. F. (2009). Macrophage phenotype and remodeling outcomes in response to biologic scaffolds with and without a cellular component. *Biomaterials* 30, 1482–1491. doi: 10.1016/j.biomaterials.2008.11.040

Butnariu-Ephrat, M., Robinson, D., Mendes, D. G., Halperin, N., and Nevo, Z. (1996). Resurfacing of goat articular cartilage by chondrocytes derived from bone marrow. *Clin. Orthop Relat. Res. 330,* 234–243.

Chen, X., McClurg, A., Zhou, G. Q., McCaigue, M., Armstrong, M. A., and Li, G. (2007). Chondrogenic differentiation alters the immunosuppressive property of bone marrow-derived mesenchymal stem cells, and the effect is partially due to the upregulated expression of B7 molecules. *Stem Cells* 25, 364–370. doi: 10.1634/stemcells.2006-0268

Colvin, R. B., and Smith, R. N. (2005). Antibody-mediated organ-allograft rejection. *Nat. Rev. Immunol.* 5, 807–817. doi: 10.1038/nri1702

Doube, M., Klosowski, M. M., Arganda-Carreras, I., Cordelieres, F. P., Dougherty, R. P., Jackson, J. S., et al. (2010). BoneJ: free and extensible bone image analysis in ImageJ. *Bone* 47, 1076–1079. doi: 10.1016/j.bone.2010.08.023

Du, W. J., Reppel, L., Leger, L., Schenowitz, C., Huselstein, C., Bensoussan, D., et al. (2016). Mesenchymal stem cells derived from human bone marrow and adipose tissue maintain their immunosuppressive properties after chondrogenic differentiation: role of HLA-G. *Stem Cells Dev.* 25, 1454–1469. doi: 10.1089/scd.2016.0022

Evans, C. H. (2013). Advances in regenerative orthopedics. *Mayo Clin. Proc.* 88, 1323–1339. doi: 10.1016/j.mayocp.2013.04.027

Evans, C. H., Palmer, G. D., Pascher, A., Porter, R., Kwong, F. N., Gouze, E., et al. (2007). Facilitated endogenous repair: making tissue engineering simple, practical, and economical. *Tissue Eng.* 13, 1987–1993. doi: 10.1089/ten.2006.0302

Farrell, E., Both, S. K., Odorfer, K. I., Koevoet, W., Kops, N., O'Brien, F. J., et al. (2011). *In-vivo* generation of bone via endochondral ossification by in-vitro chondrogenic priming of adult human and rat mesenchymal stem cells. *BMC Musculoskelet. Disord.* 12:31. doi: 10.1186/1471-2474-12-31

Gawlitta, D., Farrell, E., Malda, J., Creemers, L. B., Alblas, J., and Dhert, W. J. A. (2010). Modulating endochondral ossification of multipotent stromal cells for bone regeneration. *Tissue Engineering Part B Rev.* 16, 385–395. doi: 10.1089/ten.teb.2009.0712

Gawlitta, D., van Rijen, M. H., Schrijver, E. J., Alblas, J., and Dhert, W. J. (2012). Hypoxia impedes hypertrophic chondrogenesis of human multipotent stromal cells. *Tissue Eng. Part A* 18, 1957–1966. doi: 10.1089/ten.TEA.2011.0657

Gerstenfeld, L. C., Cullinane, D. M., Barnes, G. L., Graves, D. T., and Einhorn, T. A. (2003). Fracture healing as a post-natal developmental process: molecular, spatial, and temporal aspects of its regulation. *J. Cell. Biochem.* 88, 873–884. doi: 10.1002/jcb.10435

Gill, T. J. 3rd, Kunz, H. W., Misra, D. N., and Hassett, A. L. (1987). The major histocompatibility complex of the rat. *Transplantation* 43, 773–785.

Grinnemo, K. H., Mansson, A., Dellgren, G., Klingberg, D., Wardell, E., Drvota, V., et al. (2004). Xenoreactivity and engraftment of human mesenchymal stem cells transplanted into infarcted rat myocardium. *J. Thorac. Cardiovasc. Surg.* 127, 1293–1300. doi: 10.1016/j.jtcvs.2003.07.037

Harada, N., Watanabe, Y., Sato, K., Abe, S., Yamanaka, K., Sakai, Y., et al. (2014). Bone regeneration in a massive rat femur defect through endochondral ossification achieved with chondrogenically differentiated MSCs in a degradable scaffold. *Biomaterials* 35, 7800–7810. doi: 10.1016/j.biomaterials.2014.05.052

Huber-Lang, M., Kovtun, A., and Ignatius, A. (2013). The role of complement in trauma and fracture healing. *Semin. Immunol.* 25, 73–78. doi: 10.1016/j.smim.2013.05.006

Ide, K., Wang, H., Tahara, H., Liu, J., Wang, X., Asahara, T., et al. (2007). Role for CD47-SIRPalpha signaling in xenograft rejection by macrophages. *Proc. Natl. Acad. Sci. U.S.A.* 104, 5062–5066. doi: 10.1073/pnas.0609661104

Jukes, J. M., Both, S. K., Leusink, A., Sterk, L. M., van Blitterswijk, C. A., and de Boer, J. (2008). Endochondral bone tissue engineering using embryonic stem cells. *Proc. Natl. Acad. Sci. U.S.A.* 105, 6840–6845. doi: 10.1073/pnas.0711662105

Kiernan, C. H., Hoogduijn, M. J., Franquesa, M., Wolvius, E. B., Brama, P. A., and Farrell, E. (2016). Allogeneic chondrogenically differentiated human mesenchymal stromal cells do not induce immunogenic responses from T lymphocytes *in vitro*. *Cytotherapy* 18, 957–969. doi: 10.1016/j.jcyt.2016.05.002

Kiernan, C. H., KleinJan, A., Peeters, M., Wolvius, E. B., Farrell, E., and Brama, P. A. J. (2018). Allogeneic chondrogenically differentiated human bone marrow stromal cells do not induce dendritic cell maturation. *J. Tissue Eng. Regen. Med.* 12, 1530–1540. doi: 10.1002/term.2682

Kiernan, C. H., Wolvius, E. B., Brama, P. A. J., and Farrell, E. (2017). The immune response to allogeneic differentiated mesenchymal stem cells in the context of bone tissue engineering. *Tissue Eng. Part B Rev.* 24, 75–83. doi: 10.1089/ten.TEB.2017.0175

Kovach, T. K., Dighe, A. S., Lobo, P. I., and Cui, Q. (2015). Interactions between MSCs and immune cells: implications for bone healing. *J. Immunol. Res.* 2015:752510. doi: 10.1155/2015/752510

Le Blanc, K., Tammik, C., Rosendahl, K., Zetterberg, E., and Ringden, O. (2003). HLA expression and immunologic properties of differentiated and undifferentiated mesenchymal stem cells. *Exp. Hematol.* 31, 890–896. doi: 10.1016/s0301-472x(03)00110-3

Lohan, P., Treacy, O., Griffin, M. D., Ritter, T., and Ryan, A. E. (2017). Anti-donor immune responses elicited by allogeneic mesenchymal stem cells and their extracellular vesicles: are we still learning? *Front. Immunol* 8:1626. doi: 10.3389/fimmu.2017.01626

Longoni, A., KneŽević, L., Schepers, K., Weinans, H., Rosenberg, A. J. W. P., and Gawlitta, D. (2018). The impact of immune response on endochondral bone regeneration. *NPJ Regenerat. Med.* 3:22. doi: 10.1038/s41536-018-0060-5

Mathieux, E., Nerrière-Daguin, V., Lévèque, X., Michel-Monigadon, D., Durand, T., Bonnamain, V., et al. (2014). IgG response to intracerebral xenotransplantation: specificity and role in the rejection of porcine neurons. *Am. J. Transpl.* 14, 1109–1119. doi: 10.1111/ajt.12656

Matsiko, A., Thompson, E. M., Lloyd-Griffith, C., Cunniffe, G. M., Vinardell, T., Gleeson, J. P., et al. (2018). An endochondral ossification approach to early stage bone repair: Use of tissue-engineered hypertrophic cartilage constructs as primordial templates for weight-bearing bone repair. *J. Tissue Eng. Regen. Med.* 12, e2147–e2150. doi: 10.1002/term.2638

McDermott, A. M., Herberg, S., Mason, D. E., Collins, J. M., Pearson, H. B., Dawahare, J. H., et al. (2019). Recapitulating bone development through engineered mesenchymal condensations and mechanical cues for tissue regeneration. *Sci. Transl. Med.* 11:eaav7756. doi: 10.1126/scitranslmed.aav7756

Mödinger, Y., Löffler, B., Huber-Lang, M., and Ignatius, A. (2018). Complement involvement in bone homeostasis and bone disorders. *Semin. Immunol.* 37, 53–65. https://doi.org/10.1016/j.smim.2018.01.001

Moreau, A., Varey, E., Anegon, I., and Cuturi, M. C. (2013). Effector mechanisms of rejection. *Cold Spring Harb. Perspect. Med.* 3:a015461. doi: 10.1101/cshperspect.a015461

Navarro-Alvarez, N., and Yang, Y. G. (2014). Lack of CD47 on donor hepatocytes promotes innate immune cell activation and graft loss: a potential barrier to hepatocyte xenotransplantation. *Cell Transplant.* 23, 345–354. doi: 10.3727/096368913x663604

Niemietz, T., Zass, G., Hagmann, S., Diederichs, S., Gotterbarm, T., and Richter, W. (2014). Xenogeneic transplantation of articular chondrocytes into full-thickness articular cartilage defects in minipigs: fate of cells and the role of macrophages. *Cell Tissue Res.* 358, 749–761. doi: 10.1007/s00441-014-1982-x

Osinga, R., Di Maggio, N., Todorov, A., Allafi, N., Barbero, A., Laurent, F., et al. (2016). Generation of a bone organ by human adipose-derived stromal cells through endochondral ossification. *Stem Cells Transl. Med.* 5, 1090–1097. doi: 10.5966/sctm.2015-0256

Reinke, S., Geissler, S., Taylor, W. R., Schmidt-Bleek, K., Juelke, K., Schwachmeyer, V., et al. (2013). Terminally differentiated CD8(+) T cells negatively affect bone regeneration in humans. *Sci. Transl. Med.* 5:177ra136. doi: 10.1126/scitranslmed.3004754

Ryan, A. E., Lohan, P., O'Flynn, L., Treacy, O., Chen, X., Coleman, C., et al. (2014). Chondrogenic differentiation increases antidonor immune response to allogeneic mesenchymal stem cell transplantation. *Mol. Ther.* 22, 655–667. doi: 10.1038/mt.2013.261

Schlundt, C., Reinke, S., Geissler, S., Bucher, C. H., Giannini, C., Mardian, S., et al. (2019). Individual effector/regulator T cell ratios impact bone regeneration. *Front. Immunol.* 10:1954. doi: 10.3389/fimmu.2019.01954

Scotti, C., Piccinini, E., Takizawa, H., Todorov, A., Bourgine, P., Papadimitropoulos, A., et al. (2013). Engineering of a functional bone organ through endochondral ossification. *Proc. Natl. Acad. Sci. U.S.A.* 110, 3997–4002. doi: 10.1073/pnas.1220108110

Shapiro, F. (2008). Bone development and its relation to fracture repair. The role of mesenchymal osteoblasts and surface osteoblasts. *Eur. Cell. Mater.* 15, 53–76. doi: 10.22203/ecm.v015a05

Sivasubramaniyan, K., Ilas, D. C., Harichandan, A., Bos, P. K., Santos, D. L., de Zwart, P., et al. (2018). Bone marrow-harvesting technique influences functional heterogeneity of mesenchymal stem/stromal cells and cartilage regeneration. *Am. J. Sports Med.* 46, 3521–3531. doi: 10.1177/0363546518804807

Spees, J. L., Lee, R. H., and Gregory, C. A. (2016). Mechanisms of mesenchymal stem/stromal cell function. *Stem Cell Res. Ther.* 7:125. doi: 10.1186/s13287-016-0363-7

Su, J. A., Baxter-Lowe, L. A., Kantor, P. F., Szmuszkovicz, J. R., and Menteer, J. (2019). The clinical impact of donor-specific antibodies on antibody-mediated rejection and long-term prognosis after heart transplantation. *Curr. Opin. Organ Transplant.* 24, 245–251. doi: 10.1097/mot.0000000000000636

Thompson, E. M., Matsiko, A., Farrell, E., Kelly, D. J., and O'Brien, F. J. (2015). Recapitulating endochondral ossification: a promising route to in vivo bone regeneration. *J. Tissue Eng. Regen. Med.* 9, 889–902. doi: 10.1002/term.1918

Vadori, M., and Cozzi, E. (2015). The immunological barriers to xenotransplantation. *Tissue Antigens* 86, 239–253. doi: 10.1111/tan.12669

van der Stok, J., Koolen, M. K., Jahr, H., Kops, N., Waarsing, J. H., Weinans, H., et al. (2014). Chondrogenically differentiated mesenchymal stromal cell pellets stimulate endochondral bone regeneration in critical-sized bone defects. *Eur. Cell Mater.* 27, 137–148. doi: 10.22203/ecm.v027a11

Yang, L., Tsang, K. Y., Tang, H. C., Chan, D., and Cheah, K. S. (2014). Hypertrophic chondrocytes can become osteoblasts and osteocytes in endochondral bone formation. *Proc. Natl. Acad. Sci. U.S.A.* 111, 12097–12102. doi: 10.1073/pnas.1302703111

Zheng, Z. H., Li, X. Y., Ding, J., Jia, J. F., and Zhu, P. (2008). Allogeneic mesenchymal stem cell and mesenchymal stem cell-differentiated chondrocyte suppress the responses of type II collagen-reactive T cells in rheumatoid arthritis. *Rheumatology* 47, 22–30. doi: 10.1093/rheumatology/kem284

Conflict of Interest: The authors declare that the research was conducted in the absence of any commercial or financial relationships that could be construed as a potential conflict of interest.

frontiers in Bioengineering and Biotechnology

REVIEW
published: 28 July 2020
doi: 10.3389/fbioe.2020.00860

Infrapatellar Fat Pad/Synovium Complex in Early-Stage Knee Osteoarthritis: Potential New Target and Source of Therapeutic Mesenchymal Stem/Stromal Cells

Dylan N. Greif[1†], Dimitrios Kouroupis[1†], Christopher J. Murdock[1], Anthony J. Griswold[2], Lee D. Kaplan[1], Thomas M. Best[1] and Diego Correa[1,3‡]*

[1] Department of Orthopedics, UHealth Sports Medicine Institute, Miller School of Medicine, University of Miami, Miami, FL, United States, [2] John P. Hussman Institute for Human Genomics, Miller School of Medicine, University of Miami, Miami, FL, United States, [3] Diabetes Research Institute and Cell Transplant Center, Miller School of Medicine, University of Miami, Miami, FL, United States

The infrapatellar fat pad (IFP) has until recently been viewed as a densely vascular and innervated intracapsular/extrasynovial tissue with biomechanical roles in the anterior compartment of the knee. Over the last decade, secondary to the proposition that the IFP and synovium function as a single unit, its recognized tight molecular crosstalk with emerging roles in the pathophysiology of joint disease, and the characterization of immune-related resident cells with varying phenotypes (e.g., pro and anti-inflammatory macrophages), this structural complex has gained increasing attention as a potential therapeutic target in patients with various knee pathologies including osteoarthritis (KOA). Furthermore, the description of the presence of mesenchymal stem/stromal cells (MSC) as perivascular cells within the IFP (IFP-MSC), exhibiting immunomodulatory, anti-fibrotic and neutralizing activities over key local mediators, has promoted the IFP as an alternative source of MSC for cell-based therapy protocols. These complementary concepts have supported the growing notion of immune and inflammatory events participating in the pathogenesis of KOA, with the IFP/synovium complex engaging not only in amplifying local pathological responses, but also as a reservoir of potential therapeutic cell-based products. Consequently, the aim of this review is to outline the latest discoveries related with the IFP/synovium complex as both an active participant during KOA initiation and progression thus emerging as a potential target, and a source of therapeutic IFP-MSCs. Finally, we discuss how these notions may help the design of novel treatments for KOA through modulation of local cellular and molecular cascades that ultimately lead to joint destruction.

Keywords: infrapatellar fat pad, synovium, mesenchymal stem/stromal cells, macrophages, osteoarthritis

OPEN ACCESS

Edited by:
Roberto Narcisi, Erasmus University Rotterdam, Netherlands

Reviewed by:
Cristóbal Orellana, Corporació Sanitària Parc Taulí, Spain
Guus van den Akker, Maastricht University, Netherlands

***Correspondence:**
Diego Correa
dxc821@med.miami.edu

[†] These authors have contributed equally to this work

[‡] ORCID:
Diego Correa
orcid.org/0000-0002-9004-4300

Specialty section:
This article was submitted to Preclinical Cell and Gene Therapy, a section of the journal Frontiers in Bioengineering and Biotechnology

Received: *07 May 2020*
Accepted: *03 July 2020*
Published: *28 July 2020*

Citation:
Greif DN, Kouroupis D, Murdock CJ, Griswold AJ, Kaplan LD, Best TM and Correa D (2020) Infrapatellar Fat Pad/Synovium Complex in Early-Stage Knee Osteoarthritis: Potential New Target and Source of Therapeutic Mesenchymal Stem/Stromal Cells. Front. Bioeng. Biotechnol. 8:860. doi: 10.3389/fbioe.2020.00860

INTRODUCTION

The infrapatellar fat pad (IFP), also known as Hoffa's fat pad, is a cylinder-like piece of adipose tissue that sits posterior to the patella and fills the anterior knee compartment (Dragoo et al., 2012). Though the function of the IFP has not yet been fully defined, studies have shown that the IFP plays an important biomechanical role within the knee (Bohnsack et al., 2004; Gallagher et al., 2005). In addition, recent evidence has shown that the IFP in concert with the synovium participates in the pathogenesis and progression of various pathologies within the knee joint such as osteoarthritis (KOA) (Benito et al., 2005; Scanzello and Goldring, 2012; Sokolove and Lepus, 2013; Lieberthal et al., 2015; Felson et al., 2016; Favero et al., 2017; Mathiessen and Conaghan, 2017), given that these structures serve as sites of immune cell infiltration and origin of pro-inflammatory (*e.g.,* IFNγ, TNFα and IL1β) and articular cartilage degradative (*e.g.,* MMPs) molecules (Bondeson et al., 2010; Kalaitzoglou et al., 2017; Li et al., 2017). On the other hand, they may be related with repair attempts after injury, due to the presence of mesenchymal stem/stromal cells (MSCs) within both the IFP (IFP-MSC) (Garcia et al., 2016a; Tangchitphisut et al., 2016; Kouroupis et al., 2019a) and the synovium (sMSC) (Mizuno et al., 2018; To et al., 2019) exhibiting disease-modifying capacities (Caplan and Correa, 2011; Stagg and Galipeau, 2013; Uccelli and de Rosbo, 2015; Galipeau et al., 2016). Consequently, the IFP and synovium engage not only in amplifying local pathological responses, but also act as a reservoir of disease-modifying cellular products, promoting them as potential novel targets in joint disease (Attur et al., 2010).

IFP-MSCs have generated increased interest in recent literature due to their easy accessibility compared to other stem cell sources such as bone marrow and adipose tissue (AT), while displaying similar multipotency, growth potential, and immunomodulatory abilities (Sun et al., 2018). Their relative ease of isolation compared to bone marrow aspiration (thus removing the potential surgical complications seen with aspiration) have made them a popular resource for experimentation and regenerative medicine (Vilalta et al., 2008; Mizuno et al., 2012; Siciliano et al., 2016). However, because of its relatively newfound MSC population, current literature has re-focused on updating the knowledge of IFP anatomy, function, and most importantly its cellular composition beyond MSC. This has not only led to extensive investment in the IFP's potential for regenerative medicine in Orthopedics, but also the role the IFP may play in certain pathological processes including KOA. For example, more established theories believe that the IFP communicates with the joint via the synovium and may play a role in cartilage and/or bone regeneration via the secretion of adipose tissue derived growth factors (Jiang et al., 2019). However, a shift in our understanding of the IFP anatomy and pathophysiology demonstrates not only that the IFP and the synovium constitute one structural and functional unit (Macchi et al., 2018), but that IFP-MSCs can regulate resident immune cell infiltration and resident macrophages thus acting as local immunomodulatory players.

Therefore, the goal of this review is to outline the latest developments of the IFP/synovium complex as a tissue that actively participates in joint homeostasis and disease, while harboring cellular elements that can be harnessed for therapeutic cell-based therapy protocols. In addition, updates regarding recent discoveries in anatomy, cellular composition, function, isolation and harvest, imaging, role in certain pathologies of the knee (most importantly modulation of inflammation in the joint), current therapeutic uses, and future perspectives and goals for IFP use will be discussed.

STRUCTURE AND FUNCTION OF THE IPF/SYNOVIUM COMPLEX

Anatomy

The IFP is located deep to the patella and occupies the space between the patellar tendon, femoral condyle, and tibial plateau. It attaches to the lower border of the patella, the intercondylar notch within the femur via the ligamentum mucosum, the periosteum of the tibia, and the anterior horn of both menisci (Gallagher et al., 2005). Of note, recent study of IFP anatomy has demonstrated previously undiscovered attachments to the deep quadriceps muscle, which may assist with IFP motion during walking (Woodley et al., 2012).

Although the IFP is intracapsular, it remains extrasynovial despite its constant contact with the synovium (Clockaerts et al., 2010). Increasing evidence has demonstrated that the IFP develops as an outgrowth of the synovial tissue with regard to structure and functionality, which suggests extensive communication between the IFP and the synovium and joint capsule (**Figure 1**) (Ioan-Facsinay and Kloppenburg, 2013). Furthermore, Macchi et al. (2018) have concluded that the IFP and the synovium should be viewed as one anatomo-functional unit rather than two distinct structures that simply

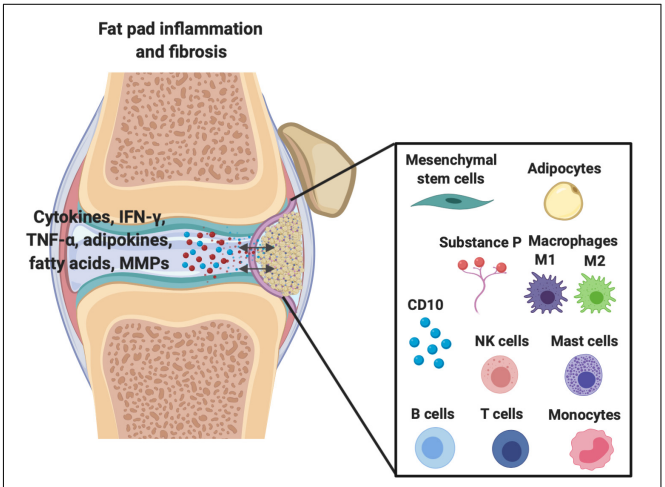

FIGURE 1 | Demonstration of the extensive molecular cross-talk and important cellular components between the IFP and the synovium within the joint capsule which are responsible for inflammation/fibrosis.

communicate with one another. The authors justified this definition because recent anatomical studies demonstrated the insertion of infrapatellar and medial synovial plicae directly onto the IFP, which suggests that the IFP may not be extrasynovial, but rather an extension of the synovium outside of the joint capsule (Macchi et al., 2018). Nevertheless, the intimate relationship between the synovium and IFP appears highly important in the release of growth factors and cytokines that help to regulate the molecular environment within the joint.

The extensive anastomotic vascular network near the IFP involves a combination of the superior and inferior geniculate arteries, the latter which passes through the IFP before supplying the patella. This matrix helps support and promote IFP-MSC proliferation, especially during injury and inflammation. It has also been hypothesized that this network is sufficient to protect the IFP during extensive surgical or arthroscopic procedures that lead to significant manipulation of the structure itself (Kohn et al., 1995).

Innervation to the IFP is just as extensive as its vasculature and typically traverses the same course across the entire tissue. Previous studies have confirmed that posterior articular branches from the tibial, saphenous, recurrent peroneal, and common peroneal nerve provide most of the innervation, however Gardner et al. recently described branches arising from the saphenous and obturator nerves as well (Freeman and Wyke, 1967; Kennedy et al., 1982). This collective peripheral sensory nociceptive innervation pattern (dense in parts of the IFP and synovium) is mediated by nerve fibers equipped with the neurotransmitter Substance P which runs separately but in parallel to sympathetic fibers and it is implicated in knee pain transmission. Additionally, within the IFP tyrosine hydroxylase (TH)-positive sympathetic fibers modulate nociception/pain signaling in sympathetic neurons, through interacting with Substance P-positive fibers (Dragoo et al., 2012; Brumovsky, 2016).

Cellular Composition and Molecular Mediators

Infrapatellar Fat Pad

The most prevalent cell is the adipocyte, which is not only responsible for the IFP's metabolism, but also endocrine and paracrine functions within the knee joint (Coelho et al., 2013; do Amaral et al., 2017). Importantly, adipose cells secrete cytokines, interferons, adipokines, and growth factors, all of which exerting local signaling effects on articular cartilage and synovial cells (Clockaerts et al., 2010).

As shown in **Figure 1**, other important cellular components of the IFP include fibroblasts, responsible for the production of extracellular matrix, and in less quantities resident monocytes, mast cells, lymphocytes, and perhaps most importantly macrophages (de Lange-Brokaar et al., 2012; Belluzzi et al., 2019; Kouroupis et al., 2019a). Barboza et al. (2017) have demonstrated that macrophages not only permanently reside within the IFP, but lie without phenotypic polarization as either classical M1 or alternative M2 variants until conditions promote their activation and subsequent conversion, such as inflammation.

Resident IFP macrophages are activated by a variety of interleukins and interferons secreted from other resident and infiltrating immune cells and adipose cells within the IFP. When converted to M1 macrophages, the IFP begins secreting vast amounts of pro-inflammatory cytokines, catabolic factors, and adipokines, and with prolonged periods of time, the IFP can also release pro-fibrotic mediators such as CTGF that may contribute to KOA progression (**Figure 2**) (Clockaerts et al., 2010). This occurs due to tight molecular crosstalk between synovial, IFP, and systemic inflammatory mediators. Consequently, these macrophages are now the target of studies assessing their release of pro-inflammatory molecular mediators (Kouroupis et al., 2019a). On the other hand, also shown in **Figure 2**, alternatively differentiated M2 macrophages exert anti-inflammatory effects, serving as counterbalance to their M1 cohorts by suppressing their proliferation and inflammatory signaling.

Finally, the IFP harbors a population of MSC (IFP-MSC), which will be discussed in detail later (see section "Synovium-Derived MSC") as a potential therapeutic tool for cell-based therapy protocols.

Synovium

Within the intimal synovial lining reside predominantly two synovial cell types: type A (Macrophage-Like synoviocytes – MLS) and type B (Fibroblast-Like-Synoviocytes – FLS) (Tu et al., 2018). The type B synoviocytes, thought to be descendants of cells of mesodermal origin, are far more abundant and display typical fibroblast markers such as surface marker Thy-1 (CD90) and integrins like ICAM1 while secreting specialized matrix constituents including hyaluronan and Type IV and V collagens (Roelofs et al., 2017; Tu et al., 2018). Thus, it can be argued that type B synoviocytes more so than type A counterparts are responsible for maintenance of synovial homeostasis.

Type B synoviocytes are subject to cytokine and growth factor regulation, which can dictate a pro or anti-inflammatory state depending on which factors are expressed in the surrounding synovial environment (Orr et al., 2017). In a chronic inflammatory state, these cells primarily act in a pro-inflammatory role. For example, in patients with rheumatoid arthritis, fibroblasts have been shown to respond to and secrete a combination of TNF-alpha, IL-1, IL-6, and granulocyte-macrophage colony-stimulating factor (GM-CSF), while expressing a multitude of toll-like receptors in order to amplify T-Cell response to TLR activation (Ospelt, 2017). In regard to patients with OA, type B synoviocytes are particularly sensitive to TLR-2, TLR-3, and TLR-4 ligands due to the active expression of CD14, a co-receptor for TLRs (Nair et al., 2012). Type B synoviocytes also secrete a multitude of chemoattractants, including CCL2, CCL5, CCL8, CXCL5, and CXCL10, designed to attract monocytes and macrophages, both resident and peripheral in nature (Bartok and Firestein, 2010). Finally, upon stimulation of TLR-3, these synoviocytes produce large quantities of IL6, B-Cell Activating Factor and proliferation-inducing ligand (Mata-Essayag et al., 2001), promoting the maturation, survival, and antibody production by B cells (Bombardieri et al., 2011).

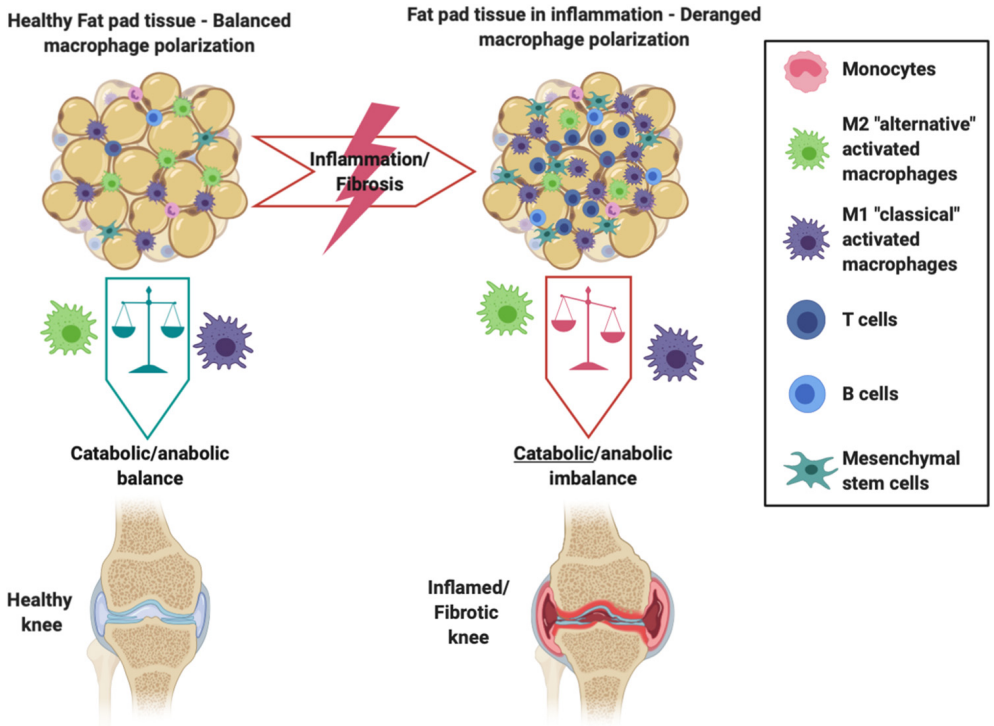

FIGURE 2 | Schematic showing the intricate balance between M1 and M2 macrophages within the IFP and synovium. Differentiated M2 macrophages exhibit anti-inflammatory effects and preserve the health of the joint, whereas an imbalance favoring M1 macrophages promotes the IFP's secretion of pro-inflammatory cytokines and catabolic factors that are seen within an inflamed/fibrotic knee.

These findings suggest that type B synoviocytes, though non-immune in nature, play a key role in autoimmune and OA disease development due to their inflammatory properties.

Type B synoviocytes can also produce a wide variety of anti-inflammatory factors such as TGF-beta, Type 1 interferons, VEG-F, indoleamine 2,3-dioxygenase (IDO enzyme), and certain prostaglandins, though some of these factors depending on concentration and exposure time may also be pro-inflammatory (Tu et al., 2018). However, the ability to harness the anti-inflammatory properties of these cells remains unknown. The recent proposition that type B synoviocytes may also contain multiple subtypes within the synovial lining which determine their secretory properties provides a future avenue for studies attempting to fully elucidate the role of these cells in arthritis development or modulation (Frank-Bertoncelj et al., 2017).

On the other hand, type A synoviocytes are far less known due to the limited number of these cells *in vivo* and their poor proliferative potential *in vitro*. They constitute resident macrophages, derived from both embryonic hematopoietic precursors and from bone marrow, although their definitive origin is still elusive (Tu et al., 2018). These resident macrophages need to be discriminated from monocytes/macrophages that extravasate into the synovium from peripheral circulation after injury or in disease. Nevertheless, it has been established that they have pro-inflammatory tendencies while exhibiting an intimate crosstalk with type B synoviocytes, especially in disease (Tu et al., 2018, 2019). Type A synoviocytes secrete soluble CD14, IL-1β, and TNFα, further potentiating the pro-inflammatory properties of type B synoviocytes and CD4 T helper cells. They also induce monocyte/macrophage-derived osteoclast activity via RANK-L secretion resulting in enhanced bone resorption (Yoshitomi, 2019). It is interesting to note given the above pro-inflammatory properties that the presence and activity levels of these tissue-resident macrophages significantly correlates with advanced stages of OA and poorer clinical outcome scores (Kriegova et al., 2018; Gomez-Aristizabal et al., 2019).

Similar to the IFP, the synovium contains a small population of cells compatible with MSC (sMSC), which will be discussed in detail in section "MSC-Induced Immunomodulation: Focus on Macrophage Polarization."

IFP/Synovium Molecular Interactions

Beyond the proximity the IFP and synovium share, there are molecular interactions between both components that support their view as a single anatomical and functional unit. For instance, both IFP and adjacent synovium experience similar structural effects in KOA, including increased inflammatory infiltration, vascularization, and thickness (Favero et al., 2017). The IFP has been shown to release prostaglandin F2a (PGF2α), IL-6, IL-8, and TNFα, inducing a profibrotic effect on the synovial membrane (Bastiaansen-Jenniskens et al., 2013; Eymard et al., 2014). Specifically, Bastiaansen-Jenniskens et al. (2013) cultured human fibroblast -like synoviocytes (type B) obtained from OA patients in conditioned medium derived from IFP tissue with and without

inhibitors of TGFβ/activin receptor-like kinase 5 or PGF2α for 4 days *in vitro*. IFP derived conditioned medium not only increased the migration and proliferation of synoviocytes but also resulted in profibrotic changes including Collagen production and *PLOD2* gene expression upregulation. Collagen production in synoviocytes was directly associated with secreted PGF2α levels in IFP derived conditioned medium. On the other hand, as the IFP is mainly composed of adipocytes, it results as a major source of various adipocyte-derived inflammatory mediators including lipids. Previous studies indicated that IFP-derived adipocytes, via secreted lipids, are able to modulate infiltrating macrophages and $CD4^+$ T cells into the OA synovium (Ioan-Facsinay et al., 2013; Klein-Wieringa et al., 2013). In adipocyte-derived conditioned medium obtained from IFP, Ioan-Facsinay et al. (2013) identified free fatty acids that enhance $CD4^+$ T cell proliferation and their capacity to produce IFN-γ. Additionally, free fatty acids secreted from IFP adipocytes can reduce the secretion of IL-12p40 cytokine by macrophages (Klein-Wieringa et al., 2013). According to previous studies (reviewed in Cooper and Khader, 2007), IL-12p40 is a chemoattractant molecule for macrophages, and which promotes inflammation and fibrosis. Furthermore, Mustonen et al. (2019) identified distinct fatty acid signature for IFP in OA and rheumatoid arthritis (RA) patients. Compared to RA, OA patients have higher total n-6, 20:4n-6 and 22:6n-3 polyunsaturated fatty acids (PUFA), and higher product/precursor ratios of n-3 PUFA. In general, n-6 PUFA such as 20:4n-6 (arachidonic acid) are precursors to pro-inflammatory mediators, whereas n-3 PUFA such as 22:6n-3 (docosahexaenoic acid) have anti-inflammatory/anti-catabolic effects (Brouwers et al., 2015). Overall, the major alterations in OA and RA joints compared to control healthy knees are an increase in monounsaturated fatty acids and a simultaneous decrease in n-6 PUFA, effects that should be further investigated in future studies (Mustonen et al., 2019).

Just as IFP influences synovium, Clements et al. (2009) demonstrated that extensive synovial proliferation and fibrosis led to marked loss of adipocytes within the IFP. Specifically, synovium secretion of pro-inflammatory cytokine IL-1β has been associated with catabolic effects in initiation and progression of OA. A previous study showed that exposure of IFP explants from OA patients to IL-1β *in vitro* result in secretion of large amounts of pro-inflammatory cytokines such as PTGS2, IL-1β, MCP-1, and IL-6. These effects can be partially ameliorated by a PPARα agonist (Clockaerts et al., 2012). Thus, recent literature has not only demonstrated extensive communication between both the IFP and synovium, but that this communication can accelerate development and progression of KOA, as elaborated below.

IFP IN THE PATHOGENESIS OF KNEE OA – POTENTIAL NEW TARGET FOR THERAPY

With the cellular composition of the IFP better elucidated and the occurrence of immune and inflammatory events within the IFP, its role in the pathophysiology of KOA is becoming the focus of multiple studies. For instance, Heilmeier et al. (2019) demonstrated that following ACL acute injury the IFP rapidly releases inflammatory cytokines that promote a sustained inflammatory response lasting for months. Consequently, various theories have emerged explaining the IFP's role in the regulation of local inflammatory cascades including adipocytes, and more recently resident macrophages as key targets (in the development of post-traumatic OA). We next explore the strengths and limitations of each prevailing theory.

IFP-Derived Adipocytes and Obesity Accelerate KOA Development

As previously discussed, adipocytes are capable of secreting certain molecular markers and products capable of initiating a local inflammatory response. Given that obesity represents a chronic inflammatory state, many studies have focused on the role of adipocytes as contributors for accelerated development of KOA (Balistreri et al., 2010; Bravo et al., 2019; Jiang et al., 2019). Consistent with this theory, the discovery of IL-1β and other pro-inflammatory cytokine production, together with matrix metalloprotease expression within KOA cartilage by adipocytes, suggests that the IFP may be intimately linked to KOA (Clockaerts et al., 2010; de Boer et al., 2012; Beekhuizen et al., 2013). Furthermore, leptin and adiponectin have been shown to be primarily secreted by IFP adipocytes into synovial fluid, with a key role influencing cartilage and synovial metabolism (Dumond et al., 2003; Toussirot et al., 2007). Therefore, the association of leptin to obesity and inflammation led to the belief that obesity itself plays a role in inducing IFP adipocyte inflammatory propagation and accelerated KOA progression (Ioan-Facsinay and Kloppenburg, 2013). Leptin has been shown to promote production of articular cartilage proteoglycans and collagen while stimulating insulin-like growth factor-1 and other growth factors that subsequently enhance chondrocyte proliferation (Bao et al., 2010, 2014). Lipid-mediated lipoxin A4, which can prevent cartilage degeneration in the knee, is also secreted by IFP adipocytes (Bastiaansen-Jenniskens et al., 2012; Gierman et al., 2013). Leptin facilitates the activation of immune cells, particularly M1 macrophages, via interferon release and nitric oxide production (Matarese et al., 2007). Moreover, recent literature suggests that obese patients with OA have either no difference in the number of M1 macrophages within the IFP, or may even have an increased number of M2 macrophages, compared to that of lean patients (de Jong et al., 2017). Lastly, even with M1 macrophages present within the IFP, the classic M1 macrophage mediated inflammation that usually occurs in abdominal adipose tissue as seen with obesity cannot be recapitulated, suggesting that IFP adipocytes are subject to distinct spatial-temporal metabolic regulation (Barboza et al., 2017).

An alternative mechanism by which obesity may affect the IFP during the progression of KOA is through altered joint mechanics. Ballegaard et al. (2014) have shown that obese patients with KOA demonstrated significantly increased inflammatory signaling within the IFP measured by contrast-enhanced perfusion variables on MRI. Cowan et al. (2015) also demonstrated that patients with patellofemoral OA have a greater

IFP volume on MRI compared to healthy knees. Because the IFP resides in a tight anatomical space, the authors suggested that increased IFP volume was an inducer of inflammation, leading to secretion of synovial inflammatory factors (Clements et al., 2009). Therefore, in this alternate hypothesis, adipocyte induced inflammation within the joint may be due to factors other than obesity (King et al., 2013). However, OA also occurs in non-weight bearing joints such as the hand, suggesting that the metabolic effects of obesity may play a greater role than altered joint mechanics (Losina et al., 2011; Yusuf, 2012; Bliddal et al., 2014).

Overall, though there is an established link between obesity and KOA, the explanation that the IFP propagates KOA development because of its primarily adipocyte-based composition remains controversial. Because the IFP has a distinct environment compared to abdominal adipose tissue, the role of this specific adipocyte population in KOA remains unclear and warrants continued investigation, as obesity related features seen in visceral adipose tissue are not present within the IFP of KOA patients (de Jong et al., 2017).

Role of IFP/Synovium Resident Macrophages

Adipocytes are not the only cellular component with potential to induce or enhance inflammation locally. The IFP and synovium are populated by macrophages, historically viewed as cells that maintain tissue homeostasis with crucial roles in early and late phases of response to injury, while more recently associated with various pathologies (Caspar-Bauguil et al., 2005; Mathis, 2013; Ginhoux and Jung, 2014). Macrophages have distinct origins resulting in significant heterogeneity, beyond the known M1 (classical pro-inflammatory) and M2 (alternative anti-inflammatory) polarization phenotypes (Ginhoux and Jung, 2014; Paul et al., 2015; Wu et al., 2020). A special population of tissue resident macrophages derive from embryonic precursors, exhibit self-renewal, and replenish after injury independently from circulating bone marrow-derived Ly6C^{High} monocytes (Ly6C^{High} is a murine marker with no current human ortholog identified) (Davies et al., 2011; Gentek et al., 2014; Ginhoux and Guilliams, 2016; Zhao et al., 2018). IFP and synovium show such resident populations with comparable immune cell profiles (Klein-Wieringa et al., 2016), also susceptible to polarize to M1 or M2 phenotypes depending on the status of the joint (Barboza et al., 2017; Sun et al., 2017; Tu et al., 2018; Wu et al., 2020).

Resident M1 pro-inflammatory macrophages are theorized to be an important driver of the host low grade chronic inflammatory state (Mathis, 2013; Kandahari et al., 2015). In fact, patients with KOA show a propensity for the M1 classical phenotype within the IFP/synovium complex, resulting in cytokine, interferon, and TNF-alpha secretion (Klein-Wieringa et al., 2011; Wu et al., 2020). Recent evidence suggests that activation of the mammalian target of rapamycin (Kuptniratsaikul et al., 2009) pathway also plays a role in M1 macrophage polarization and progression of KOA in animal models (Fernandes et al., 2020). Nevertheless, the existence of resident macrophages within the IFP exhibiting an M1 phenotype independent of the presence of local inflammation confirms their potential participation as initiators of KOA (Wu et al., 2020). Thus, the propagation of KOA is not reliant solely on immune cell extravasation, but rather on resident cells from within the IFP/synovium complex, though the precise turning point that leads to KOA still remains unknown.

Immune Infiltration to the IFP/Synovium

The aforementioned molecular markers that induce pro-inflammatory states do so in part by promoting extravasation of circulating immune cells into the IFP and synovium. The secretion of related prostaglandins, as well as IL-6 and IL-8 promote the extravasation of immune cells by attracting lymphocytes to the endothelium promoting their migration into the surrounding IFP and synovium (Schnoor et al., 2016). Substance P, a product of nociceptive nerve fibers that transmits pain signals while also modulates local inflammatory processes (*i.e.,* neurogenic inflammation), has also been shown to induce vasodilation of peripheral vessels, thus promoting the extravasation of immune cells from peripheral circulation into surrounding tissue (Clockaerts et al., 2010).

Apinun et al. (2016) described the presence of peripheral CD8 T cells, macrophages, B cells, and mast cells within the IFP of patients with OA undergoing TKA. According to the authors, the infiltration of these cells trended with disease severity (patients with severe radiographic KOA had more CD8 T cell infiltration than patients with mild KOA), thereby leading the authors to conclude that the infiltration of circulating immune cells to the IFP and synovium contribute to disease progression and severity. In addition, Klein-Wieringa et al. (2016) showed that peripheral CD4 T cells also infiltrate the IFP and synovium in a severely osteoarthritic population, and their presence correlated with pain scores ($R = 0.53$, $p < 0.01$, $N = 76$ patients). Thus, pro-inflammatory cells within the IFP and synovium not only promote localized inflammation with resident immune cells, but also promote extravasation of circulating ones potentiating the inflammatory process that are associated with poorer clinical and radiographic outcomes.

Clinical Correlation: Imaging to Assess IFP Changes During OA Progression

The IFP is best visualized on non-contrast magnetic resonance imaging (MRI) in the sagittal plane and intensity of signal alterations have recently been correlated with anterior knee pain and cartilage loss by Han et al. (OR 1.23, $p < 0.05$, $N = 374$), supporting the link between changes in IFP and KOA development (Hill et al., 2007; Roemer et al., 2009; Han et al., 2016). Though non-contrast enhanced MRI is the gold standard, contrast-enhanced MRI imaging has recently been employed to show correlations between histological synovial infiltrate and hyperplasia and KOA progression ($R = 0.63$, $p < 0.001$, $N = 30$) (Loeuille et al., 2011). Crema et al. (2013) have shown that peri-patellar synovial thickness on non-contrast-enhanced MRI images could be the culprit for KOA related pain and not the changes in signal alterations within the IFP itself.

Interestingly, the size of the IFP may play an important role in KOA risk and symptom development and intensity. Pan et al. (2015) demonstrated that decreased IFP volume in older women compared to men was significantly associated with increased total knee pain, pain at rest and during movement, and cartilage damage. However, the authors also found that total IFP maximal area appears to have a protective role for knee symptoms in older adult females, but not men. IFP signal intensity was later linked to size of IFP by Han et al. (2016), which provides support for continued use of non-contrast enhanced MRI as the gold standard. Recently, Fontanella et al. (2019) reported changes in the morphometry (i.e., reduced volume, depth, and femoral and tibial arc lengths) and increase of the MRI hypointense signal in the IFP from patients with moderate and end-stage KOA compared to healthy controls. Despite contrasting results from various groups, the description of morphological changes in the IFP by MRI warrants continued investigation into how imaging may play a future in predicting KOA risk or progression.

IFP/SYNOVIUM AS A SOURCE OF MSC FOR CELL THERAPY

IFP-MSC

In 1996 a pioneering study by Maekawa et al. (1996) firstly described a type of fibroblastic cells possessing 'stem cell-like' characteristics in synovial tissue near the IFP. Those cells reside mostly in the perivascular space surrounding vessels of small caliber and involved in the fibronectin and laminin production. Recent studies have isolated and phenotypically characterized IFP-MSC positive for CD9, CD10, CD13, CD29, CD44, CD49e, CD59, CD73, CD90, CD105, CD106, CD146, CD166, NG2, and CXCR4 markers, while negative for CD34, CD56, CD200, CD271, 3G5, LepR and STRO-1 markers (Wickham et al., 2003; Khan et al., 2008; Garcia et al., 2016a; Hindle et al., 2017; Kouroupis et al., 2019a). IFP-MSC characteristically have low or no HLA-DR expression, yet a total absent expression of co-stimulatory molecules CD40, CD80, and CD86 (Garcia et al., 2016a; Kouroupis et al., 2020). In a recent study, Hindle et al. identified two distinct IFP-MSC subpopulations within the IFP, characterized as pericytes ($CD31^-CD45^-CD34^-CD146^+$) and adventitial cells ($CD31^-CD45^-CD34^+CD146^-$), representing 3.8 and 21.2% of the IFP stromal vascular fraction, respectively (Hindle et al., 2017).

In general, IFP-MSC have comparable proliferative potential to other MSC types (Dragoo et al., 2003; Jurgens et al., 2009). In comparative studies, IFP-MSC were reported to possess similar growth kinetics to bone marrow-derived MSC (BM-MSC) (English et al., 2007) and higher proliferation to donor-matched synovial fluid-MSC (Garcia et al., 2016a). However, in order to generate clinically relevant cell numbers, IFP-MSC growth rate can be accelerated by various *in vitro* culturing conditions such as human platelet lysate (hPL) or chemically-reinforced (Ch-R) media expansion, serum and growth factor (TGF-β and FGF-2) stimulation and hypoxia exposure (Marsano et al., 2007; Khan et al., 2008; Buckley and Kelly, 2012; Liu et al., 2012; O'HEireamhoin et al., 2013). Importantly, our group recently showed that hPL and Ch-R formulations can effectively replace FBS to expand IFP-MSC, enhancing phenotypic and functional attributes (Kouroupis et al., 2020).

IFP-MSC multipotentiality toward chondrogenic, osteogenic, and adipogenic lineages has been demonstrated by previous studies (reviewed in Sun et al., 2018). However, there is evidence showing that MSC differentiation capacity is strongly related to the tissue of origin. Therefore, due to the intra-articular localization of IFP tissue, and their anatomical proximity to articular cartilage, it is not surprising that IFP-MSCs exhibit strong chondrogenic differentiation capacity both *in vitro* and *in vivo* (Dragoo et al., 2003; Khan et al., 2008; Lee et al., 2008; Jurgens et al., 2009; Buckley et al., 2010; Almeida et al., 2014, 2015, 2016; Liu et al., 2014; Ye et al., 2014). Specifically, *in vitro* IFP-MSC show stronger chondrogenic differentiation capacity than adipose- derived-, BM-, and UC-MSC (Ding et al., 2015). Others however report that they possess at least comparable chondrogenic capacity to BM-MSC (English et al., 2007) but inferior to native chondrocytes and perivascular IFP-MSC (Marsano et al., 2007; Vinardell et al., 2011; Garcia et al., 2016b; Hindle et al., 2017). On this basis, studies have shown that heterogenous IFP-MSC selection for specific subpopulations may result in further enhanced chondrogenic differentiation capacity. Moreover, perivascular IFP-MSC ($CD31^-CD45^-CD34^-CD146^+$) generate significantly more extracellular matrix than heterogenous "crude" IFP-MSC cultures (Hindle et al., 2017). Also, others reported the positive correlation of CD49c expression of donor-matched chondrocytes, BM-MSC, FP-MSC, and synovial fluid MSC with their chondrogenic capacities *in vitro* ($R = 0.2$, $p < 0.018$, $N = 5$ samples) (Garcia et al., 2016b). In *in vivo* settings, freshly isolated uncultured $CD44^+$ IFP-MSC seeded into a TGF-β3 ECM-derived scaffold and subcutaneously implanted in nude mice, are capable of producing a cartilage-like tissue rich of sGAG and Collagen type II (Almeida et al., 2015). Therefore, the selection of specific IFP-MSC subpopulations may result in improved *in vivo* chondrogenesis.

Given their high proliferation rate and superior chondrogenic differentiation capacity, IFP-MSC may be considered a suitable candidate cell to engineer cartilaginous constructs to resurface focal defects or even an entire OA joint (Liu et al., 2014; Ye et al., 2014; Prabhakar et al., 2016). In that regard, Liu et al. (2014) showed that IFP-MSC obtained from both healthy and OA individuals and cultured on PLLA fiber membranes for 6 weeks can generate robust, flexible cartilage-like grafts of clinically relevant dimensions (≥2 cm in diameter). Of note, the authors did note that donor age variability may affect the robustness of the cultured IFP-MSCs, supporting the idea that the outcome of future IFP-MSC treatments may be substantially different in certain patient populations.

However, the main limitation of MSC-based cartilage constructs is that they progress in differentiation reaching an ultimate hypertrophic phenotype and finally undergoing endochondral ossification *in vivo* (Farrell et al., 2009, 2011; Scotti et al., 2013; Correa et al., 2015; Feng et al., 2018). To overcome this limitation, co-culture of IFP-MSC with articular chondrocytes in hybrid structures result in a phenotypically

stable layer of articular cartilage with reduced mineralization upon implantation in nude mice for 8 weeks (Mesallati et al., 2015). The same group demonstrated that self-assembled IFP-MSC on top of articular cartilage agarose gels result in higher accumulation of sGAG and therefore strongly enhance the development of articular cartilage constructs (Mesallati et al., 2017). Although, articular cartilage tissue engineering is a promising approach, a significant barrier is the generation of constructs with clinically relevant dimensions and in a time/cost efficient manner ready-to-use for *in vivo* implantation, especially for large compromised surfaces such as in OA. In more simplified approaches, IFP-MSC are directly injected intra-articularly solely or embedded in hydrogel-based delivery systems with and without growth factors. Toghraie et al. (2011) showed that a single dose of intra-articularly injected IFP-MSC result in decreased cartilage degeneration, osteophyte formation, and subchondral sclerosis 20 weeks later in a rabbit OA model. Recently, Muttigi et al. (2018) directly injected IFP-MSC embedded in matrillin-3 (an essential ECM component of cartilage) and 2% hyaluronic acid in an osteochondral defect rat model, with the reasoning that Matrilin-3 alone enhances Collagen II and aggrecan expression in chondrocytes while downregulating matrix degrading enzymes such as matrix metalloproteinase-13 (MMP-13). According to the authors, Matrillin-3, when is co-delivered with IFP-MSC, indeed resulted in greatly enhanced Collagen type II and aggrecan productions, whereas the regenerated defect site possesses similarities with native cartilage (thickness, chondrocyte clustering, and hyaline-like morphology). Overall, IFP-MSC due to their advantageous intra-articular anatomical localization and ease for harvesting along with their enhanced chondrogenic capacity may be an attractive approach for addressing articular cartilage degeneration in OA.

Our group recently reported that intra-articularly injected CD10-rich IFP-MSC reverted induced synovitis and IFP fibrosis in rats which are seen in early OA (Kouroupis et al., 2020). Interestingly, the degree of *in vivo* efficacy is associated with the degree of expression of CD10 and degradation of Substance P, a local mediator of transmitting pain signals and regulator of neurogenic inflammation.

Synovium-Derived MSC

Located within the synovial intima and sub-intima lie distinct MSC populations similar to IFP-MSC, with an origin still debated (Li et al., 2019; Sivasubramaniyan et al., 2019). Though not populous within the tissue, these cells maintain high proliferative capacity and can differentiate into osteoblasts, adipocytes, and chondrocytes *in vitro* (Ferro et al., 2019). The origin of synovium-derived MSC (sMSC) in the synovial lining is still not fully defined, with groups supporting the notion of MSC infiltrating from resident vasculature or even from the neighboring bone marrow. However, two recently reports strongly support the hypothesis of the embryonic origin of synovium at the joint interzone, by showing that single or double positive Prg4-lineage and Gdf5-lineage cells, and associated sMSC as contributors to tissue homeostasis and repair in adult life (Decker et al., 2017; Roelofs et al., 2017).

Besides a similar overall immunophenotype of sMSC compared with other MSC (De Bari et al., 2001; Sakaguchi et al., 2005; Hermida-Gomez et al., 2011), CD271, a highly expressed markers in freshly isolated BM-SMC, is absent in healthy sMSC (Karystinou et al., 2009), yet expressed in cells isolated from OA patients (Hermida-Gomez et al., 2011). A topographic analysis of synovium and a full phenotypic description of sMSC are presented in our previous review (Kouroupis et al., 2019b). According to reports, sMSC show a greater proliferation rate and stronger chondrogenic capacity than BM- and adipose-derived MSC whereas they exhibit a reduced hypertrophic differentiation potential (Kubosch et al., 2018).

Previous studies have demonstrated that sMSC and IFP-MSC show comparable chondrogenic differentiation capacity (Mochizuki et al., 2006). In a comparative study of three different MSC types, Mochizuki et al. indicated that sMSC and IFP-MSC have similar chondrogenic capacity between older and younger donors but higher compared to donor-matched subcutaneous fat-derived MSC (Mochizuki et al., 2006). However, Vinardell et al. (2012) reported that when sMSC and IFP-MSC are embedded in agarose hydrogel constructs and chondrogenic induced for 49 days *in vitro*, sMSC accumulate higher levels of sGAG and Collagen than IFP-MSC. Similarly, to IFP-MSC, sMSC expansion in hPL medium result in increased proliferation rate but lower chondrogenic capacity compared to sMSC grown in the presence of FBS (Nimura et al., 2008).

In preclinical settings, Koizumi et al. (2016) isolated sMSC from both OA and RA patients and assessed their cartilage repair capacity using a scaffold-free tissue engineering approach. Interestingly, 8 weeks post-implantation both OA or RA sMSC-treated groups showed hyaline cartilage-like repair and in general higher histological scores compared to the untreated rats. In addition, various studies using animal sMSC (rabbit-, murine-, equine-, porcine-harvested synovium) showed that sMSC groups are superior to control groups in treating full thickness chondral lesions (To et al., 2019). Therefore, sMSC show good reparative capacity of chondral lesions and no adverse effects after implantation *in vivo*.

MSC-Induced Immunomodulation: Focus on Macrophage Polarization

During early phases of OA, both IFP and synovium become infiltrated by immune cells, including T cells, B cells, monocytes/macrophages, and mast cells (Pelletier et al., 2001; Sokolove and Lepus, 2013; Ioan-Facsinay and Kloppenburg, 2017; Kalaitzoglou et al., 2017). These infiltrates complement the local resident cells, especially macrophages, which as seen in **Figure 3** polarize into a pro-inflammatory classical M1 phenotype (discussed above in section "Role of IFP/Synovium Resident Macrophages"). MSC exerts immunomodulatory effects, simultaneously influencing multiple immune cells through different mechanisms including cell-cell contact, soluble factors, and released extracellular vesicles (*e.g.*, exosomes). The specific effects of MSC on T cells, B cells and other immune cells have been reviewed extensively elsewhere (Djouad et al., 2005; Hagmann et al., 2013). Herein, we emphasize on the current

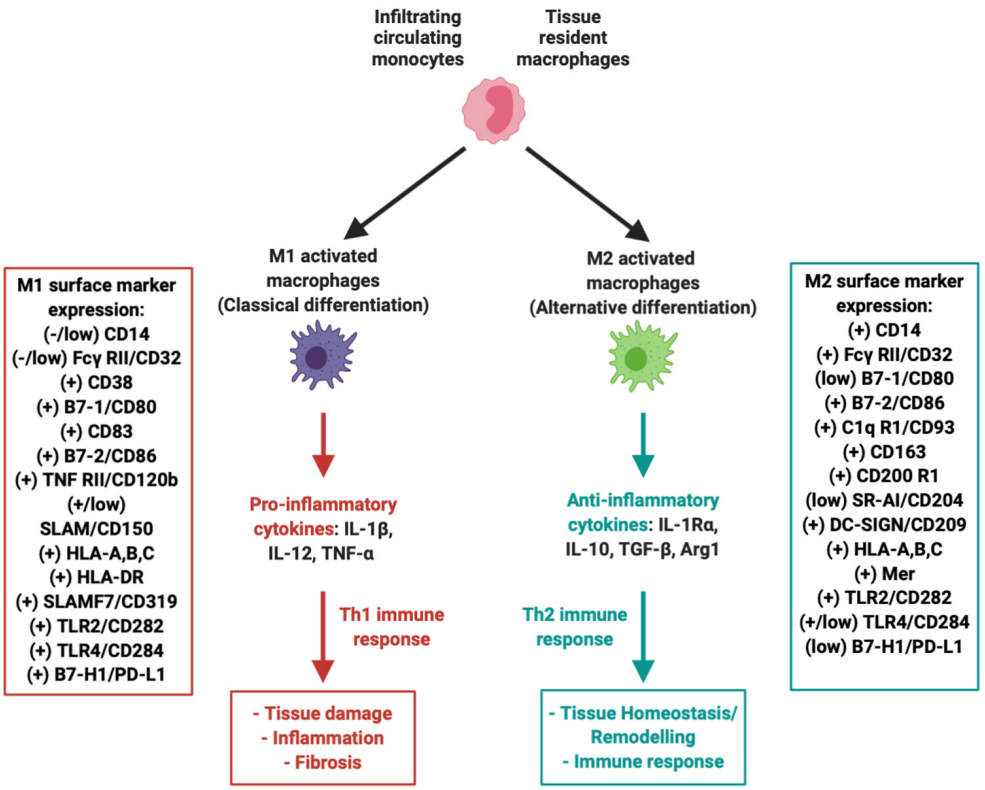

FIGURE 3 | Macrophages within the IFP can polarize into M1 (pro-inflammatory) or M2 (anti-inflammatory, tissue repair) variants. Both variants are associated with a multitude of unique surface markers with varying levels of expression that allow for proper identification.

knowledge regarding the interactions with macrophages given their pivotal role in the initiation and progression of the disease as source of inflammatory and degradative mediators.

Numerous studies have explored macrophages as potential therapeutic targets, including their pharmacological depletion from synovium and IFP and manipulation of their phenotype [reviewed in Fernandes et al. (2020) and Wu et al. (2020)]. Initial evidence suggests that polarization of macrophages back to an alternative anti-inflammatory M2 phenotype can be induced. M2 macrophages represent the other extreme in terms of functionality, as they play a major role in local tissue repair by secreting low levels of anti-inflammatory cytokines such as IL-10 at a much more accelerated rate compared to unpolarized "naïve" resident macrophages (**Figure 3**) (Zeyda et al., 2007; Fernandes et al., 2020). In fact, it has been proposed that MSC can indeed promote M2 macrophage polarization *in vitro* (Harrell et al., 2019). Furthermore, our group recently reported the switch of IFP macrophages from an M1 to an M2 phenotype *in vivo*, after a single intra-articular injection of a subset of BM-MSC ($CD146^{+}$) in rats with induced synovitis and IFP fibrosis (Bowles et al., 2020).

The effects of IFP-MSC in macrophage polarization are far less defined. Nevertheless, it has been described that Substance P within IFP actively participates in immune responses and inflammatory cascades (*i.e.,* neurogenic inflammation), enhancing the migration of monocytes to sites of inflammation (Mashaghi et al., 2016; Spitsin et al., 2017; Suvas, 2017). Relatedly, our group recently reported that upon exposure to a pro-inflammatory environment (Kouroupis et al., 2019a) and when manufactured under regulatory-compliant conditions (Kouroupis et al., 2020), IFP-MSC become enriched for CD10/neprilysin, an ectopeptidase that efficiently degrades Substance P both *in vitro* and *in vivo*. The resulting CD10-rich IFP-MSC exhibit an innate ability to selectively migrate to areas of active synovitis, reverse inflammation and fibrosis of synovium and IFP. Interestingly, these effects are directly related with the level of positivity for CD10 (Kouroupis et al., 2020). Furthermore, Substance P has been reported to induce the differentiation of pro-inflammatory macrophages into a special phagocytic M2 phenotype ($M2^{SP}$), different from previously reported M2a and M2c subphenotypes (Lim et al., 2017).

Efforts to Translate Pre-clinical Findings Into Clinical Protocols

MSC-based therapy to treat OA has received attention based on promising pre-clinical reports. Various cell sources have been successfully used in early-phase clinical trials, including bone marrow (Orozco et al., 2014; Vega et al., 2015; Soler et al., 2016), umbilical cord (Matas et al., 2019), and adipose-derived stromal vascular fraction (Garza et al., 2020). A recent systematic review summarizing available studies testing intra-articular MSC

therapy for OA and chondral defects concluded that the therapy is safe with clinical and in some cases imaging improvement (McIntyre et al., 2018). Synovial and IFP-derived MSC are starting to be explored clinically, yet only initial data is available.

In a pioneering case control study, a mean of 1.89 million (range, 1.2–2.3 $\times$ 10^6) IFP-MSC with platelet-rich plasma (PRP) were intra-articularly injected in OA patients after arthroscopic debridement, and controlled against debridement + PRP alone (Koh and Choi, 2012). Patients were followed for up to 12–18 months, reporting no adverse effects and a significant improvement in Patient Reported Outcome Measurements (PROMs) including Lysholm score, visual analog scale (VAS), and Tegner activity were noted in the study group compared with control cohorts. However, Koh et al. (2013) did note some limitations, namely that the control group was significantly different in terms of baseline radiographic and chondral lesion severity, as well as the small sample size with a focus on severe KOA patients.

The same team then in a 24–26-month follow-up study demonstrated that the significant decrease of the Western Ontario and McMaster Universities Osteoarthritis Index (WOMAC) is directly related to the amount of injected IFP-MSC (Koh et al., 2013). The authors also found that study patients demonstrated significantly improved cartilage whole-organ MRI scores that correlated strongly with decreased pain and improved function ($R = -0.588$ and -0.0536 respectively, $p < 0.05$, $N = 18$). Collectively, these initial results indicate the positive effect of intra-articularly injected IFP-MSC in reducing pain and improving knee function in OA patients, when compared with arthroscopic debridement and PRP alone. However, in addition to the various limitations acknowledged by the authors, the study population only included older patients with severe KOA, thus warranting further clinical investigation to determine the efficacy of the procedure as well as it's applicability to a broader clinical population.

Similarly, sMSC yielded encouraging results in treating symptomatic chondral lesions in patients. Sekiya et al. (2015) expanded sMSC with autologous human serum and intra-articularly injected them to treat femoral condyle chondral lesions in 10 patients. For an average follow-up of 52 months, histologic analyses indicated hyaline and fibrous cartilage formation paralleled by improved Lysholm scores (Sekiya et al., 2015). In another study, autologous sMSC scaffold-free constructs were implanted in five patients to treat 1.5–3.0 cm^2 chondral lesions (Shimomura et al., 2018). Forty-eight weeks post-implantation all patients achieved defect filling with tissue integration whereas histological analysis indicated strong cartilaginous tissue formation in all patients, with few spindle-shaped fibroblast-like cells localized only at the new-formed cartilage superficial zone. No adverse effects and significantly clinical improvements were reported at a 24-month follow-up.

These preliminary clinical studies indicated for both IFP-MSC and sMSC the overall significant improvement in cartilage repair without any complications for the patients treated. Nevertheless, the small number of patients involved and the potential confounding effect of parallel products (e.g., PRP) requires the design of prospective randomized, controlled trials to establish efficacy beyond the established safety.

FUTURE PERSPECTIVES

The involvement of immune and inflammatory events within the synovium and IFP during early KOA has led to changes in our thinking of the disease and potential treatment approaches. Furthermore, the identification of resident and infiltrating macrophages as key modulators of those events presents a novel therapeutic target in the treatment of KOA. The ability of locally delivered IFP-MSCs to regulate synovial/IFP inflammation and fibrosis then becomes a promising therapeutic alternative to mitigate disease progression of the disease. Nevertheless, more information is required to solidly connect MSC local effects, macrophage phenotypic polarization and inflammation/fibrosis control with a durable effect limiting KOA progression.

Moreover, one critical aspect to understanding the impact of macrophages in the IFP is to dissect the molecular, cellular, and genetic identities of the heterogeneous tissue. Critically, over the past decade, numerous technologies allowing single-cell RNA sequencing (scRNA-seq) have emerged to provide unprecedented ability to examine gene expression profiles at the single cell level (Svensson et al., 2018). In general, these techniques allow the deconvolution of a heterogeneous tissue into specific cell types and an examination of their abundance. Furthermore, subtle differences between cells of similar lineages can be distinguished on the basis of just a few gene expression changes. Finally, there is the ability to compare cellular profiles and gene expression across samples, conditions, or groups of individuals. While efforts are currently underway to dissect the cellular complexity of tissues throughout the body including articular cartilage during OA progression (Regev et al., 2017; Ji et al., 2019), the IFP is noticeably absent from these efforts. To our knowledge, there is no existing high throughput single cell expression profile of the IFP, either in its nascent state or following injury or in chronic disease. Given its role in the immune responses to these conditions, this remains a topic of importance moving forward in characterizing its importance.

Mechanistically, Substance P targeting and degradation by CD10-rich MSC could become a mechanism to disrupt the sustained chronic inflammation within the IFP and the transmission of nociception signals from the knee to the central nervous system. As such, the reduction of Substance P^+ nerve fibers within IFP may possibly be related to control of KOA's most prevalent clinical presentation, joint pain.

Finally, an emerging approach results from the description of extracellular vesicles (*e.g.,* exosomes) released by MSC, and their involvement in the therapeutic activities of the cells. For instance, our previous reports indicate comparable effects between cells and their supernatant in terms of their ability to degrade Substance P. These observations may support the idea of a "cell-free" product that may recapitulate the therapeutic effects of their parental cells, with manufacturing advantages as previously described (Pachler et al., 2017; Rohde et al., 2019;

Witwer et al., 2019). In fact, the potential use of exosome-based cell-free products has already sparked multiple pre-clinical studies assessing potential clinical translation of cell-free products with encouraging results (Kordelas et al., 2014; Mendicino et al., 2014; Karnieli et al., 2017; Hu et al., 2019; Cai et al., 2020; Jiang et al., 2020; Meng and Qiu, 2020).

CONCLUSION

The knowledge accrued over the last decade regarding the IFP has led to important discoveries that elucidate its role beyond that of a vascular tissue with a biomechanical role in the anterior compartment of the knee. The proposition of the IFP and the synovium functioning as a single unit and the now recognized tight molecular crosstalk between both structures has been shown to promote resident immune cells, immune cell infiltration, and the subsequent production of articular cartilage degradative molecules associated with the propagation of various knee pathologies such as KOA. On the other hand, the presence of IFP-MSC and sMSC suggest that the IFP and synovium act as a reservoir of therapeutic cellular products engaged with repair after exposure to inflammation and subsequent injury. These MSC have also been shown to modulate macrophage phenotypic polarization in favoring immunomodulatory conditions.

The ability of local MSC to regulate synovial/IFP inflammation and fibrosis poses a promising therapeutic target to mitigate disease progression. Therefore, the IFP presents an important target for limiting joint disease progression. More information is required to better understand the connection between the local MSC population and macrophage phenotypic polarization as it relates to controlling the propagation of inflammation/fibrosis and subsequent progression of KOA.

AUTHOR CONTRIBUTIONS

All authors listed have made a substantial, direct and intellectual contribution to the work, and approved it for publication.

FUNDING

The authors are in gratitude with the Soffer Family Foundation and the Diabetes Research Institute Foundation for their generous funding support.

REFERENCES

Almeida, H. V., Cunniffe, G. M., Vinardell, T., Buckley, C. T., O'Brien, F. J., and Kelly, D. J. (2015). Coupling freshly isolated CD44(+) infrapatellar fat pad-derived stromal cells with a TGF-beta3 eluting cartilage ECM-derived scaffold as a single-stage strategy for promoting chondrogenesis. *Adv. Healthc. Mater.* 4, 1043–1053. doi: 10.1002/adhm.201400687

Almeida, H. V., Eswaramoorthy, R., Cunniffe, G. M., Buckley, C. T., O'Brien, F. J., and Kelly, D. (2016). Fibrin hydrogels functionalized with cartilage extracellular matrix and incorporating freshly isolated stromal cells as an injectable for cartilage regeneration. *Acta Biomater.* 36, 55–62. doi: 10.1016/j.actbio.2016.03.008

Almeida, H. V., Liu, Y., Cunniffe, G. M., Mulhall, K. J., Matsiko, A., Buckley, C. T., et al. (2014). Controlled release of transforming growth factor-beta3 from cartilage-extra-cellular-matrix-derived scaffolds to promote chondrogenesis of human-joint-tissue-derived stem cells. *Acta Biomater.* 10, 4400–4409. doi: 10.1016/j.actbio.2014.05.030

Apinun, J., Sengprasert, P., Yuktanandana, P., Ngarmukos, S., Tanavalee, A., and Reantragoon, R. (2016). Immune mediators in osteoarthritis: infrapatellar fat pad-infiltrating CD8+ T Cells are increased in osteoarthritic patients with higher clinical radiographic grading. *Int. J. Rheumatol.* 2016:9525724.

Attur, M., Samuels, J., Krasnokutsky, S., and Abramson, S. B. (2010). Targeting the synovial tissue for treating osteoarthritis (OA): where is the evidence? *Best Pract. Res. Clin. Rheumatol.* 24, 71–79. doi: 10.1016/j.berh.2009.08.011

Balistreri, C. R., Caruso, C., and Candore, G. (2010). The role of adipose tissue and adipokines in obesity-related inflammatory diseases. *Mediat. Inflamm.* 2010:802078.

Ballegaard, C., Riis, R. G., Bliddal, H., Christensen, R., Henriksen, M., Bartels, E. M., et al. (2014). Knee pain and inflammation in the infrapatellar fat pad estimated by conventional and dynamic contrast-enhanced magnetic resonance imaging in obese patients with osteoarthritis: a cross-sectional study. *Osteoarthr. Cartilage* 22, 933–940. doi: 10.1016/j.joca.2014.04.018

Bao, J. P., Chen, W. P., Feng, J., Hu, P. F., Shi, Z. L., and Wu, L. D. (2010). Leptin plays a catabolic role on articular cartilage. *Mol. Biol. Rep.* 37, 3265–3272. doi: 10.1007/s11033-009-9911-x

Bao, J. P., Jiang, L. F., Chen, W. P., Hu, P. F., and Wu, L. D. (2014). Expression of vaspin in the joint and the levels in the serum and synovial fluid of patients with osteoarthritis. *Int. J. Clin. Exp. Med.* 7, 3447–3453.

Barboza, E., Hudson, J., Chang, W. P., Kovats, S., Towner, R. A., Silasi-Mansat, R., et al. (2017). Profibrotic infrapatellar fat pad remodeling without m1 macrophage polarization precedes knee osteoarthritis in mice with diet-induced obesity. *Arthritis Rheumatol.* 69, 1221–1232. doi: 10.1002/art.40056

Bartok, B., and Firestein, G. S. (2010). Fibroblast-like synoviocytes: key effector cells in rheumatoid arthritis. *Immunol. Rev.* 233, 233–255. doi: 10.1111/j.0105-2896.2009.00859.x

Bastiaansen-Jenniskens, Y. M., Clockaerts, S., Feijt, C., Zuurmond, A. M., Stojanovic-Susulic, V., Bridts, C., et al. (2012). Infrapatellar fat pad of patients with end-stage osteoarthritis inhibits catabolic mediators in cartilage. *Ann. Rheum. Dis.* 71, 288–294. doi: 10.1136/ard.2011.153858

Bastiaansen-Jenniskens, Y. M., Wei, W., Feijt, C., Waarsing, J. H., Verhaar, J. A., Zuurmond, A. M., et al. (2013). Stimulation of fibrotic processes by the infrapatellar fat pad in cultured synoviocytes from patients with osteoarthritis: a possible role for prostaglandin f2alpha. *Arthritis Rheum.* 65, 2070–2080. doi: 10.1002/art.37996

Beekhuizen, M., Gierman, L. M., van Spil, W. E., Van Osch, G. J., Huizinga, T. W., Saris, D. B., et al. (2013). An explorative study comparing levels of soluble mediators in control and osteoarthritic synovial fluid. *Osteoarthr. Cartilage* 21, 918–922. doi: 10.1016/j.joca.2013.04.002

Belluzzi, E., Stocco, E., Pozzuoli, A., Granzotto, M., Porzionato, A., Vettor, R., et al. (2019). Contribution of infrapatellar fat pad and synovial membrane to knee osteoarthritis pain. *Biomed. Res. Int.* 2019:6390182.

Benito, M. J., Veale, D. J., FitzGerald, O., van den Berg, W. B., and Bresnihan, B. (2005). Synovial tissue inflammation in early and late osteoarthritis. *Ann. Rheum. Dis.* 64, 1263–1267. doi: 10.1136/ard.2004.025270

Bliddal, H., Leeds, A. R., and Christensen, R. (2014). Osteoarthritis, obesity and weight loss: evidence, hypotheses and horizons - a scoping review. *Obes. Rev.* 15, 578–586. doi: 10.1111/obr.12173

Bohnsack, M., Wilharm, A., Hurschler, C., Ruhmann, O., Stukenborg-Colsman, C., and Wirth, C. J. (2004). Biomechanical and kinematic influences of a total infrapatellar fat pad resection on the knee. *Am. J. Sports Med.* 32, 1873–1880. doi: 10.1177/0363546504263946

Bombardieri, M., Kam, N. W., Brentano, F., Choi, K., Filer, A., Kyburz, D., et al. (2011). A BAFF/APRIL-dependent TLR3-stimulated pathway enhances the capacity of rheumatoid synovial fibroblasts to induce AID expression and Ig class-switching in B cells. *Ann. Rheum. Dis.* 70, 1857–1865. doi: 10.1136/ard.2011.150219

Bondeson, J., Blom, A. B., Wainwright, S., Hughes, C., Caterson, B., and van den Berg, W. B. (2010). The role of synovial macrophages and macrophage-produced mediators in driving inflammatory and destructive responses in osteoarthritis. *Arthritis Rheum.* 62, 647–657. doi: 10.1002/art.27290

Bowles, A. C., Willman, M. A., Perucca Orfei, C., Agarwal, A., and Correa, D. (2020). Signature quality attributes of CD146+ mesenchymal stem/stromal cells correlate to high therapeutic and secretory potency. *Stem Cells* [Epub ahead of print]. doi: 10.1002/stem.3196

Bravo, B., Guisasola, M. C., Vaquero, J., Tirado, I., Gortazar, A. R., and Forriol, F. (2019). Gene expression, protein profiling, and chemotactic activity of infrapatellar fat pad mesenchymal stem cells in pathologies of the knee joint. *J. Cell Physiol.* 234, 18917–18927. doi: 10.1002/jcp.28532

Brouwers, H., von Hegedus, J., Toes, R., Kloppenburg, M., and Ioan-Facsinay, A. (2015). Lipid mediators of inflammation in rheumatoid arthritis and osteoarthritis. *Best Pract. Res. Clin. Rheumatol.* 29, 741–755. doi: 10.1016/j.berh.2016.02.003

Brumovsky, P. R. (2016). Dorsal root ganglion neurons and tyrosine hydroxylase–an intriguing association with implications for sensation and pain. *Pain* 157, 314–320. doi: 10.1097/j.pain.0000000000000381

Buckley, C. T., and Kelly, D. J. (2012). Expansion in the presence of FGF-2 enhances the functional development of cartilaginous tissues engineered using infrapatellar fat pad derived MSCs. *J. Mech. Behav. Biomed. Mater.* 11, 102–111. doi: 10.1016/j.jmbbm.2011.09.004

Buckley, C. T., Vinardell, T., Thorpe, S. D., Haugh, M. G., Jones, E., McGonagle, D., et al. (2010). Functional properties of cartilaginous tissues engineered from infrapatellar fat pad-derived mesenchymal stem cells. *J. Biomech.* 43, 920–926. doi: 10.1016/j.jbiomech.2009.11.005

Cai, J., Wu, J., Wang, J., Li, Y., Hu, X., Luo, S., et al. (2020). Extracellular vesicles derived from different sources of mesenchymal stem cells: therapeutic effects and translational potential. *Cell Biosci.* 10:69.

Caplan, A. I., and Correa, D. (2011). The MSC: an injury drugstore. *Cell Stem Cell.* 9, 11–15. doi: 10.1016/j.stem.2011.06.008

Caspar-Bauguil, S., Cousin, B., Galinier, A., Segafredo, C., Nibbelink, M., Andre, M., et al. (2005). Adipose tissues as an ancestral immune organ: site-specific change in obesity. *FEBS Lett.* 579, 3487–3492. doi: 10.1016/j.febslet.2005.05.031

Clements, K. M., Ball, A. D., Jones, H. B., Brinckmann, S., Read, S. J., and Murray, F. (2009). Cellular and histopathological changes in the infrapatellar fat pad in the monoiodoacetate model of osteoarthritis pain. *Osteoarthr. Cartilage* 17, 805–812. doi: 10.1016/j.joca.2008.11.002

Clockaerts, S., Bastiaansen-Jenniskens, Y. M., Feijt, C., De Clerck, L., Verhaar, J. A., Zuurmond, A. M., et al. (2012). Cytokine production by infrapatellar fat pad can be stimulated by interleukin 1beta and inhibited by peroxisome proliferator activated receptor alpha agonist. *Ann. Rheum. Dis.* 71, 1012–1018. doi: 10.1136/annrheumdis-2011-200688

Clockaerts, S., Bastiaansen-Jenniskens, Y. M., Runhaar, J., Van Osch, G. J., Van Offel, J. F., Verhaar, J. A., et al. (2010). The infrapatellar fat pad should be considered as an active osteoarthritic joint tissue: a narrative review. *Osteoarthr. Cartilage* 18, 876–882. doi: 10.1016/j.joca.2010.03.014

Coelho, M., Oliveira, T., and Fernandes, R. (2013). Biochemistry of adipose tissue: an endocrine organ. *Arch. Med. Sci.* 9, 191–200. doi: 10.5114/aoms.2013.33181

Cooper, A. M., and Khader, S. A. (2007). IL-12p40: an inherently agonistic cytokine. *Trends Immunol.* 28, 33–38. doi: 10.1016/j.it.2006.11.002

Correa, D., Somoza, R. A., Lin, P., Greenberg, S., Rom, E., Duesler, L., et al. (2015). Sequential exposure to fibroblast growth factors (FGF) 2, 9 and 18 enhances hMSC chondrogenic differentiation. *Osteoarthr. Cartilage* 23, 443–453. doi: 10.1016/j.joca.2014.11.013

Cowan, S. M., Hart, H. F., Warden, S. J., and Crossley, K. M. (2015). Infrapatellar fat pad volume is greater in individuals with patellofemoral joint osteoarthritis and associated with pain. *Rheumatol. Int.* 35, 1439–1442. doi: 10.1007/s00296-015-3250-0

Crema, M. D., Felson, D. T., Roemer, F. W., Niu, J., Marra, M. D., Zhang, Y., et al. (2013). Peripatellar synovitis: comparison between non-contrast-enhanced and contrast-enhanced MRI and association with pain. The MOST study. *Osteoarthr. Cartilage* 21, 413–418. doi: 10.1016/j.joca.2012.12.006

Davies, L. C., Rosas, M., Smith, P. J., Fraser, D. J., Jones, S. A., and Taylor, P. R. (2011). A quantifiable proliferative burst of tissue macrophages restores homeostatic macrophage populations after acute inflammation. *Eur. J. Immunol.* 41, 2155–2164. doi: 10.1002/eji.201141817

De Bari, C., Dell'Accio, F., Tylzanowski, P., and Luyten, F. P. (2001). Multipotent mesenchymal stem cells from adult human synovial membrane. *Arthritis Rheum.* 44, 1928–1942. doi: 10.1002/1529-0131(200108)44:8<1928::aid-art331>3.0.co;2-p

de Boer, T. N., van Spil, W. E., Huisman, A. M., Polak, A. A., Bijlsma, J. W., Lafeber, F. P., et al. (2012). Serum adipokines in osteoarthritis; comparison with controls and relationship with local parameters of synovial inflammation and cartilage damage. *Osteoarthr. Cartilage* 20, 846–853. doi: 10.1016/j.joca.2012.05.002

de Jong, A. J., Klein-Wieringa, I. R., Andersen, S. N., Kwekkeboom, J. C., Herb-van Toorn, L., de Lange-Brokaar, B. J. E., et al. (2017). Lack of high BMI-related features in adipocytes and inflammatory cells in the infrapatellar fat pad (IFP). *Arthritis Res. Ther.* 19, 186.

de Lange-Brokaar, B. J., Ioan-Facsinay, A., van Osch, G. J., Zuurmond, A. M., Schoones, J., Toes, R. E., et al. (2012). Synovial inflammation, immune cells and their cytokines in osteoarthritis: a review. *Osteoarthr. Cartilage* 20, 1484–1499. doi: 10.1016/j.joca.2012.08.027

Decker, R. S., Um, H. B., Dyment, N. A., Cottingham, N., Usami, Y., Enomoto-Iwamoto, M., et al. (2017). Cell origin, volume and arrangement are drivers of articular cartilage formation, morphogenesis and response to injury in mouse limbs. *Dev. Biol.* 426, 56–68. doi: 10.1016/j.ydbio.2017.04.006

Ding, D. C., Wu, K. C., Chou, H. L., Hung, W. T., Liu, H. W., and Chu, T. Y. (2015). Human infrapatellar fat pad-derived stromal cells have more potent differentiation capacity than other mesenchymal cells and can be enhanced by hyaluronan. *Cell Transplant.* 24, 1221–1232. doi: 10.3727/096368914x681937

Djouad, F., Bony, C., Haupl, T., Uze, G., Lahlou, N., Louis-Plence, P., et al. (2005). Transcriptional profiles discriminate bone marrow-derived and synovium-derived mesenchymal stem cells. *Arthritis Res. Ther.* 7, R1304–R1315.

do Amaral, R., Almeida, H. V., Kelly, D. J., O'Brien, F. J., and Kearney, C. J. (2017). Infrapatellar fat pad stem cells: from developmental biology to cell therapy. *Stem Cells Int.* 2017:6843727.

Dragoo, J. L., Johnson, C., and McConnell, J. (2012). Evaluation and treatment of disorders of the infrapatellar fat pad. *Sports Med.* 42, 51–67. doi: 10.2165/11595680-000000000-00000

Dragoo, J. L., Samimi, B., Zhu, M., Hame, S. L., Thomas, B. J., Lieberman, J. R., et al. (2003). Tissue-engineered cartilage and bone using stem cells from human infrapatellar fat pads. *J. Bone Joint Surg. Br.* 85, 740–747. doi: 10.1302/0301-620x.85b5.13587

Dumond, H., Presle, N., Terlain, B., Mainard, D., Loeuille, D., Netter, P., et al. (2003). Evidence for a key role of leptin in osteoarthritis. *Arthritis Rheum.* 48, 3118–3129. doi: 10.1002/art.11303

English, A., Jones, E. A., Corscadden, D., Henshaw, K., Chapman, T., Emery, P., et al. (2007). A comparative assessment of cartilage and joint fat pad as a potential source of cells for autologous therapy development in knee osteoarthritis. *Rheumatology* 46, 1676–1683. doi: 10.1093/rheumatology/kem217

Eymard, F., Pigenet, A., Citadelle, D., Flouzat-Lachaniette, C. H., Poignard, A., Benelli, C., et al. (2014). Induction of an inflammatory and prodegradative phenotype in autologous fibroblast-like synoviocytes by the infrapatellar fat pad from patients with knee osteoarthritis. *Arthritis Rheumatol.* 66, 2165–2174. doi: 10.1002/art.38657

Farrell, E., Both, S. K., Odorfer, K. I., Koevoet, W., Kops, N., O'Brien, F. J., et al. (2011). In-vivo generation of bone via endochondral ossification by in-vitro chondrogenic priming of adult human and rat mesenchymal stem cells. *BMC Musculoskelet. Disord.* 12:31. doi: 10.1186/1471-2474-12-31

Farrell, E., van der Jagt, O. P., Koevoet, W., Kops, N., van Manen, C. J., Hellingman, C. A., et al. (2009). Chondrogenic priming of human bone marrow stromal cells: a better route to bone repair? *Tissue Eng. Part C Methods* 15, 285–295. doi: 10.1089/ten.tec.2008.0297

Favero, M., El-Hadi, H., Belluzzi, E., Granzotto, M., Porzionato, A., Sarasin, G., et al. (2017). Infrapatellar fat pad features in osteoarthritis: a histopathological and molecular study. *Rheumatology* 56, 1784–1793. doi: 10.1093/rheumatology/kex287

Felson, D. T., Niu, J., Neogi, T., Goggins, J., Nevitt, M. C., Roemer, F., et al. (2016). Synovitis and the risk of knee osteoarthritis: the MOST Study. *Osteoarthr. Cartilage* 24, 458–464. doi: 10.1016/j.joca.2015.09.013

Feng, X., Li, Z., Wei, J., Feng, Z., Wu, W., and Zhao, Y. (2018). Injectable cartilaginous template transformed BMSCs into vascularized bone. *Sci. Rep.* 8:8244.

Fernandes, T. L., Gomoll, A. H., Lattermann, C., Hernandez, A. J., Bueno, D. F., and Amano, M. T. (2020). Macrophage: a potential target on cartilage regeneration. *Front. Immunol.* 11:111. doi: 10.3389/fimmu.2020.00111

Ferro, T., Santhagunam, A., Madeira, C., Salgueiro, J. B., da Silva, C. L., and Cabral, J. M. S. (2019). Successful isolation and ex vivo expansion of human mesenchymal stem/stromal cells obtained from different synovial tissue-derived (biopsy) samples. *J. Cell Physiol.* 234, 3973–3984. doi: 10.1002/jcp.27202

Fontanella, C. G., Belluzzi, E., Rossato, M., Olivotto, E., Trisolino, G., Ruggieri, P., et al. (2019). Quantitative MRI analysis of infrapatellar and suprapatellar fat pads in normal controls, moderate and end-stage osteoarthritis. *Ann. Anat.* 221, 108–114. doi: 10.1016/j.aanat.2018.09.007

Frank-Bertoncelj, M., Trenkmann, M., Klein, K., Karouzakis, E., Rehrauer, H., Bratus, A., et al. (2017). Epigenetically-driven anatomical diversity of synovial fibroblasts guides joint-specific fibroblast functions. *Nat. Commun.* 8:14852.

Freeman, M. A., and Wyke, B. (1967). The innervation of the knee joint. An anatomical and histological study in the cat. *J. Anat.* 101(Pt 3), 505–532.

Galipeau, J., Krampera, M., Barrett, J., Dazzi, F., Deans, R. J., DeBruijn, J., et al. (2016). International society for cellular therapy perspective on immune functional assays for mesenchymal stromal cells as potency release criterion for advanced phase clinical trials. *Cytotherapy* 18, 151–159. doi: 10.1016/j.jcyt.2015.11.008

Gallagher, J., Tierney, P., Murray, P., and O'Brien, M. (2005). The infrapatellar fat pad: anatomy and clinical correlations. *Knee Surg. Sports Traumatol. Arthrosc.* 13, 268–272. doi: 10.1007/s00167-004-0592-7

Garcia, J., Mennan, C., McCarthy, H. S., Roberts, S., Richardson, J. B., and Wright, K. T. (2016a). Chondrogenic potency analyses of donor-matched chondrocytes and mesenchymal stem cells derived from bone marrow, infrapatellar fat pad, and subcutaneous fat. *Stem Cells Int.* 2016:6969726.

Garcia, J., Wright, K., Roberts, S., Kuiper, J. H., Mangham, C., Richardson, J., et al. (2016b). Characterisation of synovial fluid and infrapatellar fat pad derived mesenchymal stromal cells: the influence of tissue source and inflammatory stimulus. *Sci. Rep.* 6:24295.

Garza, J. R., Campbell, R. E., Tjoumakaris, F. P., Freedman, K. B., Miller, L. S., Santa Maria, D., et al. (2020). Clinical efficacy of intra-articular mesenchymal stromal cells for the treatment of knee osteoarthritis: a double-blinded prospective randomized controlled clinical trial. *Am. J. Sports Med.* 48, 588–598. doi: 10.1177/0363546519899923

Gentek, R., Molawi, K., and Sieweke, M. H. (2014). Tissue macrophage identity and self-renewal. *Immunol. Rev.* 262, 56–73. doi: 10.1111/imr.12224

Gierman, L. M., Wopereis, S., van El, B., Verheij, E. R., Werff-van, der Vat, B. J., et al. (2013). Metabolic profiling reveals differences in concentrations of oxylipins and fatty acids secreted by the infrapatellar fat pad of donors with end-stage osteoarthritis and normal donors. *Arthritis Rheum.* 65, 2606–2614.

Ginhoux, F., and Guilliams, M. (2016). Tissue-resident macrophage ontogeny and homeostasis. *Immunity* 44, 439–449. doi: 10.1016/j.immuni.2016.02.024

Ginhoux, F., and Jung, S. (2014). Monocytes and macrophages: developmental pathways and tissue homeostasis. *Nat. Rev. Immunol.* 14, 392–404. doi: 10.1038/nri3671

Gomez-Aristizabal, A., Gandhi, R., Mahomed, N. N., Marshall, K. W., and Viswanathan, S. (2019). Synovial fluid monocyte/macrophage subsets and their correlation to patient-reported outcomes in osteoarthritic patients: a cohort study. *Arthritis Res. Ther.* 21:26.

Hagmann, S., Gotterbarm, T., Muller, T., Baesig, A. M., Gantz, S., Dreher, T., et al. (2013). The influence of bone marrow- and synovium-derived mesenchymal stromal cells from osteoarthritis patients on regulatory T cells in co-culture. *Clin. Exp. Immunol.* 173, 454–462. doi: 10.1111/cei.12122

Han, W., Aitken, D., Zhu, Z., Halliday, A., Wang, X., Antony, B., et al. (2016). Signal intensity alteration in the infrapatellar fat pad at baseline for the prediction of knee symptoms and structure in older adults: a cohort study. *Ann. Rheum. Dis.* 75, 1783–1788. doi: 10.1136/annrheumdis-2015-208360

Harrell, C. R., Markovic, B. S., Fellabaum, C., Arsenijevic, A., and Volarevic, V. (2019). Mesenchymal stem cell-based therapy of osteoarthritis: current knowledge and future perspectives. *Biomed. Pharmacother.* 109, 2318–2326. doi: 10.1016/j.biopha.2018.11.099

Heilmeier, U., Mamoto, K., Amano, K., Eck, B., Tanaka, M., Bullen, J. A., et al. (2019). Infrapatellar fat pad abnormalities are associated with a higher inflammatory synovial fluid cytokine profile in young adults following ACL tear. *Osteoarthr. Cartilage* 28, 82–91. doi: 10.1016/j.joca.2019.09.001

Hermida-Gomez, T., Fuentes-Boquete, I., Gimeno-Longas, M. J., Muinos-Lopez, E., Diaz-Prado, S., de Toro, F. J., et al. (2011). Quantification of cells expressing mesenchymal stem cell markers in healthy and osteoarthritic synovial membranes. *J. Rheumatol.* 38, 339–349. doi: 10.3899/jrheum.100614

Hill, C. L., Hunter, D. J., Niu, J., Clancy, M., Guermazi, A., Genant, H., et al. (2007). Synovitis detected on magnetic resonance imaging and its relation to pain and cartilage loss in knee osteoarthritis. *Ann. Rheum. Dis.* 66, 1599–1603. doi: 10.1136/ard.2006.067470

Hindle, P., Khan, N., Biant, L., and Peault, B. (2017). The infrapatellar fat pad as a source of perivascular stem cells with increased chondrogenic potential for regenerative medicine. *Stem Cells Transl. Med.* 6, 77–87. doi: 10.5966/sctm.2016-0040

Hu, P., Yang, Q., Wang, Q., Shi, C., Wang, D., Armato, U., et al. (2019). Mesenchymal stromal cells-exosomes: a promising cell-free therapeutic tool for wound healing and cutaneous regeneration. *Burns Trauma* 7:38.

Ioan-Facsinay, A., and Kloppenburg, M. (2013). An emerging player in knee osteoarthritis: the infrapatellar fat pad. *Arthritis Res. Ther.* 15:225. doi: 10.1186/ar4422

Ioan-Facsinay, A., and Kloppenburg, M. (2017). Osteoarthritis: inflammation and fibrosis in adipose tissue of osteoarthritic joints. *Nat. Rev. Rheumatol.* 13, 325–326. doi: 10.1038/nrrheum.2017.53

Ioan-Facsinay, A., Kwekkeboom, J. C., Westhoff, S., Giera, M., Rombouts, Y., van Harmelen, V., et al. (2013). Adipocyte-derived lipids modulate CD4+ T-cell function. *Eur. J. Immunol.* 43, 1578–1587. doi: 10.1002/eji.201243096

Ji, Q., Zheng, Y., Zhang, G., Hu, Y., Fan, X., Hou, Y., et al. (2019). Single-cell RNA-seq analysis reveals the progression of human osteoarthritis. *Ann. Rheum. Dis.* 78, 100–110. doi: 10.1136/annrheumdis-2017-212863

Jiang, L. F., Fang, J. H., and Wu, L. D. (2019). Role of infrapatellar fat pad in pathological process of knee osteoarthritis: future applications in treatment. *World J. Clin. Cases* 7, 2134–2142. doi: 10.12998/wjcc.v7.i16.2134

Jiang, T., Wang, Z., and Sun, J. (2020). Human bone marrow mesenchymal stem cell-derived exosomes stimulate cutaneous wound healing mediates through TGF-beta/Smad signaling pathway. *Stem Cell Res. Ther.* 11:198.

Jurgens, W. J., van Dijk, A., Doulabi, B. Z., Niessen, F. B., Ritt, M. J., van Milligen, F. J., et al. (2009). Freshly isolated stromal cells from the infrapatellar fat pad are suitable for a one-step surgical procedure to regenerate cartilage tissue. *Cytotherapy* 11, 1052–1064. doi: 10.3109/14653240903219122

Kalaitzoglou, E., Griffin, T. M., and Humphrey, M. B. (2017). Innate immune responses and osteoarthritis. *Curr. Rheumatol. Rep.* 19:45.

Kandahari, A. M., Yang, X., Dighe, A. S., Pan, D., and Cui, Q. (2015). Recognition of immune response for the early diagnosis and treatment of osteoarthritis. *J. Immunol. Res.* 2015:192415.

Karnieli, O., Friedner, O. M., Allickson, J. G., Zhang, N., Jung, S., Fiorentini, D., et al. (2017). A consensus introduction to serum replacements and serum-free media for cellular therapies. *Cytotherapy* 19, 155–169. doi: 10.1016/j.jcyt.2016.11.011

Karystinou, A., Dell'Accio, F., Kurth, T. B., Wackerhage, H., Khan, I. M., Archer, C. W., et al. (2009). Distinct mesenchymal progenitor cell subsets in the adult human synovium. *Rheumatology* 48, 1057–1064. doi: 10.1093/rheumatology/kep192

Kennedy, J. C., Alexander, I. J., and Hayes, K. C. (1982). Nerve supply of the human knee and its functional importance. *Am. J. Sports Med.* 10, 329–335. doi: 10.1177/036354658201000601

Khan, W. S., Tew, S. R., Adesida, A. B., and Hardingham, T. E. (2008). Human infrapatellar fat pad-derived stem cells express the pericyte marker 3G5 and show enhanced chondrogenesis after expansion in fibroblast growth factor-2. *Arthritis Res. Ther.* 10:R74.

King, L. K., March, L., and Anandacoomarasamy, A. (2013). Obesity & osteoarthritis. *Indian J. Med. Res.* 138, 185–193.

Klein-Wieringa, I. R., Andersen, S. N., Kwekkeboom, J. C., Giera, M., de Lange-Brokaar, B. J., van Osch, G. J., et al. (2013). Adipocytes modulate the phenotype of human macrophages through secreted lipids. *J. Immunol.* 191, 1356–1363. doi: 10.4049/jimmunol.1203074

Klein-Wieringa, I. R., de Lange-Brokaar, B. J., Yusuf, E., Andersen, S. N., Kwekkeboom, J. C., Kroon, H. M., et al. (2016). Inflammatory cells in patients

with endstage knee osteoarthritis: a comparison between the synovium and the infrapatellar fat pad. *J. Rheumatol.* 43, 771–778. doi: 10.3899/jrheum.151068

Klein-Wieringa, I. R., Kloppenburg, M., Bastiaansen-Jenniskens, Y. M., Yusuf, E., Kwekkeboom, J. C., El-Bannoudi, H., et al. (2011). The infrapatellar fat pad of patients with osteoarthritis has an inflammatory phenotype. *Ann. Rheum. Dis.* 70, 851–857. doi: 10.1136/ard.2010.140046

Koh, Y. G., and Choi, Y. J. (2012). Infrapatellar fat pad-derived mesenchymal stem cell therapy for knee osteoarthritis. *Knee* 19, 902–907. doi: 10.1016/j.knee.2012.04.001

Koh, Y. G., Jo, S. B., Kwon, O. R., Suh, D. S., Lee, S. W., Park, S. H., et al. (2013). Mesenchymal stem cell injections improve symptoms of knee osteoarthritis. *Arthroscopy* 29, 748–755. doi: 10.1016/j.arthro.2012.11.017

Kohn, D., Deiler, S., and Rudert, M. (1995). Arterial blood supply of the infrapatellar fat pad. Anatomy and clinical consequences. *Arch. Orthop. Trauma Surg.* 114, 72–75. doi: 10.1007/bf00422828

Koizumi, K., Ebina, K., Hart, D. A., Hirao, M., Noguchi, T., Sugita, N., et al. (2016). Synovial mesenchymal stem cells from osteo- or rheumatoid arthritis joints exhibit good potential for cartilage repair using a scaffold-free tissue engineering approach. *Osteoarthr. Cartilage* 24, 1413–1422. doi: 10.1016/j.joca.2016.03.006

Kordelas, L., Rebmann, V., Ludwig, A. K., Radtke, S., Ruesing, J., Doeppner, T. R., et al. (2014). MSC-derived exosomes: a novel tool to treat therapy-refractory graft-versus-host disease. *Leukemia* 28, 970–973. doi: 10.1038/leu.2014.41

Kouroupis, D., Bowles, A. C., Willman, M. A., Perucca Orfei, C., Colombini, A., Best, T. M., et al. (2019a). Infrapatellar fat pad-derived MSC response to inflammation and fibrosis induces an immunomodulatory phenotype involving CD10-mediated Substance P degradation. *Sci. Rep.* 9:10864.

Kouroupis, D., Sanjurjo-Rodriguez, C., Jones, E., and Correa, D. (2019b). Mesenchymal stem cell functionalization for enhanced therapeutic applications. *Tissue Eng. Part B Rev.* 25, 55–77. doi: 10.1089/ten.teb.2018.0118

Kouroupis, D. B. A., Best, T. M., Kaplan, L. D., and Correa, D. (2020). CD10/neprilysin enrichment in infrapatellar fat pad-derived MSC under regulatory-compliant conditions: implications for efficient synovitis and fat pad fibrosis reversal. *Am. J. Sports Med.* 48, 2013–2027. doi: 10.1177/0363546520917699

Kriegova, E., Manukyan, G., Mikulkova, Z., Gabcova, G., Kudelka, M., Gajdos, P., et al. (2018). Gender-related differences observed among immune cells in synovial fluid in knee osteoarthritis. *Osteoarthr. Cartilage* 26, 1247–1256. doi: 10.1016/j.joca.2018.04.016

Kubosch, E. J., Lang, G., Furst, D., Kubosch, D., Izadpanah, K., Rolauffs, B., et al. (2018). The potential for synovium-derived stem cells in cartilage repair. *Curr. Stem Cell Res. Ther.* 13, 174–184. doi: 10.2174/1574888x12666171002111026

Kuptniratsaikul, V., Thanakhumtorn, S., Chinswangwatanakul, P., Wattanamongkonsil, L., and Thamlikitkul, V. (2009). Efficacy and safety of *Curcuma domestica* extracts in patients with knee osteoarthritis. *J. Altern. Complement. Med.* 15, 891–897. doi: 10.1089/acm.2008.0186

Lee, S. Y., Nakagawa, T., and Reddi, A. H. (2008). Induction of chondrogenesis and expression of superficial zone protein (SZP)/lubricin by mesenchymal progenitors in the infrapatellar fat pad of the knee joint treated with TGF-beta1 and BMP-7. *Biochem. Biophys. Res. Commun.* 376, 148–153. doi: 10.1016/j.bbrc.2008.08.138

Li, F., Tang, Y., Song, B., Yu, M., Li, Q., Zhang, C., et al. (2019). Nomenclature clarification: synovial fibroblasts and synovial mesenchymal stem cells. *Stem Cell Res. Ther.* 10:260.

Li, Y. S., Luo, W., Zhu, S. A., and Lei, G. H. (2017). T Cells in osteoarthritis: alterations and beyond. *Front. Immunol.* 8:356. doi: 10.3389/fimmu.2017.00356

Lieberthal, J., Sambamurthy, N., and Scanzello, C. R. (2015). Inflammation in joint injury and post-traumatic osteoarthritis. *Osteoarthr. Cartilage* 23, 1825–1834. doi: 10.1016/j.joca.2015.08.015

Lim, J. E., Chung, E., and Son, Y. (2017). A neuropeptide, Substance-P, directly induces tissue-repairing M2 like macrophages by activating the PI3K/Akt/mTOR pathway even in the presence of IFNgamma. *Sci. Rep.* 7:9417.

Liu, Y., Buckley, C. T., Almeida, H. V., Mulhall, K. J., and Kelly, D. J. (2014). Infrapatellar fat pad-derived stem cells maintain their chondrogenic capacity in disease and can be used to engineer cartilaginous grafts of clinically relevant dimensions. *Tissue Eng. Part A* 20, 3050–3062. doi: 10.1089/ten.tea.2014.0035

Liu, Y., Buckley, C. T., Downey, R., Mulhall, K. J., and Kelly, D. J. (2012). The role of environmental factors in regulating the development of cartilaginous grafts engineered using osteoarthritic human infrapatellar fat pad-derived stem cells. *Tissue Eng. Part A* 18, 1531–1541. doi: 10.1089/ten.tea.2011.0575

Loeuille, D., Sauliere, N., Champigneulle, J., Rat, A. C., Blum, A., and Chary-Valckenaere, I. (2011). Comparing non-enhanced and enhanced sequences in the assessment of effusion and synovitis in knee OA: associations with clinical, macroscopic and microscopic features. *Osteoarthr. Cartilage* 19, 1433–1439. doi: 10.1016/j.joca.2011.08.010

Losina, E., Walensky, R. P., Reichmann, W. M., Holt, H. L., Gerlovin, H., Solomon, D. H., et al. (2011). Impact of obesity and knee osteoarthritis on morbidity and mortality in older Americans. *Ann. Intern. Med.* 154, 217–226.

Macchi, V., Stocco, E., Stecco, C., Belluzzi, E., Favero, M., Porzionato, A., et al. (2018). The infrapatellar fat pad and the synovial membrane: an anatomo-functional unit. *J. Anat.* 233, 146–154. doi: 10.1111/joa.12820

Maekawa, K., Furukawa, H., Kanazawa, Y., Hijioka, A., Suzuki, K., and Fujimoto, S. (1996). Electron and immunoelectron microscopy on healing process of the rat anterior cruciate ligament after partial transection: the roles of multipotent fibroblasts in the synovial tissue. *Histol. Histopathol.* 11, 607–619.

Marsano, A., Millward-Sadler, S. J., Salter, D. M., Adesida, A., Hardingham, T., Tognana, E., et al. (2007). Differential cartilaginous tissue formation by human synovial membrane, fat pad, meniscus cells and articular chondrocytes. *Osteoarthr. Cartilage* 15, 48–58. doi: 10.1016/j.joca.2006.06.009

Mashaghi, A., Marmalidou, A., Tehrani, M., Grace, P. M., Pothoulakis, C., and Dana, R. (2016). Neuropeptide substance P and the immune response. *Cell Mol. Life Sci.* 73, 4249–4264. doi: 10.1007/s00018-016-2293-z

Mata-Essayag, S., Magaldi, S., de Capriles, C. H., Henao, L., Garrido, L., and Pacillo, V. (2001). Mucor indicus necrotizing fasciitis. *Int. J. Dermatol.* 40, 406–408. doi: 10.1046/j.1365-4362.2001.01246-3.x

Matarese, G., Leiter, E. H., and La Cava, A. (2007). Leptin in autoimmunity: many questions, some answers. *Tissue Antigens* 70, 87–95. doi: 10.1111/j.1399-0039.2007.00886.x

Matas, J., Orrego, M., Amenabar, D., Infante, C., Tapia-Limonchi, R., Cadiz, M. I., et al. (2019). Umbilical cord-derived mesenchymal stromal cells (MSCs) for knee osteoarthritis: repeated MSC dosing is superior to a single msc dose and to hyaluronic acid in a controlled randomized phase I/II Trial. *Stem Cells Transl. Med.* 8, 215–224. doi: 10.1002/sctm.18-0053

Mathiessen, A., and Conaghan, P. G. (2017). Synovitis in osteoarthritis: current understanding with therapeutic implications. *Arthritis Res. Ther.* 19, 18.

Mathis, D. (2013). Immunological goings-on in visceral adipose tissue. *Cell Metab.* 17, 851–859. doi: 10.1016/j.cmet.2013.05.008

McIntyre, J. A., Jones, I. A., Han, B., and Vangsness, C. T. Jr. (2018). Intra-articular mesenchymal stem cell therapy for the human joint: a systematic review. *Am. J. Sports Med.* 46, 3550–3563. doi: 10.1177/0363546517735844

Mendicino, M., Bailey, A. M., Wonnacott, K., Puri, R. K., and Bauer, S. R. (2014). MSC-based product characterization for clinical trials: an FDA perspective. *Cell Stem Cell.* 14, 141–145. doi: 10.1016/j.stem.2014.01.013

Meng, Q., and Qiu, B. (2020). Exosomal MicroRNA-320a derived from mesenchymal stem cells regulates rheumatoid arthritis fibroblast-like synoviocyte activation by suppressing CXCL9 expression. *Front. Physiol.* 11:441. doi: 10.3389/fphys.2020.00441

Mesallati, T., Buckley, C. T., and Kelly, D. J. (2017). Engineering cartilaginous grafts using chondrocyte-laden hydrogels supported by a superficial layer of stem cells. *J. Tissue Eng. Regen. Med.* 11, 1343–1353. doi: 10.1002/term.2033

Mesallati, T., Sheehy, E. J., Vinardell, T., Buckley, C. T., and Kelly, D. J. (2015). Tissue engineering scaled-up, anatomically shaped osteochondral constructs for joint resurfacing. *Eur. Cell Mater.* 30, 163–85; discussion85–86.

Mizuno, H., Tobita, M., and Uysal, A. C. (2012). Concise review: adipose-derived stem cells as a novel tool for future regenerative medicine. *Stem Cells* 30, 804–810. doi: 10.1002/stem.1076

Mizuno, M., Katano, H., Mabuchi, Y., Ogata, Y., Ichinose, S., Fujii, S., et al. (2018). Specific markers and properties of synovial mesenchymal stem cells in the surface, stromal, and perivascular regions. *Stem Cell Res. Ther.* 9:123.

Mochizuki, T., Muneta, T., Sakaguchi, Y., Nimura, A., Yokoyama, A., Koga, H., et al. (2006). Higher chondrogenic potential of fibrous synovium- and adipose synovium-derived cells compared with subcutaneous fat-derived cells: distinguishing properties of mesenchymal stem cells in humans. *Arthritis Rheum.* 54, 843–853. doi: 10.1002/art.21651

Mustonen, A. M., Kakela, R., Lehenkari, P., Huhtakangas, J., Turunen, S., Joukainen, A., et al. (2019). Distinct fatty acid signatures in infrapatellar fat pad

and synovial fluid of patients with osteoarthritis versus rheumatoid arthritis. *Arthritis Res. Ther.* 21:124. doi: 10.3109/08916934.2015.1113267

Muttigi, M. S., Kim, B. J., Choi, B., Yoshie, A., Kumar, H., Han, I., et al. (2018). Matrilin-3 codelivery with adipose-derived mesenchymal stem cells promotes articular cartilage regeneration in a rat osteochondral defect model. *J. Tissue Eng. Regen. Med.* 12, 667–675. doi: 10.1002/term.2485

Nair, A., Kanda, V., Bush-Joseph, C., Verma, N., Chubinskaya, S., Mikecz, K., et al. (2012). Synovial fluid from patients with early osteoarthritis modulates fibroblast-like synoviocyte responses to toll-like receptor 4 and toll-like receptor 2 ligands via soluble CD14. *Arthritis Rheum.* 64, 2268–2277. doi: 10.1002/art.34495

Nimura, A., Muneta, T., Koga, H., Mochizuki, T., Suzuki, K., Makino, H., et al. (2008). Increased proliferation of human synovial mesenchymal stem cells with autologous human serum: comparisons with bone marrow mesenchymal stem cells and with fetal bovine serum. *Arthritis Rheum.* 58, 501–510. doi: 10.1002/art.23219

O'HEireamhoin, S., Buckley, C. T., Jones, E., McGonagle, D., Mulhall, K. J., and Kelly, D. J. (2013). Recapitulating aspects of the oxygen and substrate environment of the damaged joint milieu for stem cell-based cartilage tissue engineering. *Tissue Eng. Part C Methods* 19, 117–127. doi: 10.1089/ten.tec.2012.0142

Orozco, L., Munar, A., Soler, R., Alberca, M., Soler, F., Huguet, M., et al. (2014). Treatment of knee osteoarthritis with autologous mesenchymal stem cells: two-year follow-up results. *Transplantation* 97, e66–e68. doi: 10.1097/tp.0000000000000167

Orr, C., Vieira-Sousa, E., Boyle, D. L., Buch, M. H., Buckley, C. D., Canete, J. D., et al. (2017). Synovial tissue research: a state-of-the-art review. *Nat. Rev. Rheumatol.* 13:630.

Ospelt, C. (2017). Synovial fibroblasts in. *RMD Open* 3:e000471. doi: 10.1136/rmdopen-2017-000471

Pachler, K., Lener, T., Streif, D., Dunai, Z. A., Desgeorges, A., Feichtner, M., et al. (2017). A good manufacturing practice-grade standard protocol for exclusively human mesenchymal stromal cell-derived extracellular vesicles. *Cytotherapy* 19, 458–472. doi: 10.1016/j.jcyt.2017.01.001

Pan, F., Han, W., Wang, X., Liu, Z., Jin, X., Antony, B., et al. (2015). A longitudinal study of the association between infrapatellar fat pad maximal area and changes in knee symptoms and structure in older adults. *Ann. Rheum. Dis.* 74, 1818–1824. doi: 10.1136/annrheumdis-2013-205108

Paul, F., Arkin, Y., Giladi, A., Jaitin, D. A., Kenigsberg, E., Keren-Shaul, H., et al. (2015). Transcriptional heterogeneity and lineage commitment in myeloid progenitors. *Cell* 163, 1663–1677. doi: 10.1016/j.cell.2015.11.013

Pelletier, J. P., Martel-Pelletier, J., and Abramson, S. B. (2001). Osteoarthritis, an inflammatory disease: potential implication for the selection of new therapeutic targets. *Arthritis Rheum.* 44, 1237–1247. doi: 10.1002/1529-0131(200106)44:6<1237::aid-art214>3.0.co;2-f

Prabhakar, A., Lynch, A. P., and Ahearne, M. (2016). Self-assembled infrapatellar fat-pad progenitor cells on a poly-epsilon-caprolactone film for cartilage regeneration. *Artif. Organs* 40, 376–384. doi: 10.1111/aor.12565

Regev, A., Teichmann, S. A., Lander, E. S., Amit, I., Benoist, C., Birney, E., et al. (2017). The human cell atlas. *eLife* 6:e27041.

Roelofs, A. J., Zupan, J., Riemen, A. H. K., Kania, K., Ansboro, S., White, N., et al. (2017). Joint morphogenetic cells in the adult mammalian synovium. *Nat. Commun.* 8:15040.

Roemer, F. W., Guermazi, A., Zhang, Y., Yang, M., Hunter, D. J., Crema, M. D., et al. (2009). Hoffa's fat pad: evaluation on unenhanced mr images as a measure of patellofemoral synovitis in osteoarthritis. *Am. J. Roentgenol.* 192, 1696–1700. doi: 10.2214/ajr.08.2038

Rohde, E., Pachler, K., and Gimona, M. (2019). Manufacturing and characterization of extracellular vesicles from umbilical cord-derived mesenchymal stromal cells for clinical testing. *Cytotherapy* 21, 581–592. doi: 10.1016/j.jcyt.2018.12.006

Sakaguchi, Y., Sekiya, I., Yagishita, K., and Muneta, T. (2005). Comparison of human stem cells derived from various mesenchymal tissues: superiority of synovium as a cell source. *Arthritis Rheum.* 52, 2521–2529. doi: 10.1002/art.21212

Scanzello, C. R., and Goldring, S. R. (2012). The role of synovitis in osteoarthritis pathogenesis. *Bone* 51, 249–257. doi: 10.1016/j.bone.2012.02.012

Schnoor, M., Alcaide, P., Voisin, M. B., and van Buul, J. D. (2016). Recruitment of immune cells into inflamed tissues: consequences for endothelial barrier integrity and tissue functionality. *Mediat. Inflamm.* 2016:1561368.

Scotti, C., Piccinini, E., Takizawa, H., Todorov, A., Bourgine, P., Papadimitropoulos, A., et al. (2013). Engineering of a functional bone organ through endochondral ossification. *Proc. Natl. Acad. Sci. U.S.A.* 110, 3997–4002. doi: 10.1073/pnas.1220108110

Sekiya, I., Muneta, T., Horie, M., and Koga, H. (2015). Arthroscopic transplantation of synovial stem cells improves clinical outcomes in knees with cartilage defects. *Clin. Orthop. Relat. Res.* 473, 2316–2326. doi: 10.1007/s11999-015-4324-8

Shimomura, K., Yasui, Y., Koizumi, K., Chijimatsu, R., Hart, D. A., Yonetani, Y., et al. (2018). First-in-human pilot study of implantation of a scaffold-free tissue-engineered construct generated from autologous synovial mesenchymal stem cells for repair of knee chondral lesions. *Am. J. Sports Med.* 46, 2384–2393. doi: 10.1177/0363546518781825

Siciliano, C., Bordin, A., Ibrahim, M., Chimenti, I., Cassiano, F., Gatto, I., et al. (2016). The adipose tissue of origin influences the biological potential of human adipose stromal cells isolated from mediastinal and subcutaneous fat depots. *Stem Cell Res.* 17, 342–351. doi: 10.1016/j.scr.2016.07.010

Sivasubramaniyan, K., Koevoet, W., Hakimiyan, A. A., Sande, M., Farrell, E., Hoogduijn, M. J., et al. (2019). Cell-surface markers identify tissue resident multipotential stem/stromal cell subsets in synovial intimal and sub-intimal compartments with distinct chondrogenic properties. *Osteoarthr. Cartilage* 27, 1831–1840. doi: 10.1016/j.joca.2019.08.006

Sokolove, J., and Lepus, C. M. (2013). Role of inflammation in the pathogenesis of osteoarthritis: latest findings and interpretations. *Ther. Adv. Musculoskelet. Dis.* 5, 77–94. doi: 10.1177/1759720x12467868

Soler, R., Orozco, L., Munar, A., Huguet, M., Lopez, R., Vives, J., et al. (2016). Final results of a phase I-II trial using ex vivo expanded autologous Mesenchymal Stromal Cells for the treatment of osteoarthritis of the knee confirming safety and suggesting cartilage regeneration. *Knee* 23, 647–654. doi: 10.1016/j.knee.2015.08.013

Spitsin, S., Meshki, J., Winters, A., Tuluc, F., Benton, T. D., and Douglas, S. D. (2017). Substance P-mediated chemokine production promotes monocyte migration. *J. Leukoc. Biol.* 101, 967–973. doi: 10.1189/jlb.1ab0416-188rr

Stagg, J., and Galipeau, J. (2013). Mechanisms of immune modulation by mesenchymal stromal cells and clinical translation. *Curr. Mol. Med.* 13, 856–867. doi: 10.2174/1566524011313050016

Sun, A. R., Panchal, S. K., Friis, T., Sekar, S., Crawford, R., Brown, L., et al. (2017). Obesity-associated metabolic syndrome spontaneously induces infiltration of pro-inflammatory macrophage in synovium and promotes osteoarthritis. *PLoS One* 12:e0183693. doi: 10.1371/journal.pone.0183693

Sun, Y., Chen, S., and Pei, M. (2018). Comparative advantages of infrapatellar fat pad: an emerging stem cell source for regenerative medicine. *Rheumatology* 57, 2072–2086. doi: 10.1093/rheumatology/kex487

Suvas, S. (2017). Role of substance P neuropeptide in inflammation, wound healing, and tissue homeostasis. *J. Immunol.* 199, 1543–1552. doi: 10.4049/jimmunol.1601751

Svensson, V., Vento-Tormo, R., and Teichmann, S. A. (2018). Exponential scaling of single-cell RNA-seq in the past decade. *Nat. Protoc.* 13, 599–604. doi: 10.1038/nprot.2017.149

Tangchitphisut, P., Srikaew, N., Numhom, S., Tangprasittipap, A., Woratanarat, P., Wongsak, S., et al. (2016). Infrapatellar fat pad: an alternative source of adipose-derived mesenchymal stem cells. *Arthritis* 2016:4019873.

To, K., Zhang, B., Romain, K., Mak, C., and Khan, W. (2019). Synovium-derived mesenchymal stem cell transplantation in cartilage regeneration: a PRISMA review of in vivo studies. *Front. Bioeng. Biotechnol.* 7:314. doi: 10.3389/fbioe.2019.00314

Toghraie, F. S., Chenari, N., Gholipour, M. A., Faghih, Z., Torabinejad, S., Dehghani, S., et al. (2011). Treatment of osteoarthritis with infrapatellar fat pad derived mesenchymal stem cells in Rabbit. *Knee* 18, 71–75. doi: 10.1016/j.knee.2010.03.001

Toussirot, E., Streit, G., and Wendling, D. (2007). The contribution of adipose tissue and adipokines to inflammation in joint diseases. *Curr. Med. Chem.* 14, 1095–1100. doi: 10.2174/092986707780362826

Tu, J., Hong, W., Guo, Y., Zhang, P., Fang, Y., Wang, X., et al. (2019). Ontogeny of synovial macrophages and the roles of synovial macrophages from different origins in arthritis. *Front. Immunol.* 10:1146. doi: 10.3389/fimmu.2019.01146

Tu, J., Hong, W., Zhang, P., Wang, X., Korner, H., and Wei, W. (2018). Ontology and function of fibroblast-like and macrophage-like synoviocytes: how do they talk to each other and can they be targeted for rheumatoid arthritis therapy? *Front. Immunol.* 9:1467. doi: 10.3389/fimmu.2018.01467

Uccelli, A., and de Rosbo, N. K. (2015). The immunomodulatory function of mesenchymal stem cells: mode of action, and pathways. *Ann. N. Y. Acad. Sci.* 1351, 114–126. doi: 10.1111/nyas.12815

Vega, A., Martin-Ferrero, M. A., Del Canto, F., Alberca, M., Garcia, V., Munar, A., et al. (2015). Treatment of knee osteoarthritis with allogeneic bone marrow mesenchymal stem cells: a randomized controlled trial. *Transplantation* 99, 1681–1690. doi: 10.1097/tp.0000000000000678

Vilalta, M., Degano, I. R., Bago, J., Gould, D., Santos, M., Garcia-Arranz, M., et al. (2008). Biodistribution, long-term survival, and safety of human adipose tissue-derived mesenchymal stem cells transplanted in nude mice by high sensitivity non-invasive bioluminescence imaging. *Stem Cells Dev.* 17, 993–1003.

Vinardell, T., Buckley, C. T., Thorpe, S. D., and Kelly, D. J. (2011). Composition–function relations of cartilaginous tissues engineered from chondrocytes and mesenchymal stem cells isolated from bone marrow and infrapatellar fat pad. *J. Tissue Eng. Regen. Med.* 5, 673–683. doi: 10.1002/term.357

Vinardell, T., Sheehy, E. J., Buckley, C. T., and Kelly, D. J. (2012). A comparison of the functionality and in vivo phenotypic stability of cartilaginous tissues engineered from different stem cell sources. *Tissue Eng. Part A* 18, 1161–1170. doi: 10.1089/ten.tea.2011.0544

Wickham, M. Q., Erickson, G. R., Gimble, J. M., Vail, T. P., and Guilak, F. (2003). Multipotent stromal cells derived from the infrapatellar fat pad of the knee. *Clin. Orthop. Relat. Res.* 412, 196–212. doi: 10.1097/01.blo.0000072467.53786.ca

Witwer, K. W., Van Balkom, B. W. M., Bruno, S., Choo, A., Dominici, M., Gimona, M., et al. (2019). Defining mesenchymal stromal cell (MSC)-derived small extracellular vesicles for therapeutic applications. *J. Extracell Vesicles* 8:1609206. doi: 10.1080/20013078.2019.1609206

Woodley, S. J., Latimer, C. P., Meikle, G. R., and Stringer, M. D. (2012). Articularis genus: an anatomic and MRI study in cadavers. *J. Bone Joint Surg. Am.* 94, 59–67. doi: 10.2106/jbjs.k.00157

Wu, C. L., Harasymowicz, N. S., Klimak, M. A., Collins, K. H., and Guilak, F. (2020). The role of macrophages in osteoarthritis and cartilage repair. *Osteoarthr. Cartilage* 28, 544–554. doi: 10.1016/j.joca.2019.12.007

Ye, K., Felimban, R., Traianedes, K., Moulton, S. E., Wallace, G. G., Chung, J., et al. (2014). Chondrogenesis of infrapatellar fat pad derived adipose stem cells in 3D printed chitosan scaffold. *PLoS One* 9:e99410. doi: 10.1371/journal.pone.0099410

Yoshitomi, H. (2019). Regulation of immune responses and chronic inflammation by fibroblast-like synoviocytes. *Front. Immunol.* 10:1395. doi: 10.3389/fimmu.2019.01395

Yusuf, E. (2012). Metabolic factors in osteoarthritis: obese people do not walk on their hands. *Arthritis Res. Ther.* 14:123. doi: 10.1186/ar3894

Zeyda, M., Farmer, D., Todoric, J., Aszmann, O., Speiser, M., Gyori, G., et al. (2007). Human adipose tissue macrophages are of an anti-inflammatory phenotype but capable of excessive pro-inflammatory mediator production. *Int. J. Obes.* 31, 1420–1428. doi: 10.1038/sj.ijo.0803632

Zhao, Y., Zou, W., Du, J., and Zhao, Y. (2018). The origins and homeostasis of monocytes and tissue-resident macrophages in physiological situation. *J. Cell Physiol.* 233, 6425–6439. doi: 10.1002/jcp.26461

Conflict of Interest: DC is a paid consultant of Lipogems USA, LLC.

The remaining authors declare that the research was conducted in the absence of any commercial or financial relationships that could be construed as a potential conflict of interest.

frontiers in Bioengineering and Biotechnology

ORIGINAL RESEARCH
published: 28 August 2020
doi: 10.3389/fbioe.2020.01036

Aggrecan and COMP Improve Periosteal Chondrogenesis by Delaying Chondrocyte Hypertrophic Maturation

Marjolein M. J. Caron[1†], Maarten P. F. Janssen[1†], Laura Peeters[1], Dominik R. Haudenschild[2], Andy Cremers[1], Don A. M. Surtel[1], Lodewijk W. van Rhijn[1], Pieter J. Emans[1†] and Tim J. M. Welting[1†]*

[1] Laboratory for Experimental Orthopedics, Department of Orthopedic Surgery, CAPHRI Care and Public Health Research Institute, Maastricht University Medical Center, Maastricht, Netherlands, [2] Department of Orthopedic Surgery, University of California Davis School of Medicine, Sacramento, CA, United States

The generation of cartilage from progenitor cells for the purpose of cartilage repair is often hampered by hypertrophic differentiation of the engineered cartilaginous tissue caused by endochondral ossification. Since a healthy cartilage matrix contains high amounts of Aggrecan and COMP, we hypothesized that their supplementation in the biogel used in the generation of subperiosteal cartilage mimics the composition of the cartilage extracellular matrix environment, with beneficial properties for the engineered cartilage. Supplementation of COMP or Aggrecan was studied *in vitro* during chondrogenic differentiation of rabbit periosteum cells and periosteum-derived chondrocytes. Low melting agarose was supplemented with bovine Aggrecan, human recombinant COMP or vehicle and was injected between the bone and periosteum at the upper medial side of the tibia of New Zealand white rabbits. Generated subperiosteal cartilage tissue was analyzed for weight, GAG and DNA content and ALP activity. Key markers of different phases of endochondral ossification were measured by RT-qPCR. For the *in vitro* experiments, no significant differences in chondrogenic marker expression were detected following COMP or Aggrecan supplementation, while *in vivo* favorable chondrogenic marker expression was detected. Gene expression levels of hypertrophic markers as well as ALP activity were significantly decreased in the Aggrecan and COMP supplemented conditions compared to controls. The wet weight and GAG content of the *in vivo* generated subperiosteal cartilage tissue was not significantly different between groups. Data demonstrate the potential of Aggrecan and COMP to favorably influence the subperiosteal microenvironment for the *in vivo* generation of cartilage for the optimization of cartilage regenerative approaches.

Keywords: chondrocyte hypertrophy, endochondral ossification, COMP, aggrecan, periosteum, periosteal chondrogenesis

OPEN ACCESS

Edited by:
Andrea Banfi,
University of Basel, Switzerland

Reviewed by:
Andrea Lolli,
Erasmus Medical Center, Netherlands
Ryan Michael Porter,
University of Arkansas for Medical Sciences, United States

***Correspondence:**
Tim J. M. Welting
t.welting@maastrichtuniversity.nl

[†] These authors have contributed equally to this work

Specialty section:
This article was submitted to Preclinical Cell and Gene Therapy, a section of the journal Frontiers in Bioengineering and Biotechnology

Received: *11 April 2020*
Accepted: *11 August 2020*
Published: *28 August 2020*

Citation:
Caron MMJ, Janssen MPF, Peeters L, Haudenschild DR, Cremers A, Surtel DAM, van Rhijn LW, Emans PJ and Welting TJM (2020) Aggrecan and COMP Improve Periosteal Chondrogenesis by Delaying Chondrocyte Hypertrophic Maturation. Front. Bioeng. Biotechnol. 8:1036. doi: 10.3389/fbioe.2020.01036

INTRODUCTION

Cartilage lesions can be debilitating, and are a high-risk factor for the development of osteoarthritis (OA) over time (Mollenhauer and Erdmann, 2002). Cartilage lesions can be treated with surgical techniques such as microfracture (MF), mosaicplasty (MP), autologous chondrocyte implantation (ACI) or implantation of a small focal prosthesis (Hunziker, 2002). Donor site morbidity, limited

donor cartilage availability, high costs, and inferior repair tissue quality, (respectively) are just some of the disadvantages of these approaches (Caldwell and Wang, 2014; Caron et al., 2014). We proposed a novel paradigm for *de novo* engineering of cartilaginous tissues, the *in vivo* bioreactor (IVB). This is an alternative cartilage repair concept that we aim to further develop (Emans et al., 2010). The IVB employs the fracture healing response as a way to generate autologous donor cartilage, suitable for implantation to repair (osteo)chondral defects (Emans et al., 2007, 2010). During bone fracture healing the local periosteum plays an important role in the healing process by providing periosteal mesenchymal progenitor cells, which differentiate into chondrocytes and form the cartilaginous callus tissue that remodels via endochondral ossification to ultimately heal the bone fracture (Nakahara et al., 1990; Jansen et al., 2008; Bahney et al., 2019). We discovered that local subperiosteal application of an agarose biogel provokes a similar cartilage callus-forming process within the created subperiosteal space, without the need of a fracture (Emans et al., 2010). This cartilaginous tissue presents all the hallmarks of hyaline cartilage, and upon transplantation, can heal an osteochondral defect out to 9 months in a rabbit model (Emans et al., 2010). However, without further optimization IVB-generated cartilage tissue is prone to further differentiate into hypertrophic cartilage, leading to unwanted ossification.

An important part of the dry-weight of articular cartilage consists of extracellular matrix (ECM) proteins (type II collagen (Col2a1), aggrecan (Acan), cartilage oligomeric matrix protein (COMP), etc.) (Mankin et al., 2000; Poole et al., 2001; Moreira-Teixeira et al., 2011). ECM proteins are thus important determinants in cartilage tissue homeostasis and their efficient synthesis is a prerequisite to creating cartilage volume. In addition, these major ECM protein species also condition the cartilage microenvironment in a unique way. Aggrecan plays a key role in generating the cartilage's fixed negative charge due to its glycosaminoglycan content, leading to its water-attracting properties (Roughley and Mort, 2014), while COMP provides the cartilage with retention capacity for TGF-β superfamily member growth factors (Haudenschild et al., 2011). Therefore, we hypothesized that the supplementation of the IVB biogel with Aggrecan or COMP mimics the composition of the native cartilage extracellular matrix microenvironment, with the potential to gain control over the chondrogenic potential of the IVB.

MATERIALS AND METHODS

Recombinant Expression and Purification of COMP

Full-length recombinant human (rh)COMP was prepared as previously described (Haudenschild et al., 2011). Briefly, human COMP cDNA was cloned into a pQE mammalian expression vector (Qiagen), which was then stably transduced into human HEK293T cells. Cells were expanded in in DMEM with 10% FBS until 15 cm tissue-culture dishes were 80% confluent, then the FBS was reduced to 0.1% FBS and conditioned media collected and replenished daily for up to 1 week. COMP was purified to near homogeneity from the conditioned culture media using nickel-nitrilotriacetic acid column affinity chromatography (Ni-NTA Agarose, Qiagen). The eluted protein was buffer-exchanged into 20 mM HEPES (pH 7.0), 2 mM $CaCl_2$, and 500 mM NaCl, at approximately 500 μg/ml, with 30% glycerol added prior to storage at −80C.

Periosteum Cell Culture

As previously described (Emans et al., 2006, 2010), the periosteum was harvested from the proximal tibia of New Zealand White Rabbits and cut into small pieces using a sterile surgical blade. Post-mortem animals were obtained from an unrelated study; no ethical approval was necessary. Periosteal pieces were digested for 3 h at 37°C in collagenase II solution [300 U/ml in HEPES buffered Dulbecco's Modified Eagle Medium (DMEM; Invitrogen, Carlsbad, CA, United States) supplemented with 1% antibiotic/antimycotic (Invitrogen)] under continuous agitation. The preparation was rinsed with 0.9% NaCl over a 70 μm cell strainer and plated in culture flasks. Cells were cultured in a humidified atmosphere at 37°C, 5% CO_2 in culture medium consisting of: Minimal Essential Medium (MEM)/D-valine (Invitrogen), 10% fetal calf serum (FCS) (Sigma-Aldrich, St Louis, MO, United States), 1% antibiotic/antimycotic (Invitrogen), 1% non-essential amino acids (NEAA, Invitrogen) and 2 mM l-glutamine (Sigma-Aldrich) (Gilbert and Migeon, 1975; Jansen et al., 2008). After reaching confluence, cells were passaged 1:2 until passage 2. Passage 2 rabbit periosteal cells from 1 donor were plated at 30.000 cells/cm^2 in triplicates per condition and the next day chondrogenic differentiation was initiated by changing the culture medium to differentiation medium consisting of: Dulbecco's Modified Eagle Medium (DMEM) high glucose (Invitrogen), 10% FCS (Sigma-Aldrich), 1% antibiotic/antimycotic (Invitrogen), 1 mM sodium pyruvate (Sigma-Aldrich), 1% insulin-transferrin-selenite solution (ITS; Sigma-Aldrich), 40 μg/ml L-proline (Sigma-Aldrich), 10 ng/ml TGF-β (Invitrogen), 25 μg/ml L-ascorbic acid-2-phosphate (Sigma-Aldrich), and 100 nM dexamethasone. Glycosaminoglycan containing bovine Aggrecan from articular cartilage (Sigma-Aldrich A1960) (**Supplementary Figure S1**) was added at 2 μg/ml concentration and rhCOMP was added at 200 μg/ml. The same volume of 0.9% sodium chloride was added as a control. Differentiation medium was changed every other day and after 0 (baseline measurement) and 21 days cells were harvested for RNA isolation and ALP activity.

Chondrocytes Derived From IVB Cartilage

Cells were obtained from cartilage out of periosteum tissue generated *in vivo* in New Zealand White Rabbits (DEC2005-159) (Emans et al., 2007). The IVB cartilage tissue was harvested directly after euthanization. The autologous IVB cartilage was

separated from the periosteum by dissecting with a scalpel and the overlying fibrous tissue was carefully removed. This cartilage tissue is distinct in phenotype and consistency so risk of contamination with other tissues in the sample is negligible. Tissue was digested for 3 h at 37°C in collagenase II solution [300 U/ml in HEPES buffered DMEM/F12 (Invitrogen) supplemented with 1% antibiotic/antimycotic (Invitrogen)] under continuous agitation. The preparation was rinsed with 0.9% NaCl over a 70 μm cell strainer and plated in culture flasks. Cells were cultured in a humidified atmosphere at 37°C, 5% CO_2 in culture medium consisting of: DMEM/F12, 10% FCS, 1% antibiotic/antimycotic and 1% NEAA. After reaching confluence, cells were passaged 1:2 until passage 6. Passage 6 cells from 1 donor were plated at 30.000 cells/cm^2 in triplicates per condition and the next day chondrogenic redifferentiation was initiated by changing the culture medium to redifferentiation medium consisting of: DMEM/F12, 1% antibiotic/antimycotic, 1% NEAA, 1% ITS, 10 ng/ml TGF-β and 25 μg/ml L-ascorbic acid-2-phosphate. Bovine Aggrecan was added at a 2 μg/ml concentration and rhCOMP was added at 200 μg/ml. The same volume of 0.9% sodium chloride was added as a control. Differentiation medium was changed every other day and after 0 (baseline measurement) and 7 days cells were harvested for RNA isolation.

Animal Study

Twenty-four knees in 12 female, specific-pathogen-free (SPF) New Zealand White Rabbits were used for this experiment (Charles River Laboratories, Wilmington, MA, United States; 107 days old, ∼1.8 kg). The experiment was approved by the Maastricht University animal ethical committee (DEC 2012-151) and we confirm that all experiments were performed in accordance with relevant guidelines and regulations (ARRIVE). Throughout the experiment, animals were housed in groups under standard conditions with *ad libitum* access to water and food and 12 h of light each day. Animal well-being and behavior (score in response to stimuli, back arch, twitch, wincing, posture, self-care, condition of skin, mobility, limb loading, difficulties in respiration/breathing, dehydration or undernourishment symptoms, color of the mucous membranes and extremities, edema/swelling/cold feeling and other notable abnormalities) were checked daily. The sample size was calculated and corrected for potential dropout, and eight animals per group were included. The IVB method described by Emans and colleagues was used for ectopically inducing cartilage formation, in which a subperiosteal space is created to induce periosteal endochondral ossification (Emans et al., 2007, 2010; Janssen et al., 2017). In short, the skin was opened over the upper medial side of the tibia, the periosteum was incised just medially of the pes anserinus, leaving the semitendinosus tendon untouched. The periosteum was elevated proximally with a probe and 0.2 ml of a 2% (w/v) agarose-based gel (2 g of ultra-pure low-melting agarose granules (Cat no: 10975035, Lot No: MO91807; Invitrogen) in 100 ml of 0.9% NaCl, followed by steam-sterilization) was injected between the bone and periosteum. Bovine Aggrecan was added at a 2% w/v or rhCOMP was added at 0.5 mg/ml to the agarose-gel. The wound was closed in separate layers with Vicryl Rapide^{TM} 4–0 absorbable sutures (Ethicon, Kirkton, United Kingdom). This procedure was repeated on the contralateral tibia. After 14 days, rabbits were euthanized by an overdose of intravenous pentobarbital. The IVB cartilage tissue was harvested directly after euthanization. The autologous IVB cartilage was separated from the periosteum by dissecting with a scalpel and the overlying fibrous tissue was carefully removed. This cartilage tissue is distinct in phenotype and consistency so risk of contamination with other tissues in the sample is negligible. Generated subperiosteal cartilage tissue was analyzed for weight, glycosaminoglycan (GAG)- and DNA content. In addition, samples were taken for gene expression analysis and ALP activity assay.

Gene Expression Analysis

Cells and ectopically formed cartilage tissue on the tibia were harvested and lysed in TRIzol (Life Technologies| Thermo Fisher Scientific, Carlsbad, CA, United States). RNA isolation, RNA quantification by ultraviolet (UV) spectrometry (Biodrop; Isogen Life Sciences, Utrecht, Netherlands) and cDNA synthesis were performed as described before (Welting et al., 2011; Caron et al., 2012). Real-time quantitative PCR (RT-qPCR) was performed using Takyon No ROX Sybr® Green MasterMix blue dTTP (Eurogentec, Seraing, Belgium). A CFX96 RealTime PCR Detection system (Biorad, Hercules, CA, United States) was used for amplification with the following protocol: initial denaturation 95°C for 10 min, followed by 40 cycles of amplification (denaturation 15 s at 95°C and annealing 1 min at 60°C). Validated primer sequences used are listed in **Table 1**. Data were analyzed using the standard curve method, mRNA expression was normalized to the reference gene (28S rRNA) and gene expression was calculated as fold change as compared to baseline conditions (*in vitro* studies) or control conditions (*in vivo* study).

sGAG Assay

The total sulfated glycosaminoglycan (sGAG) content of the ectopically formed cartilage tissue was measured using a standardized modified 1,9-dimethyl methylene blue (DMMB) assay (Polysciences) (Farndale et al., 1982, 1986). The absorbance of samples was read at 540 and 595 nm using a spectrophotometer (Multiskan FC, ThermoFisher Scientific). GAG concentrations were calculated using a standard curve of chondroitin sulfate (Sigma-Aldrich). GAG content was normalized for total DNA content or wet weight of the ectopically formed cartilage tissue.

DNA Quantification

The DNA concentration was determined using SYBR® Green I Nucleic Acid stain (Invitrogen). A serially diluted standard curve of genomic control DNA (calf thymus, Invitrogen) in TE buffer (10 mM Tris/HCl pH 8.0, 1 mM EDTA) was included to quantify the DNA concentration in the samples. Before measurement, samples were diluted in TE buffer (1 μl sample and 99 μl TE buffer) and standards were prepared. SYBR®

TABLE 1 | Primer sequences for RT-qPCR.

Oligo sets	Forward	Reverse	−ΔCt in differentiated periosteal cells	−ΔCt in IVB generated chondrocytes	−ΔCt in IVB generated cartilage
Acan	CGGGACACCAACGAGACCTAT	CTGGCGACGTTGCGTAAAA	−11,48	−14,88	−16,76
Alpl	GGAGGATGTGGCCGTCTTC	CTGCGTAAGCCATCACATGAG	−14,55	−12,82	−14,09
Nkx3-2	ACCTGGCAGCTTCGCTGAA	AGGTCGGCGGCCATCT	−21,15	−19,85	−25,96
BMP2	AGAAAAGCGTCAAGCGAAACA	GTCCACGTACAAAGGGTGTCTCT	−13,04	−12,67	−19,46
Col1a1	CTGACTGGAAGAGCGGAGAGTAC	CCATGTCGCAGAAGACCTTGA	−14,19	−14,39	−13,85
Col2a1	TGGGTGTTCTATTTATTTATTGTCTTCCT	GCGTTGGACTCACACCAGTTAGT	−11,28	−10,77	−16,57
Col10a1	AACCTGGACAACAGGGACTTACA	CCATATCCTGTTTCCCCTTTCTG	−13,50	−10,59	−18,82
Cox-2	ACCAACATGATGTTTGCATTCTTT	GGTCCCCGCTTAAGATCTGTCT	−17,27	−13,32	−21,20
ID2	CCCGATGAGCCTGCTATACAA	TGGGCACCAGCTCCTTGA	−14,85	−16,21	−17,42
Mmp13	CGATGAAGACCCCAACCCTAA	ACTGGTAATGGCATCAAGGGATA	−13,65	−17,13	−18,45
PTHrP	AAGGGCAAGTCCATCCAAGA	CTCGGCGGTGTGTGGATTTC	−12,53	−14,11	−22,40
Runx2	TGATGACACTGCCACCTCTGA	GCACCTGCCTGGCTCTTCT	−18,25	−13,94	−18,23
Smad7	GCAACCCCCATCACCTTAGTC	GTTTGAGAAAATCCATTGGGTATCTG	−15,33	−13,66	−15,38
Sox9	AGTACCCGCACCTGCACAAC	CGCTTCTCGCTCTCGTTCAG	−15,03	−12,24	−17,86
TGFb3	ACTTGCACCACCTTGGACTTC	GGTCATCACCGTTGGCTCA	−15,85	−11,76	−16,00
28S rRNA	GCCATGGTAATCCTGCTCAGTAC	GCTCCTCAGCCAAGCACATAC	Reference	Reference	Reference

The 5′ to 3′ forward and reverse oligonucleotide sequences used for RT-qPCR are listed in the table. The −ΔCt values for the control condition in the in vivo IVB generated cartilage tissue, periosteal cells and IVB-derived chondrocytes are shown.

Green was diluted 10,000 times in TE buffer and 100 μl of this solution was added to 100 μl of the above-prepared samples or standards. Fluorescence was determined in standard 96-well ELISA plates in a Spectramax M2 microplate reader (Molecular Devices, Sunnyvale, CA, United States): excitation 488 nm and emission 522 nm.

ALP Activity Assay

Cells or cartilage tissues were lysed in 1.5 M Tris–HCl pH 9.0; 2% (v/v) Triton X-100 and homogenized by sonication (Soniprep 150 MSE). Insoluble material was removed by centrifugation (5 min; 13,000 × *g*; 4°C). Total protein concentration was determined BCA assay (Sigma-Aldrich). ALP enzyme activity in-time was measured by ALP-depend enzymatic conversion of p-nitrophenyl phosphate to p-nitrophenol in buffer containing 1.5 M Tris–HCl; pH 9.0, 1 mM $ZnCl_2$, 1 mM $MgCl_2$, and 7.5 mM p-nitrophenyl phosphate. Substrate conversion was spectrophotometrically quantified at 405 nm and p-nitrophenol concentrations were determined via a p-nitrophenol calibration series. Values were normalized to total protein concentration and ALP enzyme activity was calculated as mmol/min/μg.

Statistics

Statistical significance ($p < 0.05$) was determined by student's two-tailed *t*-test for *in vitro* experiments shown in **Figures 1**, **2**, and 5 using Graphpad PRISM 5.0 (La Jolla, CA, United States). Due to limited sample size (triplicates), normal distribution of input data was assumed as normality could not be reliably tested. For the *in vivo* experiment, normal distribution of input data was tested by D'Agostino-Pearson omnibus normality tests and all data from the *in vivo* study (**Figures 3**–**5**) passed the normality tests. Statistical significance ($p < 0.05$) was determined by student's two-tailed *t*-test. Lines in graphs represent mean ± standard error of the mean (SEM).

RESULTS

Addition of Aggrecan or COMP During Chondrogenic Differentiation of Periosteal Progenitor Cells Inhibits Chondrocyte Hypertrophy

As the IVB relies on chondrogenic differentiation of the local periosteum, we determined if COMP or Aggrecan could improve the chondrogenic differentiation of periosteum-derived progenitor cells *in vitro*. These two cartilage ECM components were added to the chondrogenic differentiation media of rabbit periosteal derived cells. After 21 days, differences in chondrogenic and hypertrophic gene expression were analyzed between groups. Expression of SRY (sex-determining region Y) box9 (Sox9) was significantly increased by Aggrecan (**Figure 1A**), but not significantly by COMP. No significant differences were found in the expression of Col2a1 and Aggrecan by supplementation of either Aggrecan or COMP (**Figure 1A**). In contrast, gene expression of hypertrophic markers was all significantly repressed by Aggrecan or COMP exposure during chondrogenic differentiation of periosteum cells (**Figure 1B**). Runt-related transcription factor 2 (Runx2) expression was reduced in Aggrecan and COMP conditions. Collagen type X (Col10a1) and alkaline phosphatase (Alpl) expression responded similar as Runx2, with decreased gene expression after 21 days of exposure to Aggrecan or COMP (**Figure 1B**). This inhibition of hypertrophic maturation in

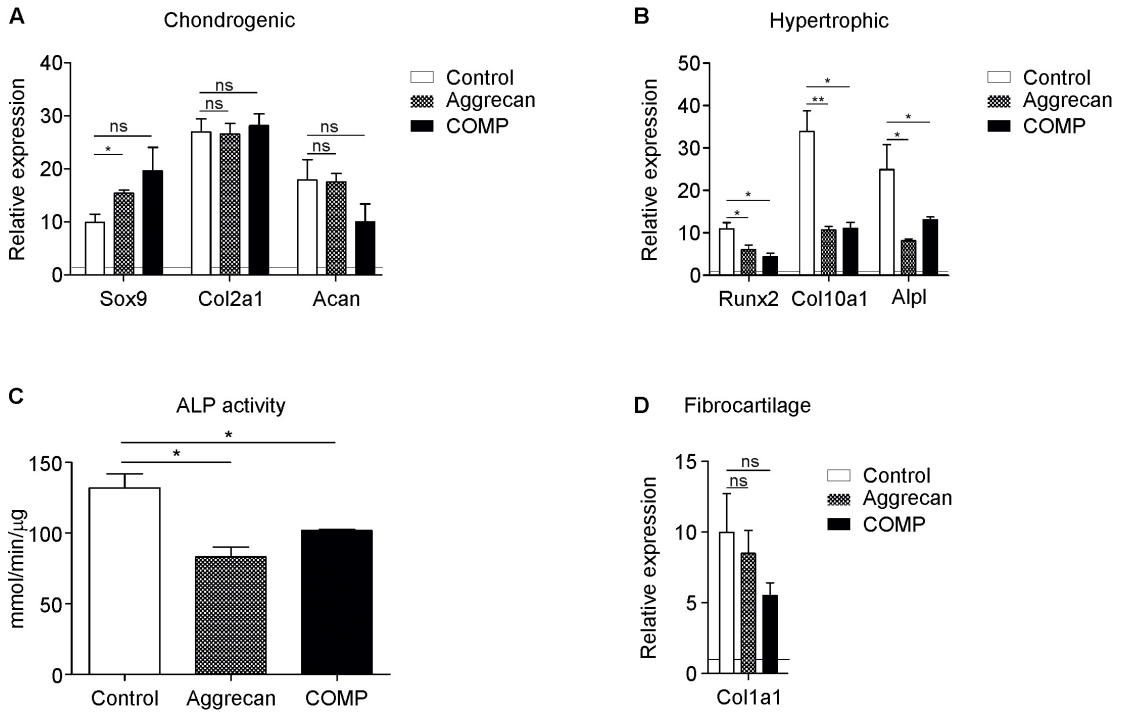

FIGURE 1 | Addition of Aggrecan or COMP during chondrogenic differentiation of rabbit periosteal cells results in decreased hypertrophic differentiation. Periosteal derived cells differentiated in chondrogenic lineage under control conditions (white bars) and with Aggrecan (2 μg/ml; dotted bars) or COMP (200 μg/ml; black bars) for 21 days. **(A)** Induction of chondrogenic markers Sox9, Col2a1, and Acan mRNA expression was determined by RT-qPCR, normalized for 28S rRNA expression and set relative to baseline ($t = 0$) values (indicated by horizontal line). **(B)** Induction of hypertrophic markers Runx2, Col10a1, and Alpl mRNA expression was determined similarly to samples from **(A)**. **(C)** ALP enzyme activity in cell lysates of same conditions was determined and normalized to total protein content. **(D)** Fibrocartilage marker Col1a1 mRNA expression as determined in similarly to from **(A)**. In graphs, error bars represent mean ± SEM. Statistically significant differences ($p < 0.05$) are shown by an *, ** = $p < 0.01$, ns = not significant.

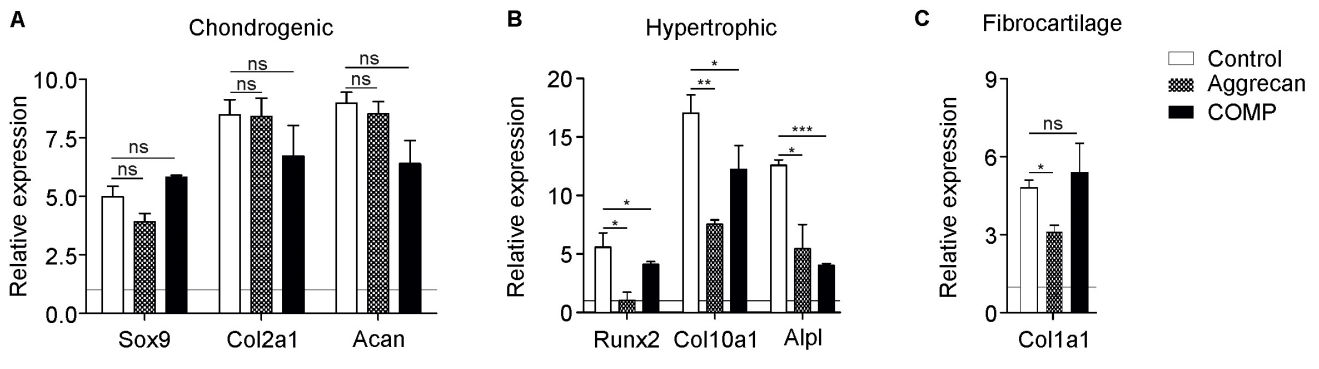

FIGURE 2 | Better cartilage quality of chondrocytes generated from periosteal tissue when exposed to Aggrecan or COMP. Chondrocytic cells derived from ectopic generated cartilage out of periosteum tissue were redifferentiated under control conditions (white bars) and with Aggrecan (2 μg/ml; dotted bars) or COMP (200 μg/ml; black bars) for 7 days. **(A)** Induction of chondrogenic markers Sox9, Col2a1, and Acan mRNA expression was determined by RT-qPCR, normalized for 28S rRNA expression and set relative to baseline ($t = 0$) values (indicated by horizontal line). **(B)** Induction of hypertrophic markers Runx2, Col10a1, and Alpl mRNA expression was determined similarly to samples from **(A). (C)** Fibrocartilage marker Col1a1 mRNA expression was determined similarly to samples from **(A)**. In graphs, error bars represent mean ± SEM. Statistically significant differences ($p < 0.05$) are shown by an *, ** = $p < 0.01$, *** = $p < 0.0001$, ns = not significant.

chondrogenic differentiation of periosteal cells by Aggrecan or COMP was further confirmed by a significant decrease in ALP enzyme activity (**Figure 1C**). No significant differences were detected for fibrotic marker collagen type I (Col1a1) expression between groups (**Figure 1D**). Collectively, these data indicate that exposure of chondrogenically differentiating periosteum cells to supplemented Aggrecan or COMP does not influence the expression of key chondrogenic markers, but specifically suppresses chondrocyte hypertrophic differentiation in these *in vitro* cell cultures.

Improved Chondrocyte Phenotype of Chondrocytes Derived From IVB Cartilage When Exposed to Aggrecan or COMP

The biogel (and additives in it) used for the IVB technique is expected to not only influence the initiation of chondrogenic differentiation but also aiding in maintaining or supporting the chondrogenic differentiation status of mature chondrocytes. Therefore, we likewise determined the effect of Aggrecan or COMP on chondrocytes that were isolated from IVB-generated cartilage from a previous *in vivo* experiment (Emans et al., 2007). After 7 days of culture with either Aggrecan or COMP, the chondrocyte phenotype was assessed by gene expression analysis. No major differences were observed in mRNA expression of chondrogenic markers Sox9, Col2a1, and Acan following the addition of Aggrecan or COMP to these cultures (**Figure 2A**). However, and in concert with results found above (**Figure 1**), the addition of Aggrecan or COMP to these cultures had a profound consequence for chondrocyte hypertrophy (**Figure 2B**). Expression of Runx2 was significantly decreased by Aggrecan or by COMP at day 7 in culture (**Figure 2B**). Significant repression of Col10A1 and Alpl was also observed following Aggrecan or COMP supplementation (**Figure 2B**). Col1a1 expression was significantly inhibited by Aggrecan in these cultures, however, not by COMP (**Figure 2C**). Together, these data indicate that Aggrecan and COMP improve the chondrocyte phenotype *in vitro* of mature chondrocytes isolated from IVB-generated cartilage by selectively decreasing chondrocyte hypertrophy.

Quality of IVB Cartilage Generated With Aggrecan or COMP Supplementation of the Biogel

We next determined if Aggrecan or COMP supplementation to the IVB biogel leads is beneficial for the quality of ectopically generated cartilage in the IVB. We used the IVB technique as described earlier (Emans et al., 2010; Janssen et al., 2017) and added either Aggrecan (2% w/v; n = 8 IVBs) or COMP (0.5 mg/ml; n = 8 IVBs) to the agarose biogel, and compared the quality of the cartilage that was generated 14 days after creation of the IVBs with a control group in which only the empty agarose biogel condition was tested (n = 8 IVBs). The wet weight of the formed IVB tissues was not significantly different between the empty agarose group versus the IVBs in which the biogel was supplemented with Aggrecan or COMP (**Figure 3A**). Also, no significant differences between the control group and Aggrecan or COMP groups were found in the DNA content of the IVB generated tissues (data not shown). When GAG content in the IVB generated tissues was determined and normalized for either DNA content or tissue wet weight, again no significant differences were found between the groups (**Figure 3B**).

To analyze the IVB-generated ectopic cartilage tissues in more bio-molecular detail we determined the expression of chondrogenic and chondrocyte hypertrophy genes. Sox9 expression in the generated cartilage tissues was not significantly different between the control and Aggrecan-supplemented or between control and COMP-supplemented groups (**Figure 4A**). Expression of Col2a1 and Acan was significantly increased in the IVBs supplemented with COMP. The IVBs supplemented with Aggrecan showed a significantly increased Col2a1 expression. However, the increase in Acan expression was not significant (**Figure 4A**). In full agreement with data obtained from above *in vitro* cultures of periosteal chondrogenesis (**Figure 1**) and the IVB-derived chondrocytes (**Figure 2**), the most profound differences in gene expression were found for chondrocyte hypertrophy genes (**Figure 4B**). Runx2, Col10a1, and Alpl expression were significantly suppressed in the IVBs supplemented with Aggrecan or COMP (**Figure 4B**). When analyzing other chondrocyte hypertrophy-associated genes such as matrix metalloproteinase 13 (MMP13) or cyclooxygenase 2 (COX-2) (Welting et al., 2011), we observed that MMP13 expression was inhibited in both the Aggrecan and COMP groups, while COX-2 expression was reduced, but not significantly (**Figure 4B**). This inhibition of hypertrophic maturation of the IVB-generated ectopic cartilage by Aggrecan or COMP was

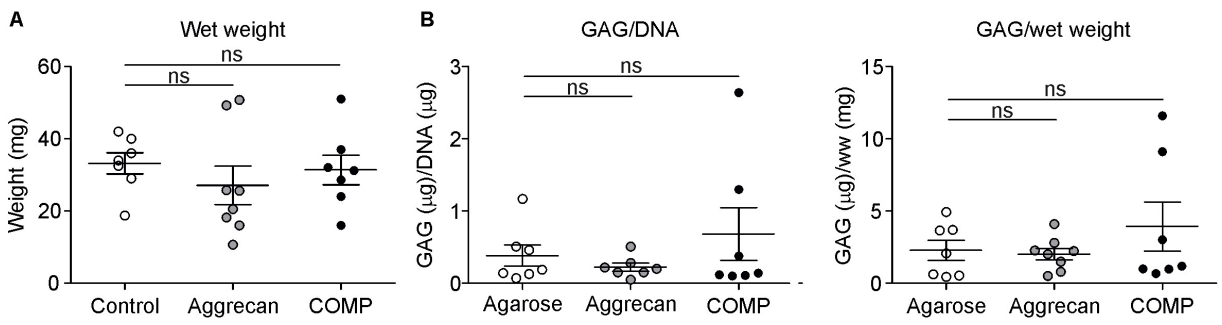

FIGURE 3 | Similar GAG content in cartilage generated out of periosteum *in vivo*. Cartilage formation was ectopically induced by injecting an agarose biogel (n = 7) with or without the addition of Aggrecan (2% w/v; n = 8) or COMP (0.5 mg/ml; n = 7) under the tibial periosteum of rabbits and after 14 days generated tissue was harvested for analysis. **(A)** Wet weight was determined for each ectopically generated cartilaginous tissue. **(B)** GAG content corrected for DNA content (left panel) or for wet weight (right panel) was determined in samples from **(A)**. Each dot represents the determined value for each of these individual generated tissues per group and lines in graphs indicate mean ± SEM. Statistically significant differences ($p < 0.05$) are shown by an *, ns = not significant.

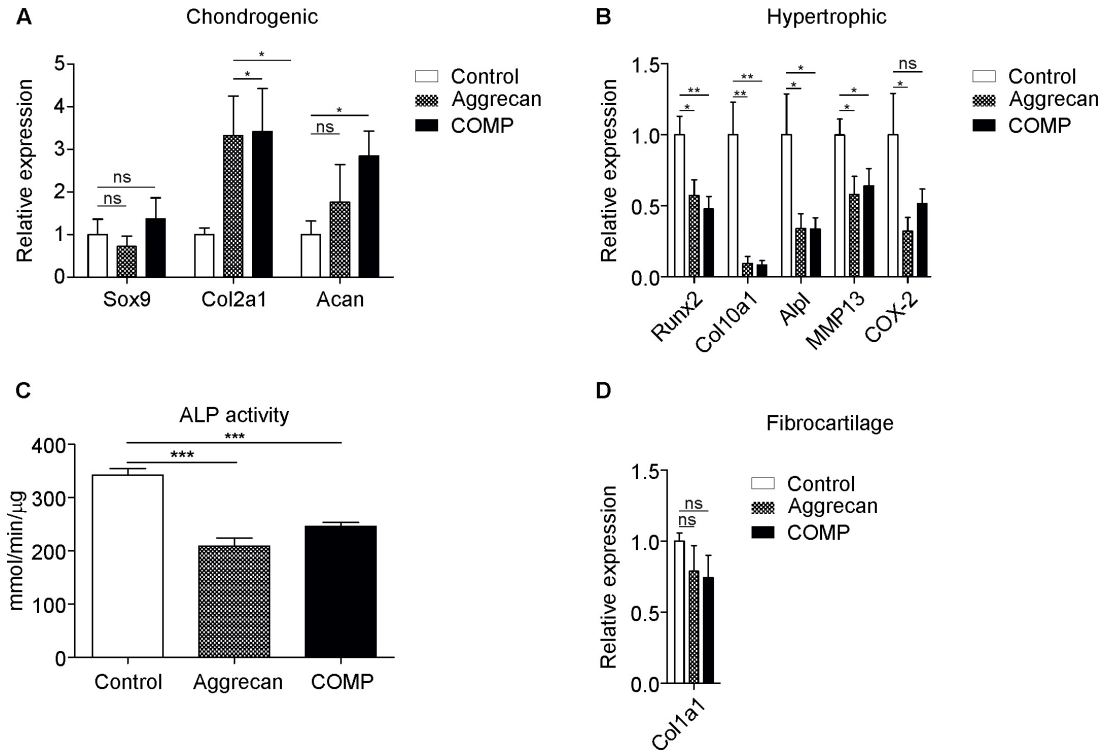

FIGURE 4 | Decreased hypertrophic marker expression in *in vivo* generated cartilage stimulated with Aggrecan or COMP. Cartilage formation was ectopically induced by injecting an agarose biogel ($n = 8$) with or without the addition Aggrecan (2% w/v; $n = 8$) or COMP (0.5 mg/ml; $n = 8$) under the tibial periosteum of rabbits and after 14 days generated tissues were harvested for gene expression analysis. **(A)** Induction of chondrogenic markers Sox9, Col2a1, and Acan mRNA expression was determined by RT-qPCR and normalized for 28S rRNA expression. **(B)** Induction of hypertrophic markers Runx2, Col10a1, and Alpl mRNA expression was determined by RT-qPCR at day 14 and normalized for 28S rRNA expression. **(C)** ALP enzyme activity in tissue lysates of same conditions was determined and normalized to total protein content. **(D)** Fibrocartilage marker Col1a1 mRNA expression as determined by RT-qPCR and normalized to 28S rRNA expression. In graphs, error bars represent mean ± SEM. Statistically significant differences ($p < 0.05$) are shown by an *, ** = $p < 0.01$, *** = $p < 0.005$, ns = not significant.

further confirmed by a significant decrease in ALP enzyme activity (**Figure 4C**). No significant differences were found for Col1a1 expression between groups (**Figure 4D**). Overall, these results demonstrate that the supplementation of Aggrecan or COMP to the IVB agarose biogel does not change the quantity or GAG content of the generated cartilaginous tissues. However, gene expression analysis shows the development of a favorable cartilage phenotype, with a specific reduction of the magnitude of chondrocyte hypertrophy in the Aggrecan and COMP groups.

Increased NKX3-2 mRNA Expression Following Aggrecan or COMP Supplementation

We next elucidated a potential biomolecular mechanism explaining the observed change in chondrogenic outcome in the chondrogenically differentiating periosteal cells, IVB-derived chondrocytes, and in the newly generated IVB tissues, as a result of exposure to Aggrecan or COMP. To this end, gene expression of important paracrine regulators (PTHrP, TGF-β3, and BMP2) of chondrogenic differentiation was determined (Kronenberg, 2003; Ripmeester et al., 2018). In addition, mRNA expression levels of Bagpipe Homeobox Protein Homolog 1 (Bapx1)/Homeobox Protein NK-3 Homolog B (NKX3-2), a transcriptional repressor of chondrocyte hypertrophic differentiation (Provot et al., 2006; Caron et al., 2013a), was determined in these samples.

At day 21 in *in vitro* chondrogenic differentiation of periosteal cells, expression of parathyroid hormone-related peptide (PTHrP), TGF-β3 and bone morphogenetic protein 2 (BMP2) was not significantly different between groups (**Figure 5A**). However, expression of NKX3-2 mRNA was significantly increased in the chondrogenic cultures supplemented with Aggrecan or COMP ($p = 0.0300$) (**Figure 5A**). Mature chondrocytes that were isolated from IVB cartilage and cultured *in vitro* for 7 days in the presence of Aggrecan or COMP did not show any significant responses of PTHrP or TGF-β3 (**Figure 5B**). Exposure of these cultures to COMP resulted in significant inhibition of BMP2 expression, while supplementation of Aggrecan to these cultures did not significantly alter BMP2 expression (**Figure 5B**). However, and similar to chondrogenesis of periosteal cells above, the gene expression of NKX3-2 was significantly increased in cultures supplemented with Aggrecan or COMP (**Figure 5B**).

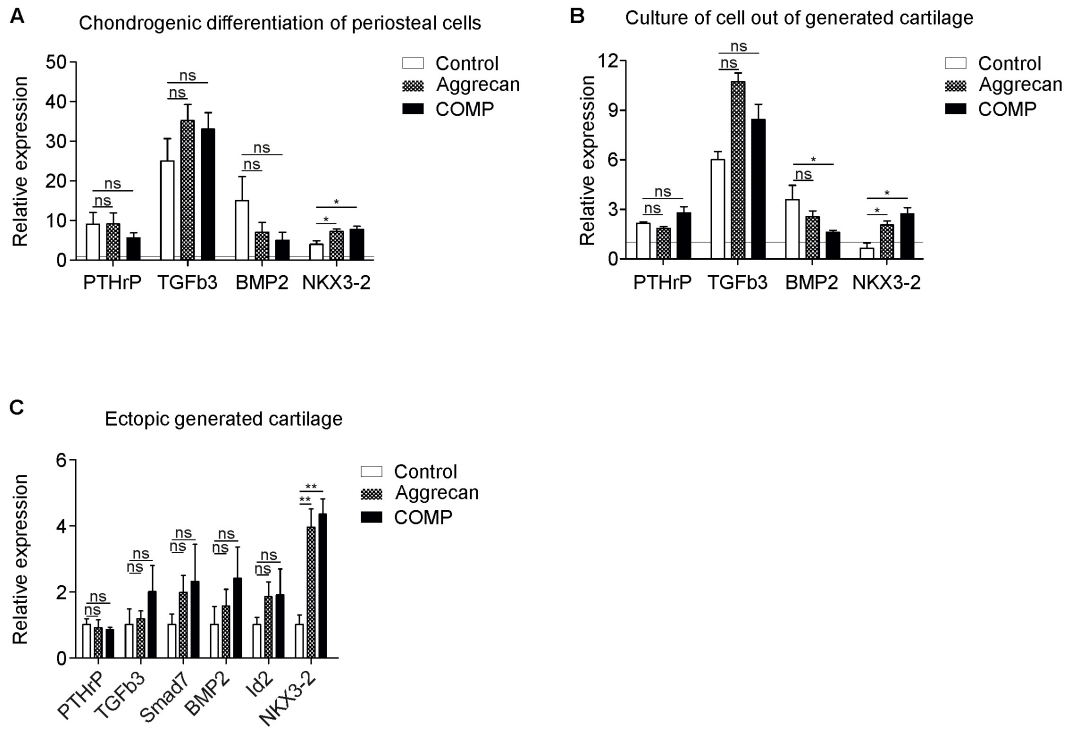

FIGURE 5 | Increased NKX3-2 mRNA expression in COMP and Aggrecan generated cartilage *in vitro* and *in vivo*. **(A)** Expression of PTHrP, TGFb3, BMP2, and NKX3-2 was determined by RT-qPCR, normalized for 28S rRNA expression and set relative to baseline ($t = 0$) values (indicated by horizontal line) in samples from **Figure 1** (chondrogenic differentiation of periosteal cells). **(B)** Expression of PTHrP, TGFb3, BMP2, and NKX3-2 was determined by RT-qPCR, normalized for 28S rRNA expression and set relative to baseline ($t = 0$) values (indicated by horizontal line) in samples from **Figure 2** (redifferentiation of cells isolated from ectopically generated cartilage). **(C)** Expression of PTHrP, TGFb3, Smad7, BMP2, Id2, NKX3-2 was determined by RT-qPCR and normalized for 28S rRNA expression in samples from **Figure 4** (ectopically generated cartilage *in vivo*). White bars represent the control condition, dotted bars the condition supplemented with Aggrecan and the black bars the condition supplemented with COMP. In graphs, error bars represent mean ± SEM. Statistically significant differences ($p < 0.05$) are shown by an *, ** = $p < 0.01$, ns = not significant.

In the *in vivo* ectopically generated IVB cartilage tissues in which the biogel was supplemented with Aggrecan or COMP, expression of PTHrP was not significantly different when compared to the control empty agarose biogel group (**Figure 5C**). Expression of TGFβ3 and TGFβ target gene Smad7 was not significantly altered in IVBs supplemented with Aggrecan or COMP (**Figure 5C**). BMP signaling, measured by BMP2 and DNA-binding protein inhibitor 2 (Id2) gene expression was not significantly different between groups (**Figure 5C**). Similar to above NKX3-2 expression data and its chondrocyte hypertrophy-suppressive action, NKX3-2 mRNA expression was significantly increased in the IVB cartilage tissues generated from biogel supplemented with Aggrecan or COMP. In conclusion, the gene expression of the chondrocyte hypertrophy transcriptional repressor NKX3-2 was significantly increased in all conditions supplemented with Aggrecan or COMP.

DISCUSSION

The goal of ectopic cartilage regeneration is to create sufficient quantity of hyaline cartilage of good quality to be used for transplantation. Limitations in quantity and progression into hypertrophy remain important drawbacks that need to be addressed in the field. In this study, we showed in three independent models that chondrogenic differentiation and cartilage homeostasis of periosteal cells *in vitro* and *in vivo* can be sustained by the supplementation of Aggrecan or COMP. It specifically leads to suppression of hypertrophic differentiation of the cartilaginous tissue, with possible involvement of NKX3-2 (Caron et al., 2013a, 2015).

Aggrecan is a key GAG-containing proteoglycan in cartilage and plays an important role in stabilizing the ECM in articular cartilage. Furthermore, due to negatively charged anionic groups of its GAG sidechains, aggrecan creates a large osmotic gradient which draws water into the tissue. This gives cartilage its unique properties (Kiani et al., 2002). Several studies have shown that articular chondrocytes and chondrogenically differentiating progenitor cells are osmolarity-responsive and increase their ECM synthesis under chondrocyte-physiological osmolarity (Urban et al., 1993; Palmer et al., 2001; Caron et al., 2013b), or after addition of oversulphated polysaccharides (Merceron et al., 2012). Likewise, plating of fibroblasts on an Aggrecan-coated surface (in the presence of TGF-β) was able to induce chondrogenic differentiation (French et al.,

2004) of these cells. We hypothesized that the addition of Aggrecan to the *in vitro* cultures of differentiating periosteal cells, IVB-derived chondrocytes and eventually also the IVB-generated cartilage tissue, would increase the chondrogenic differentiation capacity of these cells. In the *in vitro* cultures we did not observe significantly increased chondrogenic marker expression as measured by Sox9, Col2a1, and Acan, However, in the IVB-generated cartilaginous tissue, the gene expression of Col2a1 was significantly increased by Aggrecan supplementation. GAG-bound TGF-β is able to stimulate neocartilage formation (Park et al., 2008) and it was recently shown that under cartilage physiological osmolarity TGF-β signaling was increased. This was associated with an improved chondrocyte phenotype (Tan Timur et al., 2019). Indeed, also in our studies we observed increased (but not significant) TGF-β3 expression in the Aggrecan-supplemented conditions. However, we were not able to determine if the actual osmolarity of the culture conditions was significantly increased due to Aggrecan supplementation. Interestingly, in the Aggrecan-supplemented conditions we observed a significant repression of chondrocyte hypertrophy (Runx2, Col10a1, Alpl expression, and ALP enzyme activity) in all three models. These data demonstrate that periosteal chondrogenic differentiation *in vitro* and *in vivo* and homeostasis of IVB-derived chondrocytes can be influenced in a hypertrophy-suppressive manner by supplementation with Aggrecan. NKX3-2 is known as a key transcriptional repressor of Runx2 during both early and late chondrogenic differentiation (Provot et al., 2006; Rainbow et al., 2014), providing control over hypertrophic differentiation. NKX3-2 mRNA expression was significantly upregulated in the aggrecan-supplemented cultures. To the best of our knowledge, it is unknown how Aggrecan would be able to induce the expression of NKX3-2 mRNA in these cells. GAGs are described to be able to bind and regulate activity of growth factors, chemokines, cytokines and adhesion molecules (Hadler-Olsen et al., 2011). For instance, FGF and VEGF are stored, stabilized and protected from degradation in the ECM trough interactions with GAGs, and upon stimulation can be released to exert their function (Jackson et al., 1991; Vlodavsky et al., 2006). We speculate that certain NKX3-2-inducing morphogens, such as Shh, PTHrP or BMPs (Zeng et al., 2002; Provot et al., 2006; Caron et al., 2015) are being retained by the GAG-containing supplemented Aggrecan (Forsten-Williams et al., 2008), potentially potentiating their activity and leading to a hypertrophy-suppressing action via NKX3-2. Indeed, our supporting data from ATDC5 chondrogenic differentiation suggest a role for NKX3-2 in hypertrophic differentiation via specific morphogens and increased osmolarity (**Supplementary Figure S2**). However, NKX3-2 data in our present study are limited by a current lack of evidence on the protein level in periosteal cells and needs further investigation to corroborate this hypothesis.

COMP is one of the thrombospondin proteins (TSP-5) that acts as a key component in the synthesis and homeostasis of the cartilage ECM (Acharya et al., 2014). COMP is essential in chondrogenic growth plate development (DiCesare et al., 1995; Rock et al., 2010) and mutations in COMP are linked to the human skeletal disorders pseudoachondroplasia (PSACH) and multiple epiphyseal dysplasia (MED) (Briggs et al., 1995; Hecht et al., 1995). In addition, elevation of COMP levels increased chondrogenic differentiation of human bone marrow stem cells (Acharya et al., 2014). In this study, however, supplementation with COMP did not lead to significant differences in Col2a1 and Acan expression in chondrogenically differentiating periosteal cells or cultures of chondrocytes derived from IVB cartilage tissue *in vitro*. In our *in vivo* study, however, IVB biogel supplementation with COMP did significantly increase the expression of chondrogenic markers Col2a1 and Acan. In analogy with the Aggrecan supplemented condition above, supplementation with COMP significant suppressed chondrocyte hypertrophy in all three tested chondrocyte models. COMP is a homopentamer acting as a key intermolecular bridge in cartilaginous tissues (Acharya et al., 2014). COMP is described to interact with cartilage ECM proteins, including collagen type 2 and Aggrecan, and as such plays a role in matrix assembly and tissue homeostasis. COMP also interacts with endogenous growth factors, such as TGFβs and BMPs, and acts as a lattice for their presentation to cells (Haudenschild et al., 2011; Ishida et al., 2013; Acharya et al., 2014). This influences, for instance, growth factor signaling and cell differentiation processes. The activity of TGFβ1 is potentiated when bound to COMP (Haudenschild et al., 2011), potentially explaining its prochondrogenic and hypertrophy-suppressing properties in our IVB experiments. It can also be noted that COMP binds BMP7 (Haudenschild et al., 2011). Previously we reported that BMP7 suppresses chondrocyte hypertrophy in an NKX3.2 dependent fashion (Caron et al., 2013a, 2015), and we consider a BMP7 activity-potentiating role for COMP as a possible explanation for our observations. Data supporting a role for TGFβ and BMP7 in the induction of NKX3-2 levels during ATDC5 chondrogenic differentiation are presented in **Supplementary Figure S2**.

Due to a limited quantity of IVB-generated cartilage tissue in this study, we needed to select the most insightful manner of analysis. Although posing a study limitation from a histological perspective, we preferred a quantitative analysis over histology and used gene expression, GAG content, DNA content, ALP activity, and wet weight as primary read-out parameters. Also, we could only test periosteal progenitor cells and chondrocytes from periosteal cartilage from one donor each. Despite these limitations, this study demonstrates in different models that conditioning of the micro-environment with cartilage ECM components Aggrecan or COMP creates a hypertrophy-suppressive niche with prochondrogenic properties for development of cartilaginous tissue in the IVB. A more prolonged analysis of the stability of the IVB neocartilage and investigating potential synergistic consequences of COMP and Aggrecan supplementation will potentially add to the translational value of our observations. This provides novel molecular clues for the optimization of IVB cartilage graft quality for cartilage repair in particular and for endochondral ossification-based cartilage regeneration techniques in general (Emans et al., 2011, 2012). Future work should be able to address the influence of IVB cartilage graft maturation on the pre-clinical outcome of cartilage repair.

DATA AVAILABILITY STATEMENT

All datasets presented in this study are included in the article/**Supplementary Material**.

ETHICS STATEMENT

The animal study was reviewed and approved by Maastricht University animal ethical committee.

AUTHOR CONTRIBUTIONS

MC, MJ, DH, LR, PE, and TW: substantial contributions to the research design. MC, MJ, LP, AC, DS, and PE: substantial contributions to the acquisition of samples. MC, MJ, LP, AC, DS, PE, and TW: substantial contributions to analysis. MC, MJ, DH, LP, AC, DS, LR, PE, and TW: substantial contributions to the interpretation of the data, revising manuscript critically, and approval of the submitted and final versions. MC, MJ, PE, and TW: drafting the manuscript. All authors have read and approved the final submitted manuscript.

FUNDING

The authors thank the Dutch Arthritis Association (Grant LLP14) for their financial support. DH was funded by NIH/NIAMS Grant R01AR070239. The study sponsors had no involvement in study design, collection, analysis, and interpretation of data; the writing of the manuscript or in the decision to submit the manuscript for publication.

ACKNOWLEDGMENTS

The authors would like to thank the employers of the animal facility of the Maastricht University Medical Center for their assistance during this study.

SUPPLEMENTARY MATERIAL

The Supplementary Material for this article can be found online at: https://www.frontiersin.org/articles/10.3389/fbioe.2020.01036/full#supplementary-material

REFERENCES

Acharya, C., Yik, J. H., Kishore, A., Van Dinh, V., Di Cesare, P. E., and Haudenschild, D. R. (2014). Cartilage oligomeric matrix protein and its binding partners in the cartilage extracellular matrix: interaction, regulation and role in chondrogenesis. *Matrix Biol.* 37, 102–111. doi: 10.1016/j.matbio.2014.06.001

Bahney, C. S., Zondervan, R. L., Allison, P., Theologis, A., Ashley, J. W., Ahn, J., et al. (2019). Cellular biology of fracture healing. *J. Orthop. Res.* 37, 35–50. doi: 10.1002/jor.24170

Briggs, M. D., Hoffman, S. M., King, L. M., Olsen, A. S., Mohrenweiser, H., Leroy, J. G., et al. (1995). Pseudoachondroplasia and multiple epiphyseal dysplasia due to mutations in the cartilage oligomeric matrix protein gene. *Nat. Genet.* 10, 330–336. doi: 10.1038/ng0795-330

Caldwell, K. L., and Wang, J. (2014). Cell-based articular cartilage repair: the link between development and regeneration. *Osteoarthrit. Cartil.* 23, 351–362. doi: 10.1016/j.joca.2014.11.004

Caron, M. M., Emans, P. J., Coolsen, M. M., Voss, L., Surtel, D. A., Cremers, A., et al. (2012). Redifferentiation of dedifferentiated human articular chondrocytes: comparison of 2D and 3D cultures. *Osteoarthrit. Cartil.* 20, 1170–1178. doi: 10.1016/j.joca.2012.06.016

Caron, M. M., Emans, P. J., Cremers, A., Surtel, D. A., Coolsen, M. M., van Rhijn, L. W., et al. (2013a). Hypertrophic differentiation during chondrogenic differentiation of progenitor cells is stimulated by BMP-2 but suppressed by BMP-7. *Osteoarthrit. Cartil.* 21, 604–613. doi: 10.1016/j.joca.2013.01.009

Caron, M. M., Emans, P. J., Surtel, D. A., van der Kraan, P. M., van Rhijn, L. W., and Welting, T. J. (2015). BAPX-1/NKX-3.2 acts as a chondrocyte hypertrophy molecular switch in osteoarthritis. *Arthrit. Rheumatol.* 67, 2944–2956. doi: 10.1002/art.39293

Caron, M. M., van der Windt, A. E., Emans, P. J., van Rhijn, L. W., Jahr, H., and Welting, T. J. (2013b). Osmolarity determines the in vitro chondrogenic differentiation capacity of progenitor cells via nuclear factor of activated T-cells 5. *Bone* 53, 94–102. doi: 10.1016/j.bone.2012.11.032

Caron, M. M., Welting, T. J., van Rhijn, L. W., and Emans, P. J. (2014). "Targetting inflammatory processes for optimization of cartilage homeostasis and tissue repair techniques," in *ICRS: Developing Insights in Cartilage Repair*, eds L. Peterson and P. J. Emans (London: Springer), doi: 10.1007/978-1-4471-5385-6_3

DiCesare, P. E., Morgelin, M., Carlson, C. S., Pasumarti, S., and Paulsson, M. (1995). Cartilage oligomeric matrix protein: isolation and characterization from human articular cartilage. *J. Orthop. Res.* 13, 422–428. doi: 10.1002/jor.1100130316

Emans, P. J., Caron, M. M., van Rhijn, L. W., and Welting, T. J. (2012). "Endochondral bone formation as blueprint for regenerative medicine," in *Tissue Regeneration - From Basic Biology to Clinical Application*, ed. P. J. Davies (London: InTechopen), doi: 10.5772/27724

Emans, P. J., Caron, M. M. J., van Rhijn, L. W., Shastri, V. P., and Welting, T. J. M. (2011). Cartilage tissue engineering; lessons learned from periosteum. *Tissue Sci. Eng.* S2:002. doi: 10.4172/2157-7552.S2-002

Emans, P. J., Pieper, J., Hulsbosch, M. M., Koenders, M., Kreijveld, E., Surtel, D. A., et al. (2006). Differential cell viability of chondrocytes and progenitor cells in tissue-engineered constructs following implantation into osteochondral defects. *Tissue Eng.* 12, 1699–1709. doi: 10.1089/ten.2006.12.1699

Emans, P. J., Spaapen, F., Surtel, D. A., Reilly, K. M., Cremers, A., van Rhijn, L. W., et al. (2007). A novel in vivo model to study endochondral bone formation; HIF-1alpha activation and BMP expression. *Bone* 40, 409–418. doi: 10.1016/j.bone.2006.08.005

Emans, P. J., van Rhijn, L. W., Welting, T. J., Cremers, A., Wijnands, N., Spaapen, F., et al. (2010). Autologous engineering of cartilage. *Proc. Natl. Acad. Sci. U.S.A.* 107, 3418–3423. doi: 10.1073/pnas.0907774107

Farndale, R. W., Buttle, D. J., and Barrett, A. J. (1986). Improved quantitation and discrimination of sulphated glycosaminoglycans by use of dimethylmethylene blue. *Biochim. Biophys. Acta* 883, 173–177. doi: 10.1016/0304-4165(86)90306-5

Farndale, R. W., Sayers, C. A., and Barrett, A. J. (1982). A direct spectrophotometric microassay for sulfated glycosaminoglycans in cartilage cultures. *Connect. Tissue Res.* 9, 247–248. doi: 10.3109/03008208209160269

Forsten-Williams, K., Chu, C. L., Fannon, M., Buczek-Thomas, J. A., and Nugent, M. A. (2008). Control of growth factor networks by heparan sulfate proteoglycans. *Ann. Biomed. Eng.* 36, 2134–2148. doi: 10.1007/s10439-008-9575-z

French, M. M., Rose, S., Canseco, J., and Athanasiou, K. A. (2004). Chondrogenic differentiation of adult dermal fibroblasts. *Ann. Biomed. Eng.* 32, 50–56. doi: 10.1023/b:abme.0000007790.65773.e0

Gilbert, S. F., and Migeon, B. R. (1975). D-valine as a selective agent for normal human and rodent epithelial cells in culture. *Cell* 5, 11–17. doi: 10.1016/0092-8674(75)90086-0

Hadler-Olsen, E., Fadnes, B., Sylte, I., Uhlin-Hansen, L., and Winberg, J. O. (2011). Regulation of matrix metalloproteinase activity in health and disease. *FEBS J.* 278, 28–45. doi: 10.1111/j.1742-4658.2010.07920.x

Haudenschild, D. R., Hong, E., Yik, J. H., Chromy, B., Morgelin, M., Snow, K. D., et al. (2011). Enhanced activity of transforming growth factor beta1 (TGF-beta1) bound to cartilage oligomeric matrix protein. *J. Biol. Chem.* 286, 43250–43258. doi: 10.1074/jbc.M111.234716

Hecht, J. T., Nelson, L. D., Crowder, E., Wang, Y., Elder, F. F., Harrison, W. R., et al. (1995). Mutations in exon 17B of cartilage oligomeric matrix protein (COMP) cause pseudoachondroplasia. *Nat. Genet.* 10, 325–329. doi: 10.1038/ng0795-325

Hunziker, E. B. (2002). Articular cartilage repair: basic science and clinical progress. A review of the current status and prospects. *Osteoarthrit. Cartil.* 10, 432–463. doi: 10.1053/joca.2002.0801

Ishida, K., Acharya, C., Christiansen, B. A., Yik, J. H., DiCesare, P. E., and Haudenschild, D. R. (2013). Cartilage oligomeric matrix protein enhances osteogenesis by directly binding and activating bone morphogenetic protein-2. *Bone* 55, 23–35. doi: 10.1016/j.bone.2013.03.007

Jackson, R. L., Busch, S. J., and Cardin, A. D. (1991). Glycosaminoglycans: molecular properties, protein interactions, and role in physiological processes. *Physiol. Rev.* 71, 481–539. doi: 10.1152/physrev.1991.71.2.481

Jansen, E. J., Emans, P. J., Guldemond, N. A., van Rhijn, L. W., Welting, T. J., Bulstra, S. K., et al. (2008). Human periosteum-derived cells from elderly patients as a source for cartilage tissue engineering? *J. Tissue Eng. Regen. Med.* 2, 331–339. doi: 10.1002/term.100

Janssen, M. P., Caron, M. M., van Rietbergen, B., Surtel, D. A., van Rhijn, L. W., Welting, T. J., et al. (2017). Impairment of the chondrogenic phase of endochondral ossification in vivo by inhibition of cyclooxygenase-2. *Eur. Cell Mater.* 34, 202–216. doi: 10.22203/eCM.v034a13

Kiani, C., Chen, L., Wu, Y. J., Yee, A. J., and Yang, B. B. (2002). Structure and function of aggrecan. *Cell Res.* 12, 19–32. doi: 10.1038/sj.cr.7290106

Kronenberg, H. M. (2003). Developmental regulation of the growth plate. *Nature* 423, 332–336. doi: 10.1038/nature01657

Mankin, H., Mow, V., and Buckwalter, J. (2000). *Articular Cartilage Structure, Composition, and Function*. Rosemont, IL: AAOS.

Merceron, C., Portron, S., Vignes-Colombeix, C., Rederstorff, E., Masson, M., Lesoeur, J., et al. (2012). Pharmacological modulation of human mesenchymal stem cell chondrogenesis by a chemically oversulfated polysaccharide of marine origin: potential application to cartilage regenerative medicine. *Stem Cells* 30, 471–480. doi: 10.1002/stem.1686

Mollenhauer, J. A., and Erdmann, S. (2002). Introduction: molecular and biomechanical basis of osteoarthritis. *Cell Mol. Life Sci.* 59, 3–4. doi: 10.1007/s00018-002-8399-5

Moreira-Teixeira, L. S., Georgi, N., Leijten, J., Wu, L., and Karperien, M. (2011). Cartilage tissue engineering. *Endocr. Dev.* 21, 102–115. doi: 10.1159/000328140

Nakahara, H., Bruder, S. P., Goldberg, V. M., and Caplan, A. I. (1990). In vivo osteochondrogenic potential of cultured cells derived from the periosteum. *Clin. Orthop. Relat. Res.* 259, 223–232.

Palmer, G. D., Chao, P. H., Raia, F., Mauck, R. L., Valhmu, W. B., and Hung, C. T. (2001). Time-dependent aggrecan gene expression of articular chondrocytes in response to hyperosmotic loading. *Osteoarthrit. Cartil.* 9, 761–770. doi: 10.1053/joca.2001.0473

Park, J. S., Woo, D. G., Yang, H. N., Lim, H. J., Chung, H. M., and Park, K. H. (2008). Heparin-bound transforming growth factor-beta3 enhances neocartilage formation by rabbit mesenchymal stem cells. *Transplantation* 85, 589–596. doi: 10.1097/TP.0b013e3181639b3a

Poole, A. R., Kojima, T., Yasuda, T., Mwale, F., Kobayashi, M., and Laverty, S. (2001). Composition and structure of articular cartilage: a template for tissue repair. *Clin. Orthop. Relat. Res.* 391(Suppl.), S26–S33.

Provot, S., Kempf, H., Murtaugh, L. C., Chung, U. I., Kim, D. W., Chyung, J., et al. (2006). Nkx3.2/Bapx1 acts as a negative regulator of chondrocyte maturation. *Development* 133, 651–662. doi: 10.1242/dev.02258

Rainbow, R. S., Won, H. K., and Zeng, L. (2014). The role of Nkx3.2 in chondrogenesis. *Front. Biol.* 9, 376–381. doi: 10.1007/s11515-014-1321-3

Ripmeester, E. G. J., Timur, U. T., Caron, M. M. J., and Welting, T. J. M. (2018). Recent insights into the contribution of the changing hypertrophic chondrocyte phenotype in the development and progression of osteoarthritis. *Front. Bioeng. Biotechnol.* 6:18. doi: 10.3389/fbioe.2018.00018

Rock, M. J., Holden, P., Horton, W. A., and Cohn, D. H. (2010). Cartilage oligomeric matrix protein promotes cell attachment via two independent mechanisms involving CD47 and alphaVbeta3 integrin. *Mol. Cell Biochem.* 338, 215–224. doi: 10.1007/s11010-009-0355-3

Roughley, P. J., and Mort, J. S. (2014). The role of aggrecan in normal and osteoarthritic cartilage. *J. Exp. Orthop.* 1:8. doi: 10.1186/s40634-014-0008-7

Tan Timur, U., Caron, M., van den Akker, G., van der Windt, A., Visser, J., van Rhijn, L., et al. (2019). Increased TGF-beta and BMP levels and improved chondrocyte-specific marker expression in vitro under cartilage-specific physiological osmolarity. *Int. J. Mol. Sci.* 20:795. doi: 10.3390/ijms20040795

Urban, J. P., Hall, A. C., and Gehl, K. A. (1993). Regulation of matrix synthesis rates by the ionic and osmotic environment of articular chondrocytes. *J. Cell Physiol.* 154, 262–270. doi: 10.1002/jcp.1041540208

Vlodavsky, I., Abboud-Jarrous, G., Elkin, M., Naggi, A., Casu, B., Sasisekharan, R., et al. (2006). The impact of heparanese and heparin on cancer metastasis and angiogenesis. *Pathophysiol. Haemost. Thromb.* 35, 116–127. doi: 10.1159/000093553

Welting, T. J., Caron, M. M., Emans, P. J., Janssen, M. P., Sanen, K., Coolsen, M. M., et al. (2011). Inhibition of cyclooxygenase-2 impacts chondrocyte hypertrophic differentiation during endochondral ossification. *Eur. Cell Mater.* 22, 420–436.

Zeng, L., Kempf, H., Murtaugh, L. C., Sato, M. E., and Lassar, A. B. (2002). Shh establishes an Nkx3.2/Sox9 autoregulatory loop that is maintained by BMP signals to induce somitic chondrogenesis. *Genes Dev.* 16, 1990–2005. doi: 10.1101/gad.1008002

Conflict of Interest: TW and MC are listed as inventor on patents: WO2017178251, WO2017178253, and US 20130123314. TW, PE, and LR have shares in Chondropeptix BV and are CSO, CMO, and CDO of Chondropeptix, respectively. DH is listed as inventor on US patent 9,133,259 and is President and CSO of Tesio Pharmaceuticals Inc.

The remaining authors declare that the research was conducted in the absence of any commercial or financial relationships that could be construed as a potential conflict of interest.

frontiers in Bioengineering and Biotechnology

ORIGINAL RESEARCH
published: 14 October 2020
doi: 10.3389/fbioe.2020.579751

Gene Expression Signatures of Synovial Fluid Multipotent Stromal Cells in Advanced Knee Osteoarthritis and Following Knee Joint Distraction

*Clara Sanjurjo-Rodriguez[1,2], Ala Altaie[1], Simon Mastbergen[3], Thomas Baboolal[1], Tim Welting[4], Floris Lafeber[3], Hemant Pandit[1,5], Dennis McGonagle[1,5] and Elena Jones[1]**

[1] Leeds Institute of Rheumatic and Musculoskeletal Medicine, University of Leeds, Leeds, United Kingdom, [2] Physiotherapy, Medicine and Biomedical Sciences department, CIBER-BBN, Institute of Biomedical Research of A Coruña (INIBIC)-Centre of Advanced Scientific Researches (CICA), University of A Coruña, A Coruña, Spain, [3] University Medical Center Utrecht, Rheumatology & Clinical Immunology, Regenerative Medicine Center Utrecht, Utrecht University, Utrecht, Netherlands, [4] Laboratory for Experimental Orthopedics, Department of Orthopedic Surgery, Maastricht University Medical Center, Maastricht, Netherlands, [5] NIHR Leeds Musculoskeletal Biomedical Research Centre, Leeds, United Kingdom

OPEN ACCESS

Edited by:
Roberta Tasso, University of Genoa, Italy

Reviewed by:
Susanne Grässel, University of Regensburg, Germany
Ryan Michael Porter, College of Medicine, University of Arkansas for Medical Sciences, United States

***Correspondence:**
Elena Jones
e.jones@leeds.ac.uk

Specialty section:
This article was submitted to Preclinical Cell and Gene Therapy, a section of the journal Frontiers in Bioengineering and Biotechnology

Received: *03 July 2020*
Accepted: *16 September 2020*
Published: *14 October 2020*

Citation:
Sanjurjo-Rodriguez C, Altaie A, Mastbergen S, Baboolal T, Welting T, Lafeber F, Pandit H, McGonagle D and Jones E (2020) Gene Expression Signatures of Synovial Fluid Multipotent Stromal Cells in Advanced Knee Osteoarthritis and Following Knee Joint Distraction. Front. Bioeng. Biotechnol. 8:579751. doi: 10.3389/fbioe.2020.579751

Osteoarthritis (OA) is the most common musculoskeletal disorder. Although joint replacement remains the standard of care for knee OA patients, knee joint distraction (KJD), which works by temporarily off-loading the joint for 6–8 weeks, is becoming a novel joint-sparing alternative for younger OA sufferers. The biological mechanisms behind KJD structural improvements remain poorly understood but likely involve joint-resident regenerative cells including multipotent stromal cells (MSCs). In this study, we hypothesized that KJD leads to beneficial cartilage-anabolic and anti-catabolic changes in joint-resident MSCs and investigated gene expression profiles of synovial fluid (SF) MSCs following KJD as compared with baseline. To obtain further insights into the effects of local biomechanics on MSCs present in late OA joints, SF MSC gene expression was studied in a separate OA arthroplasty cohort and compared with subchondral bone (SB) MSCs from medial (more loaded) and lateral (less loaded) femoral condyles from the same joints. In OA arthroplasty cohort (n = 12 patients), SF MSCs expressed lower levels of ossification- and hypotrophy-related genes [bone sialoprotein (IBSP), parathyroid hormone 1 receptor (PTH1R), and runt-related transcription factor 2 (RUNX2)] than did SB MSCs. Interestingly, SF MSCs expressed 5- to 50-fold higher levels of transcripts for classical extracellular matrix turnover molecules matrix metalloproteinase 1 (MMP1), a disintegrin and metalloproteinase with thrombospondin motifs 5 (ADAMTS5), and tissue inhibitor of metalloproteinase-3 (TIMP3), all ($p < 0.05$) potentially indicating greater cartilage remodeling ability of OA SF MSCs, compared with SB MSCs. In KJD cohort (n = 9 patients), joint off-loading resulted in sustained, significant increase in SF MSC colonies' sizes and densities and a notable transcript upregulation of key cartilage core protein aggrecan (ACAN) (weeks 3 and 6), as well as reduction in pro-inflammatory C–C motif chemokine ligand 2 (CCL2) expression

(weeks 3 and 6). Additionally, early KJD changes (week 3) were marked by significant increases in MSC chondrogenic commitment markers gremlin 1 (GREM1) and growth differentiation factor 5 (GDF5). In combination, our results reveal distinct transcriptomes on joint-resident MSCs from different biomechanical environments and show that 6-week joint off-loading leads to transcriptional changes in SF MSCs that may be beneficial for cartilage regeneration. Biomechanical factors should be certainly considered in the development of novel MSC-based therapies for OA.

Keywords: multipotent stromal cells, synovial fluid, osteoarthritis, knee joint distraction, subchondral bone, chondrocytes

INTRODUCTION

Multipotent stromal cells (MSCs), originally termed as mesenchymal stem cells, are present in different joint structures including the synovial membrane, synovial fluid (SF), infrapatellar fat pad, ligaments/tendons, and the subchondral bone (SB) (Fellows et al., 2016; McGonagle et al., 2017). Several studies have also described the presence of MSC-like chondrogenic progenitor cells (CPCs) in the articular cartilage (Schminke and Miosge, 2014; Jayasuriya et al., 2018). SF MSCs are a particularly intriguing class of joint-resident MSCs, as unlike other MSCs, they are not attached to other cells or surfaces but instead are suspended in a viscous hyaluronan-rich SF (Jones et al., 2004; Baboolal et al., 2016; Fang et al., 2020). In healthy individuals, they are believed to be shed from the synovial intimal layer or superficial cartilage, as a result of mechanical attrition during joint movement (Jones et al., 2008; Morito et al., 2008; Lee et al., 2012; Matsukura et al., 2014). Healthy SF MSCs are highly proliferative and consistently chondrogenic (Jones et al., 2008; Katagiri et al., 2017). Combined with their ease of harvesting, despite their limited numbers, they are considered as an attractive MSC source for repairing focal osteochondral defects and potentially, joint regeneration in osteoarthritis (OA), acting via direct differentiation (McGonagle et al., 2017; Piñeiro-Ramil et al., 2017) as well as paracrine mechanisms (Garcia et al., 2016).

On the other hand, MSCs present in the SB are accessible through subchondral plate perforation and are believed to be responsible for limited cartilage regeneration following microfracture treatment of focal cartilage lesions (Dwivedi et al., 2018). In our previous work, we investigated SB MSCs in advanced knee OA and compared MSCs from the medial, commonly weight-bearing compartment, with the lateral side of the joint (Sanjurjo-Rodriguez et al., 2019). This work used collagenase-assisted release of MSCs from subchondral trabecular bone surfaces and marrow-filled bone cavities and demonstrated large MSC numbers in both lateral and medial femoral condyles. However, in more damaged, medial condyles, SB MSCs expressed higher levels of ossification-related genes compared with less-damaged lateral condyles, indicating their preference for sclerotic bone formation rather than cartilage restoration and highlighting key contribution on joint biomechanics in MSC pathophysiology in OA (Sanjurjo-Rodriguez et al., 2019). These findings are in line with previous OA animal model studies as well as our previous work on human hip OA that showed an aberrant osteogenesis of MSCs in OA SB (Zhen et al., 2013; Ilas et al., 2019, 2020).

Multipotent stromal cells numbers are increased in OA SF (Jones et al., 2008), in direct correlation with disease severity (Jones et al., 2008; Sekiya et al., 2012; Harris et al., 2013; Kim et al., 2015). This has been assumed to represent joint's repair attempt, but the source of these additional MSCs and their cartilage-supportive properties remains unclear. We and others have previously proposed that additional MSCs are shed from the synovium and accumulate inside the fluid (Jones et al., 2008; Katagiri et al., 2017), as a result of their enhanced proliferation and possibly, reduced attachment to joint structures (Jones et al., 2008; Harris et al., 2013). Another possibility is that at least a subset of these OA SF MSCs is liberated from the damaged articular cartilage, which is the prime "victim" of tissue destruction in OA (Katagiri et al., 2017). The presence of "migratory CPCs" in deep OA articular cartilage has been previously described (Koelling et al., 2009), and these CPCs may in principle enter the joint space via cracks and fissures in degenerated cartilage. In the very advanced OA stages, additional MSCs may also originate from the progressively exposed SB (Koelling et al., 2009; Iijima et al., 2016).

Knee joint distraction (KJD) is an emerging treatment for OA (Takahashi et al., 2019; Jansen et al., 2020), which is associated with impressive structural and clinical outcomes (van der Woude et al., 2017a; Jansen et al., 2018). It works by simply taking the load off the joint by surgically pulling the joint apart using an external fixation frame, which is placed on both sides of the joint, allowing distraction for a few millimeters for up to 6–8 weeks (van der Woude et al., 2017a). It is considered a good treatment option for the younger OA subjects in whom replacement might be premature and more likely to result in early failure (Schreurs and Hannink, 2017). Patients with established OA demonstrate improved knee symptoms for 5 to 9 years after the KJD (van der Woude et al., 2017b; Jansen et al., 2018). The 6-week period of the off-load leads to apparent cartilage regeneration, with increase in joint space width (JSW) on X-ray and increased articular cartilage thickness on magnetic resonance imaging (MRI) (Wiegant et al., 2013; Jansen et al., 2018, 2019). First-year minimum JSW on radiographs and cartilage thickness increase on MRI are predictive of the 9-year results (Jansen et al., 2018). As such, the initial cartilage repair activity appears to be important for long-term clinical success. This suggests that, by

temporarily off-loading the joint, KJD might trigger the intrinsic cartilaginous repair, which may be facilitated by SF MSCs. Indeed, in the canine groove model of OA, we showed that MSCs injected in the SF, following KJD, were capable of integrating into cartilage injury sites (Baboolal et al., 2016). Furthermore, a recent study provided evidence for anabolic molecular responses in SF following KJD, which may act on SF MSCs and represent potential pathways for cartilage regeneration (Watt et al., 2020).

Based on the fact that SF MSCs and SB MSCs may be present endogenously at sites of cartilage damage in OA, and that denuded bone may serve as a potential source of SF MSCs in advanced OA, we compared their gene expression signatures and assessed the MSC specificity of differentially expressed transcripts by comparing them with cultured chondrocytes from the same joints. We hypothesized that in comparison with SB MSCs, SF MSCs that are highly chondrogenic in healthy individuals may be a better MSC population for endogenous manipulation and cartilage regeneration in OA and that following KJD, their gene expression signature may change in favor of cartilage regeneration. The aims of this study were therefore to investigate gene expression signatures of SF MSCs in advanced knee OA, in comparison with SB MSCs from the same joints, and to investigate gene expression changes in SF MSCs following KJD.

MATERIALS AND METHODS

Patients and Samples

This study was performed in compliance with the Declaration of Helsinki of ethical principles for medical research involving human subjects. Ethical approval was obtained from the Yorkshire & The Humber–South Yorkshire Research Ethics Committee (14/YH/0087). For KJD study, ethical approval was obtained from the medical ethical review committee of the University Medical Center Utrecht (#15-160/D; NL51539.041.15).

Twelve patients who underwent total knee arthroplasty (median age 72 years, range 61–83; seven women and five men) were recruited after informed written consent was given, and both lateral and medial femoral condyle samples were transferred to the laboratory (**Supplementary Figure 1A**). From six patients (median age 80 years, range 64–83; three men and three women), donor-matched SFs were also collected using a syringe, after opening the joint cavity for the arthroplasty.

Patients with established symptomatic radiographic knee OA undergoing KJD gave written informed consent to participate (n = 9, median 51 age years, range 35–60; two men and seven women). SF was sampled at baseline (before distraction; pre), during (3 weeks; during), and at endpoint of distraction (6 weeks; post).

Tissue Processing for Multipotent Stromal Cell and Chondrocyte Isolation

Multipotent Stromal Cell Isolation and Expansion

For isolation of MSCs from SF, the fluid was diluted 1:4 in phosphate-buffered saline (PBS) and centrifuged 500 × g for 10 min, and pelleted cells were seeded in T25 flasks with StemMACS MSC Expansion Media (Miltenyi Biotec, Germany) supplemented with 1% penicillin/streptomycin (P/S; Thermo Fisher Scientific).

For SB MSC isolation, following cartilage removal using a scalpel, bone from the separate medial and lateral condyles was mechanically minced into small fragments with a rongeur and digested with 3,000 units of collagenase/g of tissue (Worthington Biochem Corp., United States) for 4 h (**Supplementary Figure 1A**), as previously described (Sanjurjo-Rodriguez et al., 2019). The supernatant was filtered through 22-μm cell strainer (Corning Inc., United States) before centrifugation at 450 × g for 10 min to pellet the extracted cells. After being counted, the cells were seeded for culture expansion at the seeding density of 4.0×10^4 cells/cm^2 in flasks containing StemMACS MSC Expansion Media supplemented with 1% P/S.

Media were changed twice a week, and cells were split when 80% confluence was reached for both types of MSCs. Part of passage 1 SB and SF MSCs were used for gene expression study, and passage 3–5 SF cells were used for MSC characterization. Accrued population doublings (PDs) and PD rates were calculated as previously described (Churchman et al., 2012).

Chondrocyte Isolation and Expansion

All articular cartilage was harvested from the lateral and medial condyle surfaces using a scalpel, and chondrocytes were isolated as described before and kept separate (Sanjurjo-Rodriguez et al., 2019). We were interested to see whether the nature of cells (MSCs versus chondrocytes) or their loading environment (medial versus lateral) had a stronger effect on their gene expression. Briefly, cartilage was minced using a scalpel and digested overnight with 3,000 units of collagenase/g of tissue, and the homogenate was filtered with 22-μm cell strainer. The supernatant containing cells was centrifuged at 450 × g for 10 min, cell pellet was digested 5 min with 1 × trypsin Thermo Fisher Scientific, United States), and the cells were seeded into flasks (Corning Inc.) in Dulbecco's modified Eagle's medium (DMEM; Thermo Fisher Scientific) with 10% fetal bovine serum (FBS; BioSera, France) and 1% P/S at the seeding density of 1.2×10^4 cells/cm^2. Media were changed every 3–4 days, and subculture was performed when cells reached 80% confluence. Passage 1-cultured chondrocytes were used for gene expression analysis as controls for SB and SF MSCs.

Colony-Forming Unit-Fibroblast Assay

Synovial fluid samples were diluted 1:4 in sterile PBS and thoroughly mixed before centrifuging at 500 × g for 5 min. Cells were resuspended in 1 ml of warmed StemMACS MSC Expansion media (Miltenyi Biotec, Germany) supplemented with P/S. Next, cells were diluted with 9 ml of StemMACS media to a final volume of 10 ml. Samples were plated in duplicate on colony-forming unit-fibroblast (CFU-F) dishes (60 mm) by adding 3 ml of the sample and an additional 2 ml of StemMACS to final volume of 5 ml per dish. The remaining sample (∼4 ml) was used for MSC expansion and mRNA analysis. Subsequently, the dishes were incubated at 37°C and 5% CO_2 in a humidified incubator. After 2–3 days, the media were removed and replaced with fresh StemMACS media. Thereafter, half of the media (2.5 ml) were

refreshed twice weekly. After 14 days, all media were removed, and cells fixed with 3.7% formalin (buffered with PBS) for 30 min at room temperature. Formalin was removed, and the dishes were gently washed with water.

The fixed dishes were stained with methylene blue for CFU-F counting and were scanned for CFU-F area and integrated density (ID) analysis, as previously described (Ganguly et al., 2019; Sanjurjo-Rodriguez et al., 2019). Briefly, scanned images were converted to 8-bit format, calibrated, and analyzed using ImageJ software. Colony area and ID were measured independently in all colonies after thresholding.

Synovial Fluid Multipotent Stromal Cell Characterization

Characterization of SF MSCs was performed following the minimal criteria from International Society for Cellular Therapy (ISCT) (Dominici et al., 2006).

Surface Marker Expression

Synovial fluid MSCs from three randomly selected donors were characterized by flow cytometry according to the ISCT criteria. The antibodies used were CD90-FITC (AbD Serotec, Kidlington, UK), CD73-PE and CD105-PE (both from BD Biosciences, Wokingham, UK) (MSC positive markers) and CD19-FITC, CD14-PE, CD34-PE, CD45-V450, and HLA-DR-fluorescein isothiocyanate (FITC) (hematopoietic lineage markers) (all from BD Biosciences). A minimum of 10,000 cell events per tube was acquired using Attune flow cytometer (Applied Biosystems). Data were analyzed using FlowJo (BD), and the results are expressed as percentage of positive cells.

Tri-Lineage Differentiation and Motility Assay

Tri-lineage differentiation was performed on the same cultures, as described before (Sanjurjo-Rodriguez et al., 2019). Briefly, SF MSCs were seeded in 24-well plates (Corning) for adipogenic and osteogenic differentiation. Cells were cultured in adipogenic media containing DMEM supplemented with 12.5% FBS, 12.5% horse serum, 0.5 mM of isobutylmethylxanthine, 60 μM of indomethacin, and 0.5 mM of hydrocortisone (all from Sigma) for 21 days; and adipogenesis was assessed by Oil Red O staining. Osteogenesis was assessed by Alizarin Red staining after 21-day culture in osteogenic media containing DMEM supplemented with 10% FBS, 100 nM of dexamethasone, 0.05 mM of ascorbic acid, and 100 mM of β-glycerosphosphate (all from Sigma).

Chondrogenic differentiation was performed with ChondroDiff media (Miltenyi Biotec) in a three-dimensional (3D) pellet culture for 21 days. Toluidine blue staining was performed in 5-μm paraffin-sectioned pellets to evaluate glycosaminoglycan (GAG) content.

In vitro motility of SB and SF MSCs was assessed using a scratch assay as described before (Sanjurjo-Rodriguez et al., 2019). Briefly, MSCs were grown to confluence in a 6-well plate in StemMACS MSC Expansion Media. The media were removed, and the cell monolayer was scratched with a sterile 200-μl pipette tip. The well was washed with PBS, and new fresh expansion media were added. Images were taken along the open scratch at 0 and 24 h, and measurements were calculated using the ImageJ software. The percentage of uncovered area (wound open) was normalized to time 0 and compared between SF MSCs and SB MSCs.

Gene Expression

RNA was isolated from MSCs and chondrocyte cultures, using the total RNA Purification kit (Norgen Biotek Corp., Canada). Gene expression was performed for 95 genes of interest as described in our previous work (Sanjurjo-Rodriguez et al., 2019), using standard TaqMan Assays (Thermo Fisher Scientific) and the 48.48 IFC (Integrated Fluidic Circuit) with the recommended reagents (Fluidigm Corporation, United States), following manufacturer's recommendations. Hypoxanthine phosphoribosyltransferase 1 (HPRT1) was used as a housekeeping gene. Reverse transcription was performed, followed by 14 pre-amplification cycles using a mixture of 96 TaqMan gene expression assays (**Supplementary Table 1**). The Dynamic 48.48 IFC sample compartment was loaded with the diluted pre-amplified cDNAs mixed with sample loading buffer (Fluidigm Corporation) and TaqMan Universal PCR Master mix (Applied Biosystems, United States). The IFC assay compartment was loaded with the 96 TaqMan assays mixed with assay loading buffer (Fluidigm Corporation). The IFC was then run on the Biomark Real Time PCR System using a GE 48 × 48 Standard v1 PCR thermal protocol, and data were analyzed using BioMark Gene Expression Data software and normalized to the housekeeping gene. Genes differentially expressed between chondrocytes, SB, and SF MSCs were further scrutinized for hierarchical clustering analysis using Cluster 3.0 software and Java TreeView (Churchman et al., 2012), including only samples that expressed ≥60% of all genes and genes expressed in ≥80% of the samples.

Statistical Analysis

Results were analyzed using Kruskal–Wallis and Dunn's multiple comparison tests for unpaired data and Wilcoxon signed rank tests for donor-matched data. The statistical analysis was performed using Prism software (version 7.0 a; GraphPad). The difference between the groups was considered as statistically significant only if the p value <0.05.

RESULTS

Osteoarthritis Synovial Fluid Multipotent Stromal Cell Characterization

Synovial fluid MSC cultures were established according to standard methods (Jones et al., 2004). SB MSC cultures were derived and characterized from both medial and lateral femoral condyles, as previously described (Sanjurjo-Rodriguez et al., 2019). There was no significant difference in the growth rates or surface phenotypes of SF MSC cultures and both types of SB MSCs (**Figures 1A,B**). Consistent with their MSC nature, SF cultures were tri-potential (**Figure 1C**). In motility assays, SF MSCs moved slightly faster than medial SB MSCs but were slower that lateral SB MSCs, and the differences failed to reach statistical significance (**Figure 1D**).

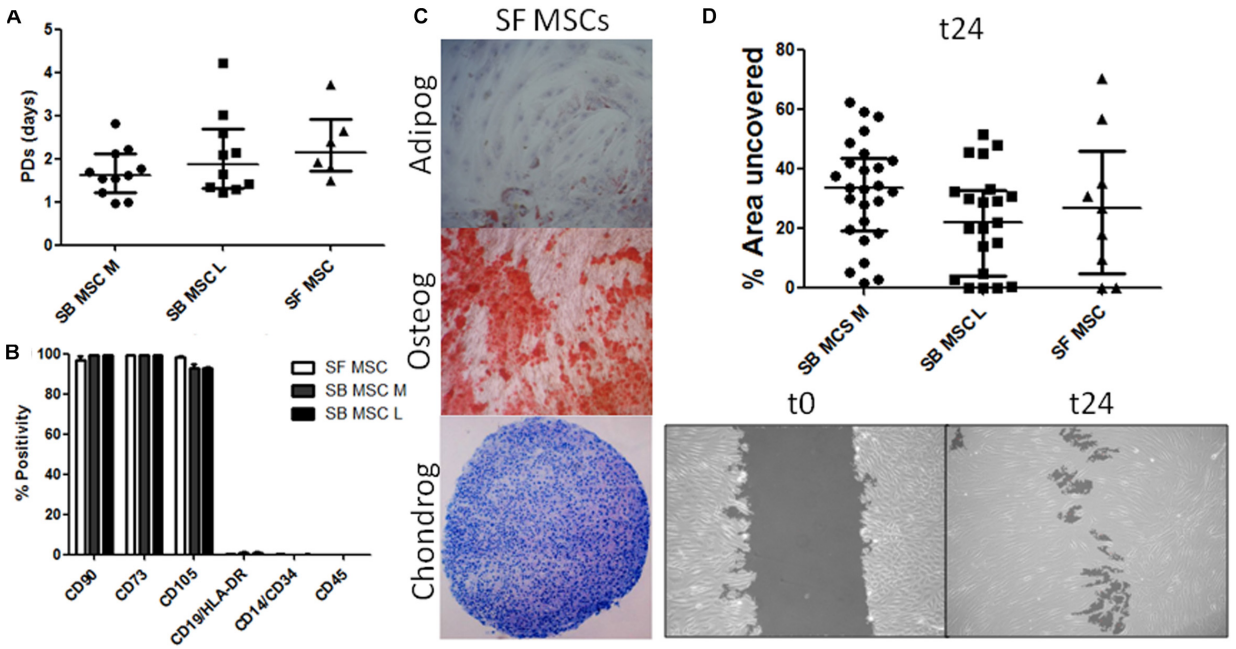

FIGURE 1 | Phenotypical and functional analyses of multipotent stromal cells (MSCs). **(A)** Comparison of growth rates of medial and lateral subchondral bone (SB) MSCs (SB MSC M and SB MSC L, respectively) and synovial fluid (SF) MSCs measured as population doubling (PD) times (in days). Dots represent individual donors; error bars represent interquartile range (IQR). **(B)** Phenotypic profile of culture-expanded SF and medial and lateral SB MSCs indicating no differences in the expression of standard MSC markers. Horizontal bars show means and error bars represent standard error (n = 3 donors). **(C)** Example images of SF MSC adipogenesis assay (Adipog) stained with Oil Red O after 14 days of adipogenic induction (top panel, original magnification ×100), osteogenesis (Osteog) showing positive alizarin red staining on day 14 post osteogenic induction (medium panel, original magnification ×100), and toluidine blue staining for glycosaminoglycan (GAG) deposition (purple) of chondrogenic (Chondrog) pellet cultures on day 21 post induction (bottom panel, original magnification ×40). **(D)** Analysis of SF MSC motility showing no significant differences between MSCs. Top panel: graph representing the median percentage of wound uncovered by migrating cells after 24 h (relative to the corresponding 0-h area); data represent individual measurements from nine SB MSC donors and three SF MSC donors; error bars represent IQR. Bottom panels: example images showing uncovered area measured at time 0 and at 24 h (t24).

Gene Expression Differences Between Synovial Fluid Multipotent Stromal Cells, Subchondral Bone Multipotent Stromal Cells, and Chondrocytes

Global gene expression differences between all culture types were first investigated using cluster analysis and revealed a clear clustering of SF MSCs and SB MSCs away from cultured chondrocytes from the same joints (**Figure 2A**). Also, within MSCs, a clear sub-cluster of SF MSCs was evident. Statistical analysis was next performed to identify differentially expressed genes between all MSCs and all chondrocytes (**Figures 2B,C**). The most differentially expressed genes highly expressed in chondrocytes were as follows: cartilage oligomeric matrix protein (COMP), lipocalin 2 (LCN2), nitric oxide synthase 2 (NOS2), interleukin 10 (IL10), C–C motif chemokine ligand 20 (CCL20), also known as macrophage inflammatory protein-3, and C–C motif chemokine receptor 7 (CCR7). All of these genes were expressed in cultured chondrocytes and low or below detection in both SF and SB MSCs (**Figure 2B**).

In contrast, four genes were significantly higher expressed in both SB and SF MSCs, compared with cultured chondrocytes (**Figure 2C**). These genes were C–X–C motif chemokine 12 (CXCL12, 58-fold higher in SB MSCs and 234-fold higher in SF MSCs), tissue inhibitor of metalloproteinase-3 (TIMP3; 7.7-fold higher in SB MSCs and 36.7-fold higher in SF MSCs), sphingosine kinase 1 (SPHK1; 6.5-fold higher in SB MSCs and 11.9-fold higher in SF MSCs), and transforming growth factor beta 1 (TGFB1; 6.9-fold higher in SB MSCs and 9.6-fold higher in SF MSCs). None of these four genes was significantly different between SB and SF MSCs. These data indicated that as expected, SF MSC gene expression signature was more similar to SB MSCs than cultured chondrocytes.

Gene Expression Comparison Between Synovial Fluid Multipotent Stromal Cells and Medial and Lateral Subchondral Bone Multipotent Stromal Cells

Synovial fluid MSC gene expression signature was next compared with medial and lateral SB MSCs. When gene expression profiles of SF MSCs were compared with those of medial SB MSCs, 82% of the measured genes showed similar levels of expression (**Supplementary Table 1**), 7% genes showed significantly >2-fold higher expression in medial SB MSCs, and 11% of genes were significantly >2-fold higher expressed in SF MSCs (**Table 1**). Similarly, when gene expression profiles of SF MSCs were compared with lateral SB MSCs, 69% of genes showed similar

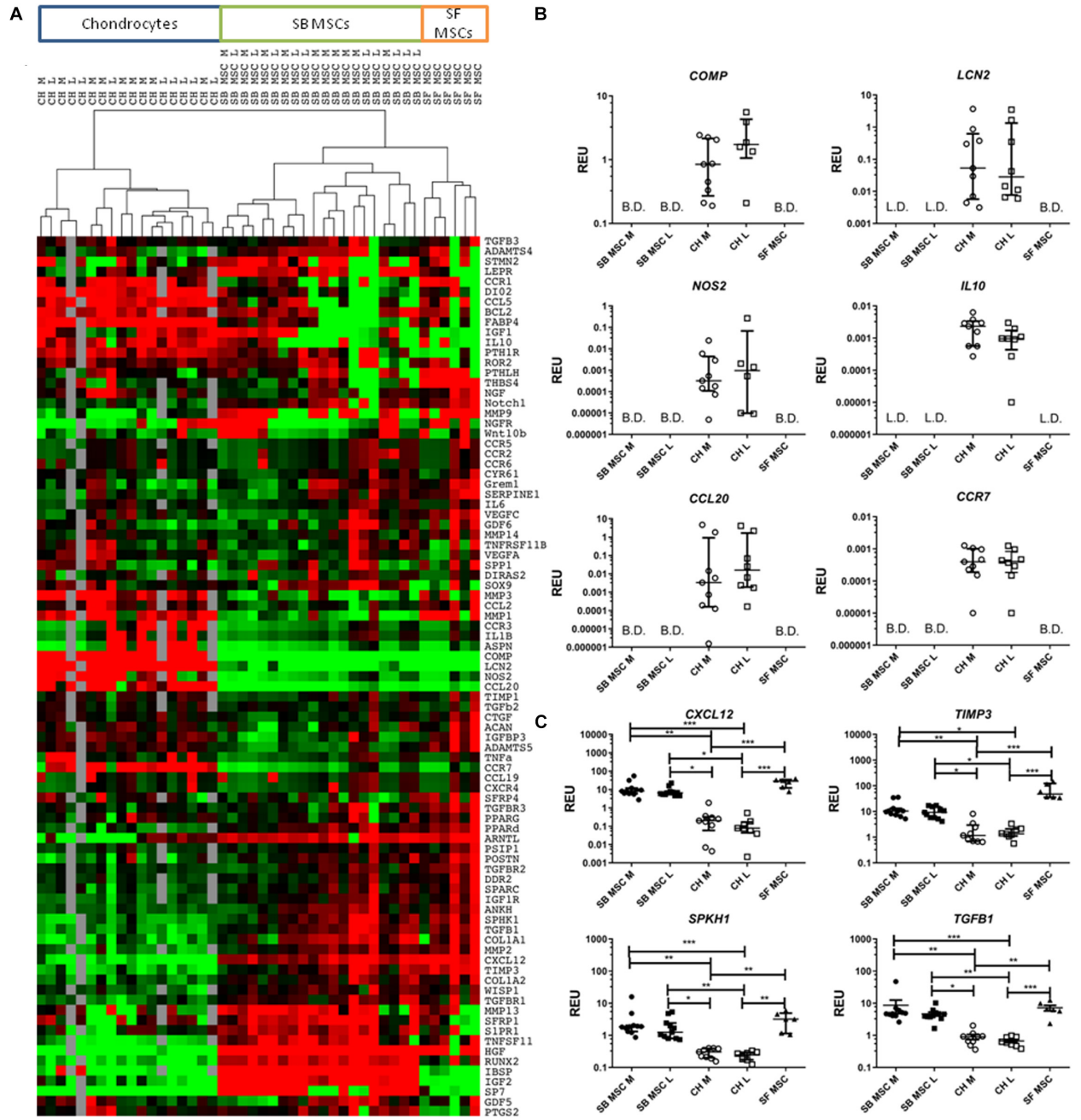

FIGURE 2 | Gene expression analysis of culture-expanded medial and lateral subchondral bone (SB) multipotent stromal cells (MSCs) (SB MSC M and SB MSC L, respectively), synovial fluid (SF) MSCs, and medial and lateral chondrocytes (CH M and CH L, respectively). **(A)** Cluster analysis between CH, SB MSCs, and SF MSCs illustrating clear clustering of MSCs away from chondrocytes. Data were normalized to the housekeeping gene HPRT and log2 transformed. Data filtering was performed according to standard methods previously described (Churchman et al., 2012). Scores were assigned as: black = 1, red > 1, green < 1; gray = missing data (below detection). **(B)** Differentially expressed genes with a significant higher expression in chondrocytes than in MSCs. L.D. indicates transcripts which were rarely expressed (in < 50% samples), and B.D. indicates transcripts below detection. **(C)** Differentially expressed genes between chondrocytes and MSCs, which were statistically significantly higher expressed in MSCs than in chondrocytes. $^{*}p < 0.05$; $^{**}p < 0.01$; $^{***}p < 0.0001$. Horizontal bars show medians and error bars represent interquartile range (IQR). REU, relative expression units [relative to housekeeping hypoxanthine phosphoribosyltransferase (HPRT)].

levels of expression (**Supplementary Table 1**), 5% genes showed significantly >2-fold higher expression in lateral SB MSCs, and 26% of genes were significantly >2-fold higher expressed in SF MSCs (**Table 1**). Interestingly, genes previously described as highly specific for synovial-origin MSCs, such as SFRP4 (Sekiya et al., 2012; Baboolal et al., 2014) and growth differentiation factor

TABLE 1 | Gene expression differences between SF and either lateral or medial SB MSCs.

Lower expression in SF than SB MSCs					
Gene symbol	**Gene name**	**Medial SB MSCs > SF**		**Lateral SB MSCs > SF**	
		Fold difference	***p*-value**	**Fold difference**	***p*-value**
SP7	Sp7 transcription factor	SF B.D.	N/A	SF B.D.	N/A
IBSP	Integrin binding sialoprotein	SF L.D.	N/A	SF L.D.	N/A
LEPR	Leptin receptor	SF L.D.	N/A	SF L.D.	N/A
PTH1R	Parathyroid hormone 1 receptor	SF L.D.	N/A	SF L.D.	N/A
RUNX2	Runt-related transcription factor 2	3.94	<0.05	6.38	<0.01
IGF2	Insulin-like growth factor 2	3.13	<0.05	4.83	<0.01
PTGS2	Prostaglandin-endoperoxide synthase 2	3.79	<0.05	4.03	NS
Higher expression in SF than SB MSCs					
Gene symbol	**Gene name**	**SF > medial SB MSCs**		**SF > lateral SB MSCs**	
		Fold difference	***p*-value**	**Fold difference**	***p*-value**
CCL5	C–C motif chemokine ligand 5	Med L.D.	N/A	Lat L.D.	N/A
PTHLH	Parathyroid hormone-like hormone	6.35	<0.05	Lat L.D.	N/A
MMP9	Matrix metalloproteinase 9	4.28	NS	Lat L.D.	N/A
STMN2	Stathmin 2	11.57	NS	Lat L.D.	N/A
ACAN	Aggrecan	1.93	<0.05	2.21	NS
THBS4	Thrombospondin 4	57.12	<0.05	78.52	<0.01
MMP1	Matrix metalloproteinase 1	36.95	<0.05	52.90	<0.01
CCR1	C–C motif chemokine receptor 1	8.08	<0.05	10.52	<0.05
ADAMTS5	A disintegrin and metalloproteinase with thrombospondin motifs 5	10.32	<0.01	8.47	<0.01
VEGFC	Vascular endothelial growth factor C	5.38	<0.01	5.46	<0.01
TIMP3	Tissue inhibitor of metalloproteinase-3	4.60	<0.01	5.20	<0.01
POSTN	Periostin	2.06	<0.05	2.59	<0.05
TGFBR3	Transforming growth factor beta receptor 3	2.59	<0.05	3.43	<0.01
TGFBR2	Transforming growth factor beta receptor 2	2.55	NS	4.87	<0.001
DDR2	Discoidin domain receptor tyrosine Kinase 2	2.31	NS	2.33	<0.01
IGFBP3	Insulin-like growth factor binding protein 3	2.37	NS	8.08	<0.001
MMP3	Matrix metalloproteinase 3	12.58	NS	24.15	<0.05
CCL2	C–C motif chemokine ligand 2	2.59	NS	3.92	<0.01
NGF	Nerve growth factor	1.73	NS	3.18	<0.01
GREM1	Gremlin 1, DAN family BMP antagonist	0.97	NS	3.14	<0.05
SERPINE1	Serpin family E member 1	2.16	NS	3.12	<0.01
CTGF	Connective tissue growth factor	1.63	NS	2.49	<0.01
PPARδ	Peroxisome proliferator activated receptor delta	1.87	NS	2.26	<0.05
MMP2	Matrix metalloproteinase 2	1.84	NS	2.23	<0.05

Kruskal–Wallis test with Dunn's correction for multiple comparisons. L.D., low detection; B.D., below detection; N/A, not applicable; NS, not significant.

5 (GDF5) (Kania et al., 2020), were not expressed at the higher levels in OA SF MSCs (**Table 1**).

To summarize, compared with both medial and lateral SB MSCs, SF MSCs expressed lower levels of osteogenesis-related genes, consistent with our original hypothesis that SF MSCs were less osteogenically committed (McGonagle et al., 2017) (**Figure 3A**). The expression of bone-anabolic insulin growth factor 2 (IGF2) (Kang et al., 2012), and the osteogenic transcription factor (TF) Runx2, was significantly lower in SF MSCs compared with SB MSCs using both unpaired and paired tests, and the expression IBSP (encoding bone sialoprotein) displayed low detection frequency in SF MSCs, precluding its full statistical analysis using paired tests but indicating its very low expression levels in SF MSCs (**Figure 3A**). Expression of parathyroid hormone 1 receptor (PTH1R) was also below detection in more than 50% of SF MSCs. PTH1R regulates cartilage hypertrophy and bone turnover (Santa Maria et al., 2016) and is indirectly implicated in promoting osteoclastogenesis, along with IGF2 and prostaglandin-endoperoxide synthase 2 (PTGS2) (Benisch et al., 2012).

Compared with SB MSCs, SF MSCs expressed similar levels of classical chondrogenesis-related TF SOX9 (**Supplementary Table 2**) but higher levels of aggrecan (ACAN) (significant in

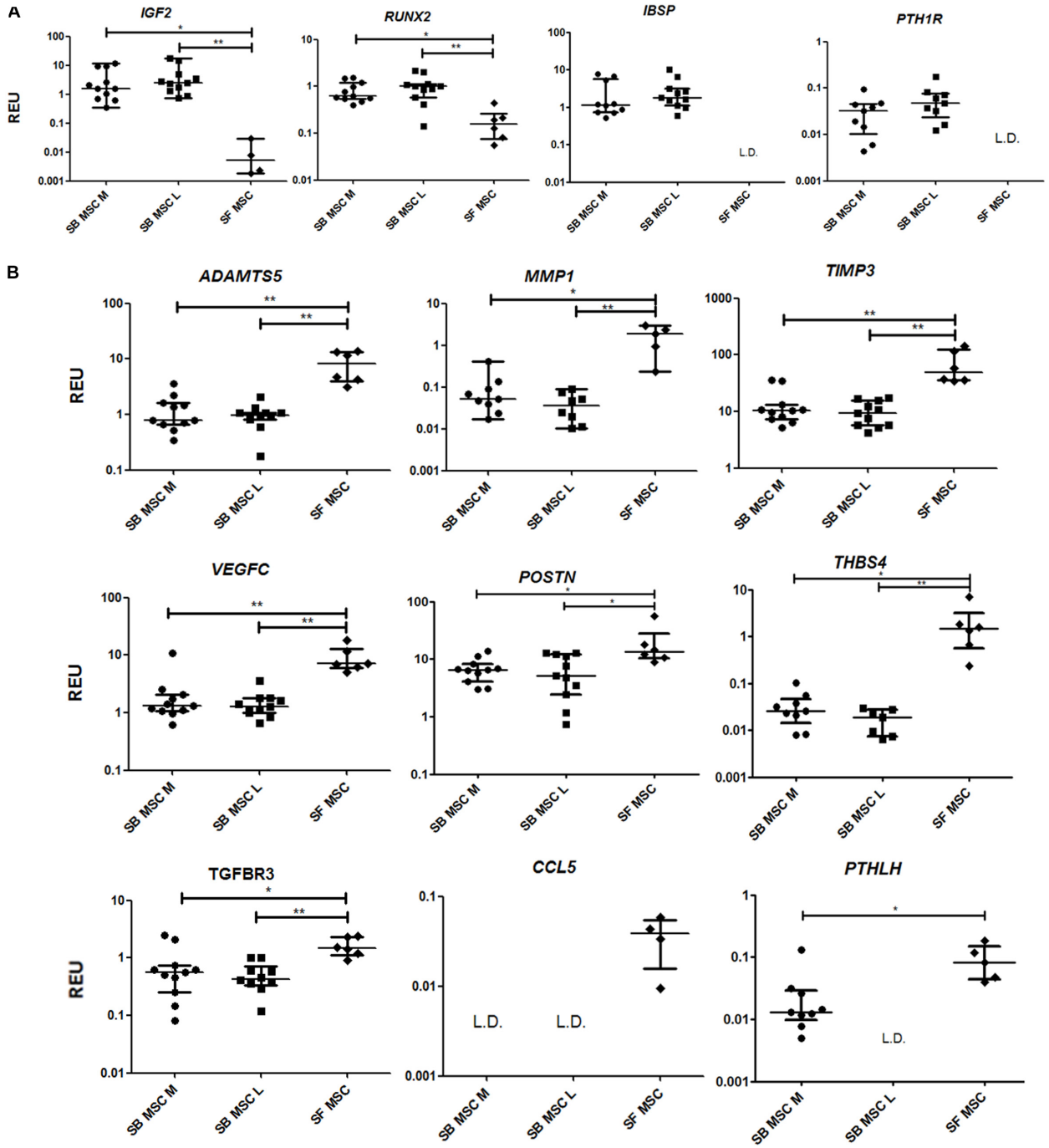

FIGURE 3 | Gene expression analysis of culture-expanded medial and lateral subchondral bone (SB) multipotent stromal cells (MSCs) (SB MSC M and SB MSC L, respectively) and synovial fluid (SF) MSCs pointing toward MMP and other pathway activation in SF MSCs. **(A)** Genes expressed significantly higher in SB MSCs than SF MSCs. **(B)** Differentially expressed genes with a significant higher expression in SF MSCs than in SB MSCs. $^{*}p < 0.05$; $^{**}p < 0.01$; $^{***}p < 0.0001$. Horizontal bars show medians, and error bars represent interquartile range (IQR). REU, relative expression units [relative to housekeeping hypoxanthine phosphoribosyltransferase (HPRT)]. L.D. indicates transcripts which were rarely expressed (detected in <50% samples).

medial SB MSCs). Unexpectedly, SF MSCs expressed significantly higher levels of genes involved in cartilage catabolism and extracellular matrix turnover (**Figure 3B**). The expression of matrix metalloproteinases 9 (MMP9) and 1 (MMP1), and tissue inhibitor of metalloproteinase-3 (TIMP3) and transforming growth factor receptor 3 (TGFBR3) were significantly higher in SF MSCs. Interestingly, high-level expression of extracellular matrix-degrading enzymes and their inhibitors has been

previously described as a distinctive feature of OA migratory CPCs (Koelling et al., 2009). Other interesting genes expressed higher in SF MSCs were thrombospondin 4 (THBS4), serpin family E member 1 (SERPINE1), and vascular endothelial growth factor C (VEGFC), among others (**Figure 3B**), all previously described as involved in cartilage formation, cartilage metabolism, or cartilage changes in OA (Hissnauer et al., 2010; Seol et al., 2012; Ludin et al., 2013).

Changes in Synovial Fluid Multipotent Stromal Cell Numbers and Colony Characteristics Following Knee Joint Distraction

A different cohort of nine OA patients was next analyzed to detect any changes in SF MSCs following KJD. CFU-F assays were first performed to quantify MSCs in donor-matched SF samples before, during, and after KJD (at weeks 0, 3, and 6, respectively). Out of nine patients studied for CFU-F, three had all three time-points available (**Figure 4A**). No particular trend was observed in relation to colony numbers following KJD (**Figure 4B**). The colony areas and IDs were next quantified to assess any potential changes in MSC proliferation. Week 0 colonies were more homogenously distributed with smaller colonies compared with week 3 and 6 colonies (**Figure 4C**). Colony IDs, which are an integrated measure of colony area and density, were significantly higher at weeks 3 and 6 compared with week 0 ($p < 0.001$) (**Figure 4D**). Correspondingly, the growth rates at early passage week 3 and week 6 MSCs were higher compared with week 0 MSCs (means of 1.65, 1.67, and 1.81 days/PD, respectively), but the differences failed to reach statistical significance. Altogether, these data indicated a slight increase in SF MSC proliferative capacity following KJD.

Changes in Synovial Fluid Multipotent Stromal Cell Gene Expression Following Knee Joint Distraction

The baseline (week 0) gene expression of SF MSCs from the KJD cohort was next compared with that of SF MSCs from OA arthroplasty cohort. No significant differences in the cell numbers at passage 0 normalized to a milliliter of SF were found between the two cohorts, indicating similarities in MSC growth potentials (**Supplementary Figure 2A**). Both cohorts had

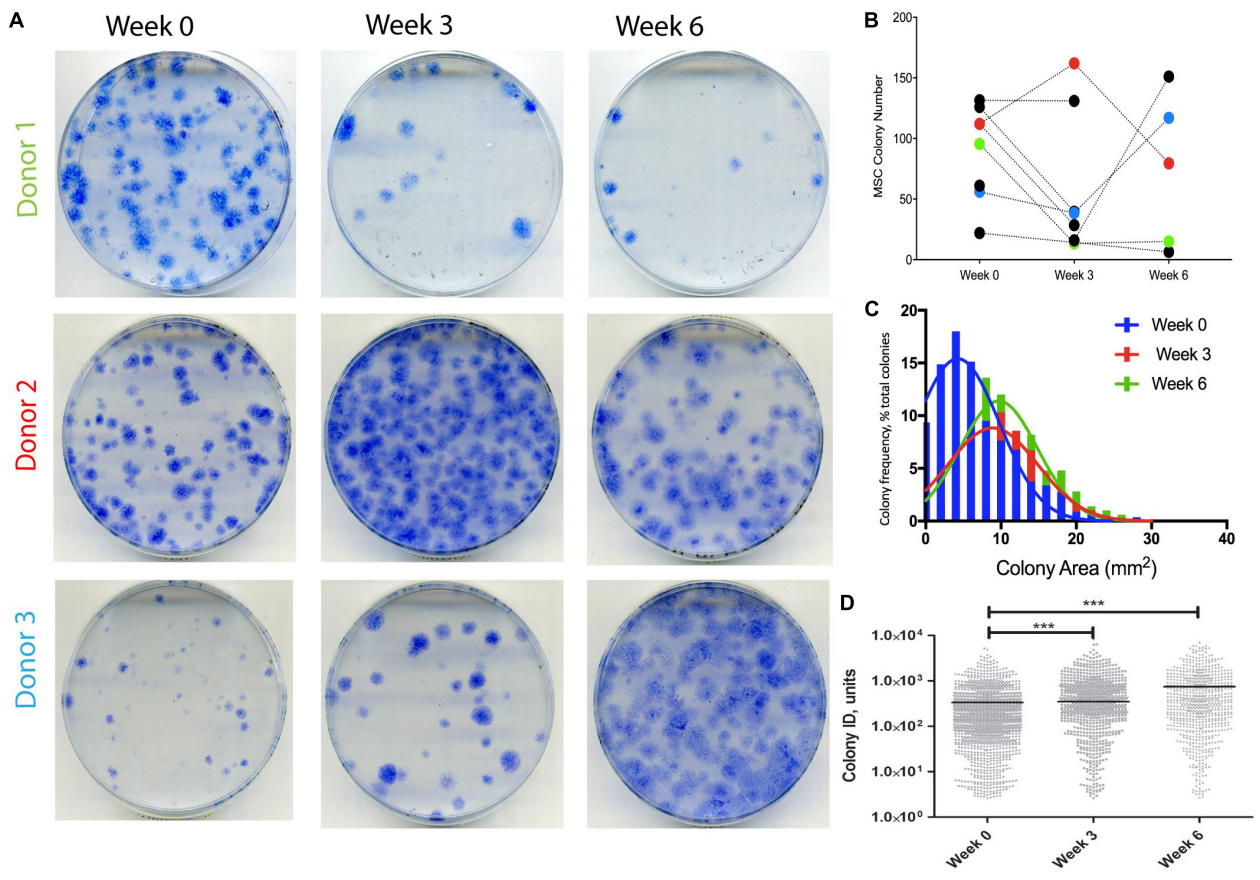

FIGURE 4 | Synovial fluid (SF) multipotent stromal cell (MSC) colony numbers and characteristics following knee joint distraction (KJD). **(A)** Colonies formed by MSCs at weeks 0, 3, and 6 from three patients. **(B)** Quantification of colony numbers (total numbers); each color represents individual patient. **(C)** Colony area frequency distribution showing a shift toward larger colonies following KJD. **(D)** Quantification of colonies integrated density using Image J (1,432, 833, and 744 total colonies at weeks 0, 3, and 6, respectively). ***$p < 0.0001$; horizontal lines represent medians.

similarly lower bone-related IGF2, IBSP, and RUNX2 transcript expression compared with SB MSCs from the arthroplasty cohort (**Supplementary Figure 2B**). Similarities in the expression of other transcripts were less obvious, and the baseline (week 0) data from the KJD cohort were next compared with week 3 and 6 data to elucidate any changes in SF MSCs toward a more chondrogenic, cartilage-anabolic, or anti-catabolic phenotype following KJD.

We first looked at transcripts overexpressed in SF MSCs compared with SB MSCs, and no significant changes or prominent trends were observed for IGFBP3, PPARδ, CCL5, TIMP3, and SERPINE1 (data not shown). However, a sustained nearly 10-fold reduction in the transcript levels for CCL2, encoding monocyte chemotactic protein 1 (MCP1), was observed in SF MSCs from the distracted joints (weeks 3 and 6) compared with week 0 (**Figure 5A**). A similar trend was observed for CCL20, encoding macrophage inflammatory protein-3 (MIP3α), but the differences failed to reach statistical significance. TNFRSF11B expression (encoding bone-anabolic osteoprotegerin) was also reduced at weeks 3 (3.8-fold) and 6 (2.5-fold) compared with week 0 ($p < 0.05$) (**Figure 5B**), and the expression of IBSP (encoding bone sialoprotein) was also consistently reduced albeit non-significantly. The expression of FABP4 (fatty acidic protein 4) or SOX9 (the master regulator of MSC chondrogenesis) was also reduced (**Figure 5C**); however, the expression of ACAN (core protein for a large cartilage proteoglycan essential for cartilage extracellular matrix maintenance) (Roughley and Mort, 2014) was, in contrast, significantly increased (**Figure 5D**).

Many transcripts displayed a trend for a decline following KJD but failed to reach significance, including MMP1, parathyroid hormone-like hormone (PTHLH), connective tissue growth factor (CTGF), THBS4, a disintegrin and metalloproteinase with thrombospondin motifs 5 (ADAMTS5), MMP9, and IL1b (interleukin 1 beta). Altogether, these data indicated a trend for a sustained reduction in cartilage-catabolic transcripts following KJD, with some evidence for increased ACAN expression (4.2-fold, $p < 0.01$ after 3 weeks) and (2.9-fold, $p < 0.05$ after 6 weeks) of KJD compared with its baseline levels (**Figure 5D**).

We next tested the hypothesis that KJD may rapidly activate joint repair pathways that would regress by 6 weeks when MSC joint repair mechanisms should be well under way (Baboolal et al., 2016). Therefore, we separately considered a group of transcripts that showed a significant change in their expression levels at week 3 followed by "return to baseline" at week 6 (**Figure 6**). Remarkably, this group included GDF5 (4.8-fold increase at week 3, $p < 0.01$), associated with chondrogenic specification in joint interzone and synovium (Kouroupis et al., 2019) and cartilage-resident progenitors (Kania et al., 2020), and gremlin 1 (GREM1) (3.9-fold at week 3, $p < 0.001$) described as characteristic for osteochondroreticular stem cells within the metaphysis of long bones (Worthley et al., 2015) and enriched in healthy articular cartilage where it regulates hypertrophy (Leijten et al., 2013) (**Figure 6A**). A similar pattern of changes was seen for TGFBR2 and TGFBR3 (**Figure 6B**) and IGFR (**Figure 6C**), the receptors for cartilage-anabolic growth factors and involved in pathogenesis of OA (Goldring, 2000). VEGFC, a well-known pro-angiogenic factor, showed a small decrease (1.6-fold, $p < 0.05$) at week 3 and returned to baseline after 6 weeks (**Figure 6C**). The VEGF family have been associated with OA progression in all tissues in the joint (Hamilton et al., 2016) and found strongly expressed in hyperplasic osteoarthritic synovium (Paavonen et al., 2002).

Overall, this pattern of gene expression indicated an early upregulation of genes associated with chondrogenic lineage specification and responsiveness to cartilage-anabolic growth factors, which may explain a more sustained increase in ACAN expression. At the end of KJD, there was also reduction in a pro-inflammatory CCL2/MCP-1 gene expression in SF MSCs as well as downregulation of typical bone- and fat-lineage genes.

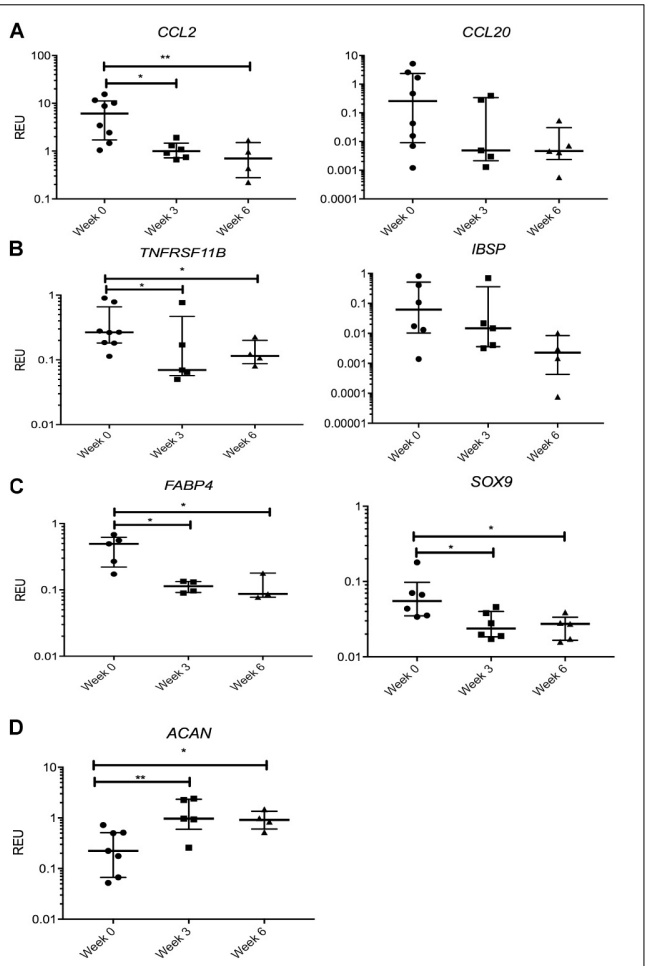

FIGURE 5 | Gene expression changes in synovial fluid (SF) multipotent stromal cells (MSCs) following knee joint distraction (KJD): sustained changes. **(A)** Reduction in chemokine transcripts CCL2 and CCL20. **(B)** Reduction in bone-anabolic transcripts TNFRSF11B and IBSP. **(C)** Reduction in FABP4 and Sox9 transcripts. **(D)** Increase in ACAN transcripts. *$p < 0.05$; **$p < 0.01$; ***$p < 0.0001$. Horizontal bars show medians, and error bars represent interquartile range (IQR). REU, relative expression units [relative to housekeeping hypoxanthine phosphoribosyltransferase (HPRT)].

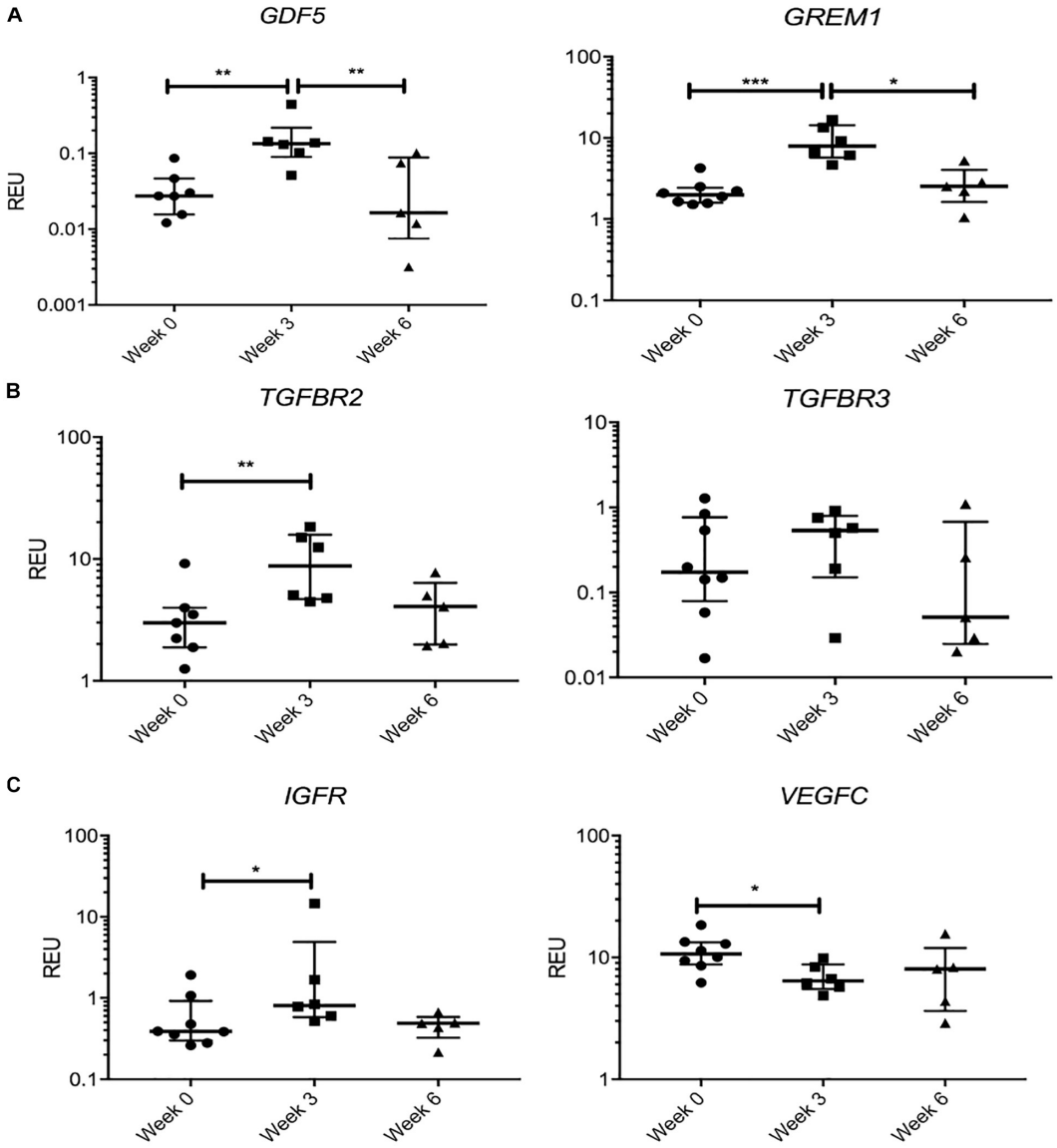

FIGURE 6 | Gene expression changes in synovial fluid (SF) multipotent stromal cells (MSCs) following knee joint distraction (KJD): temporary changes. **(A)** Increase at week 3 and reduction at week 6 in progenitor-marker transcripts GDF5 and GREM1. **(B)** Similar trend in anabolic growth factor transcripts TGFBR2 and TGFBR3. **(C)** Increase in insulin growth factor receptor (IGFR) and reduction in vascular endothelial growth factor C (VEGFC) transcripts at week 3. $^{*}p < 0.05$; $^{**}p < 0.01$; $^{***}p < 0.0001$. Horizontal bars show medians, and error bars represent interquartile range (IQR). REU, relative expression units [relative to housekeeping hypoxanthine phosphoribosyltransferase (HPRT)].

DISCUSSION

Novel therapeutic interventions based on the modulation of local biomechanical or biological environments within the OA-affected joint have recently emerged as potential joint-sparing alternatives to joint replacement surgery (Sánchez et al., 2012; Jansen et al., 2018; Goh et al., 2019; Jansen et al., 2019; Takahashi et al., 2019). Harnessing endogenous joint repair mechanisms following biomechanical correction of OA joints following KJD appears to hold particular promise (Mastbergen et al., 2013; McGonagle et al., 2017). While their mechanisms of action remain to be fully elucidated, endogenous SB and SF MSCs have been suggested as potential contributors to structural improvements and cartilage regeneration following these treatments (Chen et al., 2015; Baboolal et al., 2016; Sánchez et al., 2016). In this study, we investigated gene expression profiles of SF and SB MSCs in advanced knee OA and explored whether KJD, a successful treatment for advanced OA, leads to any favorable cartilage-anabolic changes in SF MSCs.

At the beginning, we compared gene expression profiles of SF MSCs and SB MSCs with articular chondrocytes enzymatically extracted from the same joints. Our results showed clear

clustering of chondrocytes away from both types of MSCs indicating toward less-differentiated nature of both types of MSCs. Recent studies have indicated the existence, within the OA cartilage, of highly proliferative and migrating CPCs (Koelling et al., 2009; Fellows et al., 2017; Carluccio et al., 2020), which could in theory, be shed into the SF and contribute to increased levels of matrix-turnover molecules in SF MSCs. Chondrocyte cultures, which were derived from the full-depth OA cartilage in the present study, could also contain the progeny of these migrating CPCs. Our data on chondrocyte cultures showed their higher-level expression of typical cartilage-specific molecules, compared with MSCs, as well as some evidence of chondrocyte inflammation, based on increased expression of pro-inflammatory molecules lipocalin-2 (LCN2) (Choi and Chun, 2017), NOS2 (Ahmad et al., 2020), CCL20 (Alaaeddine et al., 2015), and C–C motif chemokine receptor 7 (CCR7). These data indicated clear differences in gene expression profiles between cultured full-depth cartilage-resident cells and MSCs from the same late-OA joints and pointed toward cartilage degradation and inflammation as potential contributing factors to MSC gene expression signatures in late-stage OA joints.

In agreement with Djouad et al. (2005) for healthy bone marrow MSCs and SF MSCs, SB MSCs and SF MSCs formed separate sub-clusters within the MSC cluster in our study. This could indicate different tissue origins of these MSCs (Sekiya et al., 2012; McGonagle et al., 2017), but this could also be a reflection of different biomechanical environments that these MSCs reside in. We have previously shown that SB MSCs from medial (more loaded) femoral condyles had a gene expression profile enriched for bone-anabolic genes compared with MSCs from lateral (less loaded) condyles, implicating joint biomechanics as a potential main driver of SB MSC commitment to osteogenesis and sclerotic plate formation in late-OA joints (Sanjurjo-Rodriguez et al., 2019). In the present study, SF MSCs under-expressed many of these osteogenic and hypertrophy-related genes compared with SB MSCs (IGF2, RUNX2, IBSP, and PTH1R) supporting SF MSC role in endogenous cartilage repair *in vivo* in experimental OA (Wiegant et al., 2015) and arguing for better suitability of SF MSCs for cartilage regeneration in OA in humans (Baboolal et al., 2016).

The lack of a clear pro-chondrogenic or cartilage anabolic phenotype of OA SF MSCs could at least in part be related to pro-inflammatory mediators present in late-OA SF (Monibi et al., 2016). Indeed, OA SF MSCs expressed higher levels of many genes related to cartilage catabolism and extracellular matrix turnover (including ADAMTS5, MMP1, and TIMP3) compared with SB MSCs. This is similar to CPCs, which express high levels of these molecules, possibly to facilitate their tissue egress and remodeling of damaged extracellular matrix (Koelling et al., 2009). Such a unique gene expression profile may also reflect a strong effect of cartilage breakdown and joint inflammation on SF MSCs (Leijs et al., 2012; Neybecker et al., 2018). Regardless of the cause, this gene expression profile might be of relevance to remodeling the damaged cartilage matrix and enabling endogenous repair by SF MSCs.

Higher numbers, but reduced functionalities of MSCs in OA SF compared with healthy donors, have been reported in many previous studies (Jones et al., 2008; Sekiya et al., 2012; Kim et al., 2015), but the precise mechanisms behind this unexpected increase remain unknown. The molecular and metabolic milieu of OA SF may encourage resident MSC self-renewal (Jones et al., 2008; Harris et al., 2013), but it may also induce the egress of CPCs and SB MSCs from their natural niches (Sánchez et al., 2016; De Luca et al., 2019) or reduce their homing and attachment to damaged cartilage and other joint tissues (Endres et al., 2007; Baboolal et al., 2016; De Luca et al., 2019). Another promising joint-preserving regenerative treatment for severe OA, a combination of intra-articular and intra-osseous infiltrations of autologous platelet-rich plasma (PRP), has been shown to reduce SF MSC numbers measured by flow cytometry (Muiños-López et al., 2016; Sánchez et al., 2016), presumably by attraction of MSCs to the exposed osseous surface. In our cohort of KJD patients, SF MSC numbers measured by CFU-F assay did not increase or fall following the treatment, although higher colony densities during treatment pointed toward their slightly increased proliferative capacity that may in part be driven by KJD-associated changes in SF FGF2 concentration (Coutu et al., 2011; Watt et al., 2020). We acknowledge that aspirated SF MSC numbers could not be volumetrically counted, as the volumes of fluid taken from the patients could not be precisely controlled and depended on patient's clinical status; therefore, the data were presented as total aspirated MSCs. Nevertheless, SF MSC responses to KJD appeared to be different to those reported following PRP infiltrations.

Our analysis of SF MSC transcriptome half-way through (week 3) and in the end of KJD (week 6) provided interesting insights into the dynamics of SF MSC responses in relation to previously reported SF cytokine changes (Watt et al., 2020). In a separate cohort of 20 KJD patients, mild but sustained increases in SF levels of FGF2 and TGFb1 have been recently documented, which were particularly prominent in patients who responded better to their treatment (Watt et al., 2020). Our data showed an increase in TGFβ receptor 2 and 3 expression in SF MSCs early in KJD, which may represent an enrichment in TGFβ-responsive MSCs during early stages of treatment. Interestingly, this coincided with higher-level GREM1 and GDF5 transcripts in week 3 MSCs, the molecules associated with chondrogenesis and healthy cartilage homeostasis (Leijten et al., 2013; Worthley et al., 2015; Kouroupis et al., 2019; Kania et al., 2020). A sustained increase in ACAN expression in SF MSCs following KJD suggests some degree of their chondrogenic commitment and may be explained by the activity of these GREM1- and GDF5-expressing cells.

It is difficult to directly compare the gene expression of SF MSCs following KJD with our results obtained for their comparison with SB MSCs, as different patient cohorts were used. Some key similarities in SF MSCs from both cohorts were however found, particularly in relation to their reduced levels of osteogenic transcripts IGF2, IBSP, and RUNX2, compared with SB MSCs, as well as similar growth potentials. However, it was noted that several genes higher expressed in the OA SF MSCs and assumed to be upregulated in response to pro-inflammatory SF mediators (ADAMTS5, IL1b, MMP9, or MMP1) in our OA arthroscopy cohort did not show a significant change

following KJD, but they tended to decrease. Interestingly, SF MSC expression of pro-inflammatory chemokines (CCL2/MCP1 and CCL20/MIP1α) was reduced. MCP1 is associated with synovial inflammation (Wang et al., 2013) and implicated in joint pain (Miotla Zarebska et al., 2017), as well as an inhibition of SF MSC chondrogenesis (Harris et al., 2013). In contrast to an animal model studies where a significant effect of KJD on joint inflammation was found (Chen et al., 2015; Wiegant et al., 2015), early results on the effects of KJD on SF pro-inflammatory mediators in OA patients remain puzzling. For example, pro-inflammatory IL-6 and MCP1 SF levels were found increased following KJD in Watt et al. (2020) study, although IL-6 was negatively correlated with pro-chondrogenic TGFb1, as would be expected (Wiegertjes et al., 2019). Larger studies investigating more SF analytes and SF MSC transcripts using the same cohort of patients (validation cohort), ideally at more time-points, during the course of distraction and comparing responders and non-responders, would be needed to shed more light on the effects of joint off-loading on SF cellular and molecular responses. Changes in SF MSC secretome and their immunomodulation, chondrogenic and chondroprotective potencies using appropriate assays (Cassano et al., 2018; Amemiya et al., 2020; Watanabe et al., 2020) would be needed to confirm the functional significance of the observed transcript changes. In addition to MSCs, the investigations of SF immune cells, and particularly macrophage subsets in terms of their pro- and anti-inflammatory polarization states (Fahy et al., 2014; Daghestani et al., 2015), would be necessary.

This study is limited by small numbers of samples tested and by the analysis of SB and SF MSC expression in culture-expanded MSCs, which is known to influence gene expression (Churchman et al., 2012; Sanjurjo-Rodriguez et al., 2019). We have previously demonstrated the feasibility of analyzing gene expression in uncultured SB MSCs from knee OA patients where differentially expressed genes between lateral and medial femoral condyles were discovered using cultured MSCs and subsequently confirmed using CD271-selected uncultured MSCs (Sanjurjo-Rodriguez et al., 2019). However, the isolation of uncultured SF MSCs, which are significantly rarer (Jones et al., 2004, 2008; Morito et al., 2008; Altaie et al., 2018), remains a challenge. New methodologies involving single-cell quantitative PCR or RNA sequencing, as utilized for other types of rare stem cells (Ayyaz et al., 2019; Tricoire et al., 2019; Zhou et al., 2019), provide a future way forward. Our chondrocyte cultures were derived from full-depth OA cartilage and grown in culture media different from MSC-expansion media; this could have partially contributed to differences in their gene expression compared with MSCs. Similarly, single-cell RNA sequencing (Ji et al., 2019) or mass cytometry (Grandi et al., 2020) on cartilage-resident cells including uncultured CPCs and comparing their profiles with single MSCs would provide future valuable insights into different progenitor and stem cell types present in OA-affected human joints. If cultured, the same early passage cells should be used for transcript analysis and functional assays.

Apart from SF MSCs, joint off-loading following KJD is likely to have an impact on SB MSCs, but bone biopsy was considered too invasive and therefore deemed unethical. The assessment of SB microstructural changes using CT scans (Intema et al., 2011) and correlating them with SB MSC changes and cartilage regeneration (Hyodo et al., 2019) would be valuable for future evaluation of the roles of SB MSCs in osteochondral structural improvements and cartilage metabolism (Westacott et al., 1997) following KJD. Finally, primary biomechanical effects of joint off-loading are also possible, for example, SF viscosity changes, hyaluronan content, or cartilage swelling, which are potential drivers for SF attachment to cartilage occurred within the first week following off-loading (Baboolal et al., 2016) and were therefore missed in the present study protocol. Future studies should also include investigations of synovial MSC subpopulations and comparing them, through high-throughput single cell-based analysis, to SF MSCs. Up to now, there exist multiple studies presenting different phenotypes and topographies of MSCs in human synovium (Sivasubramaniyan et al., 2012; O'Brien et al., 2017; Mizuno et al., 2018; Affan et al., 2019) or rodent synovium (Roelofs et al., 2017); and their relationships with synovial fibroblasts (Croft et al., 2019), which may be pro-inflammatory, remain unclear. In the future, it would be interesting to establish which subset of synovial MSCs may be preferentially shed into the fluid, using recently developed *in vitro* methodologies (Kohno et al., 2018). Endogenous manipulations of the osteoarthritic synovium toward inflammation inhibition and increased MSC shedding into the fluid could be the next step toward KJD efficacy augmentation.

Our findings have broad implications for the development of novel joint-sparing regenerative strategies as they highlight the complexity of different joint-resident MSC niches, MSC responses to the disease itself, and dynamic changes favoring tissue repair following biomechanical correction by joint off-loading. Many clinical investigations employ MSC intra-articular injections as a sole therapy based on their tissue repair and immunomodulatory activities *in vitro* (Chahal et al., 2019; Matas et al., 2019), but long-term clinical benefits are not always guaranteed (Shariatzadeh et al., 2019). Our data highlight the importance of considering complex cellular and biomechanical environments into which these cells are delivered for the development of more effective joint-sparing treatments for OA.

DATA AVAILABILITY STATEMENT

The analyzed datasets for this study can be found in the University of Leeds data depository on https://doi.org/10.5518/837.

ETHICS STATEMENT

The studies involving human participants were reviewed and approved by Yorkshire & The Humber – South Yorkshire Research Ethics Committee (14/YH/0087), UK; University Medical Center Utrecht (#15-160/D; NL51539.041.15), Netherlands. The patients/participants provided their written informed consent to participate in this study.

AUTHOR CONTRIBUTIONS

EJ, DM, FL, SM, TB, and CS-R performed conception and design. HP, CS-R, AA, TW, SM, and TB acquired data. CS-R, AA, TB, and EJ performed the data analysis. CS-R, AA, EJ, TB, SM, FL, TW, and DM carried out data interpretation. CS-R, AA, and EJ contributed to manuscript preparation. All authors performed manuscript review and editing for important intellectual content.

FUNDING

This study was supported by FOREUM: foundation for research in rheumatology grant number 104929. The institution of SC Mastbergen and FPJG Lafeber has, during the study period, received funding from Dutch Arthritis Society (ReumaNederland), project number LLP-9, https://reumanederland.nl/. The institution of TJM Welting received funding from Dutch Arthritis Society (ReumaNederland), project number LLP-14, https://reumanederland.nl/. The funders had no role in study design, data collection and analysis, decision to publish, or preparation of the manuscript.

ACKNOWLEDGMENTS

CS-R is beneficiary of a postdoctoral fellowship from Xunta de Galicia (Spain). We gratefully acknowledge Dr. Agata Burska and Dr. Frederique Ponchel for qPCR analysis support; Adam Davison and Liz Straszynski for research support services at the Leeds Institute of Rheumatic and Musculoskeletal Medicine; surgeons, patients, and staff of Chapel Allerton Orthopaedic Centre; Arno Concepcion for research support services at the University Medical Center Utrecht; and Andy Crèmers for research support services at the Maastricht University Medical Center. Professor Pandit is a National Institute for Health Research (NIHR) Senior Investigator. The views expressed in this article are those of the authors and not necessarily those of the NIHR or the Department of Health and Social Care.

SUPPLEMENTARY MATERIAL

The Supplementary Material for this article can be found online at: https://www.frontiersin.org/articles/10.3389/fbioe.2020.579751/full#supplementary-material

Supplementary Figure 1 | Tissue processing **(A)** and the immunohistochemical staining of an example osteochondral specimen **(B)** showing an absence of intact cartilage superficial layer and the presence of CD271 + MSCs in marrow cavities (dotted arrows) and in bone-lining locations (black arrows). Dotted line represents an approximate position of slicing-off the cartilage using a scalpel. The method for processing and immunohistochemical staining of OA knee osteochondral specimens can be found in "Materials and Methods" and "**Supplementary Material**".

Supplementary Figure 2 | Comparison between SF MSCs from OA arthroplasty (OA/A) cohort and SF MSCs from KJD cohort at baseline (week 0). Similar growth potentials were observed **(A)** (lines represent medians, each symbol represents an individual donor). Gene expression heatmap of SF MSCs from both cohorts: OA/A (n = 6), KJD (n = 8), and SB MSCs from OA/A cohort (n = 11) used as comparator **(B)**. Heatmap is generated using Graphpad Prism version 8.4.3. Log2 transformation and data filtering (filter = 67% present) were performed on the data and color coding represents medians. Osteogenic genes differentially expressed between SB MSCs and both groups of SF MSCs are shown in yellow brackets.

Supplementary Table 1 | Taqman probes used to assess the gene expression.

Supplementary Table 2 | Genes not differentially expressed between SF and SB MSCs.

REFERENCES

Affan, A., Al-Jezani, N., Railton, P., Powell, J. N., and Krawetz, R. J. (2019). Multiple mesenchymal progenitor cell subtypes with distinct functional potential are present within the intimal layer of the hip synovium. *BMC Musculoskelet. Disord.* 20:125. doi: 10.1186/s12891-019-2495-2

Ahmad, N., Ansari, M. Y., and Haqqi, T. M. (2020). Role of iNOS in osteoarthritis: pathological and therapeutic aspects. *J. Cell Physiol.* 235, 6366–6376. doi: 10.1002/jcp.29607

Alaaeddine, N., Antoniou, J., Moussa, M., Hilal, G., Kreichaty, G., Ghanem, I., et al. (2015). The chemokine CCL20 induces proinflammatory and matrix degradative responses in cartilage. *Inflamm. Res.* 64, 721–731. doi: 10.1007/s00011-015-0854-5

Altaie, A., Baboolal, T. G., Wall, O., Jones, E., and McGonagle, D. (2018). Platelet lysate enhances synovial fluid multipotential stromal cells functions: implications for therapeutic use. *Cytotherapy* 20, 375–384. doi: 10.1016/j.jcyt.2017.12.003

Amemiya, M., Tsuji, K., Katagiri, H., Miyatake, K., Nakagawa, Y., Sekiya, I., et al. (2020). Synovial fluid-derived mesenchymal cells have non-inferior chondrogenic potential and can be utilized for regenerative therapy as substitute for synovium-derived cells. *Biochem. Biophys. Res. Commun.* 523, 465–472. doi: 10.1016/j.bbrc.2019.12.068

Ayyaz, A., Kumar, S., Sangiorgi, B., Ghoshal, B., Gosio, J., Ouladan, S., et al. (2019). Single-cell transcriptomes of the regenerating intestine reveal a revival stem cell. *Nature* 569, 121–125. doi: 10.1038/s41586-019-1154-y

Baboolal, T. G., Boxall, S. A., Churchman, S. M., Buckley, C. T., Jones, E., and McGonagle, D. (2014). Intrinsic multipotential mesenchymal stromal cell activity in gelatinous Heberden's nodes in osteoarthritis at clinical presentation. *Arthritis Res. Ther.* 16:R119. doi: 10.1186/ar4574

Baboolal, T. G., Mastbergen, S. C., Jones, E., Calder, S. J., Lafeber, F. P., and McGonagle, D. (2016). Synovial fluid hyaluronan mediates MSC attachment to cartilage, a potential novel mechanism contributing to cartilage repair in osteoarthritis using knee joint distraction. *Ann. Rheum. Dis.* 75, 908–915. doi: 10.1136/annrheumdis-2014-206847

Benisch, P., Schilling, T., Klein-Hitpass, L., Frey, S. P., Seefried, L., Raaijmakers, N., et al. (2012). The transcriptional profile of mesenchymal stem cell populations in primary osteoporosis is distinct and shows overexpression of osteogenic inhibitors. *PLoS One* 7:e45142. doi: 10.1371/journal.pone.0045142

Carluccio, S., Martinelli, D., Palamà, M. E. F., Pereira, R. C., Benelli, R., Guijarro, A., et al. (2020). Progenitor cells activated by platelet lysate in human articular cartilage as a tool for future cartilage engineering and reparative strategies. *Cells* 9:52. doi: 10.3390/cells9041052

Cassano, J. M., Schnabel, L. V., Goodale, M. B., and Fortier, L. A. (2018). Inflammatory licensed equine MSCs are chondroprotective and exhibit enhanced immunomodulation in an inflammatory environment. *Stem Cell Res. Ther.* 9:82. doi: 10.1186/s13287-018-0840-2

Chahal, J., Gómez-Aristizábal, A., Shestopaloff, K., Bhatt, S., Chaboureau, A., Fazio, A., et al. (2019). Bone marrow mesenchymal stromal cell treatment in patients with osteoarthritis results in overall improvement in pain and symptoms and reduces synovial inflammation. *Stem Cells Transl. Med.* 8, 746–757. doi: 10.1002/sctm.18-0183

Chen, Y., Sun, Y., Pan, X., Ho, K., and Li, G. (2015). Joint distraction attenuates osteoarthritis by reducing secondary inflammation, cartilage degeneration and subchondral bone aberrant change. *Osteoarthr. Cartil.* 23, 1728–1735. doi: 10.1016/j.joca.2015.05.018

Choi, W. S., and Chun, J. S. (2017). Upregulation of lipocalin-2 (LCN2) in osteoarthritic cartilage is not necessary for cartilage destruction in mice. *Osteoarthr. Cartil.* 25, 401–405. doi: 10.1016/j.joca.2016.07.009

Churchman, S. M., Ponchel, F., Boxall, S. A., Cuthbert, R., Kouroupis, D., Roshdy, T., et al. (2012). Transcriptional profile of native CD271+ multipotential stromal cells: evidence for multiple fates, with prominent osteogenic and wnt pathway signaling activity. *Arthrit. Rheum.* 64, 2632–2643. doi: 10.1002/art.34434

Coutu, D. L., François, M., and Galipeau, J. (2011). Inhibition of cellular senescence by developmentally regulated FGF receptors in mesenchymal stem cells. *Blood* 117, 6801–6812. doi: 10.1182/blood-2010-12-321539

Croft, A. P., Campos, J., Jansen, K., Turner, J. D., Marshall, J., Attar, M., et al. (2019). Distinct fibroblast subsets drive inflammation and damage in arthritis. *Nature* 570, 246–251. doi: 10.1038/s41586-019-1263-7

Daghestani, H. N., Pieper, C. F., and Kraus, V. B. (2015). Soluble macrophage biomarkers indicate inflammatory phenotypes in patients with knee osteoarthritis. *Arthrit. Rheumatol.* 67, 956–965. doi: 10.1002/art.39006

De Luca, P., Kouroupis, D., Viganò, M., Perucca-Orfei, C., Kaplan, L., Zagra, L., et al. (2019). Human diseased articular cartilage contains a mesenchymal stem cell-like population of chondroprogenitors with strong immunomodulatory responses. *J. Clin. Med.* 8:jcm8040423.

Djouad, F., Bony, C., Haupl, T., Uze, G., Lahlou, N., Louis-Plence, P., et al. (2005). Transcriptional profiles discriminate bone marrow-derived and synovium-derived mesenchymal stem cells. *Arthrit. Res. Ther.* 7, R1304–R1315. doi: 10.1186/ar1827

Dominici, M., Le Blanc, K., Mueller, I., Slaper-Cortenbach, I., Marini, F. C., Krause, D. S., et al. (2006). Minimal criteria for defining multipotent mesenchymal stromal cells. the international society for cellular therapy position statement. *Cytotherapy* 8, 315–317. doi: 10.1080/14653240600855905

Dwivedi, G., Chevrier, A., Alameh, M. G., Hoemann, C. D., and Buschmann, M. D. (2018). Quality of cartilage repair from marrow stimulation correlates with cell number, clonogenic, chondrogenic, and matrix production potential of underlying bone marrow stromal cells in a rabbit model. *Cartilage* 2018:1947603518812555. doi: 10.1177/1947603518812555

Endres, M., Neumann, K., Haeupl, T., Erggelet, C., Ringe, J., Sittinger, M., et al. (2007). Synovial fluid recruits human mesenchymal progenitors from subchondral spongious bone marrow. *J. Orthop. Res.* 25, 1299–1307. doi: 10.1002/jor.20394

Fahy, N., de Vries-van Melle, M. L., Lehmann, J., Wei, W., Grotenhuis, N., Farrell, E., et al. (2014). Human osteoarthritic synovium impacts chondrogenic differentiation of mesenchymal stem cells via macrophage polarisation state. *Osteoarthr. Cartil.* 22, 1167–1175. doi: 10.1016/j.joca.2014.05.021

Fang, W., Sun, Z., Chen, X., Han, B., and Vangsness, C. T. (2020). Synovial fluid mesenchymal stem cells for knee arthritis and cartilage defects: a review of the literature. *J. Knee Surg.* doi: 10.1055/s-0040-1710366. [Epub ahead of print].

Fellows, C. R., Matta, C., Zakany, R., Khan, I. M., and Mobasheri, A. (2016). Adipose, bone marrow and synovial joint-derived mesenchymal stem cells for cartilage repair. *Front. Genet.* 7:213. doi: 10.3389/fgene.2016.00213

Fellows, C. R., Williams, R., Davies, I. R., Gohil, K., Baird, D. M., Fairclough, J., et al. (2017). Characterisation of a divergent progenitor cell sub-populations in human osteoarthritic cartilage: the role of telomere erosion and replicative senescence. *Sci. Rep.* 7:41421. doi: 10.1038/srep41421

Ganguly, P., El-Jawhari, J. J., Burska, A. N., Ponchel, F., Giannoudis, P. V., and Jones, E. A. (2019). The analysis of in vivo aging in human bone marrow mesenchymal stromal cells using colony-forming unit-fibroblast assay and the CD45lowCD271+ phenotype. *Stem Cells Int.* 2019:5197983. doi: 10.1155/2019/5197983

Garcia, J., Wright, K., Roberts, S., Kuiper, J. H., Mangham, C., Richardson, J., et al. (2016). Characterisation of synovial fluid and infrapatellar fat pad derived mesenchymal stromal cells: the influence of tissue source and inflammatory stimulus. *Sci. Rep.* 6:24295. doi: 10.1038/srep24295

Goh, E. L., Lou, W. C. N., Chidambaram, S., and Ma, S. (2019). The role of joint distraction in the treatment of knee osteoarthritis: a systematic review and quantitative analysis. *Orthop. Res. Rev.* 11, 79–92. doi: 10.2147/ORR.S211060

Goldring, M. B. (2000). The role of the chondrocyte in osteoarthritis. *Arthrit. Rheum.* 43, 1916–1926.

Grandi, F. C., Baskar, R., Smeriglio, P., Murkherjee, S., Indelli, P. F., Amanatullah, D. F., et al. (2020). Single-cell mass cytometry reveals cross-talk between inflammation-dampening and inflammation-amplifying cells in osteoarthritic cartilage. *Sci. Adv.* 6:eaay5352. doi: 10.1126/sciadv.aay5352

Hamilton, J. L., Nagao, M., Levine, B. R., Chen, D., Olsen, B. R., and Im, H. J. (2016). Targeting VEGF and its receptors for the treatment of osteoarthritis and associated pain. *J. Bone. Miner. Res.* 31, 911–924. doi: 10.1002/jbmr.2828

Harris, Q., Seto, J., O'Brien, K., Lee, P. S., Kondo, C., Heard, B. J., et al. (2013). Monocyte chemotactic protein-1 inhibits chondrogenesis of synovial mesenchymal progenitor cells: an in vitro study. *Stem Cells* 31, 2253–2265. doi: 10.1002/stem.1477

Hissnauer, T. N., Baranowsky, A., Pestka, J. M., Streichert, T., Wiegandt, K., Goepfert, C., et al. (2010). Identification of molecular markers for articular cartilage. *Osteoarthr. Cartil.* 18, 1630–1638. doi: 10.1016/j.joca.2010.10.002

Hyodo, A., Ozeki, N., Kohno, Y., Suzuki, S., Mizuno, M., Otabe, K., et al. (2019). Projected cartilage area ratio determined by 3-dimensional MRI analysis: validation of a novel technique to evaluate articular cartilage. *JB JS Open Access* 4:e0010. doi: 10.2106/JBJS.OA.19.00010

Iijima, H., Aoyama, T., Tajino, J., Ito, A., Nagai, M., Yamaguchi, S., et al. (2016). Subchondral plate porosity colocalizes with the point of mechanical load during ambulation in a rat knee model of post-traumatic osteoarthritis. *Osteoarthr. Cartil.* 24, 354–363. doi: 10.1016/j.joca.2015.09.001

Ilas, D. C., Baboolal, T. G., Churchman, S. M., Jones, W. G., Giannoudis, P. V., Bühring, H. J., et al. (2020). The osteogenic commitment of CD271+CD56+ bone marrow stromal cells (BMSCs) in osteoarthritic femoral head bone. *Sci. Rep.* 10:11145. doi: 10.1038/s41598-020-67998-0

Ilas, D. C., Churchman, S. M., Baboolal, T., Giannoudis, P. V., Aderinto, J., McGonagle, D., et al. (2019). The simultaneous analysis of mesenchymal stem cells and early osteocytes accumulation in osteoarthritic femoral head sclerotic bone. *Rheumatology* 58, 1777–1783. doi: 10.1093/rheumatology/kez130

Intema, F., Thomas, T. P., Anderson, D. D., Elkins, J. M., Brown, T. D., Amendola, A., et al. (2011). Subchondral bone remodeling is related to clinical improvement after joint distraction in the treatment of ankle osteoarthritis. *Osteoarthr. Cartil.* 19, 668–675. doi: 10.1016/j.joca.2011.02.005

Jansen, M. P., Besselink, N. J., van Heerwaarden, R. J., Custers, R. J. H., Emans, P. J., Spruijt, S., et al. (2019). Knee joint distraction compared with high tibial osteotomy and total knee arthroplasty: two-year clinical, radiographic, and biochemical marker outcomes of two randomized controlled trials. *Cartilage* 2019:1947603519828432. doi: 10.1177/1947603519828432

Jansen, M. P., Mastbergen, S. C., van Heerwaarden, R. J., Spruijt, S., van Empelen, M. D., Kester, E. C., et al. (2020). Knee joint distraction in regular care for treatment of knee osteoarthritis: a comparison with clinical trial data. *PLoS One* 15:e0227975. doi: 10.1371/journal.pone.0227975

Jansen, M. P., van der Weiden, G. S., Van Roermund, P. M., Custers, R. J. H., Mastbergen, S. C., and Lafeber, F. P. J. G. (2018). Initial tissue repair predicts long-term clinical success of knee joint distraction as treatment for knee osteoarthritis. *Osteoarthr. Cartil.* 26, 1604–1608. doi: 10.1016/j.joca.2018.08.004

Jayasuriya, C. T., Hu, N., Li, J., Lemme, N., Terek, R., Ehrlich, M. G., et al. (2018). Molecular characterization of mesenchymal stem cells in human osteoarthritis cartilage reveals contribution to the OA phenotype. *Sci. Rep.* 8:7044. doi: 10.1038/s41598-018-25395-8

Ji, Q., Zheng, Y., Zhang, G., Hu, Y., Fan, X., Hou, Y., et al. (2019). Single-cell RNA-seq analysis reveals the progression of human osteoarthritis. *Ann. Rheum. Dis.* 78, 100–110. doi: 10.1136/annrheumdis-2017-212863

Jones, E. A., Crawford, A., English, A., Henshaw, K., Mundy, J., Corscadden, D., et al. (2008). Synovial fluid mesenchymal stem cells in health and early osteoarthritis - Detection and functional evaluation at the single-cell level. *Arthrit. Rheum.* 58, 1731–1740. doi: 10.1002/art.23485

Jones, E. A., English, A., Henshaw, K., Kinsey, S. E., Markham, A. F., Emery, P., et al. (2004). Enumeration and phenotypic characterization of synovial fluid multipotential mesenchymal progenitor cells in inflammatory and degenerative arthritis. *Arthrit. Rheum.* 50, 817–827. doi: 10.1002/art.20203

Kang, H., Sung, J., Jung, H. M., Woo, K. M., Hong, S. D., and Roh, S. (2012). Insulin-like growth factor 2 promotes osteogenic cell differentiation in the

parthenogenetic murine embryonic stem cells. *Tissue Eng Part A* 18, 331–341. doi: 10.1089/ten.TEA.2011.0074

Kania, K., Colella, F., Riemen, A. H. K., Wang, H., Howard, K. A., Aigner, T., et al. (2020). Regulation of Gdf5 expression in joint remodelling, repair and osteoarthritis. *Sci. Rep.* 10:157. doi: 10.1038/s41598-019-57011-8

Katagiri, K., Matsukura, Y., Muneta, T., Ozeki, N., Mizuno, M., Katano, H., et al. (2017). Fibrous synovium releases higher numbers of mesenchymal stem cells than adipose synovium in a suspended synovium culture model. *Arthroscopy* 33, 800–810. doi: 10.1016/j.arthro.2016.09.033

Kim, Y. S., Lee, H. J., Yeo, J. E., Kim, Y. I., Choi, Y. J., and Koh, Y. G. (2015). Isolation and characterization of human mesenchymal stem cells derived from synovial fluid in patients with osteochondral lesion of the talus. *Am. J. Sports Med.* 43, 399–406. doi: 10.1177/0363546514559822

Koelling, S., Kruegel, J., Irmer, M., Path, J. R., Sadowski, B., Miro, X., et al. (2009). Migratory chondrogenic progenitor cells from repair tissue during the later stages of human osteoarthritis. *Cell Stem Cell* 4, 324–335. doi: 10.1016/j.stem.2009.01.015

Kohno, Y., Mizuno, M., Ozeki, N., Katano, H., Otabe, K., Koga, H., et al. (2018). Comparison of mesenchymal stem cells obtained by suspended culture of synovium from patients with rheumatoid arthritis and osteoarthritis. *BMC Musculoskelet. Disord.* 19:78. doi: 10.1186/s12891-018-1998-6

Kouroupis, D., Sanjurjo-Rodriguez, C., Jones, E., and Correa, D. (2019). Mesenchymal stem cell functionalization for enhanced therapeutic applications. *Tissue Eng Part B Rev.* 25, 55–77. doi: 10.1089/ten.TEB.2018.0118

Lee, D. H., Sonn, C. H., Han, S. B., Oh, Y., Lee, K. M., and Lee, S. H. (2012). Synovial fluid CD34− $CD44^+$ $CD90^+$ mesenchymal stem cell levels are associated with the severity of primary knee osteoarthritis. *Osteoarthr. Cartil.* 20, 106–109. doi: 10.1016/j.joca.2011.11.010

Leijs, M. J., van Buul, G. M., Lubberts, E., Bos, P. K., Verhaar, J. A., Hoogduijn, M. J., et al. (2012). Effect of arthritic synovial fluids on the expression of immunomodulatory factors by mesenchymal stem cells: an explorative in vitro study. *Front. Immunol.* 3:231. doi: 10.3389/fimmu.2012.00231

Leijten, J. C., Bos, S. D., Landman, E. B., Georgi, N., Jahr, H., Meulenbelt, I., et al. (2013). GREM1, FRZB and DKK1 mRNA levels correlate with osteoarthritis and are regulated by osteoarthritis-associated factors. *Arthrit. Res. Ther.* 15:R126. doi: 10.1186/ar4306

Ludin, A., Sela, J. J., Schroeder, A., Samuni, Y., Nitzan, D. W., and Amir, G. (2013). Injection of vascular endothelial growth factor into knee joints induces osteoarthritis in mice. *Osteoarthr. Cartil.* 21, 491–497. doi: 10.1016/j.joca.2012.12.003

Mastbergen, S. C., Saris, D. B., and Lafeber, F. P. (2013). Functional articular cartilage repair: here, near, or is the best approach not yet clear? *Nat. Rev. Rheumatol.* 9, 277–290. doi: 10.1038/nrrheum.2013.29

Matas, J., Orrego, M., Amenabar, D., Infante, C., Tapia-Limonchi, R., Cadiz, M. I., et al. (2019). Umbilical cord-derived mesenchymal stromal cells (MSCs) for knee osteoarthritis: repeated MSC dosing is superior to a single MSC dose and to hyaluronic acid in a controlled randomized Phase I/II Trial. *Stem Cells Transl. Med.* 8, 215–224. doi: 10.1002/sctm.18-0053

Matsukura, Y., Muneta, T., Tsuji, K., Koga, H., and Sekiya, I. (2014). Mesenchymal stem cells in synovial fluid increase after meniscus injury. *Clin. Orthop. Relat. Res.* 472, 1357–1364. doi: 10.1007/s11999-013-3418-4

McGonagle, D., Baboolal, T. G., and Jones, E. (2017). Native joint-resident mesenchymal stem cells for cartilage repair in osteoarthritis. *Nat. Rev. Rheumatol.* 13, 719–730. doi: 10.1038/nrrheum.2017.182

Miotla Zarebska, J., Chanalaris, A., Driscoll, C., Burleigh, A., Miller, R. E., Malfait, A. M., et al. (2017). CCL2 and CCR2 regulate pain-related behaviour and early gene expression in post-traumatic murine osteoarthritis but contribute little to chondropathy. *Osteoarthr. Cartil.* 25, 406–412. doi: 10.1016/j.joca.2016.10.008

Mizuno, M., Katano, H., Mabuchi, Y., Ogata, Y., Ichinose, S., Fujii, S., et al. (2018). Specific markers and properties of synovial mesenchymal stem cells in the surface, stromal, and perivascular regions. *Stem Cell Res. Ther.* 9:123. doi: 10.1186/s13287-018-0870-9

Monibi, F., Roller, B. L., Stoker, A., Garner, B., Bal, S., and Cook, J. L. (2016). Identification of synovial fluid biomarkers for knee osteoarthritis and correlation with radiographic assessment. *J. Knee Surg.* 29, 242–247. doi: 10.1055/s-0035-1549022

Morito, T., Muneta, T., Hara, K., Ju, Y. J., Mochizuki, T., Makino, H., et al. (2008). Synovial fluid-derived mesenchymal stem cells increase after intra-articular ligament injury in humans. *Rheumatology* 47, 1137–1143. doi: 10.1093/rheumatology/ken114

Muiños-López, E., Delgado, D., Sánchez, P., Paiva, B., Anitua, E., Fiz, N., et al. (2016). Modulation of Synovial fluid-derived mesenchymal stem cells by intra-articular and intraosseous platelet rich plasma administration. *Stem Cells Int.* 2016:1247950. doi: 10.1155/2016/1247950

Neybecker, P., Henrionnet, C., Pape, E., Mainard, D., Galois, L., Loeuille, D., et al. (2018). In vitro and in vivo potentialities for cartilage repair from human advanced knee osteoarthritis synovial fluid-derived mesenchymal stem cells. *Stem Cell Res. Ther.* 9:329. doi: 10.1186/s13287-018-1071-2

O'Brien, K., Tailor, P., Leonard, C., DiFrancesco, L. M., Hart, D. A., Matyas, J. R., et al. (2017). Enumeration and localization of mesenchymal progenitor cells and macrophages in synovium from normal individuals and patients with pre-osteoarthritis or clinically diagnosed osteoarthritis. *Int. J. Mol. Sci.* 18:774. doi: 10.3390/ijms18040774

Paavonen, K., Mandelin, J., Partanen, T., Jussila, L., Li, T. F., Ristimaki, A., et al. (2002). Vascular endothelial growth factors C and D and their VEGFR-2 and 3 receptors in blood and lymphatic vessels in healthy and arthritic synovium. *J. Rheumatol.* 29, 39–45.

Piñeiro-Ramil, M., Castro-Viñuelas, R., Sanjurjo-Rodríguez, C., Hermida-Gómez, T., Fuentes-Boquete, de Toro-Santos, F. J., et al. (2017). "Cell therapy and tissue engineering for cartilage repair," in *Cartilage Repair and Regeneration*, eds A. R. Zorzi and J. B. D. Miranda (London: IntechOpen), doi: 10.5772/intechopen.70406

Roelofs, A. J., Zupan, J., Riemen, A. H. K., Kania, K., Ansboro, S., White, N., et al. (2017). Joint morphogenetic cells in the adult mammalian synovium. *Nat. Commun.* 8:15040. doi: 10.1038/ncomms15040

Roughley, P. J., and Mort, J. S. (2014). The role of aggrecan in normal and osteoarthritic cartilage. *J. Exp. Orthop.* 1:8. doi: 10.1186/s40634-014-0008-7

Sánchez, M., Andia, I., Anitua, E., and Pello, S. (2012). "Platelet rich plasma (PRP) biotechnology: concepts and therapeutic applications in orthopedics and sports medicine," in *Innovations in Biotechnology*, ed. E. C. Agbo (London: IntechOpen), doi: 10.5772/28908

Sánchez, M., Delgado, D., Sánchez, P., Muiños-López, E., Paiva, B., Granero-Moltó, F., et al. (2016). Combination of intra-articular and intraosseous injections of platelet rich plasma for severe knee osteoarthritis: a pilot study. *Biomed. Res. Int.* 2016:4868613. doi: 10.1155/2016/4868613

Sanjurjo-Rodriguez, C., Baboolal, T. G., Burska, A. N., Ponchel, F., El-Jawhari, J. J., Pandit, H., et al. (2019). Gene expression and functional comparison between multipotential stromal cells from lateral and medial condyles of knee osteoarthritis patients. *Sci. Rep.* 9:9321. doi: 10.1038/s41598-019-45820-w

Santa Maria, C., Cheng, Z., Li, A., Wang, J., Shoback, D., Tu, C. L., et al. (2016). Interplay between CaSR and PTH1R signaling in skeletal development and osteoanabolism. *Semin. Cell Dev. Biol.* 49, 11–23. doi: 10.1016/j.semcdb.2015.12.004

Schminke, B., and Miosge, N. (2014). Cartilage repair in vivo: the role of migratory progenitor cells. *Curr. Rheumatol. Rep.* 16:461. doi: 10.1007/s11926-014-0461-4

Schreurs, B. W., and Hannink, G. (2017). Total joint arthroplasty in younger patients: heading for trouble? *Lancet* 389, 1374–1375. doi: 10.1016/S0140-6736(17)30190-3

Sekiya, I., Ojima, M., Suzuki, S., Yamaga, M., Horie, M., Koga, H., et al. (2012). Human mesenchymal stem cells in synovial fluid increase in the knee with degenerated cartilage and osteoarthritis. *J. Orthop. Res.* 30, 943–949. doi: 10.1002/jor.22029

Seol, D., McCabe, D. J., Choe, H., Zheng, H., Yu, Y., Jang, K., et al. (2012). Chondrogenic progenitor cells respond to cartilage injury. *Arthrit. Rheum.* 64, 3626–3637. doi: 10.1002/art.34613

Shariatzadeh, M., Song, J., and Wilson, S. L. (2019). The efficacy of different sources of mesenchymal stem cells for the treatment of knee osteoarthritis. *Cell Tissue Res.* 378, 399–410. doi: 10.1007/s00441-019-03069-9

Sivasubramaniyan, K., Lehnen, D., Ghazanfari, R., Sobiesiak, M., Harichandan, A., Mortha, E., et al. (2012). Phenotypic and functional heterogeneity of human bone marrow- and amnion-derived MSC subsets. *Hematopoiet. Stem Cells* 8, 94–106. doi: 10.1111/j.1749-6632.2012.06551.x

Takahashi, T., Baboolal, T. G., Lamb, J., Hamilton, T. W., and Pandit, H. G. (2019). Is knee joint distraction a viable treatment option for Knee OA?-a literature review and meta-analysis. *J. Knee Surg.* 32, 788–795. doi: 10.1055/s-0038-1669447

Tricoire, L., Cauli, B., and Lambolez, B. (2019). Gene expression analysis by multiplex single-cell RT-PCR. *Methods Mol. Biol.* 1941, 139–154. doi: 10.1007/978-1-4939-9077-1_10

van der Woude, J. A. D., Wiegant, K., van Heerwaarden, R. J., Spruijt, S., Emans, P. J., Mastbergen, S. C., et al. (2017a). Knee joint distraction compared with total knee arthroplasty: a randomised controlled trial. *Bone Joint J.* 99, 51–58. doi: 10.1302/0301-620X.99B1.BJJ-2016-0099.R3

van der Woude, J. A. D., Wiegant, K., van Roermund, P. M., Intema, F., Custers, R. J. H., Eckstein, F., et al. (2017b). Five-year follow-up of knee joint distraction: clinical benefit and cartilaginous tissue repair in an open uncontrolled prospective study. *Cartilage* 8, 263–271. doi: 10.1177/1947603516665442

Wang, Z., Qiu, Y., Lu, J., and Wu, N. (2013). Connective tissue growth factor promotes interleukin-1β-mediated synovial inflammation in knee osteoarthritis. *Mol. Med. Rep.* 8, 877–882. doi: 10.3892/mmr.2013.1570

Watanabe, N., Endo, K., Komori, K., Ozeki, N., Mizuno, M., Katano, H., et al. (2020). Mesenchymal stem cells in synovial fluid increase in knees with degenerative meniscus injury after arthroscopic procedures through the endogenous effects of CGRP and HGF. *Research Square* [Preprint], doi: 10.21203/rs.3.rs-42459/v1

Watt, F. E., Hamid, B., Garriga, C., Judge, A., Hrusecka, R., Custers, R. J. H., et al. (2020). The molecular profile of synovial fluid changes upon joint distraction and is associated with clinical response in knee osteoarthritis. *Osteoarthr. Cartil.* 28, 324–333. doi: 10.1016/j.joca.2019.12.005

Westacott, C. I., Webb, G. R., Warnock, M. G., Sims, J. V., and Elson, C. J. (1997). Alteration of cartilage metabolism by cells from osteoarthritic bone. *Arthrit. Rheum.* 40, 1282–1291. doi: 10.1002/1529-0131(199707)40:7<1282::aid-art13>3.0.co;2-e

Wiegant, K., Intema, F., van Roermund, P. M., Barten-van Rijbroek, A. D., Doornebal, A., Hazewinkel, H. A., et al. (2015). Evidence of cartilage repair by joint distraction in a canine model of osteoarthritis. *Arthrit. Rheumatol.* 67, 465–474. doi: 10.1002/art.38906

Wiegant, K., van Roermund, P. M., Intema, F., Cotofana, S., Eckstein, F., Mastbergen, S. C., et al. (2013). Sustained clinical and structural benefit after joint distraction in the treatment of severe knee osteoarthritis. *Osteoarthr. Cartil.* 21, 1660–1667. doi: 10.1016/j.joca.2013.08.006

Wiegertjes, R., van Caam, A., van Beuningen, H., Koenders, M., van Lent, P., van der Kraan, P., et al. (2019). TGF-β dampens IL-6 signaling in articular chondrocytes by decreasing IL-6 receptor expression. *Osteoarthr. Cartil.* 27, 1197–1207. doi: 10.1016/j.joca.2019.04.014

Worthley, D. L., Churchill, M., Compton, J. T., Tailor, Y., Rao, M., Si, Y., et al. (2015). Gremlin 1 identifies a skeletal stem cell with bone, cartilage, and reticular stromal potential. *Cell* 160, 269–284. doi: 10.1016/j.cell.2014.11.042

Zhen, G., Wen, C., Jia, X., Li, Y., Crane, J. L., Mears, S. C., et al. (2013). Inhibition of TGF-beta signaling in mesenchymal stem cells of subchondral bone attenuates osteoarthritis. *Nat. Med.* 19, 704–712. doi: 10.1038/nm.3143

Zhou, W., Lin, J., Zhao, K., Jin, K., He, Q., Hu, Y., et al. (2019). Single-cell profiles and clinically useful properties of human mesenchymal stem cells of adipose and bone marrow origin. *Am. J. Sports Med.* 47, 1722–1733. doi: 10.1177/0363546519848678

Conflict of Interest: The authors declare that the research was conducted in the absence of any commercial or financial relationships that could be construed as a potential conflict of interest.

frontiers in Bioengineering and Biotechnology

ORIGINAL RESEARCH
published: 13 November 2020
doi: 10.3389/fbioe.2020.590743

Physioxia Stimulates Extracellular Matrix Deposition and Increases Mechanical Properties of Human Chondrocyte-Derived Tissue-Engineered Cartilage

James E. Dennis[1], George Adam Whitney[1], Jyoti Rai[2], Russell J. Fernandes[2] and Thomas J. Kean[1†]*

[1] Benaroya Research Institute, Seattle, WA, United States, [2] Department of Orthopaedics and Sports Medicine, University of Washington, Seattle, WA, United States

Cartilage tissue has been recalcitrant to tissue engineering approaches. In this study, human chondrocytes were formed into self-assembled cartilage sheets, cultured in physiologic (5%) and atmospheric (20%) oxygen conditions and underwent biochemical, histological and biomechanical analysis at 1- and 2-months. The results indicated that sheets formed at physiological oxygen tension were thicker, contained greater amounts of glycosaminoglycans (GAGs) and type II collagen, and had greater compressive and tensile properties than those cultured in atmospheric oxygen. In all cases, cartilage sheets stained throughout for extracellular matrix components. Type II-IX-XI collagen heteropolymer formed in the neo-cartilage and fibrils were stabilized by trivalent pyridinoline cross-links. Collagen cross-links were not significantly affected by oxygen tension but increased with time in culture. Physiological oxygen tension and longer culture periods both served to increase extracellular matrix components. The foremost correlation was found between compressive stiffness and the GAG to collagen ratio.

Keywords: tissue-engineered cartilage, type II collagen, biomechanical testing, articular cartilage, chondrocyte, chondrogenesis, collagen cross linking, hypoxia

OPEN ACCESS

Edited by:
Roberto Narcisi, Erasmus University Rotterdam, Netherlands

Reviewed by:
Lucienne A. Vonk, CO.DON AG, Germany
Ryan Michael Porter, University of Arkansas for Medical Sciences, United States

***Correspondence:**
Thomas J. Kean
thomas.kean@ucf.edu

†Present address:
Thomas J. Kean, Biionix Cluster, Internal Medicine, College of Medicine, University of Central Florida, Orlando, FL, United States

Specialty section:
This article was submitted to Preclinical Cell and Gene Therapy, a section of the journal Frontiers in Bioengineering and Biotechnology

Received: *02 August 2020*
Accepted: *14 October 2020*
Published: *13 November 2020*

Citation:
Dennis JE, Whitney GA, Rai J, Fernandes RJ and Kean TJ (2020) Physioxia Stimulates Extracellular Matrix Deposition and Increases Mechanical Properties of Human Chondrocyte-Derived Tissue-Engineered Cartilage. Front. Bioeng. Biotechnol. 8:590743. doi: 10.3389/fbioe.2020.590743

INTRODUCTION

Cartilage tissue has very poor intrinsic repair capacity. While osteoarthritis is a complex, multifaceted disease, cartilage degradation is a core component. Autologs chondrocyte implantation and matrix assisted autologs chondrocyte implantation have provided relief to patients but commonly result in fibrocartilage repair (Shekkeris et al., 2012). Tissue engineering could potentially address this through *in vitro* culture methods to produce functional hyaline cartilage tissue, with several examples currently in clinical trials (Kwon et al., 2019). We, and others, have investigated media supplements and growth factors to improve the expansion and re-differentiation of the expanded chondrocytes (Vunjak-Novakovic et al., 1999; Enochson et al., 2012; Makris et al., 2013a; Dennis et al., 2020).

Cartilage, being avascular, is normally exposed to low levels of oxygen (2–5%), meaning that this would be physiological conditions (Pattappa et al., 2019). It is increasingly apparent that physiological oxygen tension should be the standard culture method to grow tissue engineered human articular cartilage whether it be from mesenchymal stem cells (Pattappa et al., 2019), articular chondrocytes (Kean and Dennis, 2012a,b, 2013, 2015; Kean et al., 2013, 2015, 2016, 2019; Markway et al., 2013; Bianchi et al., 2017) or chondroprogenitors (Anderson et al., 2018). The selection of cell type for engineered tissue raises some interesting issues, mesenchymal stromal cells (MSC) commonly progress to hypertrophy (Mueller and Tuan, 2008) as do iPSCs driven down the mesenchymal pathway (Adkar et al., 2019), a negative scenario for the production of hyaline cartilage. Hypertrophy has been reduced but not eliminated during MSC culture (Gawlitta et al., 2012) and subcutaneous implants by pharmacological and/or culture-dependent methods (Diederichs et al., 2019). This study focuses on the use of human articular chondrocytes derived from discarded total joint replacement tissue as both a clinically relevant and non-hypertrophic cell source (in our hands). We, and others, have focused on scaffold-free self-assembly of tissue-engineered cartilage, as significant similarities to native tissue structure can be achieved (Weidenbecher et al., 2008; Gilpin et al., 2010; Whitney et al., 2012; Kean et al., 2016; Anderson et al., 2018; Dennis et al., 2018; Huang et al., 2018; Mansour et al., 2018; Whitney et al., 2018). Significant expansion, up to eight population doublings, of human chondrocytes while maintaining their differentiation capacity has been achieved through their culture on devitalized synoviocyte matrix (Kean and Dennis, 2015). Using these methods, we produced sheets of human articular chondrocyte-derived cartilage and investigated the effect of low, physiological, oxygen tension and duration of culture on cartilage quality in terms of biomechanics and biochemical content. It was hypothesized that physiological oxygen tension and increased culture duration would improve the mechanical properties of the tissue engineered cartilage through an increase in extracellular matrix content. This study adds to the current body of literature by expanding the donor pool, focuses on chondrocytes isolated from total joint replacement tissue as a cell source, and includes analysis of cartilage-typic collagen heteropolymer formation, collagen cross-links and tensile properties of tissue engineered cartilage.

MATERIALS AND METHODS

Cell and Tissue Culture

Human articular chondrocytes were thawed from frozen stocks obtained from discarded surgical tissue of patients (n = 6) undergoing total joint replacement collected with IRB approval. Human articular chondrocytes were expanded under physiological oxygen tension (5%; Physioxia) on synoviocyte derived extracellular matrix in growth media (DMEM-LG supplemented with 10% FBS and 1% penicillin/streptomycin) (Kean and Dennis, 2015). Synoviocyte derived extracellular matrix was generated using the method described in Kean et al. (2015) Briefly, synoviocytes from porcine knees were isolated using sequential digest with hyaluronidase, trypsin/EDTA then collagenase. Synoviocytes were expanded for two passages then seeded at 6,000 cells/cm^2, grown until 70–80% confluence (˜5 days) in DMEM-LG + 10% FBS + 1% pen/strep, then switched to ascorbate containing media (DMEM-LG + 10% FBS + 1% pen/strep + 50 μM ascorbate-2-phosphate for a further 7 days. At this point, cells were washed with PBS then the flask flash frozen on dry ice-cooled ethanol. Dry ice-cooled ethanol was then pipetted into the flask to devitalize the synoviocytes, removed and evaporated. Devitalized synoviocyte matrix covered flasks were stored at 4°C until use (<6-months). At the end of first passage (six experiments) or second passage (two experiments), cells were trypsinized and seeded at high density (4.4×10^6 cells/cm^2) in a custom stainless steel biochamber (**Figure 1**) (Whitney et al., 2012). Partner biochambers for large (16 cm^2) (Whitney et al., 2012), seeded at the same cell density, were made in several experiments for other studies. All assays were performed on the 1.13 cm^2 pieces of tissue engineered cartilage (**Figure 1**). Biochambers were assembled and sterilized by autoclave. The polyester membrane was coated with fibronectin (8 μg/cm^2 in PBS) and allowed to dry in a biosafety cabinet. Biochambers were used much as previously described but with a stacked, 1.1 cm^2 circular seeding chamber with longer screws creating greater space above and below the chamber for media exchange (**Figure 1**). Biochambers were cultured at either atmospheric oxygen tension (20%; Atm O_2) or Physioxia (5% O_2) in defined chondrogenic medium [DMEM-HG containing 1% ITS + premix, dexamethasone (100 nM), ascorbate-2-phosphate (120 μM), 1% MEM NEAA, 1% Pen/Strep, 1% glutamax, TGFβ1 (10 ng/ml)] for 21 days (3-weeks) and 46–56 days (7-weeks) with 50% media changes every other day. All cultures were grown at 37°C with 5% CO_2 in a humidified atmosphere. After 5-days in static culture, all biochambers were put on a rotating shaker (60 RPM). At the end of culture, three 5mm skin biopsy punches were taken for mechanical assessment (equilibrium modulus and tensile modulus). Remaining tissue was assessed by biochemical [glycosaminoglycan (GAG), DNA, hydroxyproline (HDP), and collagen cross-link content (hydroxylysyl pyridinoline + lysyl pyridinoline (HP + LP); moles/mole collagen)] and histological assays.

Biochemical Assays

Glycosaminoglycan, DNA and HDP assays were conducted much as previously described (Kean et al., 2016). Briefly, tissue engineered cartilage was digested with papain solution (25 μg/mL papain, 2 mM cysteine, 50 mM sodium phosphate, and 2 mM EDTA adjusted to pH 6.5 [all from Sigma-Aldrich]) at 65°C for 3 h. Digested tissue was then split between the HDP assay and GAG/DNA assays. For the GAG/DNA portion of the assay, papain digested samples were inactivated by sodium hydroxide (2 volumes 0.1 M NaOH) then neutralized with acidified phosphate buffer (2 volumes 100 mM sodium phosphate pH 7.2 acidified with 0.1 M HCl). GAG was assessed using safranin-O: Neutralized samples were incubated with Safranin-O solution (0.05% in 50 mM sodium acetate) on a dot blot apparatus (BioRad) with a 0.45 μm nitrocellulose membrane in duplicate. Dots were punched from the membrane and incubated

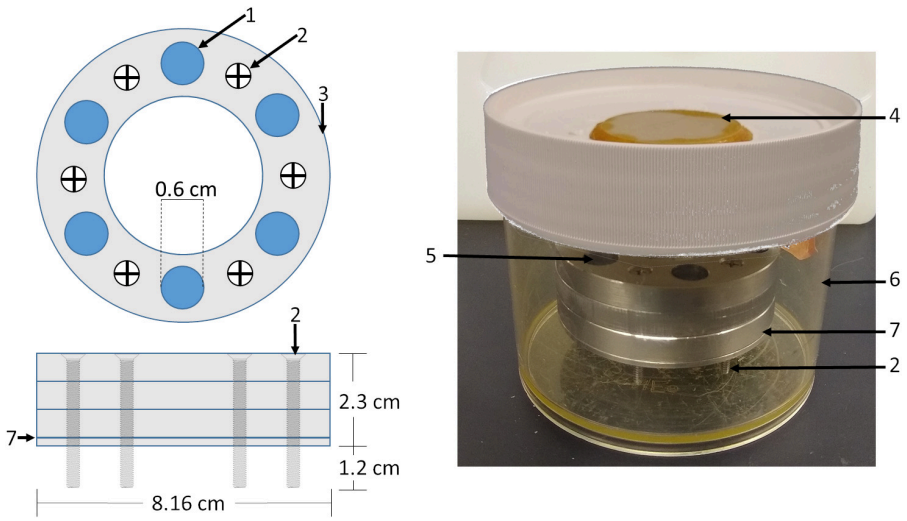

FIGURE 1 | Biochamber model and setup. A circular biochamber design with a 1.13 cm^2 cell seeding area (1) was used with three seeding chambers (3) stacked on top of each other giving a 2.1 ml seeding volume. Stainless steel screws (2) were used to raise the biochambers 1.2 cm allowing media access to the cell sheet through the polyester membrane (7) sandwiched between the bottom 0.2 cm plate and the seeding chambers. Biochambers were assembled and placed in Nalgene containers (6) with a ceramic filter on the lid (4). Defined chondrogenic media was added to the level of the membrane, cells seeded, then media added to 0.2 cm below the top of the topmost seeding chamber.

in cetylpyridinium chloride solution (10%, Alpha Aesar) at 37°C for 20 min. The extract was then transferred in triplicate to a clear 96-well microplate and absorbance measured (536 nm; Tecan M200). GAG concentrations were calculated from a standard curve produced with chondroitin sulfate (Seikagaku Chemicals). DNA was assessed from neutralized samples using buffered Hoechst solution (0.667 μg/ml in 0.2 M pH 8.0 phosphate buffer; 33258; Sigma-Aldrich). Neutralized digest (20μl) was transferred to a black 96-well plate in duplicate and Hoechst solution added (100 μl) then fluorescence read (Ex 365 nm, Em 460 nm; Tecan M200). DNA content was calculated from a standard curve (calf thymus DNA; Sigma-Aldrich) made in neutralized papain buffer. For the assessment of HDP, papain digested samples were acid hydrolyzed overnight (10:1 vol/vol, 6 M HCl, 110°C). Acid hydrolysate was then evaporated to dryness by incubation at 70°C 1–2 days. Samples and HDP standards were then resuspended in ddH_2O, mixed with 1 volume copper sulfate (0.15 M), 1 volume NaOH (2.5 M) and incubated (50°C, 5 min). Samples were then oxidized by incubation with hydrogen peroxide (1 volume, 6% H_2O_2; 50°C, 10 min). To this solution, 4 volumes of sulfuric acid were added (1.5 M H_2SO_4) then reacted with Ehrlich's reagent (2 volumes: 10% w/v 4-dimethylamino benzaldehyde in 60% isopropanol, 26% perchloric acid, 14% MΩ water) at 70°C for 16 min. After cooling, samples and standard absorbance was read on a plate reader (505 nm, Tecan M200). Collagen content was estimated from HDP concentration by a conversion factor of 7.6 (Venn and Maroudas, 1977).

Collagen Cross-Link Analysis

Samples were dried, weighed and then acid hydrolyzed in 6 M HCl, 110°C for 24 h. HP and LP cross-linking residues were resolved and quantified by C-18 reverse phase HPLC with fluorescence detection (excitation 297 nm, emission 396 nm) and total collagen content was determined as described (Fernandes et al., 1998).

Collagen Heteropolymer Analysis

Unused portions of the samples used for mechanical analyses were used to qualitatively fingerprint cross-linked collagen types by western blots. The heteropolymeric collagen network formed in the samples was depolymerized in equal volumes of 0.5 M acetic acid containing 100 μg/ml pepsin for 18h at 4°C. Unused portions of neo-cartilage after mechanical tests were used for SDS-PAGE, these were normalized by wet weight within oxygen tension. Equal aliquots of solubilized collagen were analyzed by SDS-PAGE and the separated collagen chains visualized by Coomassie blue staining. Pepsin-extracted type II collagen from human articular cartilage was used as a control. The separated collagen chains were also blotted onto PVDF membranes and probed with mAb 1C10 to identify α1(II) chains and with mAb 10F2, pAb 5890, mAb 2B4 to identify collagen chains cross-linked to the *C*-telopeptide of α1(II), to the *N*-telopeptide of α1(XI) chains and to the α1(IX) chains, respectively (Fernandes et al., 2003). As we have described before, this validates if a heteropolymer of type II and type XI collagen had formed (Murdoch et al., 2016).

Histological Analysis

Samples were fixed in neutral buffered formalin overnight at 4°C then switched to PBS at 4°C until embedded. Samples were embedded by sequential dehydration in graded ethanols, xylene, and paraffin. Paraffin sections (8 μm) were deparaffinized and hydrated before staining with safranin-O (Sigma-Aldrich) for GAG with a Fast Green (AA16520-06, Alfa Aesar) counterstain.

For immunohistochemistry, hydrated sections were subjected to antigen retrieval by pronase (1 mg/ml in PBS containing 5 mM calcium chloride; Sigma-Aldrich) incubation for 10 min at room temperature. Primary antibodies against type I collagen (631703, MP Biomedical, 1:1,000), type II collagen (DSHB II-II6B3 cell culture supernatant, 1:500) and type X collagen (kind gift of Gary Gibson, Henry Ford Hospital, Detroit, MI, United States; 1:500) were incubated with tissue sections at 4°C overnight. Sections were then rinsed and stained with secondary antibody (biotinylated horse anti-mouse; Gibco; BA2000; 1:2,000) for 1 h at room temperature before rinsing and incubation with streptavidin-HRP (SNN1004, Invitrogen, 1:5,000) 30 min at room temperature. Detection was then made with VIP substrate (Vectashield) by incubation at room temperature for 10 min. Slides were rinsed and counterstained with Fast Green before mounting.

Mechanical Analysis

Samples were thawed in PBS solution equilibrated to room temperature for at least 30 min. Punches were measured three times with digital calipers to assess thickness. Compressive equilibrium moduli were determined as previously described (Lima et al., 2007). Briefly, after an initial tare load of 0.2 N, 4 sequential strains of 5, 10, 15, and 20% were applied, with a stress-equilibration period of 30 min between each strain step. The stress measured at the end of each strain period was taken as the apparent stress at the corresponding strain level. The equilibrium modulus was determined as the slope between the apparent stress and the strain.

To test elastic tensile Young's moduli, a custom dogbone punch was made from skin biopsy punches and punches taken from the 5 mm punch (**Figure 2A**). Custom holders were made from overhead projector sheets (**Supplementary File 1**) and dogbones attached using cyanoacrylate glue (**Figure 2A4**), tissue hydration was maintained with PBS. Tissues were stretched to failure (**Figures 2B,C**) and the tensile Young's modulus, ultimate tensile stress and yield stress calculated. Residual pieces of cartilage from the dogbone punch were used for collagen typing and heteropolymer analysis.

Samples and Statistics

Eight separate experiments were performed with chondrocytes from six human donors. For the analysis of GAG/DNA/HDP, three samples per sheet were taken from up to two replicate sheets and assayed in duplicate. Each experiment was averaged and data shown represents the average for the experiment. When sheets were too flimsy to be manipulated, GAG/DNA/HDP was not performed (three experiments, three donors, five data points, all Atm O_2). A mixed-effects model was used to analyze log transformed values (GAG/DNA and Collagen/DNA) and collagen crosslink density with Sidak's multiple comparisons test (GraphPad Prism, V8.4.2).

For mechanical tests two sheets were made for each donor and 2–3 5 mm biopsy punches were taken from each sheet. Punch thickness was measured with digital calipers three times and the average value taken for the thickness. Thickness data was analyzed by a mixed-effects model with Sidak's multiple comparisons test (GraphPad Prism, V8.4.2). Punches that were incomplete circles, curled too much to get a flat sheet in testing were excluded from analysis. Atmospheric oxygen tension sheets from donors that were insufficiently sturdy or were too thin to be manipulated (2 of 6) have the imputed compressive modulus value of the weakest sheet tested (0.3129 kPa). All data represent the average of the samples tested (n = 1–4) for each independent experiment (n = 8). Data were analyzed by repeated measures two-way ANOVA with Sidak's multiple comparisons test (GraphPad Prism, V8.4.2). Four donors were included in the tensile testing experiments, two of which failed to form sheets that were sturdy enough to be tested when cultured at Atm O_2. Data were analyzed by two-way ANOVA with Sidak's multiple comparisons test (GraphPad Prism, V8.4.2).

RESULTS

Handleable tissue-engineered human cartilage sheets formed in all eight experiments in Physioxia vs five of eight experiments at week 3 and six of eight experiments by week 7 at Atm O_2 (**Figure 3**).

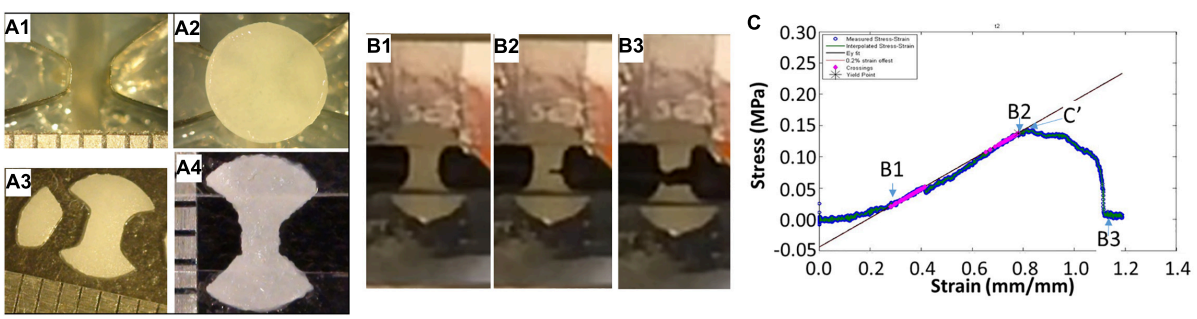

FIGURE 2 | Tissue engineered cartilage sample preparation and tensile testing. Panel **(A)** shows the custom manufactured dog bone punch **(A1)**, the 5 mm punched tissue-engineered human cartilage sheet on the dogbone punch **(A2)**, the resulting dogbone **(A3)**, and the dogbone fixed to the OHP film adapter to insert into the grips of the mechanical testing device. Panel **(B)** shows sequential images of a piece of tissue-engineered human cartilage being tested in tension to failure. Panel **(C)** shows the stress strain curve of the cartilage piece with approximate points shown in the graph of the images in **(B)**, with **(B2)** indicating the yield stress, in this case close to the ultimate yield stress **(C')**, and the best fit line showing the tensile Young's modulus.

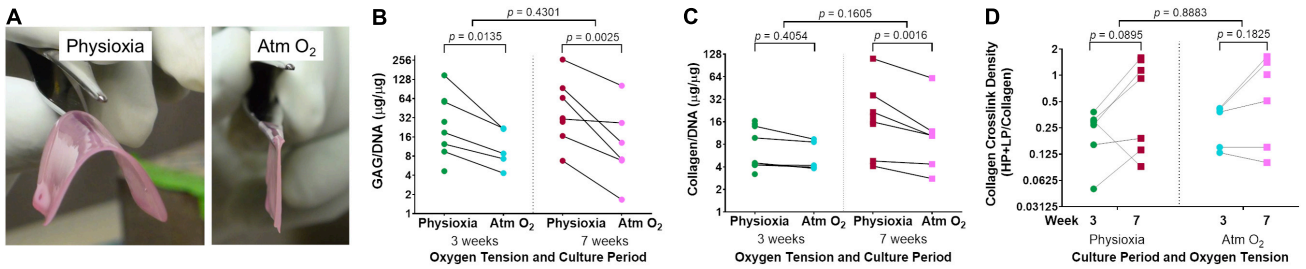

FIGURE 3 | Extracellular matrix deposition in tissue-engineered human cartilage sheets. Sheets grown under Physioxia are more easily manipulated than those grown in Atm O_2; an example of a large (16 cm^2) sheet from a single donor grown in Physioxia or Atm O_2 at 7-weeks **(A)**. Cell normalized glycosaminoglycan (GAG/DNA) content of cartilage from samples grown at Physioxia and Atm O_2 are shown at 3- and 7-weeks **(B)**. Cell normalized total collagen content of tissue-engineered cartilage when grown in Physioxia and Atm O_2 at 3 and 7 weeks is shown **(C)**. Trivalent collagen cross-link density (HP + LP/Collagen) at 3- and 7-weeks under both Physioxia and Atm O_2 are shown **(D)**. Note, all measures are shown on a log (base 2) scale. The average of data for each experiment is shown by a symbol with lines connecting an experiment, six donors, eight experiments.

Biochemical Assays

There was a significant increase in extracellular matrix content, both in terms of GAG/DNA (**Figure 3B**) and collagen/DNA (**Figure 3C**) in human tissue-engineered cartilage sheets when cultured in Physioxia vs Atm O_2. This increase in GAG/DNA was not significantly affected by time in culture (**Figure 3B**). Only under Physioxia was the accumulation of collagen/DNA greater at the 7-week time point (**Figure 3C**).

Collagen trivalent HP and LP cross-links were formed in culture at both oxygen tensions and increased with time in culture, with no apparent effect of oxygen tension (**Figure 3D**). To determine if cartilage-specific collagen type II-IX-XI heteropolymer formed in culture we used specific antibodies to qualitatively fingerprint cross-linked collagen chains as we previously established (Murdoch et al., 2016). **Figure 4A** shows an SDS-PAGE gel of pepsin extracted collagen from human tissue engineered cartilage grown under Atm O_2 and Physioxia. Purified human type II collagen (lane 1) and tissue engineered human cartilage is shown in the lanes 2–5. Only a qualitative evaluation of collagen in these samples was possible. The major Coomassie blue stained pepsin-resistant chain observed was the α1(II) collagen chain which migrates similarly to the chain seen for human type II collagen purified from adult articular cartilage. Two other pepsin-resistant chains of varying intensities were observed (lanes 2–5), migrating above the α1(II) chains. The chains migrate similarly to the α1(XI) and α2(XI) chains in type XI collagens. Faint bands in the region of α2(I) and β2(I) chain characteristic of type I collagen are seen in all lanes including the human type II control. Immunohistochemical analysis does reveal type I collagen in the matrix of the week 3 (Atm O_2 and Physioxia) and week 7 (Atm O_2) tissue engineered cartilage (**Figure 6**). Indeed, we have determined by mass spectrometry that type I collagen is a minor component of neo-cartilage from human bone marrow derived mesenchymal cells (Murdoch et al., 2016). A similar band was also observed in normal and chondrodysplastic human cartilage and was presumed to be the α2(I) chain (Fernandes et al., 1998). However, by *N*-terminal amino-acid sequencing the band was identified as a pepsin over-cleavage product of the α1(II) chain (Wu and Eyre, 1995; Fernandes et al., 1998).

Western Blot using the type II collagen antibody 1C10 (**Figure 4B**) confirmed the α1(II) and the β1(II) chains of type II collagen (lanes 2–5) indicating the chondrocytes elaborated an extensive extracellular matrix containing type II collagen. The antibody also recognized the band below β1(II) chains (distinct in lanes 4, 5 but obscured in lanes 1, 2 due to intense immunoreactivity of the β1(II) band) and the band below the α1(II) chains (lanes 4, 5) indicating these are over-cleavage products of the α1(II) chain. The antibody 10F2 reacted with the α1(II) chain, β1(II) chain and their over-cleavage products as expected for a cross-linked type II collagen polymer (**Figure 4C**), (*C*-telopeptide of type II collagen cross-linked to α1(II) collagen chains) indicating a cross-linked collagen network assembled in the all the neo-cartilages. Following an extended exposure, the antibody also reacted with α1(XI) collagen chains implying this chain was cross-linked to the *C*-telopeptide of type II collagen and that type XI collagen was copolymerized and cross-linked to *C*-telopeptides of type II collagen (data not shown). A similar blot when probed with the antibody 5890 clearly reacted with the α1(II) chain and the α3(XI) chain in the neo-cartilages (**Figure 4D**). (The α1(II) and α3(XI) chains are the identical product of the type II collagen gene but post translational modifications causes the chains to migrate differently on SDS-PAGE). This indicated that the *N*-telopeptide of the α1(XI) collagen chain was cross-linked to the α3(XI) and the α1(II) chain and thus a heteropolymer of type XI-type II collagen molecules had formed. The antibody 2B4 strongly reacted with the β1(II) chain of type II collagen in the neo-cartilages (**Figure 4E**) indicating that this chain was cross-linked to the α1(IX) chain of type IX collagen and a heteropolymer of type IX-type II had formed. This fingerprint pattern on western blots showed that a cross-linked heteropolymer of type II-IX-XI had assembled in the neo-cartilages. **Figure 4F** shows molecular interpretations of collagen heteropolymer assembly from Western blot analysis. Locations of the epitopes in the α1(II) chain or in telopeptide stubs cross-linked to the chains are also shown (McAlinden et al., 2014).

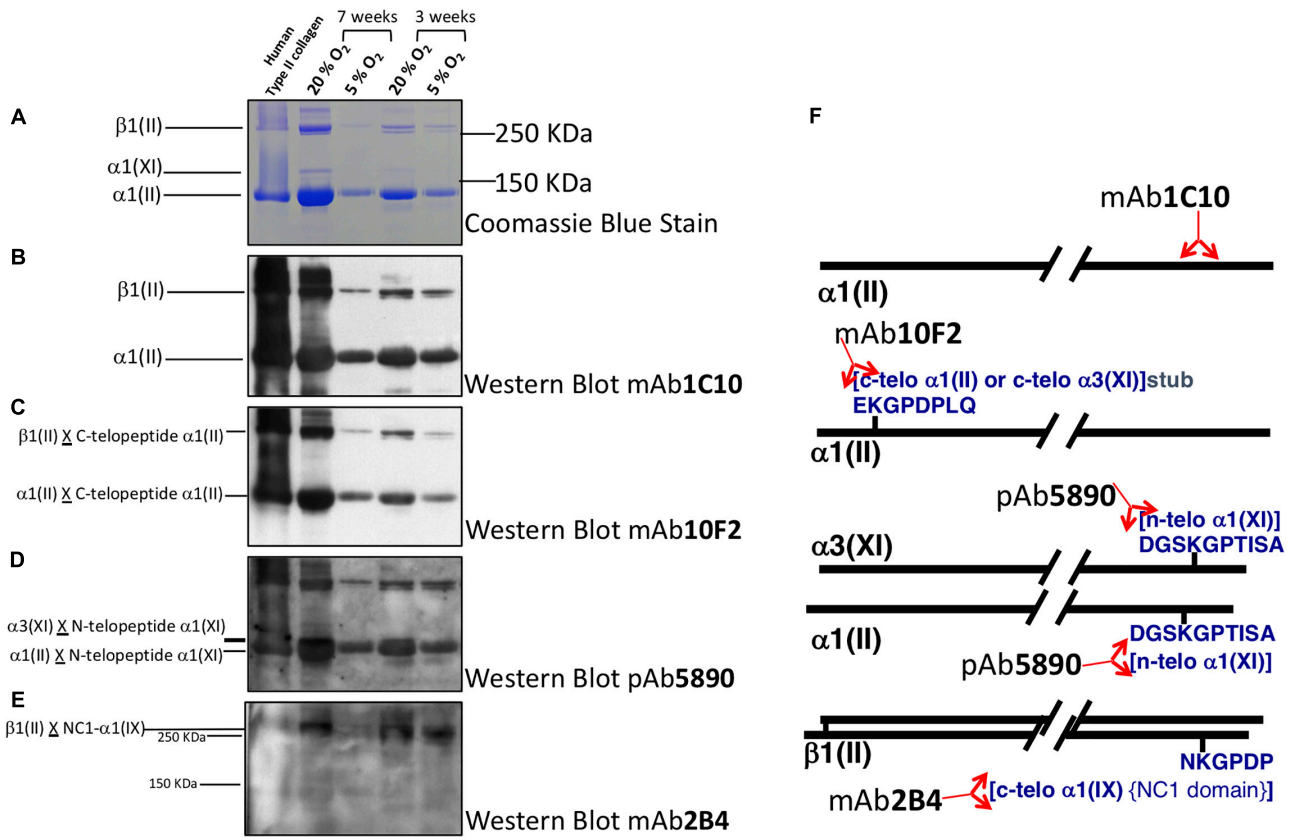

FIGURE 4 | Collagen heteropolymer crosslink analysis. Collagen in human tissue-engineered cartilage was analyzed by SDS page and western blot. *Lane 1* human type II collagen (control); *Lane 2* 7-week Atm O_2 (20%); *Lane 3* 7-week Physioxia (5%); *Lane 4* 3-week Atm O_2; *Lane 5* 3-week Physioxia. Panels **(A)** Coomassie blue stain; **(B)** Western blot type using II collagen antibody to α1(II) chain in helical region; **(C)** Western blot using antibody to *C*-telopeptide of α1(II) chains of type II collagen; **(D)** Western blot using antibody to *N*-telopeptide of α1(XI) chains of type IX collagen; **(E)** Western blot of antibody that recognizes C-telopeptide of the non-collagenous domain of α1(IX) chains of type IX collagen of type IX collagen. **(F)** Locations of the epitopes in the α1(II) chain or in telopeptide stubs crosslinked to the collagen chains in type II-IX-XI heteropolymer.

Mechanical Assays

Tissue-engineered human cartilage sheet thickness increased with time in culture at both physiological and Atm O_2 (**Figure 5A**). Sheets produced in Physioxia were significantly thicker than those produced in Atm O_2 (**Figure 5A**). Compressive stiffness of the cartilage sheets was greater in sheets grown in Physioxia at both 3-weeks and 7-weeks (**Figure 5B**), time in culture was only a significant factor for sheets grown in Physioxia. Tensile stiffness of sheets increased with time in culture at both physiological and Atm O_2 (**Figure 5C**), for this measure there was no appreciable effect of oxygen tension. The highest correlation for compressive mechanical stiffness with biochemical measures was achieved with the ratio of GAG/collagen (**Figure 5D**). None of the biochemical data showed significant correlation with elastic tensile modulus (Data not shown).

Histological Analyses

Tissue-engineered human cartilage sheets were stained for GAG content (safranin-O) and types I, II, and X collagen. At the 3-week time point, sheets were thicker when grown in physioxic conditions vs Atm O_2 (0.77 ± 0.33 vs 0.52 ± 0.18 mm; mean ± S.D.; **Figures 6** and **5A**). Thickness increased over time in physioxic conditions but not in Atm O_2 (7-week thickness 1.0 ± 0.42 vs 0.52 ± 0.19 mm Phsioxia vs Atm O_2; mean ± S.D.). GAG staining was more intense in sheets grown under physioxic conditions (**Figure 6A2**) vs Atm O_2 (**Figure 6A1**). Type I collagen and type II collagen staining was similar under both oxygen tensions at 3-weeks (**Figures 6B1,B2,C1,C2**). Type X collagen staining was slightly increased under Atm O_2 (**Figure 6D1**) vs Physioxia (**Figure 6D2**) conditions at week 3. At the 7-week time point, safranin-O staining in sheets grown in Atm O_2 (**Figure 6A3**) had increased to a similar level as sheets grown in physioxic conditions (**Figure 6A4**). Type I collagen staining under Atm O_2 at week 7 (**Figure 6B3**) has decreased intensity vs the 3-week time point (**Figure 6B1**). Similarly, the sheets grown under physioxic conditions at week 7 have reduced or minimal staining for type I collagen (**Figure 6B4**) vs (**Figure 6B2**). Type II collagen was relatively intense under both oxygen tensions (**Figures 6C3,C4**). Type X collagen staining was more intense on the upper surface of the sheet grown under Atm O_2 at week 7 (**Figure 6D3**). In sheets grown under physioxic conditions,

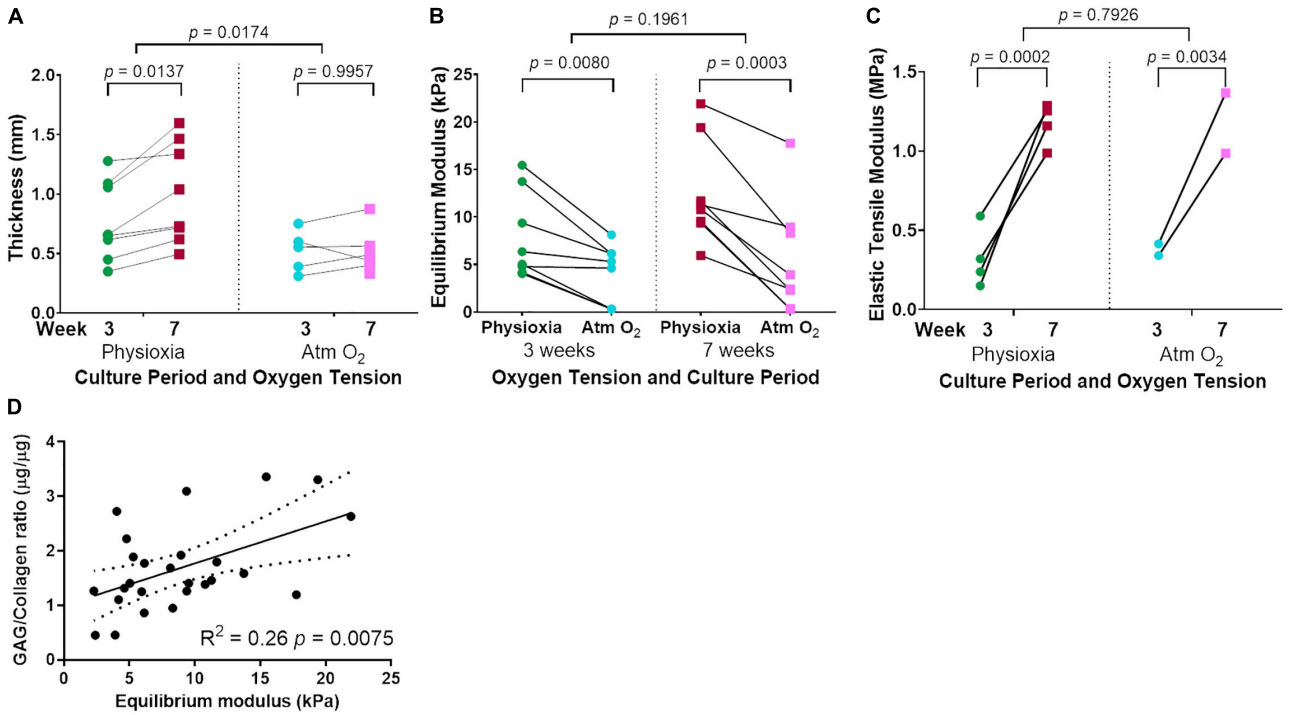

FIGURE 5 | Mechanical testing of tissue-engineered human cartilage sheets. Tissue-engineered human cartilage sheet thickness over time (3- and 7-weeks) in both Physioxia and Atm O_2 **(A)**. Compressive stiffness (Equilibrium Modulus) of tissue-engineered human cartilage sheets when grown in Physioxia vs Atm O_2 both at 3- and 7-weeks **(B)**. Elastic tensile Modulus of tissue engineered human cartilage sheets in Physioxia and Atm O_2 at 3- and 7-weeks **(C)**. Correlation of GAG/Collagen ratio with Equilibrium modulus **(D)**. **(A–C)** The average of data for each experiment is shown by a symbol with lines connecting a donor/experiment, **(A,B)** six donors, eight experiments, **(C)** 4 donors, 4 experiments. In **(D)** the symbols represent average sheet data regardless of the time or oxygen tension.

type X collagen staining was predominantly intracellular vs. extracellular (**Figure 6D4**).

DISCUSSION

Critically, scaffold-free human tissue-engineered cartilage sheets were successfully formed in physioxic conditions for all donors. There was a large degree of variation between donors in terms of GAG deposition, collagen deposition and crosslink density. Even with this wide variation in donor response, a consistent effect of increased GAG deposition through growth under physioxic conditions was remarkable. Similarly, a consistent increase in total collagen deposition was also found through culture under physiological oxygen conditions. Unfortunately, the biochemical assay for collagen does not discriminate between the different types of collagen. This shortcoming is apparent when looking at the histological data, where temporal and regional variation in collagen type and intensity are evident. Initial expression and replacement of type I collagen has been documented developmentally *in vivo* (Morrison et al., 1996; Sasano et al., 1996) and, as we have also shown in human bone marrow derived stem cell neo-cartilage, engineered *in vitro* (Murdoch et al., 2016). This could indicate that expression and replacement is a normal progression in tissue-engineered cartilage development and that replacement of type I with type II collagen is aided by Physioxia. Growth on synoviocyte matrix in the absence of any synthetic scaffold allows for significant population doublings while retaining chondrogenic capacity, enough that large (16 cm^2) pieces of tissue engineered human cartilage can be grown (**Figure 3A**). There was no apparent effect of oxygen tension on trivalent collagen cross-linking, but significant increases in total HP and LP cross-link formation were observed with longer culture duration. This indicates that under both physioxic and normoxic conditions a fibrillar network of collagen with mature cross-links had formed in neo-cartilage. Western blot analyses using established antibodies to specific collagen peptides involved in covalent cross-link formation (Fernandes et al., 2003; McAlinden et al., 2014) indicated that a cross-linked hetropolymer of type II-IX-XI collagen had formed in the tissue engineered cartilage. This cross-linked collagen heteropolymer is typical of cartilage and is essential in the proper assembly of the cartilage collagen fibril (Eyre et al., 2002). Our findings that a similar nascent heteropolymeric template is formed in human neo-cartilage with increased cross-linking with time in culture point to a progressive formation of type II collagen based fibril network typical of cartilage.

There are multiple mechanisms by which Physioxia is thought to increase GAG, collagen deposition and biomechanics. An excellent review by Pattappa et al. (2019) highlights the many mechanisms that have been identified in MSC chondrogenesis. Briefly, they identified inhibition of IL1B effects, upregulation of

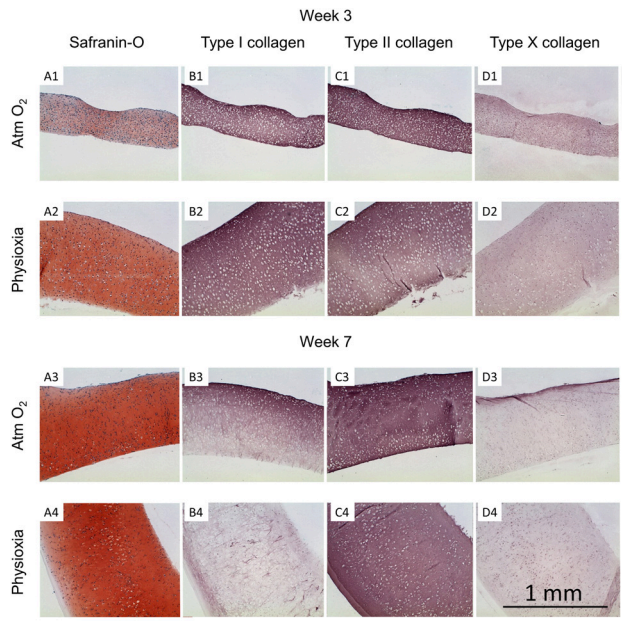

FIGURE 6 | Histological analysis of human tissue-engineered cartilage sheets. Tissue-engineered human cartilage sheets from a single donor are shown (see **Supplementary Figures 1,2** for other donors and **Supplementary Figure 3** for native immunohistochemistry controls), they were stained for GAG (safranin-O, column **A**), type I collagen (column **B**), type II collagen (column **C**), and type X collagen (column **D**). Rows 1 and 2 show data from the 3-week time point and rows 3 and 4 show data from week-7. Atm O_2 sheets are shown in rows 1 and 3, Physioxic sheets are shown in rows 2 and 4. The scale bar indicates a 1 mm distance.

TGFβ receptors, HIF stabilization and expression and stimulation of SOX9 (Pattappa et al., 2019). It is likely that some, if not most, of these factors would be mechanisms by which tissue engineered cartilage derived from articular chondrocytes would benefit. Others have focused on the hypoxia inducible factors HIF1α, HIF2α and HIF3α, and HIF3α was found to be particularly important for cartilage health from both MSCs and chondrocytes (Markway et al., 2015).

Subjective assessment of the sheets (physical handling) indicate that longer culture durations gave stronger sheets in all cases, although this was not fully supported by the equilibrium moduli which only showed a benefit in sheets grown under Physioxia. This is potentially due to untestable sheets formed under Atm O_2 culture (5 of 16 sheets). However, the results did show an increase in both total collagen content and collagen cross-link content with time. These increases correlated with the increased tensile properties of the tissues. Makris et al. (2013b) also found that hypoxia (4% O_2) increased collagen crosslinks in tissue engineered bovine cartilage constructs but that they also found weak correlations to compressive mechanical properties. The combined increase in compressive and tensile stiffness, along with the greater accumulation of extracellular matrix components, through culture under Physioxia leads us to recommend this culture method for chondrogenic experiments.

While autologs chondrocytes have many benefits, without a mechanism to improve poor responders they may not be the best cell choice for tissue engineered grafts. Indeed, the relatively immunopriveledged site of the joint does seem to accept grafts without the need for any HLA matching. This creates an opportunity for a well characterized donor pool of chondrocytes to be created to make tissue engineered cartilage grafts. There remain significant challenges in producing autologs, tissue-engineered cartilage with sufficient biomechanical properties to be implanted as a functional replacement. Current clinical trials cover a wide range of approaches, many using allogenic cells (for review see Kwon et al., 2019). The advantages of a well characterized allogenic cell bank are clear given the range of GAG and collagen contents due to donor variability. In chondrocyte progenitor experiments, this has been further focused in on showing clonal variability (Anderson et al., 2016). Interestingly, while there was a wide range of extracellular matrix component concentrations detected, the distribution in mechanical properties was actually relatively narrow. Evans and Quinn (2005) found that cartilage compressive stiffness correlated with GAG density in native tissues. Roeder et al. (2002) found that tensile modulus increased with increasing concentration of type I collagen engineered constructs in a linear manner. Our data showed the greatest correlation of biochemical measures with compressive moduli when the GAG/Collagen ratio was used but, probably due to the four conditions and six donors, this correlation was relatively weak. When looking at biochemical content correlations with tensile properties, nothing gave a significant correlation; this analysis was hampered by the number of conditions analyzed and lack of sheet formation for two of the four donors at Atm O_2. Similarly, Williamson et al. (2003) found no significant correlation between bovine fetal cartilage and tensile tests. Overall, the data indicate that physiological oxygen tension is beneficial to chondrogenesis of human tissue-engineered cartilage sheets formed through scaffold-free culture of human articular chondrocytes.

Another issue to be addressed is the timing of implantation of tissue-engineered sheets. The methods used in this study pre-suppose the formation of a rigid cartilage matrix prior to implantation, which is a different approach to that of many others (Kwon et al., 2019). This raises the issue of the timing of implantation. If the implant is made too early, the construct may be compromised by the loads experienced *in vivo*. Alternatively, if the material is too stiff, there may be problems related to the integration into the underlying bone or along the lateral edges. One approach is to engineer the constructs such that the lateral edges are in a non-load or minimally-loaded area. Alternatively, it may be necessary to engineer the edges differently so that they might withstand tensional forces of suture material.

CONCLUSION

Tissue-engineered human cartilage sheets, formed through scaffold free self-assembly of articular chondrocytes, in Physioxia have significantly more extracellular matrix with correlative

increases in compressive stiffness than sheets grown under Atm O_2. The combination of Physioxia with longer culture duration resulted in the formation of the type II-IX-XI collagen heteropolymer with greater collagen crosslinks vs sheets grown in Atm O_2 conditions.

DATA AVAILABILITY STATEMENT

The original contributions presented in the study are included in the article/**Supplementary Material**, further inquiries can be directed to the corresponding author.

AUTHOR CONTRIBUTIONS

TK, JD, GW, and RF: concept and manuscript writing. TK, JD, GW, and RF: design, data analysis and interpretation, and manuscript editing. TK, JD, and RF: financial support. TK, GW, JR, and RF: collection of the data. TK, JD, GW, and RF: final approval of the manuscript. All authors contributed to the article and approved the submitted version.

FUNDING

This work was supported in part by NIH grants AR053622 (JD), DE015322 (JD), AR057025 (RF and JR), and AR037318 (JR and RF). Publication costs were paid by UCF College of Medicine (TK).

ACKNOWLEDGMENTS

We would like to thank Geoffrey R. Traeger for his technical expertise and Dr. Gary Gibson (Henry Ford Hospital) for the type X collagen antibody.

SUPPLEMENTARY MATERIAL

The Supplementary Material for this article can be found online at: https://www.frontiersin.org/articles/10.3389/fbioe.2020.590743/full#supplementary-material

Supplementary Figure 1 | Week 3 histology images of donors (B,C,D) sheets produced under Physioxia and Atm O_2. 1st passage sheets are p1 and second passage sheets are p2.

Supplementary Figure 2 | Week 7 histology images of donors (A,B,C,E) sheets produced under Physioxia and Atm O_2. 1st passage sheets are p1.

Supplementary Figure 3 | Immunohistochemistry controls, type I collagen showing staining in the perichondrium of the rabbit (Rb) ear and in the bone of the Rb Knee. Type II collagen showing staining in the cartilage of the Rb ear, human (Hu) knee and Rb knee articular and growth plate cartilage. Type X collagen showing staining in the Rb Ear, and Rb knee hypertrophic and calcified growth plate cartilage.

Supplementary Data Sheet 1 | Template for printing overhead projector sheets to create clamps for the cartilage tissue tension tests. Dotted line indicates where the testing machine clamps should go, window in center is cut out with craft knife or scalpel, tissue adhered with dog bone over window, kept hydrated until placed in testing device then edges of the window cut before applying load.

REFERENCES

Adkar, S. S., Wu, C.-L., Willard, V. P., Dicks, A., Ettyreddy, A., Steward, N., et al. (2019). Step-Wise chondrogenesis of human induced pluripotent stem cells and purification via a reporter allele generated by CRISPR-Cas9 Genome editing. *Stem Cell.* 37, 65–76. doi: 10.1002/stem.2931

Anderson, D. E., Markway, B. D., Bond, D., McCarthy, H. E., and Johnstone, B. (2016). Responses to altered oxygen tension are distinct between human stem cells of high and low chondrogenic capacity. *Stem Cell Res. Ther.* 7:154. doi: 10.1186/s13287-016-0419-8

Anderson, D. E., Markway, B. D., Weekes, K. J., McCarthy, H. E., and Johnstone, B. (2018). Physioxia promotes the articular chondrocyte-like phenotype in human chondroprogenitor-derived self-organized tissue. *Tissue Eng. Part A* 24, 264–274. doi: 10.1089/ten.TEA.2016.0510

Bianchi, V. J., Weber, J. F., Waldman, S. D., Backstein, D., and Kandel, R. A. (2017). Formation of hyaline cartilage tissue by passaged human osteoarthritic chondrocytes. *Tissue Eng. Part A* 23, 156–165. doi: 10.1089/ten.TEA.2016.0262

Dennis, J. E., Bernardi, K. G., Kean, T. J., Liou, N. E., and Meyer, T. K. (2018). Tissue engineering of a composite trachea construct using autologous rabbit chondrocytes. *J. Tissue Eng. Regen. Med.* 12, e1383–e1391. doi: 10.1002/term.2523

Dennis, J. E., Splawn, T., and Kean, T. J. (2020). High-Throughput, temporal and dose dependent, effect of vitamins and minerals on Chondrogenesis. *Front. Cell Dev. Biol.* 8:92. doi: 10.3389/fcell.2020.00092

Diederichs, S., Tonnier, V., Marz, M., Dreher, S. I., Geisbusch, A., and Richter, W. (2019). Regulation of WNT5A and WNT11 during MSC in vitro chondrogenesis: WNT inhibition lowers BMP and hedgehog activity, and reduces hypertrophy. *Cell. Mol. Life Sci.* 76, 3875–3889. doi: 10.1007/s00018-019-03099-0

Enochson, L., Brittberg, M., and Lindahl, A. (2012). Optimization of a chondrogenic medium through the use of factorial design of experiments. *Biores. Open Access* 1, 306–313. doi: 10.1089/biores.2012.0277

Evans, R. C., and Quinn, T. M. (2005). Solute diffusivity correlates with mechanical properties and matrix density of compressed articular cartilage. *Arch. Biochem. Biophys.* 442, 1–10. doi: 10.1016/j.abb.2005.07.025

Eyre, D. R., Wu, J. J., Fernandes, R. J., Pietka, T. A., and Weis, M. A. (2002). Recent developments in cartilage research: matrix biology of the collagen II/IX/XI heterofibril network. *Biochem. Soc. Trans.* 30(Pt 6), 893–899. doi: 10.1042/bst0300893

Fernandes, R. J., Schmid, T. M., and Eyre, D. R. (2003). Assembly of collagen types II, IX and XI into nascent hetero-fibrils by a rat chondrocyte cell line. *Eur. J. Biochem.* 270, 3243–3250. doi: 10.1046/j.1432-1033.2003.03711.x

Fernandes, R. J., Wilkin, D. J., Weis, M. A., Wilcox, W. R., Cohn, D. H., Rimoin, D. L., et al. (1998). Incorporation of structurally defective type II collagen into cartilage matrix in kniest chondrodysplasia. *Arch. Biochem. Biophys.* 355, 282–290. doi: 10.1006/abbi.1998.0745

Gawlitta, D., van Rijen, M. H., Schrijver, E. J., Alblas, J., and Dhert, W. J. (2012). Hypoxia impedes hypertrophic chondrogenesis of human multipotent stromal cells. *Tissue Eng. Part A* 18, 1957–1966. doi: 10.1089/ten.TEA.2011.0657

Gilpin, D. A., Weidenbecher, M. S., and Dennis, J. E. (2010). Scaffold-free tissue-engineered cartilage implants for laryngotracheal reconstruction. *Laryngoscope* 120, 612–617. doi: 10.1002/lary.20750

Huang, B. J., Brown, W. E., Keown, T., Hu, J. C., and Athanasiou, K. A. (2018). Overcoming challenges in engineering large, Scaffold-Free Neocartilage with functional properties. *Tissue Eng. Part A* 24, 1652–1662. doi: 10.1089/ten.TEA.2017.0495

Kean, T. J., and Dennis, J. E. (2012a). "Tissue Engineered, Scaffold Free, Human Cartilage Sheets," in *Proceedings of the International Conference on Tissue Science & Engineering* (Chicago, IL), 40.

Kean, T. J., and Dennis, J. E. (2012b). *Improved Expansion of Human Chondrocytes*. San Francisco, CA: Orthopaedic Research Society, 1757.

Kean, T. J., and Dennis, J. E. (2013). *Effects of TGF-β1 on Chondrogenesis*. San Antonio, TX: Orthopaedic Research Society Growth Factor Interest Group.

Kean, T. J., and Dennis, J. E. (2015). Synoviocyte derived-extracellular matrix enhances human articular chondrocyte proliferation and maintains re-differentiation capacity at both low and atmospheric oxygen tensions. *PLoS One* 10:e0129961. doi: 10.1371/journal.pone.0129961

Kean, T. J., Ge, Z., Li, Y., Chen, R., and Dennis, J. E. (2019). Transcriptome-Wide analysis of human chondrocyte expansion on Synoviocyte Matrix. *Cells* 8:85. doi: 10.3390/cells8020085

Kean, T. J., Mera, H., Whitney, G. A., MacKay, D. L., Awadallah, A., Fernandes, R. J., et al. (2016). Disparate response of articular- and auricular-derived chondrocytes to oxygen tension. *Connect Tissue Res.* 57, 319–333. doi: 10.1080/03008207.2016.1182996

Kean, T. J., Whitney, G. A., MacKay, D. L., and Dennis, J. E. (2013). "Generation of clinical scale tissue engineered human cartilage sheets," in *Proceedings of the ORS Annual Meeting* (San Antonio, TX).

Kean, T. J., Whitney, G. A., Traeger, G., Fernandes, R. J., and Dennis, J. E. (2015). "Tissue Engineered Human Cartilage Sheets are Significantly Stiffer When Re-Differentiated at Low Oxygen Tension," in *Proceedings of the ORS Annual Meeting* (Las Vegas, NV).

Kwon, H., Brown, W. E., Lee, C. A., Wang, D., Paschos, N., Hu, J. C., et al. (2019). Surgical and tissue engineering strategies for articular cartilage and meniscus repair. *Nat. Rev. Rheumatol.* 15, 550–570. doi: 10.1038/s41584-019-0255-1

Lima, E. G., Bian, L., Ng, K. W., Mauck, R. L., Byers, B. A., Tuan, R. S., et al. (2007). The beneficial effect of delayed compressive loading on tissue-engineered cartilage constructs cultured with TGF-beta3. *Osteoarthritis Cartilage* 15, 1025–1033. doi: 10.1016/j.joca.2007.03.008

Makris, E. A., Hu, J. C., and Athanasiou, K. A. (2013b). Hypoxia-induced collagen crosslinking as a mechanism for enhancing mechanical properties of engineered articular cartilage. *Osteoarthritis Cartilage* 21, 634–641. doi: 10.1016/j.joca.2013.01.007

Makris, E. A., MacBarb, R. F., Responte, D. J., Hu, J. C., and Athanasiou, K. A. (2013a). A copper sulfate and hydroxylysine treatment regimen for enhancing collagen cross-linking and biomechanical properties in engineered neocartilage. *FASEB J.* 27, 2421–2430. doi: 10.1096/fj.12-224030

Mansour, J. M., Motavalli, M., Dennis, J. E., Kean, T. J., Caplan, A. I., Berilla, J. A., et al. (2018). Rapid detection of shear-induced damage in tissue-engineered cartilage using ultrasound. *Tissue Eng. Part C Methods* 24, 443–456. doi: 10.1089/ten.TEC.2017.0513

Markway, B. D., Cho, H., and Johnstone, B. (2013). Hypoxia promotes redifferentiation and suppresses markers of hypertrophy and degeneration in both healthy and osteoarthritic chondrocytes. *Arthritis Res. Ther.* 15:R92. doi: 10.1186/ar4272

Markway, B. D., Cho, H., Zilberman-Rudenko, J., Holden, P., McAlinden, A., and Johnstone, B. (2015). Hypoxia-inducible factor 3-alpha expression is associated with the stable chondrocyte phenotype. *J. Orthop. Res.* 33, 1561–1570. doi: 10.1002/jor.22930

McAlinden, A., Traeger, G., Hansen, U., Weis, M. A., Ravindran, S., Wirthlin, L., et al. (2014). Molecular properties and fibril ultrastructure of types II and XI collagens in cartilage of mice expressing exclusively the alpha1(IIA) collagen isoform. *Matrix Biol.* 34, 105–113. doi: 10.1016/j.matbio.2013.09.006

Morrison, E. H., Ferguson, M. W., Bayliss, M. T., and Archer, C. W. (1996). The development of articular cartilage: I. The spatial and temporal patterns of collagen types. *J. Anat.* 189(Pt 1), 9–22.

Mueller, M. B., and Tuan, R. S. (2008). Functional characterization of hypertrophy in chondrogenesis of human mesenchymal stem cells. *Arthritis Rheum.* 58, 1377–1388. doi: 10.1002/art.23370

Murdoch, A. D., Hardingham, T. E., Eyre, D. R., and Fernandes, R. J. (2016). The development of a mature collagen network in cartilage from human bone marrow stem cells in Transwell culture. *Matrix Biol.* 50, 16–26. doi: 10.1016/j.matbio.2015.10.003

Pattappa, G., Johnstone, B., Zellner, J., Docheva, D., and Angele, P. (2019). The importance of physioxia in mesenchymal stem cell Chondrogenesis and the mechanisms controlling its response. *Int. J. Mol. Sci.* 20:484. doi: 10.3390/ijms20030484

Roeder, B. A., Kokini, K., Sturgis, J. E., Robinson, J. P., and Voytik-Harbin, S. L. (2002). Tensile mechanical properties of three-dimensional type I collagen extracellular matrices with varied microstructure. *J. Biomech. Eng.* 124, 214–222. doi: 10.1115/1.1449904

Sasano, Y., Furusawa, M., Ohtani, H., Mizoguchi, I., Takahashi, I., and Kagayama, M. (1996). Chondrocytes synthesize type I collagen and accumulate the protein in the matrix during development of rat tibial articular cartilage. *Anat. Embryol. (Berl)* 194, 247–252. doi: 10.1007/BF00187135

Shekkeris, A., Perera, J., Bentley, G., Flanagan, A., Miles, J., Carrington, R., et al. (2012). Histological results of 406 biopsies following ACI/MACI procedures for Osteochondral defects in the Knee. *J. Bone Joint Surg. Br.* 94-B(Suppl. XXXVI):12.

Venn, M., and Maroudas, A. (1977). Chemical composition and swelling of normal and osteoarthrotic femoral head cartilage. I. Chemical composition. *Ann. Rheum. Dis.* 36, 121–129. doi: 10.1136/ard.36.2.121

Vunjak-Novakovic, G., Martin, I., Obradovic, B., Treppo, S., Grodzinsky, A. J., Langer, R., et al. (1999). Bioreactor cultivation conditions modulate the composition and mechanical properties of tissue-engineered cartilage. *J. Orthop. Res.* 17, 130–138. doi: 10.1002/jor.1100170119

Weidenbecher, M., Tucker, H. M., Awadallah, A., and Dennis, J. E. (2008). Fabrication of a neotrachea using engineered cartilage. *Laryngoscope* 118, 593–598. doi: 10.1097/MLG.0b013e318161f9f8

Whitney, G. A., Kean, T. J., Fernandes, R. J., Waldman, S., Tse, M. Y., Pang, S. C., et al. (2018). Thyroxine increases collagen type II expression and accumulation in scaffold-free tissue-engineered articular cartilage. *Tissue Eng. Part A* 24, 369–381. doi: 10.1089/ten.TEA.2016.0533

Whitney, G. A., Mera, H., Weidenbecher, M., Awadallah, A., Mansour, J. M., and Dennis, J. E. (2012). Methods for producing scaffold-free engineered cartilage sheets from auricular and articular chondrocyte cell sources and attachment to porous tantalum. *Biores. Open Access* 1, 157–165. doi: 10.1089/biores.2012.0231

Williamson, A. K., Chen, A. C., Masuda, K., Thonar, E. J. M. A., and Sah, R. L. (2003). Tensile mechanical properties of bovine articular cartilage: variations with growth and relationships to collagen network components. *J. Orthop. Res.* 21, 872–880. doi: 10.1016/s0736-0266(03)00030-5

Wu, J. J., and Eyre, D. R. (1995). Structural analysis of cross-linking domains in cartilage type XI collagen. Insights on polymeric assembly. *J. Biol. Chem.* 270, 18865–18870. doi: 10.1074/jbc.270.32.18865

Conflict of Interest: The authors declare that the research was conducted in the absence of any commercial or financial relationships that could be construed as a potential conflict of interest.

frontiers in Bioengineering and Biotechnology

ORIGINAL RESEARCH
published: 25 May 2021
doi: 10.3389/fbioe.2021.591126

Measuring and Modeling Oxygen Transport and Consumption in 3D Hydrogels Containing Chondrocytes and Stem Cells of Different Tissue Origins

Simon F. Carroll[1,2], *Conor T. Buckley*[1,2,3,4] *and Daniel J. Kelly*[1,2,3,4]*

[1] *Trinity Centre for Biomedical Engineering, Trinity Biomedical Sciences Institute, Trinity College Dublin, Dublin, Ireland,* [2] *Department of Mechanical, Manufacturing and Biomedical Engineering, School of Engineering, Trinity College Dublin, Dublin, Ireland,* [3] *Department of Anatomy, Royal College of Surgeons in Ireland, Dublin, Ireland,* [4] *Advanced Materials and BioEngineering Research (AMBER) Centre, Trinity College Dublin, Dublin, Ireland*

OPEN ACCESS

Edited by:
Roberto Narcisi,
Erasmus University Rotterdam, Netherlands

Reviewed by:
Elena Jones,
University of Leeds, United Kingdom
Debby Gawlitta,
University Medical Center Utrecht, Netherlands

***Correspondence:**
Daniel J. Kelly
kellyd9@tcd.ie

Specialty section:
This article was submitted to Preclinical Cell and Gene Therapy, a section of the journal Frontiers in Bioengineering and Biotechnology

Received: *03 August 2020*
Accepted: *06 April 2021*
Published: *25 May 2021*

Citation:
Carroll SF, Buckley CT and Kelly DJ (2021) Measuring and Modeling Oxygen Transport and Consumption in 3D Hydrogels Containing Chondrocytes and Stem Cells of Different Tissue Origins. Front. Bioeng. Biotechnol. 9:591126. doi: 10.3389/fbioe.2021.591126

Understanding how the local cellular environment influences cell metabolism, phenotype and matrix synthesis is crucial to engineering functional tissue grafts of a clinically relevant scale. The objective of this study was to investigate how the local oxygen environment within engineered cartilaginous tissues is influenced by factors such as cell source, environmental oxygen tension and the cell seeding density. Furthermore, the subsequent impact of such factors on both the cellular oxygen consumption rate and cartilage matrix synthesis were also examined. Bone marrow derived stem cells (BMSCs), infrapatellar fat pad derived stem cells (FPSCs) and chondrocytes (CCs) were seeded into agarose hydrogels and stimulated with transforming growth factor-β3 (TGF- β3). The local oxygen concentration was measured within the center of the constructs, and numerical modeling was employed to predict oxygen gradients and the average oxygen consumption rate within the engineered tissues. The cellular oxygen consumption rate of hydrogel encapsulated CCs remained relatively unchanged with time in culture. In contrast, stem cells were found to possess a relatively high initial oxygen consumption rate, but adopted a less oxidative, more chondrocyte-like oxygen consumption profile following chondrogenic differentiation, resulting in net increases in engineered tissue oxygenation. Furthermore, a greater reduction in oxygen uptake was observed when the oxygen concentration of the external cell culture environment was reduced. In general, cartilage matrix deposition was found to be maximal in regions of low oxygen, but collagen synthesis was inhibited in very low (less than 2%) oxygen regions. These findings suggest that promoting an oxygen consumption profile similar to that of chondrocytes might be considered a key determinant to the success of stem cell-based cartilage tissue engineering strategies.

Keywords: tissue engineering, oxygen consumption, cellular metabolism, chondrogenesis, stem cell differentiation, cartilage

INTRODUCTION

The efficacy of stem cell based cartilage tissue engineering strategies is typically evaluated based on changes in the expression of chondrogenic matrix related genes, as well as the resulting biochemical composition and biomechanical function of the graft (Kafienah and Sims, 2004; Cernanec et al., 2007; Fehrer et al., 2007; Buckley et al., 2010; Meyer et al., 2010; Farrell et al., 2012, 2014; Thorpe et al., 2012; Carroll et al., 2014). However, other changes in phenotype, such as cellular metabolic activity, may play an equally important role in determining whether a stem cell can differentiate to fulfill a tissue specific function. In the case of cartilage tissue engineering strategies, it would seem reasonable to assume that chondrogenically primed mesenchymal stem cells (MSCs) would need to adopt oxygen and nutrient consumption rates approaching that of chondrocytes in order to thrive following implantation into an articular cartilage defect.

Chondrocytes are known to reside in an avascular, low oxygen *in vivo* environment, which ranges from around 6% in the superficial zone to as low as 1% in the deep zone (Zhou et al., 2004; Fermor et al., 2007). MSCs, however, typically reside in tissues such as bone marrow, which has been shown to possess oxygen levels in the range of 4–7% *in vivo* (Grant and Smith, 1963; Kofoed et al., 1985; Harrison et al., 2002), and due to their perivascular niche (as reviewed by Caplan, 2007; da Silva Meirelles et al., 2008), are likely to experience oxygen levels at least at the higher end of this range. This would suggest that undifferentiated MSCs possess a different oxygen consumption rate to that of differentiated chondrocytes. Therefore, determining if MSCs used to engineer cartilage grafts adopt a metabolic profile similar to chondrocytes might be considered a key determinant of the success of stem cell-based cartilage tissue engineering strategies. Furthermore, given that MSC phenotype and its biosynthetic activity is influenced by the local oxygen tension (Malladi et al., 2006; Fehrer et al., 2007; Buckley et al., 2010; Meyer et al., 2010; Sheehy et al., 2012; Pattappa et al., 2013), a detailed knowledge of how MSCs consume factors such as oxygen will play a key role in successfully engineering tissues of clinically relevant scales. Introducing gradients of regulatory factors such as oxygen into cell laden constructs, for example through the use of novel culture systems (Thorpe et al., 2013), may also be critical to engineering tissues with spatial complexity mimicking that observed in articular cartilage.

Chondrocytes are well adapted to low oxygen environments, deriving over 95% of their energy from glycolysis and demonstrating minimal oxygen consumption (Rajpurohit et al., 1996; Lee and Urban, 1997; Heywood and Lee, 2008). Undifferentiated MSCs possess a higher oxygen consumption rate than chondrocytes and derive a significantly larger portion of ATP generation via oxidative phosphorylation (Pattappa et al., 2011). Both osteogenic and chondrogenic differentiation of MSCs have been shown to alter the balance of oxidative phosphorylation and glycolysis, with culture of MSC pellets in chondrogenic media shown to result in a reduction in the oxygen consumption rate, and MSCs undergoing osteogenesis increasing their glucose consumption rate (Pattappa et al., 2011). In hypoxic conditions, MSCs have also been shown to derive a greater proportion of their ATP production from glycolysis (Pattappa et al., 2013).

In a tissue engineering context, while the external culture environment can be controlled with relative ease, depending on construct geometry, scale and cellular seeding density, large gradients in oxygen availability (and thus spatial gradients in cell viability and matrix deposition) can arise between the periphery and center of *in vitro* engineered grafts (Martin et al., 1999; Malda et al., 2004; Meyer et al., 2010; Buckley et al., 2011; Thorpe et al., 2013; Murphy et al., 2017; Westphal et al., 2017), potentially resulting in a necrotic core and graft failure. Understanding how parameters such as cell source, cell seeding density, oxygen consumption rate and culture environment influence oxygen gradients, and thus cellular metabolism and matrix synthesis, within engineered tissues will be critical to developing functional cartilage grafts of scale. The first objective of this study was to compare the oxygen consumption rate of chondrocytes and stem/progenitor cells isolated from bone marrow and infrapatellar fat pad following encapsulation into three dimensional hydrogels. Cell seeded constructs were maintained in chondrogenic medium supplemented with TGF-β3 for 24 days, with the oxygen levels measured within the engineered tissues at day 0 and day 24. The oxygen consumption rate was determined by fitting a computational model of oxygen transport and consumption within MSC laden hydrogels to experimental data obtained using implanted oxygen-sensitive micro-sensors. The second objective of this study was to explore how altering the external oxygen tension would affect local levels of oxygen availability and gradients within the engineered tissue. The final objective was to measure how oxygen levels and subsequent levels of matrix synthesis within engineered tissues depended on the initial cell seeding density.

MATERIALS AND METHODS

Cell Isolation and Expansion

Bone marrow derived stem cells (BMSCs), infrapatellar fat pad derived stem cells (FPSCs) and chondrocytes (CCs) were isolated aseptically from the femoral diaphysis, the knee joint capsule and the femoral condyle, respectively, of 4 month old porcine donors as described previously (Buckley et al., 2010, 2011). Each group consisted of cells from a single donor (i.e., donors were not pooled). CCs were isolated from cartilage slices obtained from porcine femoral condyles via digestion with collagenase type II (0.5 mg/mL, Sigma–Aldrich, Dublin, Ireland) under constant rotation at 37°C until the tissue had visibly dissolved. The solution was filtered through a 40 μm nylon cell strainer (B.D. Falcon–Unitech) and centrifuged at 650 g for 10 min and the cells were then resuspended in expansion media consisting of high glucose Dulbecco's modified Eagle's medium (hgDMEM) GlutaMAX supplemented with 10% fetal bovine serum and 100 U/mL penicillin/streptomycin (all Gibco–Biosciences). Porcine infrapatellar fat pad harvested from the donor was washed with phosphate buffered saline (PBS), diced, and digested in the same

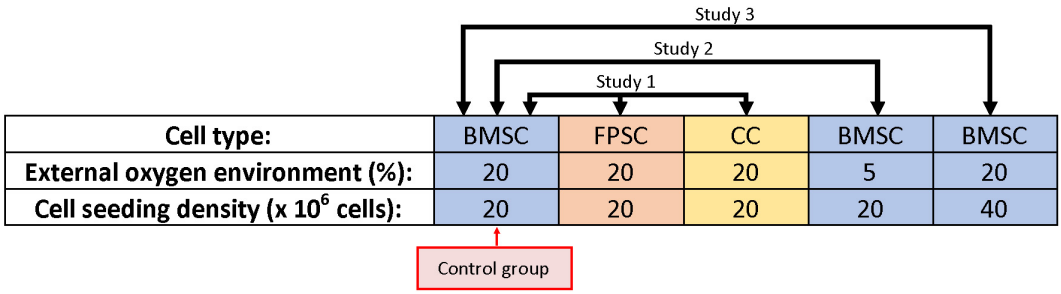

FIGURE 1 | Study schematic; three studies were performed in parallel using a shared control group.

manner as CCs. Bone marrow was aseptically harvested from the femoral diaphysis and the marrow was repeatedly aspirated by using a 16-gauge needle to break up large aggregates before centrifugation at 650 g for 5 min. The separated floating adipose layer was discarded, and the cell pellet was then resuspended in expansion media.

For cell counting, all cell suspensions (BMSCs, FPSCs and CCs) were triturated through 20-gauge needles to create single-cell suspensions and filtered through 40 μm nylon cell strainers. An aliquot of each suspension was treated with 4% acetic acid to lyse the red blood cells (BMSCs only) and viable mononuclear cells were counted by using a hemocytometer in the presence of 0.4% trypan blue. Mononuclear cells were initially seeded at a density of 5×10^3 cells/cm^2 (for FPSCs and CCs) or 50×10^3 cells/cm^2 (for BMSCs) in T-175 cm^2 flasks (Sarstedt, Wexford, Ireland) and expanded in a 20% oxygen, 5% CO_2 environment at 37°C. Following colony formation of BMSCs and FPSCs, cells were trypsinised, counted and expanded to passage 3 at a seeding density of 5×10^3 cells/cm^2 at each passage. CCs were expanded to passage 3 in the same manner. Complete media exchanges were performed twice weekly. We have previously demonstrated that porcine BMSCs isolated and expanded in this manner can differentiate down an osteogenic, adipogenic or chondrogenic pathway (Vinardell et al., 2011).

Agarose Gel Constructs Fabrication and Culture

BMSC, FPSC and CC constructs were fabricated separately. Cell suspensions were mixed with 4% agarose (Type VII; Sigma-Aldrich) at a ratio of 1:1 at ∼40°C to yield a final gel concentration of 2% at a density of either 20 or 40 million cells/mL. The agarose/cell suspension was cast in stainless steel molds and allowed to set for 20 min to produce a solid slab, which was then cored with sterile biopsy punches to produce cylindrical constructs (Ø5 × 3 mm). Constructs were maintained for 24 days in a chemically defined chondrogenic medium consisting of high glucose DMEM supplemented with 100 U/mL penicillin/streptomycin (both from Gibco), 100 mg/mL sodium pyruvate, 40 mg/mL L-proline, 50 mg/mL L-ascorbic acid-2-phosphate, 1.5 mg/mL bovine serum albumin, 1 × insulin–transferrin–selenium, 100 nM dexamethasone (all Sigma-Aldrich), and 10 ng/mL of transforming growth factor-β3 (TGF-β3, ProSpec-Tany TechnoGene, Ltd.). Constructs were cultured in either a nominally 20 or 5% oxygen-controlled CO_2 incubator (New Brunswick, Galaxy 48R). Each construct was cultured in an individual test dish (**Figure 2**) on an agarose bed to allow for greater, more homogenous oxygen distribution throughout the construct. Constructs were held firmly in position by the surrounding agarose bed to ensure that their position and orientation remained constant throughout the culture period. Complete media exchanges were performed twice weekly under atmospheric oxygen conditions using non-deoxygenated media.

Experimental Design

Three studies were performed in parallel using a shared control group (**Figure 1**):

1. Hydrogels were seeded with BMSCs, FPSCs or CCs at a cell density of 20×10^6 cells/mL and cultured in 20% oxygen to investigate the influence of cell source on oxygen gradients and matrix deposition.
2. Hydrogels were seeded with BMSCs at a cell density of 20×10^6 cells/mL and cultured in either 20 or 5% oxygen to investigate the influence of external oxygen environment.
3. Hydrogels were seeded with BMSCs at a cell density of either 20×10^6 or 40×10^6 cells/mL and cultured in 20% oxygen to investigate the influence of cell seeding density.

Measurement of Local Oxygen Concentrations

A novel test rig (**Figure 2A**) was developed to allow accurate spatial positioning of sensor tips within the engineered constructs. Sample test dishes were prepared by pouring acellular 2% agarose into cell culture dishes (Iwaki, Ø60 mm), thus creating a 3 mm deep agarose bed. A recess (1.5 mm deep, Ø5 mm) was created in the center of the dish, into which samples to be tested were placed (thus leaving a 1.5 mm deep agarose bed underneath the sample). Sufficient medium was added to the dish resulting in a consistent depth of approximately 1 mm of medium above the construct.

Oxygen concentration at the center of each construct (O_{2c}) was measured using a fiber optic oxygen transmitter (Microx TX; PreSens—Precision Sensing GmbH, Regensburg, Germany)

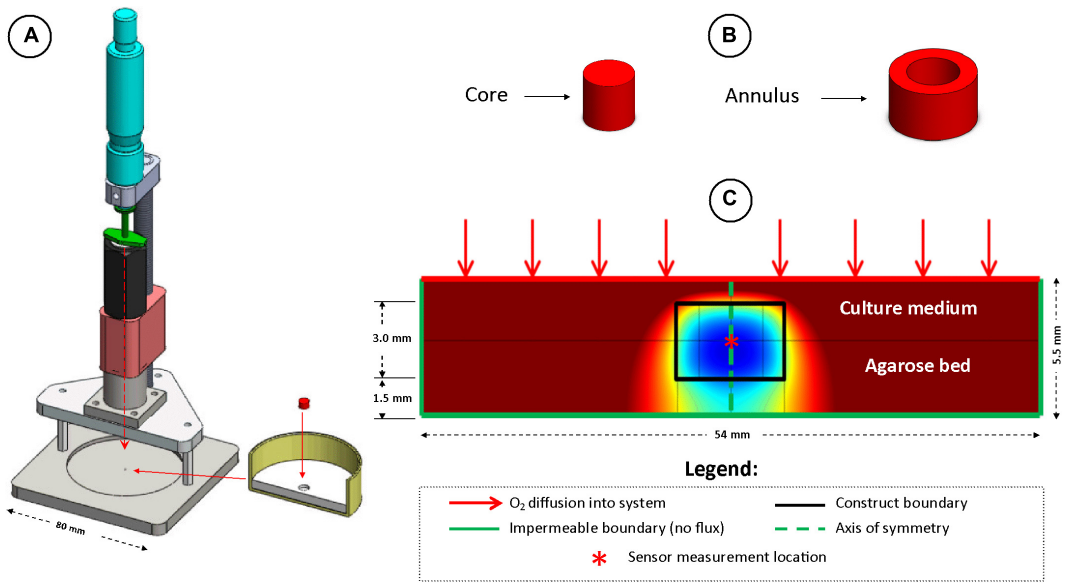

FIGURE 2 | The local oxygen concentration in the center of *in vitro* engineered cartilage tissue grafts cultured in chondrogenic media was measured using a custom designed oxygen testing rig, test dish and **fiber** optic sensor **(A)**. Samples were separated into cores and annuli for spatial biochemical analysis **(B)**. Schematic of the finite element model developed to predict oxygen concentration gradients throughout constructs **(C)**.

and implantable, 140 μm tip diameter, fiber optic, oxygen microsensors. The sensors were calibrated using two-point calibration in oxygen free (nitrogen saturated and containing sodium sulphite) and air saturated medium at 37°C. At each time-point, a micrometer was used to accurately position the sensor tip at the geometrical center of the construct and the system was allowed to equilibrate for at least 3 h prior to each oxygen measurement.

Prediction of Oxygen Concentration Within Agarose Constructs

Oxygen concentration in the constructs and throughout the culture dish was modeled using commercially available finite element modeling software (COMSOL Multiphysics 4.3) and is described by a diffusion-reaction type equation. The parameters used in the models are summarized in **Table 1**.

The reaction term followed Michaelis-Menten kinetics:

$$\frac{\partial c}{\partial t} = D\nabla^2 c - \rho\frac{Q_m c}{K_m + c}$$

This equation describes a quasi-steady state reaction, which assumes that after an initial time period, the concentration of the reaction intermediates remains constant with time. Here, c is the oxygen concentration, D is the diffusion coefficient, ρ is the cell density and K_m is the oxygen concentration at which the reaction rate is at 50% of Q_m. Q_m is defined as the maximum cellular oxygen consumption rate. However, the actual oxygen consumption rate of each cell is a function of the oxygen concentration at that particular location in accordance with Michaelis Menten kinetics. The value of Q_m was determined for each sample by using a linear regression approach (i.e., varying the value of Q_m that was input into the model until the output matched the experimentally observed O_{2c} value). Since oxygen concentration was measured at one location only, each Q_m value calculated was assumed to be representative of the maximum oxygen cellular consumption rate of each cell within the construct.

The diffusion coefficient in 2% agarose was determined using the Mackie and Meares relation:

$$\frac{D_{ag}}{D_{H_2O}} = \frac{\phi_f^2}{(2-\phi_f)}$$

so that $D_{ag} = 2.77 \times 10^{-3}$ mm^2/s, where ϕ_f (= 0.98) is the fluid phase volume fraction (Gu et al., 2003; Sengers et al., 2005). The Michaelis-Menten constant, K_m was set to 63 μmol/mm^3 (Heywood et al., 2010). The construct was modeled as axisymmetric (**Figure 2C**). Oxygen diffusion through the culture media, D_{media} (= 3.0×10^{-3} mm^2/s), was assumed to be the same as in water (Haselgrove et al., 1993; Lightfoot and Duca, 1999).

The oxygen concentration at the media surface was prescribed as 185 μM (measured using independently calibrated oxygen sensors) in the case of constructs cultured in the nominally 20% oxygen incubator and 50 μM for the constructs cultured in the 5% oxygen incubator. At the dish walls, base and at the axis of symmetry, the flux was set to zero. Day 0 time-point simulations were performed assuming uniform cell concentrations of $\rho = 20 \times 10^6$ or 40×10^6 cells/mL throughout the construct. For day 24 simulations, however, the core and outer annular regions were modeled using separate ρ values derived from experimental data, to allow for discrepancies in cell proliferation/death between each region. The percentage change in cell concentration was calculated separately for each sample

TABLE 1 | Summary of parameters used for oxygen diffusion-reaction model.

Parameter	Symbol	Value	Units	Source
O_2 diffusion coefficient in water	D_{media}	3.0×10^{-3}	mm^2/s	Haselgrove et al., 1993; Lightfoot and Duca, 1999
O_2 diffusion coefficient in 2% agarose	D_{ag}	2.77×10^{-3}	mm^2/s	Gu et al., 2003; Sengers et al., 2005
Fluid phase volume fraction for 2% agarose	ϕ_f	0.98		Calculated
Cell density at day 0 (low seeding density condition)	ρ	20×10^6	cells/mL	Direct measurement (cell counting)
Cell density at day 0 (high seeding density condition)	ρ	40×10^6	cells/mL	Direct measurement (cell counting)
O_2 concentration at media surface (low O_2 conditions)	C	50	μM	Direct measurement (oxygen sensor)
O_2 concentration at media surface (high O_2 conditions)	C	185	μM	Direct measurement (oxygen sensor)
O_2 concentration at geometrical center of construct	O_{2c}	measured	%	Direct measurement (oxygen microsensor)
Cell density at day 24 (core)	ρ_{core}	measured	cells/mL	Direct measurement (DNA quantification)
Cell density at day 24 (annulus)	ρ_{ann}	measured	cells/mL	Direct measurement (DNA quantification)
Michaelis—Menten constant	K_m	63	$\mu mol/mm^3$	Heywood et al., 2010
Cellular oxygen consumption rate	Q_m	Unknown	mol/cell/s	Output predicted by numerical model

core and annulus by normalizing day 24 DNA values to mean day 0 DNA values. ρ values for day 24 models were then calculated by multiplying this ratio by the initial (day 0) seeding density, giving cell concentrations in each sample core (ρ_{core}) and annulus (ρ_{ann}), thereby accounting for spatial changes in cell number over the study duration. The cellular oxygen consumption rate Q_m was determined for each cell type and culture condition by systematically adjusting Q_m until the predicted O_{2c} matched the experimentally observed O_{2c}. It should be noted that Q_m represents the mean oxygen consumption value for all cells in each construct and, in the case of an experimentally measured O_{2c} of 0%, the predicted value of Q_m is a minimum value of the oxygen consumption rate required to deplete oxygen to 0% at the center of the construct. Contour plots were then produced showing predicted oxygen gradients throughout the tissues. This modeling process was repeated for 3 different samples for each culture condition and time-point, using unique input parameters for Q_m, ρ_{core}, and ρ_{ann}. Furthermore, frequency plots were also produced to demonstrate the volumetric fraction of each construct at specific oxygen levels.

Biochemical Analysis

Each construct ($n \geq 3$ per group) was separated into a core and annulus (to allow for spatial biochemical analyses (**Figure 2B**); using a 3 mm biopsy punch and their respective wet weights were measured. Each sample was then used for quantitative analysis of DNA, sulphated glycosaminoglycan (sGAG) and collagen content. For the former analyses, samples were digested with papain (125 μg/mL) in 0.1M sodium acetate, 5 mM L-cysteine-HCl, and 0.05M EDTA (pH 6.0, all Sigma-Aldrich) at 60°C under constant rotation for 18 h. DNA content was quantified using the Hoechst Bisbenzimide 33258 dye assay as described previously (Kim et al., 1988), with a calf thymus DNA standard. sGAG content was quantified using the dimethylmethylene blue dye-binding assay (DMMB; Blyscan, Biocolor Ltd., Northern Ireland) with a chondroitin sulfate standard. Collagen content was determined by measuring the hydroxyproline content. Samples were hydrolyzed at 110°C for 18 h in 38% HCl and assayed using a chloramine-T assay with a hydroxyproline : collagen ratio of 1:7.69 (Kafienah and Sims, 2004; Ignat'eva et al., 2007). Total sGAG and hydroxyproline values were normalized to DNA values.

Histology and Immunohistochemistry

At selected time-points, constructs ($n = 2$) were fixed in 4% paraformaldehyde (Sigma-Aldrich) overnight at 4°C, rinsed with phosphate buffered saline (PBS), dehydrated and embedded in paraffin wax. Constructs were then cut in half and sectioned perpendicular to the disc face yielding 8 μm thick sections. Sections were stained with either 1% alcian blue 8GX (Sigma-Aldrich, Ireland) in 0.1M HCl for sGAG or picrosirius red for collagen. The deposition of collagen type II was identified through immunohistochemistry. Briefly, sections were rinsed with PBS and quenched of peroxidase activity for 20 min and treated with chondroitinase ABC (Sigma, 0.25 units/mL) in a humidified environment at 37°C for 1 h to enhance the permeability of the extracellular matrix by removal of chondroitin sulfate. Slides were again rinsed with PBS and blocked with 10% goat serum for 30 min. Sections were incubated with mouse monoclonal anti-collagen type II diluted 1:100 (Abcam, United Kingdom) (concentration 1 mg/mL) for 1 h at room temperature. After washing in PBS, the secondary antibody for type II collagen (Anti-Mouse IgG Biotin antibody produced in goat) (concentration 1 g/L) binding was applied for 1 h. Color was developed using the Vectastain ABC reagent (Vectastain ABC kit, Vector Laboratories, United Kingdom) for 45 min, followed by 5 min of exposure to peroxidase DAB substrate kit (Vector laboratories, United Kingdom). Slides were dehydrated through ethanol and xylene and mounted with Vectamount medium (Vector Laboratories, United Kingdom). Positive and negative controls (porcine cartilage and ligament) were included in the immunohistochemistry staining protocol for each batch.

Statistical Analysis

All statistical analyses were performed using GraphPad Prism (Version 8.3) software. Results are reported as mean ± standard deviation. Groups were analyzed by a general linear model for analysis of variance. Tukey's test was used to compare conditions. Significance was accepted at a level of $P < 0.05$ and population size n is stated where applicable.

RESULTS

MSCs Adopt a Chondrocyte-Like Oxygen Consumption Rate Following Hydrogel Encapsulation and Stimulation With TGF-β3

Agarose hydrogels seeded with either BMSCs, FPSCs or CCs were cultured for 24 days in chondrogenic medium. The level of oxygen at the center of the construct (O_{2c}) was measured at day 0 and 24 (**Figures 3A,C**). On day 0, the lowest O_{2c} levels were measured in BMSC seeded constructs (0.0% ± 0.0), whereas the highest levels were measured in the CC seeded constructs (4.6% ± 0.3). By day 24, O_{2c} levels had increased in BMSC constructs (4.2% ± 0.3) and were similar to those observed in FPSC seeded constructs (3.0% ± 1.0). The oxygen levels in CC constructs also increased over the duration of the study (from 4.6% ± 0.3 at day 0 to 7.6% ± 0.7 at day 24), whereas no significant change in oxygen levels were measured in FPSC constructs. Similar results were observed in a replicate study performed with cells isolated from a different donor (**Supplementary Figure 1A**).

While a likely explanation for the observed increases in oxygen levels within the constructs is a change in cellular metabolism as MSCs adopt a more chondrogenic phenotype with time in culture, an alternative explanation could be a change in total number of cells within the engineered tissue due to proliferation or cell death. To investigate this, average DNA content at day 24 was normalized to that of day 0 and the percentage change was calculated (**Supplementary Figure 2A**). Both BMSCs and FPSCs proliferated in both the annuli and the central core section of the samples over the study duration, with a ∼40% increase in DNA content. However, a reduction in CC cell numbers was observed, as evidenced by a ∼20% decrease in overall DNA content, with cell death being more prevalent in the higher oxygen annular section than in the core.

This experimental data on core oxygen levels and cell numbers was next used to develop finite element (FE) models of oxygen transport within the hydrogels and to predict cellular oxygen consumption rates. FE modeling of oxygen transport revealed that BMSCs were found to have highest cellular oxygen consumption rate at day 0 (**Figure 3B**), but this value dropped by approximately 70% (Q_m = 43.2 ± 6.2 vs. 13.1 ± 0.6 amol/cell/s) to a level similar to that of CCs by day 24. The CC oxygen consumption rate remained relatively unchanged throughout the study (Q_m = 18.1 ± 0.6 vs. 14.9 ± 0.9 amol/cell/s), suggesting that the observed change in oxygen concentration in CC constructs can be attributed to cell death (and hence a decrease in the number of oxygen consuming cells), as opposed to altered cell metabolism. Q_m values extrapolated for FPSCs show a significant decrease of approximately 30% in cellular oxygen consumption rate during the 24 days of culture (Q_m = 28.1 ± 0.7 vs. 19.1 ± 2.5 amol/cell/s). Despite this, oxygen gradients remained consistent throughout FPSC constructs over the duration of the study, as decreases in FPSC oxygen consumption rate were balanced with increases in cell numbers (**Figure 3C**).

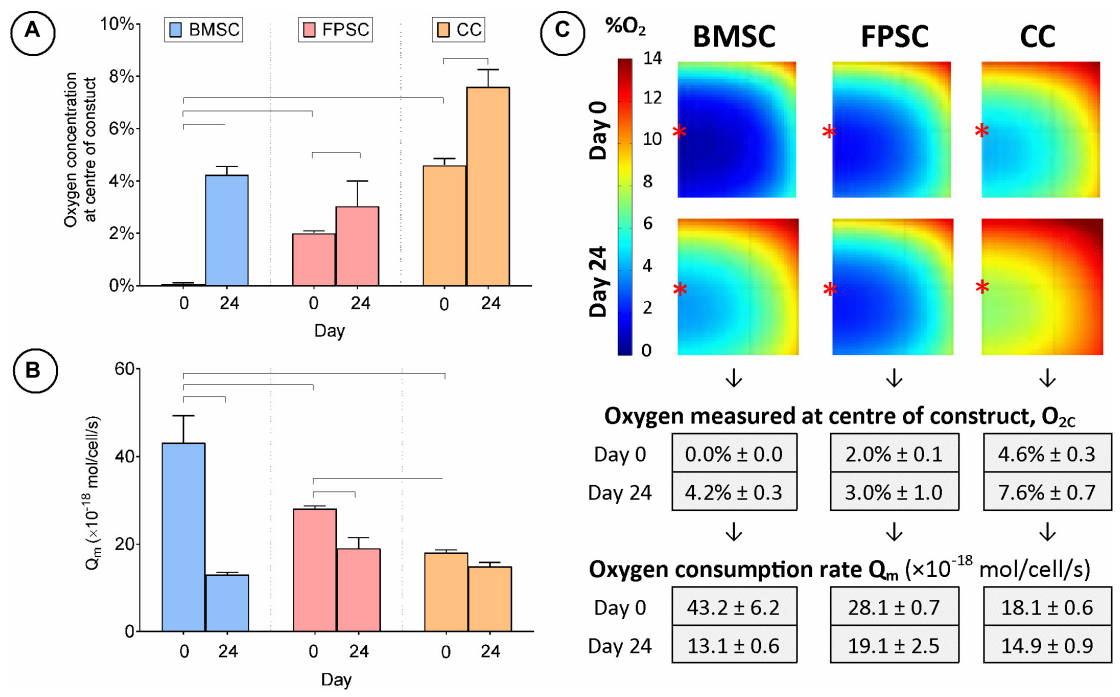

FIGURE 3 | Cartilage tissue grafts engineered using various cell sources were cultured for 24 days. **(A)** Oxygen concentration at center of constructs. **(B)** Cellular oxygen consumption rate extrapolated from FE model. **(C)** FE contour plots showing predicted oxygen gradients and table of values from **(A,B)** (± SD). Significant differences between groups are indicated where $P < 0.05$ ($n = 3$). *Indicates the location of oxygen sensor measurement within the constructs.

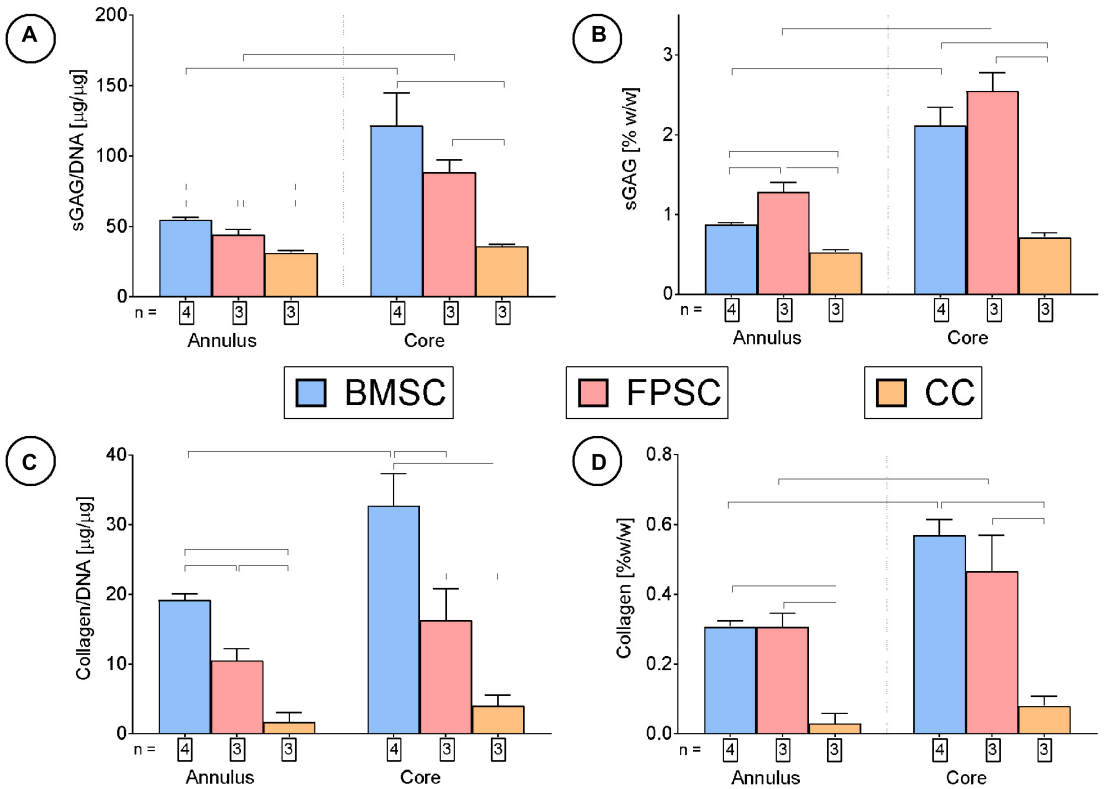

FIGURE 4 | Cartilage tissue grafts engineered using various cell sources were cultured for for 24 days, then subsequently separated into cores and annuli and analyzed for DNA, sGAG and collagen content. Significant differences between groups are indicated where $P < 0.05$ (n shown on graph).

After 24 days in culture, BMSCs had synthesized higher quantities of sGAG on a per-cell basis compared to FPSCs or CCs (**Figure 4A**). On a wet weight basis (%ww), greater levels of sGAG accumulation were observed in FPSC seeded constructs compared to both BMSC seeded constructs and CC seeded constructs (FPSC: 1.75 ± 0.08 %ww; BMSC: 1.29 ± 0.04 %ww; CC: 0.59 ± 0.01 %ww, for whole constructs). Spatial analysis of ECM deposition revealed higher levels of sGAG accumulation in the more hypoxic core than in the outer annulus of tissues engineered using stem cells (**Figures 4A,B**). Similar trends were observed for collagen deposition, with BMSCs synthesizing the most collagen when normalized to DNA content (**Figure 4C**), and with the greatest levels of accumulation also observed in the core (**Figure 4D**). On a percentage weight basis, comparable levels of total collagen accumulation were observed in FPSC and BMSC seeded constructs, which were higher than those observed in CC seeded constructs (FPSC: 0.36 ± 0.02 %ww; BMSC: 0.4 ± 0.02 %ww; CC: 0.04 ± 0.01 %ww, for whole constructs). Histological analysis revealed more intense staining for sGAG and collagen in BMSC and FPSC constructs when compared to CCs (**Figure 5**). Morphologically cells appeared similar in the central and peripheral regions of these engineered constructs, with a more well developed pericellular matrix observed in BMSC groups (**Supplementary Figure 3**). Only weak/negative staining for collagen type II was observed in FPSC and CC constructs, with BMSC constructs staining more strongly for type II collagen, particularly in the more hypoxic core region of the engineered tissue.

Decreasing the External Oxygen Tension Reduces the Rate at Which BMSCs Consume Oxygen and Leads to Increased Matrix Accumulation

Although regions of low oxygen concentration correlated with increased ECM deposition in stem cell seeded constructs, it was unclear whether these low oxygen conditions were directly enhancing chondrogenesis, or if these regions of low oxygen within the engineered tissues were simply a function of the high levels of oxygen consumption by encapsulated cells. To address this question, BMSC-seeded constructs were cultured in either a 20 or 5% environment and local levels of oxygen availability in the engineered grafts were measured experimentally and oxygen consumption rates (Q_m) were subsequently predicted using numerical models. O_{2c} was observed to be close to 0% for both external oxygen conditions at day 0 (**Figures 6A,C**). However, by day 24, local O_{2c} levels had increased significantly for both external oxygen environments (4.2% ± 0.3 for 20% oxygen and 1.1% ± 0.2 for 5% oxygen conditions).

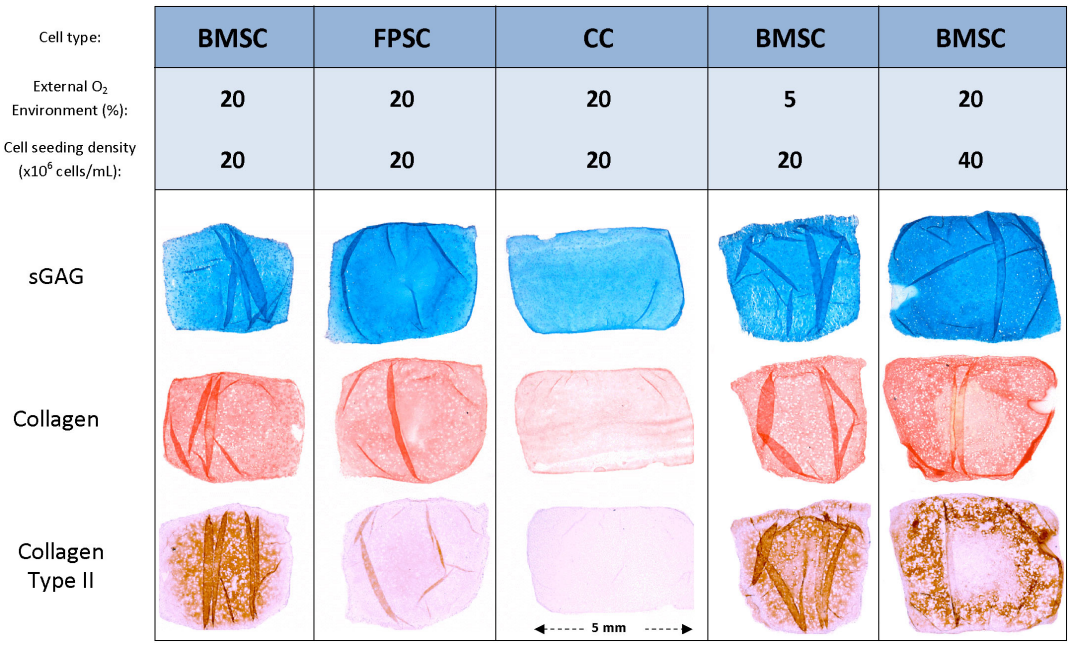

FIGURE 5 | Histological and immuno-histochemical staining was performed on representative sections of cartilage tissue grafts engineered using various cell sources and cultured for 24 days.

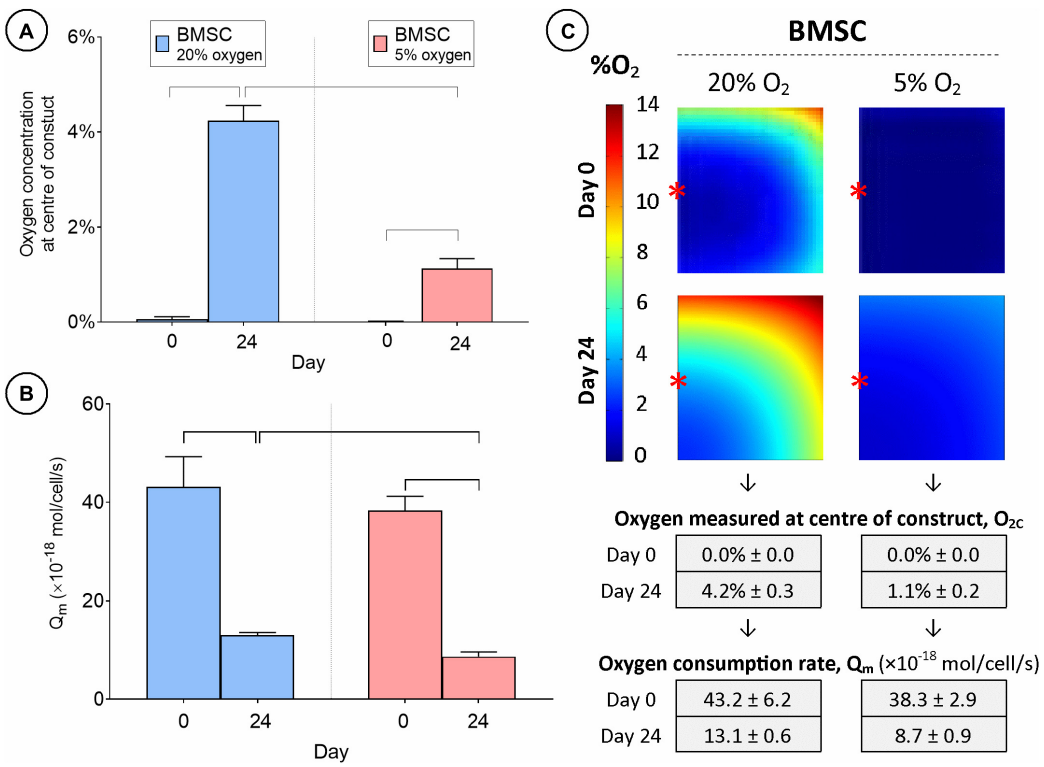

FIGURE 6 | Cartilage tissue grafts engineered using bone marrow MSCs were cultured in either a 20% or low (5%) external oxygen environment for 24 days. **(A)** Oxygen concentration at center of constructs. **(B)** Cellular oxygen consumption rate extrapolated from FE model. **(C)** FE contour plots showing predicted oxygen gradients and table of values from **(A,B)** (± SD). Significant differences between groups are indicated where $P < 0.05$ ($n = 3$). *Indicates the location of oxygen sensor measurement within the constructs.

Unsurprisingly, oxygen levels in the core of BMSC constructs cultured in a low (5%) oxygen environment were still lower than those in the core of constructs cultured in 20% oxygen conditions at day 24. While the boundary conditions of the FE model were set so that the O_2 concentration at the air/media interface was equivalent to that of the air within the incubator, it was expected that O_2 levels would drop across the 1 mm vertical diffusion distance between the media surface and the upper surface of the construct and that the maximum oxygen levels within the construct would be significantly lower than that of the air. FE simulations predicted higher concentrations of oxygen (ranging from 0 to 14% O_2) throughout the constructs maintained in 20% oxygen compared to those maintained in low oxygen conditions, where the oxygen levels throughout much of the construct were less than 2% (**Figure 6C** and **Supplementary Figure 4B**). Q_m was shown to decrease in both cases over the culture period duration, but was significantly lower in the 5% oxygen (Q_m = 8.7 ± 0.7 amol/cell/s) condition than in 20% oxygen (Q_m = 13.1 ± 0.6 amol/cell/s) by day 24 (**Figures 6B,C**).

Although decreasing the external oxygen concentration to 5% had no effect on sGAG accumulation in the already low oxygen core, sGAG accumulation in the annulus of the construct maintained at an external oxygen concentration of 5% was approximately twice that measured in the annulus of the construct maintained at 20% oxygen (**Figures 7A,B**). Collagen deposition also increased in the annulus of the constructs maintained at 5% oxygen but decreased in the core (**Figures 7C,D**). The mean predicted oxygen level in the annulus was 9.0% for BMSC constructs maintained in 20% oxygen and 2.3% for those maintained in 5% oxygen, while the mean predicted oxygen level in the core was 6.4% for constructs cultured in 20% oxygen and 1.7% for those in 5% oxygen (see **Supplementary Figure 4B** for further details). This suggests that while environments of less than 2% oxygen concentration can continue to support sGAG synthesis, collagen synthesis can be negatively impacted. Positive alcian blue, picrosirius red and type II collagen staining was observed in all constructs (**Figure 5**), with the latter staining maximally in the core of constructs maintained at 20% oxygen.

Increasing the Cell Seeding Density Lowers Oxygen Levels in Tissue Engineered Cartilage and Increases Extracellular Matrix Synthesis

To investigate the influence of cell seeding density on engineered cartilage tissue development, constructs were seeded at either 20 or 40 million cells/mL and cultured in chondrogenic medium for 24 days with the external oxygen concentration maintained at 20%. On day 0, O_{2c} was measured to be approximately 0% in both groups (**Figure 8A**). This value increased for both conditions over the study period despite significant cell proliferation (**Supplementary Figure 2C**) but as expected was significantly greater in the lower seeding density group by day 24 (4.2% ± 0.3 vs. 1.5% ± 0.4 O_{2c}). A higher cell seeding density was predicted to lead to the development of a much larger hypoxic core region at both day 0 and 24 (**Figure 8C**), although the size of this region was not as large as that for the lower cell seeding density when maintained at 5% external oxygen concentration (compare **Figures 6C**, **8C**). Extrapolated values for the average cellular oxygen consumption rate at day 24 were similar for both cell seeding densities, but significantly lower than day 0 values (**Figure 8B**).

Spatial biochemical analysis revealed that doubling the initial seeding density resulted in a large increase in sGAG synthesis (on a per cell basis) and accumulation in the construct annulus, as measured by increases in sGAG/DNA (×3.5 times, **Figure 9A**) and sGAG as a % of wet weight (×6.7 times, **Figure 9B**). Increasing the seeding density also led to higher sGAG accumulation in the core region, but not when sGAG accumulation was normalized to DNA content. Collagen synthesis was also enhanced in the annulus with increasing seeding density but was reduced in the core region (**Figures 9C,D**). More intense staining for sGAG was observed throughout the high seeding density constructs (**Figure 5**), while collagen staining was located primarily in the annular region. Immuno-histochemical staining for collagen type II clearly showed the effects of varying the seeding density, with collagen II concentrated in the core of the low seeding density constructs and around the periphery of the high seeding density constructs.

DISCUSSION

It has previously been demonstrated that the external oxygen concentration can influence MSC metabolism, differentiation and matrix synthesis (Fehrer et al., 2007; Buckley et al., 2010; Meyer et al., 2010; Pattappa et al., 2013). In the current study, a combined experimental and numerical approach was utilized to characterize the spatial oxygen environment within cartilage tissues engineered using various sources of cells. Oxygen levels measured within tissues seeded with BMSCs and CCs increased significantly over the study duration. However, biochemical analysis and finite element modeling revealed different causes for these increases: MSCs were found to possess a high initial oxygen uptake rate, but to adopt a more chondrocyte-like oxygen consumption profile following chondrogenic differentiation, whereas increases in oxygen concentration within CC constructs were attributed to decreases in cell number. Spatial biochemical analysis of the engineered tissues revealed a correlation between low oxygen regions and enhanced levels of cartilage specific extra cellular matrix deposition.

Direct measurements of oxygen levels within the constructs provided an insight into the local cellular environment during chondrogenesis in 3D hydrogels. BMSCs and FPSCs were found to have proliferated significantly over the study duration, while the CC population reduced in number. Using this data, the average oxygen consumption rate of BMSCs was estimated to be 43.2 amol/cell/s prior to chondrogenic differentiation, which is comparable to values previously reported for BMSCs of 33 amol/cell/s (Pattappa et al., 2013). FPSCs were estimated to utilize oxygen at a rate of 28.1 amol/cell/s at day 0. CC oxygen consumption did not change significantly throughout the study,

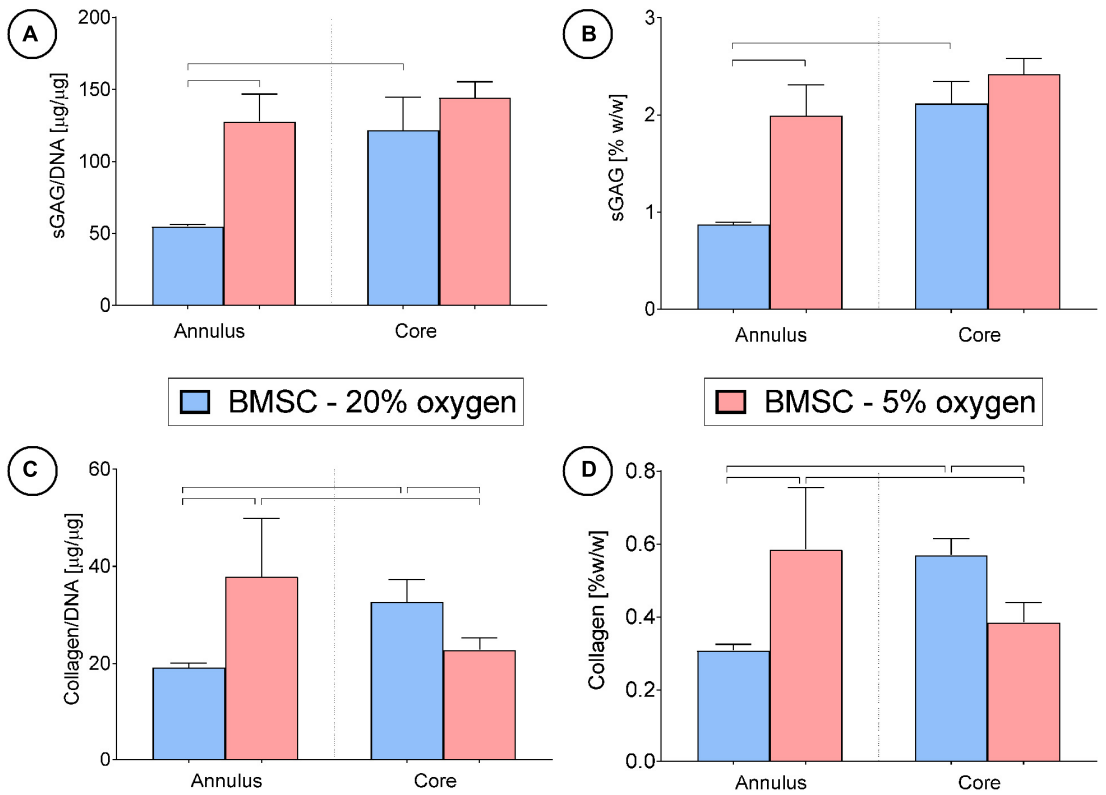

FIGURE 7 | Cartilage tissue grafts engineered using bone marrow MSCs were cultured in either a 20% or low (5%) external oxygen environment for 24 days were separated into cores and annuli, then analyzed for DNA, sGAG and collagen content. Significant differences between groups are indicated where $P < 0.05$ ($n = 4$).

with an average rate of 16.5 amol/cell/s, which is reasonably consistent with previously reported values of 19.4 amol/cell/s (Heywood and Lee, 2010). However, by day 24, both BMSCs and FPSCs had adopted a similar oxygen uptake (13.1 and 19.1 amol/cell/s, respectively) to that of CCs. In fact, it appears that this switch occurred prior to day 14 (see **Supplementary Figure 5**), but continuous monitoring of oxygen levels within the construct and an increased number of FE models and analyses would be required to pinpoint when this switch occurs. During monolayer expansion, MSCs are known to possess the ability to adapt their oxygen consumption to changes in the oxygen environment (Pattappa et al., 2013). The apparent switch to a more glycolytic metabolism reported in the current study has also been observed previously in MSC pellets (Pattappa et al., 2011), whereas increases in oxidative metabolism has been associated with a loss of chondrocyte phenotype (Heywood and Lee, 2008).

In the current study, it was demonstrated that BMSCs possess a higher initial oxygen uptake rate than FPSCs and this resulted in an O_{2C} measurement of 0% for all BMSC-laden constructs at day 0. A possible explanation for this is that these cells reside within different oxygenated niches *in vivo* and have adapted metabolisms to reflect this. Despite this, both groups were successfully induced to adopt a more chondrogenic oxygen consumption rate and synthesize cartilage-specific extracellular matrix. Consistent with previously reported findings (Meyer et al., 2010; Buckley et al., 2011), matrix deposition was generally maximal in regions of low oxygen. Even when cultured at 20% oxygen, a hypoxic core region developed in MSC laden hydrogels where matrix deposition was greatest. Culturing in a low oxygen environment effectively expanded this hypoxic region to include the entirety of the construct, thereby enhancing matrix synthesis within the annular region also. However, this also had the effect of further reducing oxygen levels in the core from an average concentration (by volume) of 6.4–1.7% oxygen, which, while having no net effect on sGAG content, appeared to inhibit collagen synthesis. This suggests that, while both sGAG and collagen synthesis is enhanced by culture in 5% oxygen, very low oxygen environments can be detrimental to collagen production. However, since MSCs have been observed to increase their glucose uptake when maintained in hypoxia (Pattappa et al., 2013; Naqvi and Buckley, 2015), the lower oxygen environment predicted throughout the entirety of the constructs cultured in 5% oxygen will also likely lead to a depletion of glucose in the core region, thus potentially inhibiting collagen synthesis. Indeed, it has been reported that, while collagen deposition by MSCs remains unaffected in either low oxygen or low glucose environments, hypoxia combined with deprivation of glucose leads to significantly reduced collagen synthesis, whereas sGAG synthesis is enhanced under these conditions, when compared to those cultured in 20% oxygen (Naqvi and Buckley, 2015). Follow-up studies measuring glucose consumption in engineered tissues are required to further test this hypothesis.

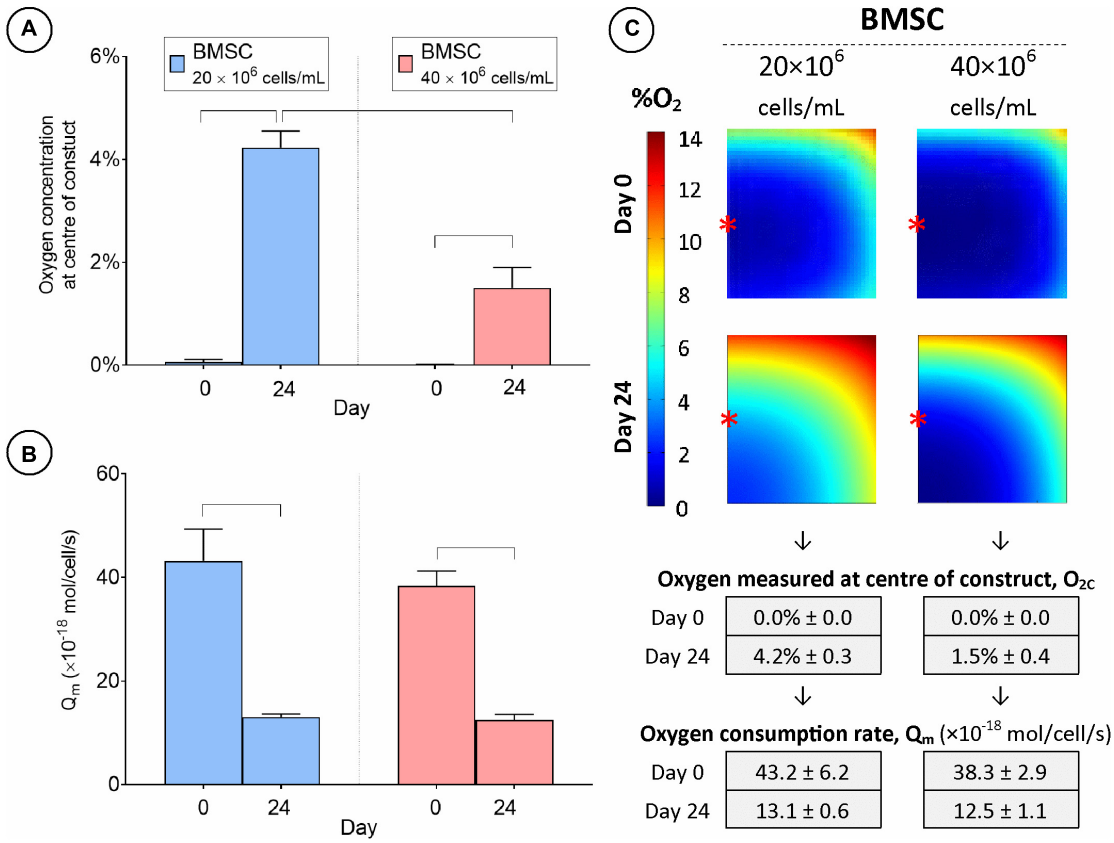

FIGURE 8 | Cartilage tissue grafts engineered using bone marrow MSCs were seeded initially at a density of either 20 or 40 million cells/mL and cultured for 24 days. **(A)** Oxygen concentration at center of constructs. **(B)** Cellular oxygen consumption rate extrapolated from FE model. **(C)** FE contour plots showing predicted oxygen gradients and table of values from **(A,B)** (± SD). Significant differences between groups are indicated where $P < 0.05$ ($n = 3$). *Indicates the location of oxygen sensor measurement within the constructs.

Both FPSCs and BMSCs secreted higher levels of sGAG and collagen compared to CCs. While we have previously observed that FPSCs and BMSCs secrete higher levels of cartilage matrix specific extracellular matrix components *in vitro* (Sheehy et al., 2011; Vinardell et al., 2012), others have reported superior chondrogenesis with CCs compared to BMSCs following hydrogel encapsulation (Mauck et al., 2006; Farrell et al., 2012). It should be noted that the CCs used in this study were first expanded on tissue culture plastic prior to hydrogel encapsulation, which is known to result in dedifferentiation of the cells. This is similar to what occurs with clinical cell-based therapies such as autologous chondrocyte implantation. This likely contributes to the relatively lower levels of chondrogenesis observed with the CCs compared to the other cell types. Further studies are required to assess how such monolayer expansion influences the metabolic phenotype of CCs.

Increasing the cell seeding density also had the effect of expanding the hypoxic core region (**Figure 8C**) and again enhancing matrix accumulation in the annulus, at the cost of reduced collagen synthesis (on a per cell basis) in the core. As discussed previously, this may be due to low oxygen conditions and/or glucose depletion in constructs seeded at high densities. However, as native cartilage consists of a zonal architecture, with gradients in biochemical content and functional properties throughout the tissue (Chen et al., 2001; Julkunen et al., 2009; Gannon et al., 2012), introducing nutrient gradients, and even selective localized scarcity in nutrient availability, may be ultimately desirable when attempting to recapitulate native-like tissue composition and architecture.

This paper presents a novel approach to measuring and modeling the oxygen consumption rates of stem cells within engineered tissues, although it does involve making certain assumptions. While cell density was estimated separately for each core and annulus region, cell density gradients, which are not fully accounted for, will likely develop within these regions. Relying solely on a DNA assay to measure changes in cell number within the hydrogels is also a limitation; DNA of dead cells may remain trapped within the hydrogel and be detected by the biochemical assay. Future studies should look to combine such assays with imaging to assess spatial changes in cell proliferation and death. Also, the K_m value used for all cell types was a value reported for bovine articular chondrocytes and was assumed not to vary throughout the study. Therefore, it is proposed that future studies should involve accurately measuring cell density

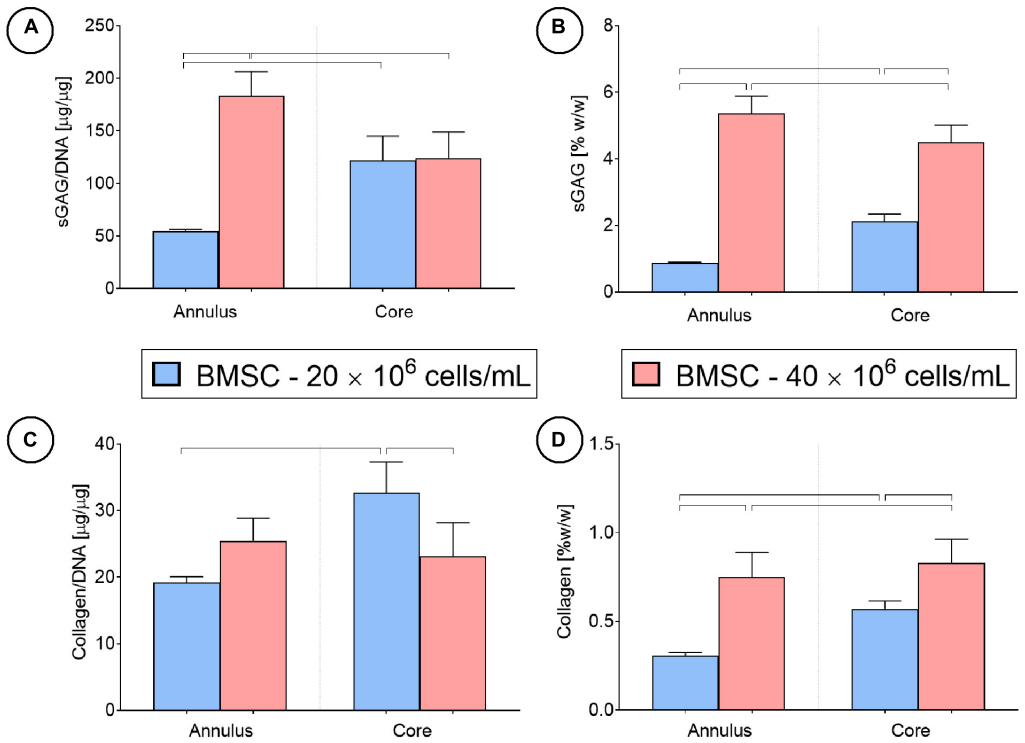

FIGURE 9 | Cartilage tissue grafts engineered using bone marrow MSCs were seeded initially at a density of either 20 or 40 million cells/mL for 24 days, then separated into cores and annuli and analyzed for DNA, sGAG and collagen content. Significant differences between groups are indicated where $P < 0.05$ ($n = 4$).

gradients, quantifying temporal changes in K_m for each culture condition, monitoring both oxygen and glucose concentrations more frequently (particularly in the early phase to monitor the onset of differentiation) and at multiple locations throughout the tissues and the development of dual-species oxygen/glucose diffusion-reaction numerical models. Other improvements to the model would include altering the diffusion rate of different species through the hydrogel as a function of matrix deposition by cells, locations and considering factors such as acidification and changing lactate concentrations. Furthermore, exploring the donor-to-donor variability in oxygen consumption rates should be more robustly addressed in future studies.

The results of this study can also inform the future clinical development of cell and tissue engineering based strategies for articular cartilage regeneration. By understanding, monitoring and modeling how oxygen consumption rates change with time in culture, in the future it should be possible to use such data as a metric of MSC differentiation and in the design of culture environments that temporally modulate external oxygen levels to accelerate chondrogenesis and the functional development of tissue engineered cartilage grafts. For allogenic tissue engineering strategies, this might be achieved by first carefully characterizing the oxygen consumption rates of a specific lot of donor MSCs as they undergo chondrogenesis, and then implementing donor-specific culture conditions when scaling-up the engineering of grafts using banks of these donor cells. For autologous tissue engineering strategies, it will likely require the on-line monitoring of oxygen consumption within each culture, with real-time control of the external oxygen conditions to provide the ideal conditions for these patient-specific grafts.

CONCLUSION

Understanding how the local cellular environment influences cell metabolism, phenotype and matrix synthesis will be crucial to engineering functional cartilage tissue grafts of a clinically relevant scale. Oxygen and nutrient gradients and consumption rates within tissue grafts can be influenced by varying factors such as the external culture environment oxygen tension, cell seeding density and construct scale. However, these gradients will be often in a state of flux, varying both spatially and temporally, where the local environment will influence cell metabolism, which in turn will influence the cellular environment. These studies present a combined experimental and numerical approach to characterizing these gradients and cellular responses and, potentially provides a framework which in the future may allow tissue engineers to control these gradients to engineer native-like articular cartilage. It was demonstrated that MSCs undergoing chondrogenesis adapt their oxygen consumption profile to be more similar to that of chondrocytes. Therefore, determining if MSCs used to engineer cartilage grafts adopt an oxygen consumption profile similar to chondrocytes might be considered a key determinant of the success of stem cell-based cartilage tissue engineering strategies.

DATA AVAILABILITY STATEMENT

The raw data supporting the conclusions of this article will be made available by the authors, without undue reservation.

AUTHOR CONTRIBUTIONS

SC performed all the experimental activities and sample analyses. All authors were involved in study design, interpretation and presentation of data and preparation of this article.

FUNDING

Funding was provided by Science Foundation Ireland (President of Ireland Young Researcher Award: 08/YI5/B1336) and the European Research Council (StemRepair – Project no. 258463).

SUPPLEMENTARY MATERIAL

The Supplementary Material for this article can be found online at: https://www.frontiersin.org/articles/10.3389/fbioe.2021.591126/full#supplementary-material

Supplementary Figure 1 | A replicate study was performed using cells from a separate set of donors and oxygen concentration in the center of each construct was measured.

Supplementary Figure 2 | The percentage change in cell density in sample cores and annuli following 24 days of culture.

Supplementary Figure 3 | High-magnification (20x) images of representative sections stained with Alcian Blue and Nuclear Fast Red following 24 days of culture.

Supplementary Figure 4 | FEA models were analyzed to determine the percentage volume of each sample that contained nodes with O_2 values that lay within the specified oxygen ranges at day 24.

Supplementary Figure 5 | Oxygen concentration as measured in the center of constructs from each study group for both the main and replicate studies combined.

REFERENCES

Buckley, C. T., Meyer, E. G., and Kelly, D. J. (2011). The influence of construct scale on the composition and functional properties of cartilaginous tissues engineered using bone marrow-derived mesenchymal stem cells. *Tissue Eng. Part A.* 18, 382–396. doi: 10.1089/ten.tea.2011.0145

Buckley, C. T., Vinardell, T., and Kelly, D. J. (2010). Oxygen tension differentially regulates the functional properties of cartilaginous tissues engineered from infrapatellar fat pad derived MSCs and articular chondrocytes. *Osteoarthr. Cartil. OARS Osteoarthr. Res. Soc.* 18, 1345–1354. doi: 10.1016/j.joca.2010.07.004

Caplan, A. I. (2007). Adult mesenchymal stem cells for tissue engineering versus regenerative medicine. *J. Cell. Physiol.* 213, 341–347. doi: 10.1002/jcp.21200

Carroll, S. F., Buckley, C. T., and Kelly, D. J. (2014). Cyclic hydrostatic pressure promotes a stable cartilage phenotype and enhances the functional development of cartilaginous grafts engineered using multipotent stromal cells isolated from bone marrow and infrapatellar fat pad. *J. Biomech.* 47, 2115–2121. doi: 10.1016/j.jbiomech.2013.12.006

Cernanec, J. M., Weinberg, J. B., Batinic-Haberle, I., Guilak, F., and Fermor, B. (2007). Influence of oxygen tension on interleukin 1-induced peroxynitrite formation and matrix turnover in articular cartilage. *J. Rheumatol.* 34, 401–407.

Chen, S. S., Falcovitz, Y. H., Schneiderman, R., Maroudas, A., and Sah, R. L. (2001). Depth-dependent compressive properties of normal aged human femoral head articular cartilage: relationship to fixed charge density. *Osteoarthr. Cartil. OARS Osteoarthr. Res. Soc.* 9, 561–569. doi: 10.1053/joca.2001.0424

da Silva Meirelles, L., Caplan, A. I., and Nardi, N. B. (2008). In search of the in vivo identity of mesenchymal stem cells. *Stem cells* 26, 2287–2299. doi: 10.1634/stemcells.2007-1122

Farrell, M. J., Comeau, E. S., and Mauck, R. L. (2012). Mesenchymal stem cells produce functional cartilage matrix in three-dimensional culture in regions of optimal nutrient supply. *Eur. Cells Materials* 23, 425–440. doi: 10.22203/ecm.v023a33

Farrell, M. J., Fisher, M. B., Huang, A. H., Shin, J. I., Farrell, K. M., and Mauck, R. L. (2014). Functional properties of bone marrow-derived MSC-based engineered cartilage are unstable with very long-term in vitro culture. *J. Biomech.* 47, 2173–2182. doi: 10.1016/j.jbiomech.2013.10.030

Fehrer, C., Brunauer, R., Laschober, G., Unterluggauer, H., Reitinger, S., Kloss, F., et al. (2007). Reduced oxygen tension attenuates differentiation capacity of human mesenchymal stem cells and prolongs their lifespan. *Aging Cell* 6, 745–757. doi: 10.1111/j.1474-9726.2007.00336.x

Fermor, B., Christensen, S. E., Youn, I., Cernanec, J. M., Davies, C. M., and Weinberg, J. B. (2007). Oxygen, nitric oxide and articular cartilage. *Eur. Cells Materials* 13, 56–65;discussion.

Gannon, A. R., Nagel, T., and Kelly, D. J. (2012). The role of the superficial region in determining the dynamic properties of articular cartilage. *Osteoarthr. Cartil. OARS Osteoarthr. Res. Soc.* 20, 1417–1425. doi: 10.1016/j.joca.2012.08.005

Grant, J. L., and Smith, B. (1963). Bone marrow gas tensions, bone marrow blood flow, and erythropoiesis in man. *Ann. Int. Med.* 58, 801–809. doi: 10.7326/0003-4819-58-5-801

Gu, W. Y., Yao, H., Huang, C. Y., and Cheung, H. S. (2003). New insight into deformation-dependent hydraulic permeability of gels and cartilage, and dynamic behavior of agarose gels in confined compression. *J. Biomech.* 36, 593–598. doi: 10.1016/s0021-9290(02)00437-2

Harrison, J. S., Rameshwar, P., Chang, V., and Bandari, P. (2002). Oxygen saturation in the bone marrow of healthy volunteers. *Blood* 99:394. doi: 10.1182/blood.v99.1.394

Haselgrove, J. C., Shapiro, I. M., and Silverton, S. F. (1993). Computer modeling of the oxygen supply and demand of cells of the avian growth cartilage. *Am. J. Physiol.* 265(2 Pt 1), C497–C506.

Heywood, H. K., and Lee, D. A. (2008). Monolayer expansion induces an oxidative metabolism and ROS in chondrocytes. *Biochem. Biophys. Res. Commun.* 373, 224–229. doi: 10.1016/j.bbrc.2008.06.011

Heywood, H. K., and Lee, D. A. (2010). Low oxygen reduces the modulation to an oxidative phenotype in monolayer-expanded chondrocytes. *J. Cell. Physiol.* 222, 248–253. doi: 10.1002/jcp.21946

Heywood, H. K., Knight, M. M., and Lee, D. A. (2010). Both superficial and deep zone articular chondrocyte subpopulations exhibit the crabtree effect but have different basal oxygen consumption rates. *J. Cell. Physiol.* 223, 630–639.

Ignat'eva, N. Y., Danilov, N. A., Averkiev, S. V., Obrezkova, M. V., Lunin, V. V., and Sobol', E. N. (2007). Determination of hydroxyproline in tissues and the evaluation of the collagen content of the tissues. *J. Anal. Chem.* 62, 51–57. doi: 10.1134/s106193480701011x

Julkunen, P., Harjula, T., Iivarinen, J., Marjanen, J., Seppanen, K., Narhi, T., et al. (2009). Biomechanical, biochemical and structural correlations in immature and mature rabbit articular cartilage. *Osteoarthr. Cartil. OARS Osteoarthr. Res. Soc.* 17, 1628–1638. doi: 10.1016/j.joca.2009.07.002

Kafienah, W., and Sims, T. J. (2004). Biochemical methods for the analysis of tissue-engineered cartilage. *Methods Mol. Biol.* 238, 217–230. doi: 10.1385/1-59259-428-x:217

Kim, Y.-J., Sah, R. L. Y., Doong, J.-Y. H., and Grodzinsky, A. J. (1988). Fluorometric assay of DNA in cartilage explants using Hoechst 33258. *Anal. Biochem.* 174, 168–176. doi: 10.1016/0003-2697(88)90532-5

Kofoed, H., Sjontoft, E., Siemssen, S. O., and Olesen, H. P. (1985). Bone marrow circulation after osteotomy. blood flow, pO2, pCO2, and pressure studied in dogs. *Acta Orthopaed. Scand.* 56, 400–403. doi: 10.3109/17453678508994357

Lee, R. B., and Urban, J. P. (1997). Evidence for a negative Pasteur effect in articular cartilage. *Biochem. J.* 321(Pt. 1), 95–102. doi: 10.1042/bj3210095

Lightfoot, E. N., and Duca, K. A. (1999). "The roles of mass transfer in tissue function," in *The Biomedical Engineering Handbook*, 2d Edn, Vol. 2, ed. J. D. Bronzino (Boca Raton, FL: Electrical Engineering Handbook: CRC Press).

Malda, J., Rouwkema, J., Martens, D. E., Le Comte, E. P., Kooy, F. K., Tramper, J., et al. (2004). Oxygen gradients in tissue-engineered PEGT/PBT cartilaginous constructs: measurement and modeling. *Biotechnol. Bioeng.* 86, 9–18. doi: 10.1002/bit.20038

Malladi, P., Xu, Y., Chiou, M., Giaccia, A. J., and Longaker, M. T. (2006). Effect of reduced oxygen tension on chondrogenesis and osteogenesis in adipose-derived mesenchymal cells. *Am. J. Physiol. Cell Physiol.* 290, C1139–C1146.

Martin, I., Obradovic, B., Freed, L. E., and Vunjak-Novakovic, G. (1999). Method for quantitative analysis of glycosaminoglycan distribution in cultured natural and engineered cartilage. *Ann. Biomed. Eng.* 27, 656–662. doi: 10.1114/1.205

Mauck, R., Yuan, X., and Tuan, R. S. (2006). Chondrogenic differentiation and functional maturation of bovine mesenchymal stem cells in long-term agarose culture. *Osteoarthr. Cartil.* 14, 179–189. doi: 10.1016/j.joca.2005.09.002

Meyer, E. G., Buckley, C. T., Thorpe, S. D., and Kelly, D. J. (2010). Low oxygen tension is a more potent promoter of chondrogenic differentiation than dynamic compression. *J. Biomech.* 43, 2516–2523. doi: 10.1016/j.jbiomech.2010.05.020

Murphy, K. C., Hung, B. P., Browne-Bourne, S., Zhou, D., Yeung, J., Genetos, D. C., et al. (2017). Measurement of oxygen tension within mesenchymal stem cell spheroids. *J. R. Soc. Interf.* 14:20160851. doi: 10.1098/rsif.2016.0851

Naqvi, S. M., and Buckley, C. T. (2015). Extracellular matrix production by nucleus pulposus and bone marrow stem cells in response to altered oxygen and glucose microenvironments. *J. Anatomy* 227, 757–766. doi: 10.1111/joa.12305

Pattappa, G., Heywood, H. K., de Bruijn, J. D., and Lee, D. A. (2011). The metabolism of human mesenchymal stem cells during proliferation and differentiation. *J. Cell. Physiol.* 226, 2562–2570. doi: 10.1002/jcp.22605

Pattappa, G., Thorpe, S. D., Jegard, N. C., Heywood, H. K., de Bruijn, J. D., and Lee, D. A. (2013). Continuous and uninterrupted oxygen tension influences the colony formation and oxidative metabolism of human mesenchymal stem cells. *Tissue Eng. Part C Methods.* 19, 68–79. doi: 10.1089/ten.tec.2011.0734

Rajpurohit, R., Koch, C. J., Tao, Z., Teixeira, C. M., and Shapiro, I. M. (1996). Adaptation of chondrocytes to low oxygen tension: relationship between hypoxia and cellular metabolism. *J. Cell. Physiol.* 168, 424–432. doi: 10.1002/(sici)1097-4652(199608)168:2<424::aid-jcp21>3.0.co;2-1

Sengers, B. G., Heywood, H. K., Lee, D. A., Oomens, C. W., and Bader, D. L. (2005). Nutrient utilization by bovine articular chondrocytes: a combined experimental and theoretical approach. *J. Biomech. Eng.* 127, 758–766. doi: 10.1115/1.1993664

Sheehy, E. J., Buckley, C. T., and Kelly, D. J. (2011). Chondrocytes and bone marrow-derived mesenchymal stem cells undergoing chondrogenesis in agarose hydrogels of solid and channelled architectures respond differentially to dynamic culture conditions. *J. Tissue Eng. Regenerat. Med.* 5, 747–758. doi: 10.1002/term.385

Sheehy, E. J., Buckley, C. T., and Kelly, D. J. (2012). Oxygen tension regulates the osteogenic, chondrogenic and endochondral phenotype of bone marrow derived mesenchymal stem cells. *Biochem. Biophys. Res. Commun.* 417, 305–310. doi: 10.1016/j.bbrc.2011.11.105

Thorpe, S. D., Buckley, C. T., Steward, A. J., and Kelly, D. J. (2012). European society of biomechanics S.M. Perren Award 2012: the external mechanical environment can override the influence of local substrate in determining stem cell fate. *J. Biomech.* 45, 2483–2492. doi: 10.1016/j.jbiomech.2012.07.024

Thorpe, S. D., Nagel, T., Carroll, S. F., and Kelly, D. J. (2013). Modulating gradients in regulatory signals within mesenchymal stem cell seeded hydrogels: a novel strategy to engineer zonal articular cartilage. *PLoS One* 8:e60764. doi: 10.1371/journal.pone.0060764

Vinardell, T., Buckley, C., Thorpe, S., and Kelly, D. (2011). Composition–function relations of cartilaginous tissues engineered from chondrocytes and mesenchymal stem cells isolated from bone marrow and infrapatellar fat pad. *J. Tissue Eng. Regenerat. Med.* 5, 673–683. doi: 10.1002/term.357

Vinardell, T., Sheehy, E. J., Buckley, C. T., and Kelly, D. J. (2012). A comparison of the functionality and in vivo phenotypic stability of cartilaginous tissues engineered from different stem cell sources. *Tissue Eng. Part A.* 18, 1161–1170. doi: 10.1089/ten.tea.2011.0544

Westphal, I., Jedelhauser, C., Liebsch, G., Wilhelmi, A., Aszodi, A., and Schieker, M. (2017). Oxygen mapping: probing a novel seeding strategy for bone tissue engineering. *Biotechnol. Bioeng.* 114, 894–902. doi: 10.1002/bit.26202

Zhou, S., Cui, Z., and Urban, J. P. (2004). Factors influencing the oxygen concentration gradient from the synovial surface of articular cartilage to the cartilage-bone interface: a modeling study. *Arthr.Rheumat.* 50, 3915–3924. doi: 10.1002/art.20675

Conflict of Interest: The authors declare that the research was conducted in the absence of any commercial or financial relationships that could be construed as a potential conflict of interest.

Advantages of publishing in Frontiers

OPEN ACCESS
Articles are free to read for greatest visibility and readership

FAST PUBLICATION
Around 90 days from submission to decision

HIGH QUALITY PEER-REVIEW
Rigorous, collaborative, and constructive peer-review

TRANSPARENT PEER-REVIEW
Editors and reviewers acknowledged by name on published articles

Frontiers
Avenue du Tribunal-Fédéral 34
1005 Lausanne | Switzerland

Visit us: www.frontiersin.org
Contact us: frontiersin.org/about/contact

REPRODUCIBILITY OF RESEARCH
Support open data and methods to enhance research reproducibility

DIGITAL PUBLISHING
Articles designed for optimal readership across devices

FOLLOW US
@frontiersin

IMPACT METRICS
Advanced article metrics track visibility across digital media

EXTENSIVE PROMOTION
Marketing and promotion of impactful research

LOOP RESEARCH NETWORK
Our network increases your article's readership